Universitat Autònoma de Barcelona

Characterization of the Circadian Clock Function in the Control of Cell Cycle Progression to Modulate Growth in Arabidopsis thaliana

Jorge Alberto Fung Uceda

ADVERTIMENT. L'accés als continguts d'aquesta tesi queda condicionat a l'acceptació de les condicions d'ús establertes per la següent llicència Creative Commons: http://cat.creativecommons.org/?page_id=184

ADVERTENCIA. El acceso a los contenidos de esta tesis queda condicionado a la aceptación de las condiciones de uso establecidas por la siguiente licencia Creative Commons: http://es.creativecommons.org/blog/licencias/

WARNING. The access to the contents of this doctoral thesis it is limited to the acceptance of the use conditions set by the following Creative Commons license: https://creativecommons.org/licenses/?lang=en

UAB
Universitat Autònoma de Barcelona

crag
CENTRE FOR RESEARCH
IN AGRICULTURAL GENOMICS

Characterization of the Circadian Clock Function in the Control of Cell Cycle Progression to Modulate Growth in *Arabidopsis thaliana*

PhD Thesis

Jorge Alberto Fung Uceda

Barcelona, 2018

Universitat Autònoma de Barcelona

CRAG
CENTRE FOR RESEARCH
IN AGRICULTURAL GENOMICS

Universidad Autónoma de Barcelona
Facultad de Biociéncias
Departamento de Biología Animal, Biología Vegetal y Ecología
Programa de Doctorado en Biología y Biotecnología Vegetal

Characterization of the Circadian Clock Function in the Control of Cell Cycle Progression to Modulate Growth in *Arabidopsis thaliana*

Memoria presentada por Jorge Alberto Fung Uceda para optar por el título de doctor por la Universidad Autónoma de Barcelona

Directora

Doctorando

Dra. Paloma Mas Martínez

Jorge Alberto Fung Uceda

Barcelona, 2018

“*Pour domaine une baie,*
Pour château, une cabane,
Pour Fou, une mésange,
Pour sujets, mes souvenirs.”

Dans les forêts de Sibérie, Sylvain Tesson 2011

ACKNOWLEDGMENTS

No podría dejar de agradecer a todas las personas que han formado y siguen formando parte de este camino. El doctorado ha sido probablemente hasta el día de hoy una de las etapas mas interesantes y personalmente desafiantes que me ha tocado vivir. He tenido la suerte de contar con mucha gente que me ha apoyado de distintas maneras desde antes, durante y posiblemente espero que algunas lo sigan haciendo después del final de esta aventura.

Esta tesis doctoral ha sido el producto no sólo de mi esfuerzo y trabajo sino también del de mi directora de tesis Paloma Mas. Mis logros han sido el producto de un trabajo en equipo y los resultados que hemos obtenido son la prueba de ello.

Hay muchas maneras de llevar a cabo con éxito un doctorado y yo no cambiaría por nada como decidí llevar el mío. Con risas, muchos buenos momentos y algunas crisis existenciales que he compartido con gente de dentro y fuera del CRAG. Muchos llegaron y se fueron, algunos siguen conmigo y otros aunque llegaron al final, se han vuelto imprescindibles en mi día a día. Como fuese, no visualizo la totalidad de este camino sin ninguno de ellos. Si me detuviese a nombrar a cada uno de ustedes probablemente terminaría escribiendo una segunda tesis. Por ello y mucho más gracias.

Finalmente quiero agradecer a las cuatro personas sin las cuales nada de esto hubiera sido posible, mis padres y mis hermanas. Por estar ahí desde el inicio de mis tiempos y porque estarán ahí hasta el final.

TABLE OF CONTENTS

Table of contents

Introduction 7

1. Circadian clocks and circadian networks 7

2. The circadian clock in plants 8

  2.1. The Arabidopsis central oscillator: components and regulatory networks 9

    2.1.1. Role of TOC1 at the center of the circadian clock molecular architecture 15

      2.1.1.1. Transcriptional regulation of TOC1 15

      2.1.1.2. Post-translational regulation of TOC1 16

      2.1.1.3. Epigenetic regulation of TOC1 rhythmic oscillation 19

  2.2. Input pathways: synchronization of the circadian clock 20

  2.3. Output pathways: biological processes under circadian control 24

    2.3.1. Circadian regulation of hypocotyl elongation 24

    2.3.2. Circadian regulation of leaf growth 26

3. The cell cycle in plants 28

  3.1. Role of the cell cycle controlling leaf growth 28

  3.2. The plant mitotic cycle 30

  3.3. The plant endocycle 33

  3.4. Importance of G1/S phase transition during the plant cell cycle 36

  3.5. DNA replication during the S-phase 37

    3.5.1. Role of CDC6 in the formation of the Arabidopsis pre-replication complex 39

Objectives 45

Results 49

1. TOC1 regulates the timing of cell division in developing leaves 49

2. TOC1 controls the timing of the endocycle in leaves 53

4. The developmental expression of cell cycle genes is altered in TOC1-ox 60

5. The diurnal expression of cell cycle genes is altered in TOC1-ox 64

6. TOC1 directly binds to the CDC6 promoter 68

7. Tumor progression is affected in TOC1-ox inflorescence stalks 73

Discussion 77

Conclusions 87

Resumen en castellano **91**

Summary in english **95**

Materials and methods **99**

1. DNA constructs and plant transformation 99
2. Hypocotyl measurements 99
3. Kinematic analyses and flow cytometry 100
4. Real-time PCR analysis 101
5. Protoplast transfection 102
6. Chromatin immunoprecipitation 103
7. Tumor induction and progression 103
8. Quantification and statistical analysis 104

Bibliography **113**

Annexes **135**

INTRODUCTION

Introduction

---

1. Circadian clocks and circadian networks

The earth rotation around its axis has shaped the rhythmic behavior of living organisms in consonance with the 24 hours changes in environmental cues such as light and temperature. In order to anticipate these periodic changes, organisms have developed an endogenous timekeeping mechanism known as circadian clock. Circadian clocks are self-sustaining machineries that are responsible for sensing and integrating the predictable environmental fluctuations to efficiently generate rhythmic biological oscillations that enhance the organism’s fitness (Bell-Pedersen et al., 2005, Terzibasi-Tozzini et al., 2017).

The circadian system is composed of three main pathways: inputs, the central oscillator and outputs. The clock components responsible for the synchronization of the circadian rhythmic oscillations with the environmental cues are known as inputs (Stratmann and Schibler, 2006, Husse et al., 2015). The clock components responsible for generating and sustaining the rhythms form part of the central oscillator, which is the core of the clock (Partch et al., 2014, Mendoza-Viveros et al., 2017). Lastly, the biological processes that are rhythmically controlled by the clock are known as outputs (Pilorz et al., 2018). Although this is a very simplified model of the circadian system, it provides a clear and simple view to understand how the clock is working and regulating the rhythms in organisms (Masri et al., 2012, Panda, 2016).

In spite of the independent evolutionary steps, nearly all eukaryotic circadian clocks share functional similarities such as (1) the persistence of rhythmicity with endogenous period of about 24 hours, even in the absence of environmental changes in light and temperature (free-running or constant conditions); (2) the ability to be synchronized or entrained every day by light and/or temperature cycles and (3) their capacity to buffer changes in temperature within a physiological range, a property known as clock temperature compensation (Dunlap and Loros, 2017).

The basic architectural regulation of the eukaryotic central oscillator is based on interconnected transcriptional and post-transcriptional feedback loops as well as epigenetic regulation that altogether ensure the maintenance of robust rhythms (Stevenson, 2017). The complex regulatory networks result in circadian waves of clock core gene expression that oscillate at different phases during the day and night. These rhythms in gene expression are ultimately responsible for the generation of the rhythmic oscillations in physiological and developmental outputs (van der Veen et al., 2017).

2. The circadian clock in plants

The circadian clock organization in plants has been the subject of different studies focused on the specific circadian function in cells, tissues and organs. In *Arabidopsis thaliana*, almost all cells possess self-sustained clocks exhibiting different degrees of circadian synchronization in accordance to tissue specificity and the environmental conditions. The shoot apex clocks have been described to function as master clocks (Takahashi et al., 2015) with properties similar to those of the SCN (Suprachiasmatic Nucleus) in mammals (Dibner et al., 2010, Welsh et al., 2010). The shoot apex clocks are closely coupled, displaying a high degree of circadian communication. This strong coupling leads to robust and stable circadian rhythmic oscillations with improved capacity for phase readjustments. Furthermore, signals coming from the shoot apex clocks are able to synchronize distant clocks like the one in roots (Takahashi et al., 2015). Analyses of cell-and tissue-specific clock function were also explored in other studies. They showed that the circadian clockwork operates differently in distinct tissues and organs. Indeed, different tissues display diverse degrees of circadian coupling in spite of being physically close to each other (Thain et al., 2000, Yakir et al., 2011, Wenden et al., 2012, Endo et al., 2014, Bordage et al., 2016).

The three main components of the circadian system described in other organisms have been also identified in plants. In the following sections, we briefly describe these three main pathways, their components and regulatory interactions. We mostly focus on the *Arabidopsis thaliana* circadian system, which is one of the best-studied plant models thus far (Figure 1).

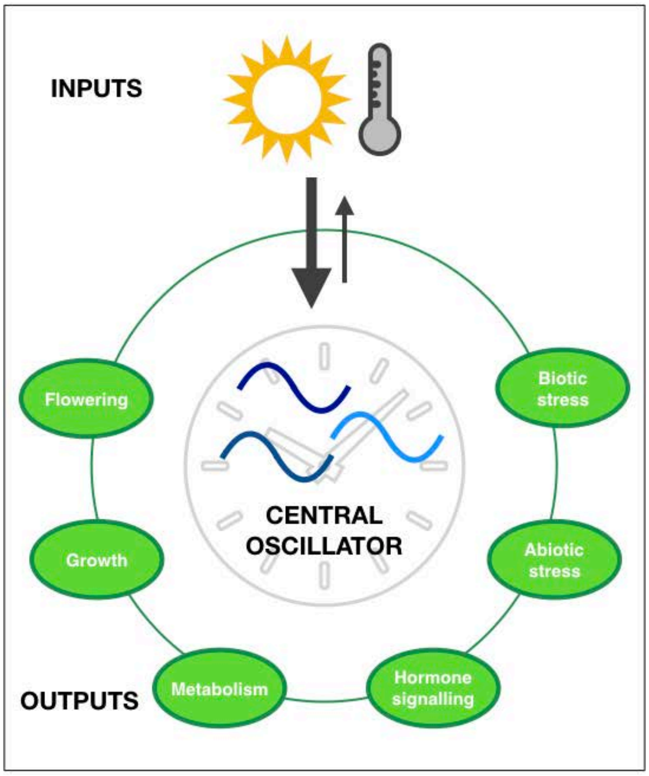

Figure 1. Schematic view of the circadian clock system. This simplified depiction of the circadian clock components shows the input pathways that include the environmental cues such as light or temperature in charge of synchronizing the clock every day. The central oscillator that translates the external signals into rhythmic oscillation of about 24 hours and the output pathways that are the rhythmic biological processes regulated by the circadian clock. Arrows indicate the interrelationship between the different pathways, the arrow going from the central oscillator to the input pathways indicate the property of the circadian clock to modulate its sensibility in the perception of external stimuli. Modified from (Greenham and McClung, 2015).

2.1. The Arabidopsis central oscillator: components and regulatory networks

Many different genetic and biochemical approaches have provided a wealth of information about the *Arabidopsis* central oscillator (Nohales and Kay, 2016). The initial identification of core clock components was carried out using plants expressing the promoter of the morning-expressed circadian output gene *CHLOROPHYLL A/B-BINDING PROTEIN 2* (*CAB2*) fused to the *luciferase* gene (*LUC*) as reporter. Induced mutagenesis followed by *in-vivo* bioluminescence assays identified a number of mutants with altered circadian period, phase or amplitude (Millar et al., 1995). These initial studies were followed by reverse genetic studies in which the characterization by miss-expression (mutation or over-expression) of the putative circadian clock genes provided important insights into the circadian regulatory network.

The first clock components to be characterized included two single MYB-domain transcription factors showing strong sequence homology within their MYB domain. The *CIRCADIAN CLOCK ASSOCIATED 1* (*CCA1*) (Wang and Tobin, 1998) and *LONG ELONGATED HYPOCOTYL* (*LHY*) (Schaffer et al., 1998) are expressed early in the morning, close to dawn. Their proteins are partially redundant (Mizoguchi et al., 2002) and heterodimerize (Lu et al., 2009, Yakir et al., 2011) to repress the expression of evening-phased genes. The importance of these two components in accurate timekeeping was also inferred by studies of circadian phenotypes of the mutants. While single loss-of-function mutants of either *CCA1* or *LHY* showed a short circadian period and advance phase under free-running conditions, the *cca1/lhy* double mutant was found to be arrhythmic (Alabadi et al., 2002, Mizoguchi et al., 2002). Furthermore, over-expression of either gene results in arrhythmic clock gene expression as well as severe phenotypes of various clock outputs (Schaffer et al., 1998, Wang and Tobin, 1998).

One of the evening-expressed genes repressed by CCA1 and LHY is the *TIMING OF CAB EXPRESSION 1* (*TOC1*) or *PSEUDO RESPONSE REGULATOR* (*PRR1*), one of the five members of the PRR family. TOC1 protein contains an N-terminus domain similar to the receiver domain of response regulators. However, TOC1 domain lacks the conserved phospho-accepting aspartate residue present in canonical response regulators (Strayer et al., 2000, Makino et al., 2002). In addition, TOC1 contains a C-terminal motif similar to the one found in the flowering-related CONSTANS (CO) family of transcription factors. The regulatory network among CCA1, LHY and TOC1 was described as the first transcriptional feedback loop in the *Arabidopsis* central oscillator (Alabadi et al., 2001). Based on this loop, CCA1 and LHY repressed the expression of *TOC1*, and in turn, TOC1 was proposed to activate the expression of these *MYB* transcription factors (Alabadi et al., 2001). However, a number of studies have recently shown that TOC1 actually function as a repressor of *CCA1* and *LHY* expression (Gendron et al., 2012, Huang et al., 2012, Pokhilko et al., 2012). Furthermore, TOC1 seems to function as a repressor of nearly all oscillator genes (Huang et al., 2012). The importance of TOC1 within the clock was also demonstrated in studies of the circadian phenotypes of TOC1 miss-expressing plants. While a loss-of-function mutation advanced the phase and shortened the circadian period (Millar et al., 1995, Somers et al., 1998, Strayer et al., 2000), TOC1 over-expression showed arrhythmia under constant light conditions (Mas et al., 2003a). Interestingly, additional copies of rhythmic TOC1 in transgenic plants expressing TOC1 under its own promoter (TOC1 MiniGene) showed delayed phase and longer period than WT (Wild-Type) plants (Mas et al., 2003b), suggesting that both proper accumulation and rhythmic oscillation of *TOC1* is central for circadian function (Figure 2).

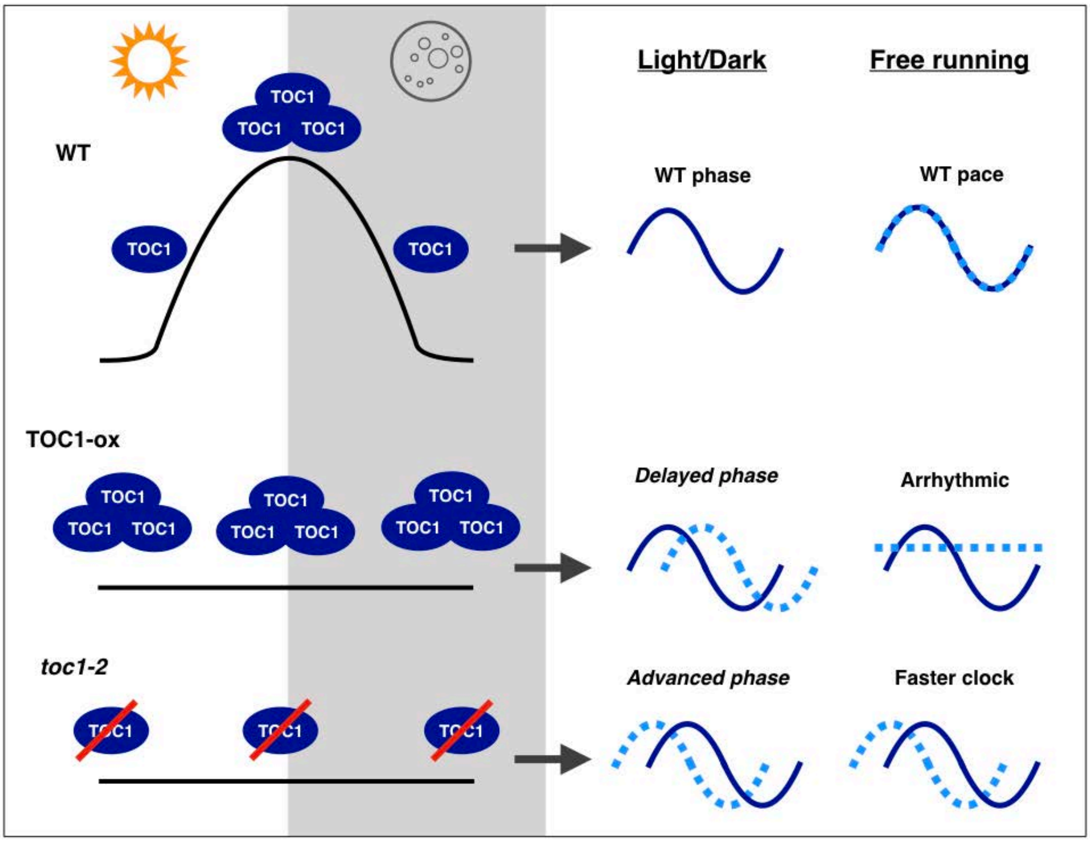

Figure 2. TOC1 accumulation alters the phase and the pace of the circadian clock. Diagrammatic scheme illustrating the effects of the different degree of TOC1 accumulation in the phase and the pace of the central oscillator. High levels of TOC1 lead to clocks with a delayed phase, while lower or non accumulation arises in clocks with an advanced phase. Under free running conditions (constant light) the circadian clock becomes arrhythmic in presence of high levels of TOC1 while it runs faster in absence of TOC1.

Research over the past years has aided on the identification of a myriad of additional clock components. For instance, the other members of the PRR family PRR3, PRR5, PRR7 and PRR9 were described as important clock-related components (Makino et al., 2001, Adams et al., 2015, Kamioka et al., 2016). The PRRs are sequentially expressed from close to dawn (PRR9 and PRR7) to midday (PRR5 and 3) and dusk (TOC1) (Matsushika et al., 2000). PRRs appear to repress the expression of *CCA1* and *LHY* during the day, shaping their oscillatory waveform that leads to their peak-expression at dawn (Nakamichi et al., 2010). Although the PRRs repress *CCA1* and *LHY* expression, phenotypic studies of plants miss-expressing one or more members of the family showed that they affect clock function differently. Mutation of *prr9* or *prr7* resulted in slightly long circadian periods (Farre et al., 2005) while *prr5* mutant plants displayed a short period phenotype (Fujiwara et al., 2008), following a similar trend but not as severe as the short period phenotype of *toc1* mutant plants (Strayer et al., 2000). The *prr7/prr9* double mutant showed stronger phenotypes than single loss-of-function mutants (Farre et al., 2005, Nakamichi et al., 2005) while the *prr5/prr7/prr9* triple mutants are arrhythmic under free-running conditions (Nakamichi et al., 2005). These results suggest a possible partially redundant function for some PRRs. The PRRs play important roles not only in the regulation of the central oscillator but also in their connection to inputs and outputs. Chromatin immunoprecipitation followed by massive parallel sequencing (ChIP-seq) experiments of TOC1 (Huang et al., 2012) and PRR5 (Nakamichi et al., 2012) provided a genome-wide view of the regulatory networks regulated by TOC1 and PRR5. The studies defined the function of TOC1 as a global repressor of oscillator expression (Huang et al., 2012) and established that PRR5 modulates the expression of key players involved in multiple clock output processes (Nakamichi et al., 2012).

Clock components expressed during the evening also include three other clock-related proteins that interact with each other to form the so-called EVENING COMPLEX (EC) (Nusinow et al., 2011, Herrero et al., 2012). The EC is composed of a single MYB-like GARP transcription factor known as LUX ARRHYTHMO or PHYTOCLOCK1 (LUX/PCL1) (Hazen et al., 2005, Onai and

Ishiura, 2005) and two plant-specific proteins without recognizable domains known as EARLY FLOWERING 3 (ELF3) (McWatters et al., 2000) and EARLY FLOWERING 4 (ELF4) (Doyle et al., 2002). Loss-of-function of any of the components of the EC results in arrhythmia (Helfer et al., 2011, Herrero et al., 2012). These results explain the tight transcriptional regulation of EC gene expression exerted by CCA1 and LHY in the morning (Portoles and Mas, 2010, Li et al., 2011, Lu et al., 2012) and TOC1 in the evening (Huang et al., 2012). The EC works as a nighttime transcriptional repressor and binds directly to the *PRR9* and *PRR7* promoters (Dixon et al., 2011, Helfer et al., 2011, Chow et al., 2012). Thus, *PRR9* and *PRR7* repression by the EC may indirectly promote *CCA1* expression at the end of the night. The EC also regulates *GIGANTEA* (*GI*), a plant-specific protein involved in the regulation of many processes including the circadian clock (Gould et al., 2006, Nagel et al., 2014).

The EC has been shown to connect the oscillator with various output pathways. For example, seedling hypocotyl elongation is coordinated through the direct repression of the bHLH transcription factor *PHYTOCHROME-INTERATING FACTOR* (*PIF4* and *PIF5*) by the EC (Thines and Harmon, 2010, Nusinow et al., 2011, Filo et al., 2015), which is required for hypocotyl elongation (Niwa et al., 2009). Recent studies have also shown that the EC and phytochrome B (PHYB) act in a temperature-dependent manner as regulators of key players involved in the control of diverse clock outputs such as photosynthesis, growth, hormone signaling and environmental responses (Ezer et al., 2017).

All these studies highlight the prevalence of repressor components within the *Arabidopsis* circadian system (Millar, 2016). However, a number of studies have also identified a number of key positive regulators. For instance, the rhythmic deposition of activating histone marks at the promoter of clock genes was identified as an important mechanism correlating with the activation of circadian gene expression (Perales and Mas, 2007). Other specific clock-related factors have been proposed to act as circadian activators. For instance, the LIGHT REGULATED WD 1 (LWD1) and LIGHT REGULATED WD 2 (LWD2) were found to bind to the promoters of *CCA1*, *PRR9*, *PRR5* and *TOC1* to activate their expression (Wang et al., 2011, Wu et al., 2016). Another example of clock-related activating component includes the CCA1 and LHY homolog known as REVEILLE 8 (RVE8 also known as LHY-CCA1-LIKE5 or LCL5). RVE8 belongs to the CCA1 and LHY single MYB protein family, presenting high sequence homology particularly in the MYB domain (Schmied and Merkle, 2005). Despite the sequence homology, RVE8 function in the clock is antagonistic to that of CCA1/LHY since RVE8 promotes the expression of *TOC1* and *PRR5* (as opposed to the repressing function exerted by CCA1/LHY) (Farinas and Mas, 2011, Rawat et al., 2011, Hsu et al., 2013). The RVE8-mediated activation correlates with increased accumulation of histone acetylation at the *TOC1* and *PRR5* promoters (Farinas and Mas, 2011). The activation also requires the function of the clock-related NIGHT LIGHT-INDUCIBLE AND CLOCK-REGULATED (LNK) factors, which interact with RVE8 and act as transcriptional co-activators of *TOC1* and *PRR5* expression (Xie et al., 2014). Two members of the LNK family, LNK1 and LNK2 have been shown to be responsible for promoting the expression of *TOC1*, *PRR5* and other evening-expressed circadian genes (Rugnone et al., 2013). Because of the absence of DNA binding domains, LNKs need to interact with MYB transcription factors in order to perform their role as activators (Xie et al., 2014, Perez-Garcia et al., 2015). Interaction with RVE8 and RVE4 is therefore necessary for the LNKs to be recruited to the *PRR5* and *TOC1* promoters (Xie et al., 2014, Perez-Garcia et al., 2015) (Figure 3).

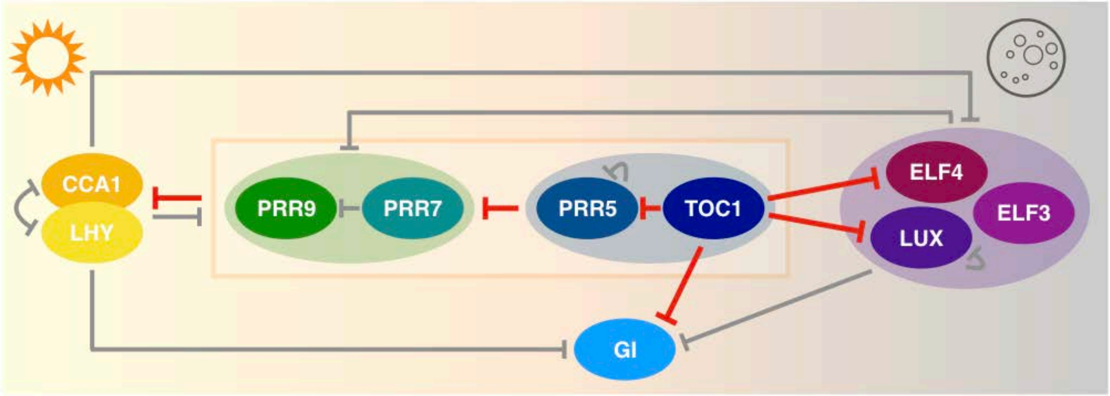

Figure 3. Role of TOC1 at the center of the *Arabidopsis* central oscillator. Scheme describing the main components of the transcriptional feedback loops in the *Arabidopsis* circadian clock, highlighting the role of TOC1 as a general repressor of the circadian transcriptional machinery. Lines ending with perpendicular dashes denote gene repression, the ones in red indicate the direct repressive role of TOC1 over other circadian clock components. (Please see section 2.1.1. for details). (Modified from Nohales and Kay, 2016).

2.1.1. Role of TOC1 at the center of the circadian clock molecular architecture

Proper expression and activity of TOC1 is essential for circadian function. Therefore, over the years, a number of studies have focused on the regulatory mechanisms responsible for ensuring proper rhythms of TOC1 gene and protein expression and activity. The mechanisms involve epigenetic, transcriptional, translational and post-translational regulation. In the following sections, some of the components and mechanisms involved in TOC1 regulation are briefly described. We also describe the function of TOC1 as a global repressor of oscillator gene expression.

2.1.1.1. Transcriptional regulation of TOC1

Under light:dark cycles, *TOC1* mRNA displays a robust rhythmic oscillation with a peak around dusk and a progressive transcript decline during the night. The diurnal oscillatory pattern of *TOC1* transcripts is maintained under constant free-running conditions (Matsushika et al., 2000, Strayer et al., 2000). The oscillation of *TOC1* is essential for its proper function at the core of the circadian clock. As mentioned above, TOC1 forms part of a complex transcriptional network within the *Arabidopsis* circadian clock. In this network, the morning expressed *MYB* transcription factors CCA1 and LHY repress the expression of *TOC1* during the day by direct binding to a motif known as Evening Element (EE) present in its promoter. Reduced accumulation of *TOC1* mRNA in plants over-expressing *CCA1* or *LHY* and their direct binding to the *TOC1* promoter supported the hypothesis of their repressive function.

As mentioned above, activation of *TOC1* transcriptional expression relies on the positive function of one of the members of the CCA1 and LHY single MYB protein family known as RVE8. This protein activates *TOC1* and *PRR5* through binding to their EE motif (Hsu et al., 2013). RVE8 directly interacts with LNKs and this interaction is important for their function as co-transcriptional activators of *TOC1* and *PRR5* (Xie et al., 2014, Perez-Garcia et al., 2015). RVE8 and LNKs activate transcriptional initiation and elongation of TOC1 and PRR5 expression by direct interaction with the transcriptional machinery and its recruitment to the *TOC1* and *PRR5* promoters (Ma et al., 2018). Notably, members of the PRR family, PRR9, PRR7, PRR5 and TOC1 are able to bind to the LNK's promoters to negatively regulate their expression from midday to the early evening. This regulatory network establishes a negative feedback loop, with LNKs as activators and PRRs as repressors (Nakamichi et al., 2012, Rugnone et al., 2013).

Regarding TOC1 function at the core of the clock, several studies have recently showed that in contrast to the initial idea of TOC1 being an activator of *CCA1* and *LHY* expression, TOC1 in fact acts as a repressor of these genes (Gendron et al., 2012, Huang et al., 2012, Pokhilko et al., 2012). Further studies shown that TOC1 is in fact a general repressor of nearly all of the circadian oscillator components (Huang et al., 2012). ChIP-Seq experiments revealed that TOC1 binds to G-box-related and EE motifs present in the oscillator gene promoters (Huang et al., 2012). These motifs were displayed in the promoters of morning-expressed core clock genes, including *CCA1*, *LHY*, *PRR9* and *PRR7* and also in the promoters of evening-expressed genes including, *GI*, *LUX*, *ELF4* and *TOC1* itself. Repression occurs through rhythmic binding of TOC1 to its target promoters with the highest enrichment observed just after dusk, when TOC1 protein accumulation reaches its peak (Huang et al., 2012). Additionally, the high and constant occupancy at the target promoters displayed in TOC1 over-expressing plants, as well as the decreased expression of core circadian genes in plants transiently over-expressing TOC1 confirmed the function of TOC1 as general repressor of the circadian clock, linking the evening and morning oscillator loops through its repressive function (Huang et al., 2012) (Figure 3).

2.1.1.2. Post-translational regulation of TOC1

TOC1 protein robustly cycles with increasing protein accumulation reaching a peak around dusk and following a progressive decline during the night. The rhythmic oscillatory pattern of TOC1 protein accumulation is also observed under free-running conditions (Mas et al., 2003b). This rhythmic pattern is controlled by direct and indirect regulatory mechanisms that shape the circadian waveform of TOC1 accumulation. On one hand, TOC1 protein stability is modulated by the dark-induced proteasome degradation mediated by the F-box protein ZETLUPE (ZTL) (Mas et al., 2003b). ZTL is member of the E3 ubiquitin ligase Skp-Cullin-F-box (SCF) complex, containing a blue-light-sensing light, oxygen and voltage (LOV) domain, and F-box domain and a Kelch repeat domain (Somers et al., 2000). In *Arabidopsis*, besides ZTL, two other proteins are part of the LOV domain protein family, FLAVIN-BINDING, KELCH REPEAT AND F-BOX 1 (FKF1) and LOV KELCH PROTEIN 2 (LKP2) (Nelson et al., 2000, Schultz et al., 2001). TOC1 interaction with ZTL is necessary for proper regulation of circadian period by the clock (Mas et al., 2003b). Hence, their interaction is tightly controlled through several mechanisms. For instance, the time-dependent and tissue-specific interaction of TOC1 and PRR3 prevents ZTL interaction with TOC1, and thus impeding TOC1 degradation (Para et al., 2007, Fujiwara et al., 2008). Also, TOC1 nuclear accumulation is enhanced by its interaction with PRR5, which prevents the cytoplasmic degradation of TOC1 by ZTL (Wang et al., 2010). In addition, ZTL stabilization by the blue-light-dependent interaction with GI enhances the stability and oscillation of TOC1 and PRR5 (Kim et al., 2007, Fujiwara et al., 2008), which in turn are also regulated through degradation by direct interaction with the two other ZTL homologs, FKF1 and LKP2 (Baudry et al., 2010, Wang et al., 2010).

Protein phosphorylation is also important in the regulation of several clock components. Specifically for TOC1 and PRR5, their increased phosphorylation leads to enhance binding to ZTL, therefore favoring their degradation (Fujiwara et al., 2008). On the other hand, phosphorylation of TOC1 and PRR3 is necessary for their interaction so that TOC1 protein stability is regulated by a complex phosphorylation-dependent mechanism (Fujiwara et al., 2008). The kinases responsible for the rhythmic phosphorylation of TOC1 and PRR5 remain unknown (Figure 4).

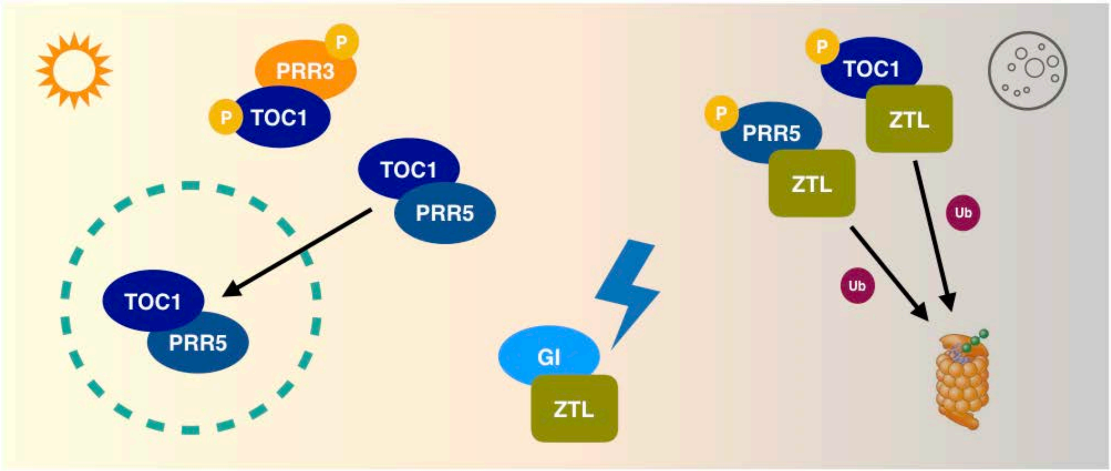

Figure 4. TOC1 post-translational regulation in the *Arabidopsis* central oscillator. Scheme describing the main components of the post-translational regulatory circuits in the *Arabidopsis* circadian clock involving TOC1. Arrows indicate the fate of clock proteins in the plant cell. P refers to phospho groups, Ub to ubiquitin and blue bolt to blue light sensing (Please see section 2.1.1.2. for details). (Modified from Nohales and Kay. 2016).

TOC1 protein also directly interacts with additional clock components. For instance, direct interaction of TOC1 with CCA1 HIKING EXPEDITION (CHE), a transcription factor of the TEOSINTE BRANCHED 1, CYCLOIDEA AND PROLIFERATING CELL FACTOR 1 & 2 (TCP) family, was proposed to be important for *CCA1* repression (Pruneda-Paz et al., 2009). Furthermore, TOC1 also interacts with the EC through direct association with ELF3. The EC can also interact with LWD1 through the presence of the photoreceptor PHYB (Huang et al., 2016). Although the functional relevance of these interactions remain to be fully explored, the results open the possibility of a direct link between light input and the central oscillator through protein-protein interactions (Huang et al., 2016).

In addition to clock components, recent studies have shown that TOC1 can also physically interact with the transcription factors PIF3 and PIF4 (Soy et al., 2016, Zhu et al., 2016, Martin et al., 2018). PIFs have been described as been involved in a myriad of developmental processes (Leivar and Quail, 2011), one of them being their collective activity to promote maximal hypocotyl elongation at dawn (Nozue et al., 2007). Even though PIF transcription is known to be circadianly regulated (Yamashino et al., 2003, Kidokoro et al., 2009), their interaction with TOC1 and other members of the PRR family has been recently shown to be important for the joint regulation of PIF activity by sequential modulation of common PRR-PIF target genes, which ultimately control proper hypocotyl growth (Martin et al., 2018). PIF interaction with TOC1 provides a mechanism for integrating circadian clock regulation to exogenous signal prediction in order to coordinate growth and development.

2.1.1.3. Epigenetic regulation of TOC1 rhythmic oscillation

Changes in chromatin architecture are directly linked to regulation of gene expression. Modifications of DNA and histones affect the degree of chromatin compaction and therefore modulates the accessibility of the transcriptional machinery and other regulators to chromatin (Li et al., 2007). Histones are modified at their N-terminal tails by a number of covalent modifications, including among others acetylation, methylation and ubiquitination. Histone hyper-acetylation has been proposed to open chromatin conformation, therefore facilitating transcriptional activation. Histone hypo-acetylation on the other hand correlates with transcriptional repression by chromatin compaction (Sequeira-Mendes et al., 2014).

Over the years, a number of regulatory activities have been identified at the *TOC1* promoter, including a complex array of clock transcription factors as well as chromatin-related activities. The first report correlating the rhythmic oscillation of *TOC1* gene expression with changes in chromatin conformation showed the circadian changes in histone H3 acetylation at the *TOC1* promoter (Perales and Mas, 2007). The study demonstrated that the mechanism behind *TOC1* repression by CCA1 might involve increased H3 deacetylation (Perales and Mas, 2007). Indeed, CCA1 over-expression favored a hypo-acetylated state of H3 at the *TOC1* promoter correlating with its transcriptional repression. Contrarily, RVE8, the MYB transcription factor with high sequence homology to CCA1 and LHY mentioned above, facilitated a hyper-acetylated state of H3 that correlated with increased *TOC1* transcriptional accumulation during its circadian raising phase (Perales and Mas, 2007, Farinas and Mas, 2011, Malapeira et al., 2012). Thus, and despite the sequence similarity, CCA1 and RVE8 play antagonistic functions in the epigenetic and transcriptional regulation of *TOC1* expression (Farinas and Mas, 2011).

The rhythmic oscillation of H3 acetylation and deacetylation as well as other chromatin modifications are not exclusive to the *TOC1* locus, as they were also described at the promoters of other oscillator genes such as *CCA1*, *LHY*, *PRR9*, *PRR7*, *GI* and *LUX*, thus suggesting a coupling between histone modifications and the generation of rhythms at the core of the circadian clock oscillator (Ni et al., 2009, Malapeira et al., 2012, Song and Noh, 2012). Spatio-temporal studies of chromatin transitions at the loci of core circadian genes showed that the accurate timing and combinatorial accumulation of H3 acetylation and H3K4 trimethylation (H3K4me3) at the 5' end of the genes are essential for their proper transcriptional regulation. Interestingly, these two histone marks oscillated with different phases, thus suggesting a degree of specificity in their activating roles within the core circadian genes. Additionally, low H3K4me3 levels were shown to correlate with increased clock repressor binding, therefore indicating a role of this histone mark in the proper control of the activation to repression transition (Malapeira et al., 2012). It is noteworthy that the coupling of circadian clock gene activation with changes in H3 acetylation and H3K4me3 is a common chromatin-dependent activation mechanism shared by the plant and mammalian circadian systems.

2.2. Input pathways: synchronization of the circadian clock

The predictable diurnal changes in environmental signals synchronize the circadian rhythms in resonance with the day and night cycles. Two of the main synchronizers of the plant circadian clock are light and temperature. Light plays a major role setting the pace of the clock. Light intensity and quality can affect gene transcription (Lu et al., 2009, Rugnone et al., 2013), mRNA stability (Yakir et al., 2007), translation (Kim et al., 2003) and protein stability (Mas et al., 2003b, Kim et al., 2007, Yu et al., 2008). However, how this information is transmitted to and incorporated by the central oscillator is not fully understood. Clock synchronization was proposed to occur by the alteration of core clock gene expression and protein activity. These changes are ultimately translated into variations in amplitude, period and phase of the rhythms. In this way, the endogenous internal period of the clock is daily adjusted every day to the external environmental time.

Given the importance of light as a clock synchronizer and resetting signal, its perception and signaling are in turn regulated by the clock. Photoreceptors are circadianly regulated (Fankhauser and Staiger, 2002), and several other clock and light-signaling components are also involved in modulating light sensitivity to the clock (Li et al., 2011, Wenden et al., 2011). In *Arabidopsis*, red and far-red light are sensed by the members of the phytochrome photoreceptor family (PHYA to PHYE) (Sharrock and Quail, 1989, Clack et al., 1994, Rockwell et al., 2006). Cryptochromes (CRY1, 2 and 3) are responsible for the UV-A/blue light perception (Ahmad and Cashmore, 1993, Lin et al., 1996) together with phototropins (PHOT1 and PHOT2) (Huala et al., 1997, Kagawa et al., 2001), members of the ZTL family (Nelson et al., 2000, Somers et al., 2000, Schultz et al., 2001) and UV-B RESISTANCE 8 (UVR8) as the UV-B light photoreceptor (Rizzini et al., 2011).

The role of some of these photoreceptors in the light input to the clock has been identified. For instance, the blue-light photoreceptor ZTL is involved in clock protein stability and the mechanistic behind this regulation has been well described (see section 2.1.1.2.). Indeed, as mentioned above, the TOC1-ZTL interaction is important for regulation of TOC1 protein stability and proper control of circadian period by the clock (Mas et al., 2003b). Phytochromes, cryptochromes and UVR8 photoreceptors are also involved in clock synchronization but the mechanisms behind their function are less well known. Phytochromes are necessary for sustaining proper circadian period (Devlin and Kay, 2000). Analyses of phytochrome-null-mutants showed that low and high light fluence rates affect period length in opposite ways. This suggests a possible antagonistic role of the inactive and light-activated forms of phytochromes in the determination of the clock's pace (Hu et al., 2013). PHYB signaling is required in the nucleus in order to sustain rhythmicity in response to red light (Jones et al., 2015). PHYB can also bind directly to multiple clock proteins in a light-dependent manner (Yeom et al., 2014). For instance, PHYB interacts with ELF3 and the photomorphogenesis repressor CONSTITUTIVE PHOTOMORPHOGENIC 1 (COP1). The functional interaction is important in the control of the photoperiodic regulation of flowering time through the destabilization of GI cyclic accumulation. The complex thus allows temporal information of seasonal changes to be transferred from photoreceptors to the circadian clock in order to allow the resetting and permit the transition to flowering (Liu et al., 2001, Yu et al., 2008). Moreover, affinity purification and mass spectrometry studies have shown that in addition to this interaction, PHYB also plays a role in mediating ELF3's interaction with several other components of different process (Huang et al., 2016).

The convergence of light signaling and circadian rhythmicity is well exemplified in many clock components. For instance, the transcriptional regulation of *ELF4* requires the coordination of both light and the clock for its proper rhythmic expression (Li et al., 2011). Three positive regulators of PHYA signaling, ELONGATED HYPOCOTYL 5 (HY5), FAR RED IMPAIRED RESPONSE 1 (FAR1) and FAR RED ELONGATED HYPOCOTYL 3 (FHY3) bind directly to the *ELF4* promoter to progressively promote its expression during the day (Li et al., 2011). *ELF4* activation is inhibited at dawn by the repressive action of the core clock components CCA1 and LHY (Li et al., 2011).

In addition to light, the circadian clock can also be entrained by temperature. The transcription of several clock genes is sensitive to temperature. The temperature-dependent regulation of PRR7 and PRR9 play an important role in temperature responsiveness (Salome and McClung, 2005). Repression of *PRR7* by direct binding of HEAT SHOCK TRANSCRIPTION FACTOR B2B (HSFB2B) has been proposed to be involved in temperature resetting (Kolmos et al., 2014). On the other hand, low temperature entrainment has been shown to act through the transcriptional regulation of *LUX* by the cold-induced transcription factor C-REPEATED/DRE BINDING FACTOR 1 (CBF1) (Chow et al., 2014). It is noteworthy that *HSFB2B* and *CBF1* are both regulated by the circadian clock. These results open up the possibility of the clock gating its own sensitivity to external environmental cues.

Besides transcriptional regulation, temperature variations have been found to influence clock gene expression through alternative splicing. Various clock genes undergo alternative splicing, including *CCA1*, *LHY*, *RVE8*, *PRR7*, *PRR9*, *TOC1*, *ELF3* and *GI* (James et al., 2012, Wang et al., 2012, Kwon et al., 2014). Even though other processes have been reported to influence alternative splicing of clock genes (Kwon et al., 2014, Mancini et al., 2016), the abundance of various splicing variants seems to be regulated overall by temperature (James et al., 2012, Seo et al., 2012).

In spite of its ability to reset and entrain every day the clock, changes in temperature can be also buffered by the clock in order to maintain a relatively constant pace (Gould et al., 2006). This property, known as temperature compensation, is intrinsic to circadian oscillators and ensures the accuracy of the clock regardless the temperature changes within a physiological range. PRR9, PRR7, CCA1, LHY and GI have been described as important players in this mechanism. PRR7 and PRR9 are necessary for temperature entrainment of the *Arabidopsis* clock as double mutant *prr7-3/prr9-1* plants are not able to properly respond and entrain to variations in temperature (Salome and McClung, 2005). Further analyses showed that the inability of *prr7-3/prr9-1* to maintain proper circadian rhythmicity in response to changes in temperature is due to the increased activation of *CCA1* and *LHY*. Indeed, PRR7 and PRR9 are in charge of repressing *CCA1* and *LHY* expression during the early morning (Nakamichi et al., 2010). Induced down-regulation of these morning-expressed genes in the *prr7/prr9* double mutant rescued the long period phenotype and abolished the over-compensation defects observed at high temperatures (Salome et al., 2010). Moreover, proper *GI* expression is needed to extend the range of temperatures at which robust and accurate circadian rhythmicity can be maintained. This is achieved by GI-mediated regulation of *CCA1* and *LHY* expression in a temperature-dependent manner (Salome and McClung, 2005, Gould et al., 2006). Other studies have shown that the molecular mechanism underlying temperature compensation might rely on the balance between two antagonistic activities: phosphorylation by the protein kinase CK2 (CASEIN KINASE 2) and the transcriptional activity of *CCA1*. Both activities are antagonistic but they are similarly regulated by high temperature. As CCA1 function is essential for maintaining the period of the clock, its regulation by CK2 provides an accurate means for avoiding that the clock runs faster at high temperatures (Portoles and Mas, 2010).

Besides light and temperature, other external stimuli can play a role on clock synchronization. For instance, *PRR7* is transcriptionally repressed by photosynthetically-derived sugars (Haydon et al., 2013). *PRR7* repression results in an early activation of *CCA1* (at the so-called metabolic dawn), thus contributing to the gated entrainment of the *Arabidopsis* circadian oscillator (Haydon et al., 2013).

2.3. Output pathways: biological processes under circadian control

As mentioned in section 1, the circadian clock controls the rhythmic oscillation of a myriad of processes that are essential for plants. Some of these processes include among others, photoperiodic flowering, metabolism, hormone signaling, responses to biotic and abiotic stresses and growth responses. In the following sections, we briefly describe some studies reporting the connection of the circadian clock with hypocotyl elongation and leaf growth, as these processes are directly related to the results described in this Thesis.

2.3.1. Circadian regulation of hypocotyl elongation

Hypocotyls in dicotyledonous plants are stems that connect the leaves or cotyledons with the seedling root. After seed germination and radical emergence, hypocotyls rapidly elongate in a process that is controlled by a vast number of external and internal cues (Vandenbussche et al., 2005). Due to their plasticity and morphological simplicity, hypocotyls have become a recurrent model in the study of various processes controlling their growth and cell expansion.

Light, gravity, temperature, hormone and the circadian clock directly influence hypocotyl growth (Vandenbussche et al., 2005). Hypocotyls follow a phototropic growth response after germination by bending and growing toward light. This process is characterized by an uneven elongation of their cells (Gendreau et al., 1997). Seedling growth under dark conditions or skotomorphogenesis renders highly elongated hypocotyls due to a rapid response of plants germinating under the soil (Gendreau et al., 1997). The induction of the photomorphogenic program by light relies on the action of a vast array of photoreceptors including PHYs, CRYs and PHOTs (Kami et al., 2010). Consistent with their role, loss-of-function mutants of the photoreceptors showed long hypocotyl phenotypes under different quality and intensity of light.

The mechanisms governing hypocotyl elongation are different in seedling grown in the presence or absence of light. Under constant darkness cells at the base of the hypocotyl are the first ones to elongate, followed by those in the middle and finally the ones close to the apex. Under constant light conditions, hypocotyl elongation is very much reduced and only a slight expansion is observed in epidermal cells. Additionally, DNA content analysis of hypocotyl cells showed that seedlings grown under dark conditions showed an extra round of endoreplication (please see section 3) compared to seedlings grown under light (Gendreau et al., 1997).

The circadian clock plays an essential role in the regulation of hypocotyl elongation. Although growth under constant darkness is arrhythmic (Nozue et al., 2007), under constant light conditions, hypocotyl growth follows a circadian pattern, with fastest growth around the subjective dusk (subjective is the name assigned to the day and night cycle under constant, free-running conditions). The rhythmic elongation is affected in several clock mutants leading to long or short hypocotyl length phenotypes depending on the light conditions and the genotypes. These results clearly show a direct connection of the circadian clock regulating hypocotyl growth. Notably, under light/dark cycles the peak of hypocotyl rhythmic growth is shifted 12h compared to free-running conditions (Dowson-Day and Millar, 1999, Nozue et al., 2007). The molecular mechanism behind this regulation relies on the light and clock regulation of two bHLH (basic Helix-Loop-Helix) transcription factors, PIF4 and PIF5, whose activity directly correlates with growth (Nozue et al., 2007). Under light-dark cycles, the expression patterns of these positive regulators of hypocotyl growth correlate with the end of night phase of elongation. During the day, PIF4 and PIF5 protein abundance is negatively regulated by light, whereas the clock in turn represses their transcript accumulation during the early night. At the end of the night, the clock repression on *PIF4* and *PIF5* transcripts is relieved, enabling protein accumulation and function. The coincidence of high transcripts and protein accumulation at the end of the night, allows PIF4 and PIF5 to promote hypocotyl growth. Additionally, the circadian regulation of *PIF4* and *PIF5* relies on their early evening repression by the EC (Nusinow et al., 2011). The activity of PIF4 is inhibited through the direct interaction with ELF3 (Nieto et al., 2015) during the early night (Nozue et al., 2007).

Plants miss-expressing TOC1 display significant hypocotyl phenotypes. The circadian oscillation of *TOC1* is antiphasic with the transcriptional activation of PIF3, specifically under Short-Day conditions. In fact, and as mentioned above, TOC1 directly interacts with PIF3 after dusk and repress its transcriptional activity. The decreasing accumulation of TOC1 from the middle of the night relieves the repression on PIF3 and thereby, aiding in the control of PIF-related growth just before dawn (Soy et al., 2016). Similarly to what it was proposed for flowering time, hypocotyl elongation might be controlled by an external coincidence model by which hypocotyl growth relies on the coincidence of a particular phase of the external light-dark cycle with the oscillatory phase of a molecular component essential for growth (Niwa et al., 2009).

2.3.2. Circadian regulation of leaf growth

Leaf growth is regulated by many exogenous (e.g. temperature, light, water and carbon availability) and endogenous factors (e.g. developmental stages, cell cycle). The interaction among these factors and pathways ultimately determines optimal leaf growth. Notably, leaf expansion in vascular plants present a rhythmic diurnal growth and in some cases, this is maintained under constant light and temperature conditions (Walter et al., 2009). Despite its relevance, little is known about the spatiotemporal mechanisms underlying circadian control of rhythmic leaf growth (Walter et al., 2009).

Studies using the model plant *Arabidopsis* revealed that during early stages, the rhythmic growth oscillated with a 24-hour period, with maximum growth during the day and with a trough at night (Poire et al., 2010). Interestingly, the maximum rate of leaf growth shifted towards the night, with low growth rates during the day at later stages of development (Poire et al., 2010). This occurred progressively over time and has been described as the result of the shift from metabolic growth control during the day at early stages to hydraulic growth control during the night at older stages of development. The maximum growth rate shift has been proposed to be a response to the transition of leaf growth limitation from carbon to water (Pantin et al., 2011).

With the aim of elucidating the molecular mechanisms by which the circadian clock may regulate growth during leaf development, recent studies have showed the importance of the clock component ELF3 in the maintenance of rhythmic leaf growth (Dornbusch et al., 2014). In *Arabidopsis*, leaf growth preceded upward leaf movement (hyponasty) by several hours, and both of these processes displayed circadian oscillations. ELF3 is required for the proper phasing between elongation growth in leaves and upward leaf movement. Consistent with this notion, leaf growth in early developing leaves of *elf3* mutants showed that the peak of maximum growth rate moved towards the end of the night while the wild-type maximum growth peaked during the day (Dornbusch et al., 2014). Furthermore, similar to hypocotyl growth, leaf growth also relies on the interplay between light and the circadian clock. However, the molecular mechanisms underlying these regulations seemed to differ. Indeed, analysis of leaf growth in the *pif4*/*pif5* mutant revealed that PIF4 and PIF5 are not essential for sustaining rhythmic leaf growth although they influence its amplitude (Dornbusch et al., 2014). Overall, these results highlight the importance of light and the circadian clock shaping the rhythms of growth in young leaves.

3. The cell cycle in plants

Plant growth and development also rely on a flexible and highly controlled balance between cell division and cell expansion, which are controlled by the different variants of the cell cycle. Studies carried on *Arabidopsis* have contributed to our understanding of how these processes control growth and development. The results described in this Doctoral Thesis link the circadian clock function with plant growth through the regulation of cell cycle progression. Therefore, in the next sections, we briefly described the role of the cell cycle controlling leaf development. We also describe the cell cycle machinery, including the mitotic cycle and the endocycle. The section ends with a brief description of the S-phase and the role of CDC6 (CELL DIVISION CONTROL 6) within the cell cycle.

3.1. Role of the cell cycle controlling leaf growth

Post-embryonic plant development relies primarily on the ability to produce leaves, which are the plant's main photosynthetic organs (Barber, 2009, Zhu et al., 2010). In eudicots, leaves are initiated at the flank of the shoot apical meristem (SAM) in a zone known as primordium (Efroni et al., 2010, Traas and Moneger, 2010). Initially, growth is sustained by cell division (mitotic cycle) throughout the entire primordium generating new cells of relative constant and small size in what is known as proliferation. Later in development, and once proliferation has stopped, cells increase their size rapidly, mainly by cell expansion (Donnelly et al., 1999, De Veylder et al., 2001, Breuninger and Lenhard, 2010). This occurs by cell wall loosening, which allows cell growth (Cosgrove, 2005). Interestingly, inhibition of cell proliferation is very often compensated by an enhancement of cell expansion, and an increase in cell proliferation can be balanced by decreased cell expansion, so that the effects on the whole size are often diminished (De Veylder et al., 2001, Tsukaya, 2002, Beemster et al., 2003, Tsukaya, 2003) (Figure 5). The duration of proliferation and expansion as well as the appropriate timing for the transition remain key processes in the determination of the final organ and therefore plant size

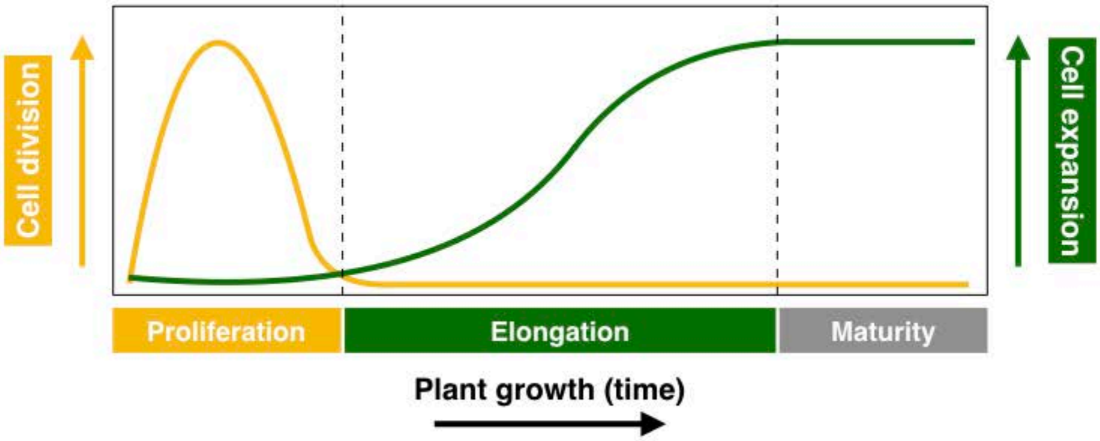

Figure 5. Kinematics parameters of leaf growth during development. Diagrammatic scheme illustrating the phases of leaf growth during time. On the left axis and in yellow the curve depicts the timing of cell division during the phase of proliferation (yellow box). On the right axis and in green the curve depicts the timing of cell elongation during the phase of expansion (green box). The box in gray indicates the maturity phase in which cells have stopped proliferating and elongating (Modified from Fiorani and Beemster 2006).

As for hypocotyls, leaf cell expansion is often associated with endoreplication, a variant of the cell cycle in which successive rounds of DNA replication occurs without further division (Beemster et al., 2005) (please see section 3.3). During the transition from proliferation to expansion cells stop dividing gradually from the tip to the base of the leaf as they exit the mitotic cycle. Meanwhile, they start to expand in the same direction (Donnelly et al., 1999, Nath et al., 2003). Thus, at the cellular level, cell division and cell expansion are essential for the final leaf size. Leaf development is extremely plastic and besides the balance between cell growth and division rates, final leaf size depends on genetic predisposition, leaf position, and environmental conditions (Andriankaja et al., 2012).

Because of the importance of the mitotic cycle as basis for growth by proliferation and the endocycle as indicator of growth by cell expansion, the plant cell cycle has been studied for a number of years in plants. Studies carried on the model plant *Arabidopsis*, revealed that many of the cell-cycle-related genes share similarities with their homologues in yeast and animals, while most of them are encoded by multiple loci. Key elements and pathways have been discovered and new players are being identified and characterized.

3.2. The plant mitotic cycle

As in other eukaryotes, the plant mitotic cycle consists of four consecutive phases: the Gap 1 phase (G1-phase), the DNA synthesis (S-phase), the Gap 2 phase (G2-phase) and mitosis (M-phase). A highly conserved basic molecular control of the mitotic cycle progression relies on the oscillatory activation/ deactivation of CYCLIN-DEPENDENT KINASES (CDKs) (Francis, 2007). The interaction of these kinases with the key cell cycle components cyclins (CYCs) triggers the transition from G1 to S-phase (G1/S) and from G2 to M-phase (G2/ M) (Figure 6).

The oscillatory pattern of CDK phosphorylating activity specifically at the G1/S and G2/M transitions ensure the unidirectional progression of the cell cycle. Their function is particularly relevant at the onset of DNA replication (S-phase) and mitosis (M-phase). CDKs are regulated at multiple levels, including transcriptional control, protein-protein interactions, post-translational modifications and degradation (Inagaki and Umeda, 2011). In *Arabidopsis,* eight classes of CDKs have been identified (A-type to G-type and CDK-like kinases, CDKLs). Only the A-type (CDKA) and B-type (CDKB) CDKs have been clearly shown to be directly involved in the control of the cell cycle progression (Vandepoele et al., 2002, Menges et al., 2005, Dudits et al., 2007, Andersen et al., 2008).

CDK activity relies on the timely regulated direct interaction with CYCs, which provide substrate specificity. CYCs display phase-specific patterns of expression along the cell cycle, thus defining the timing of the CDK-CYC protein complex activity (Inagaki and Umeda, 2011). Although a large number of cyclin-related proteins have been found in *Arabidopsis*, only 32 have been proposed to play a role in cell cycle regulation (Menges et al., 2005). Broadly speaking, A-type cyclins (CYCAs) control S- to M-phase progression, B-type cyclins (CYCBs) control the G2/M transition and M-phase progression, while D-type cyclins (CYCDs) control the G1/S transition (Inze and De Veylder, 2006). CYCDs are also involved in the regulation of cell proliferation in response to endogenous and exogenous stimuli like hormone signaling and nutrient availability that are sensed during G1 (Riou-Khamlichi et al., 2000, Menges et al., 2006, Dewitte et al., 2007).

CDKs are controlled not only by cyclins as activators but also by a wide array of inhibitors that directly bind to CDKs to negatively regulate their activity (Morgan, 1997, Nakayama and Nakayama, 1998). Two classes of main CDK inhibitors have been described in plants. The first class, the so-called Kip-related proteins (KRP) or CDK inhibitors (CKI) includes a family of small proteins with a specific C-terminal domain (CTD) that is necessary for inhibition of CDK activity (De Veylder et al., 2001, De Clercq and Inze, 2006). In *Arabidopsis,* the KRP family is composed of seven members, ICK1/KRP1, ICK2/KRP2 and KRP3 to KRP7 (De Veylder et al., 2001). Over-expression of some of these members result in strong inhibition of the overall organ growth and morphology, suggesting a role for these proteins in repressing the progression of the mitotic cycle (Wang et al., 2000, De Veylder et al., 2001, Zhou et al., 2003). Supporting this idea, yeast two-hybrid analyses showed that all KRPs except KRP5 are able to bind to CDKA;1 (De Veylder et al., 2001) and inhibit the activity of the CYCD-CDKA protein complex. Furthermore, all KRPs interact with at least one member of the CYCD sub-families (Wang et al., 1998, Zhou et al., 2003).

The second class of CDK inhibitors is composed of the plant-specific proteins SIAMESE (SIM) and SIM-related (SMR) (Churchman et al., 2006). The proteins show sequence similarities with KRPs in their C-terminal cyclin-binding domain (Churchman et al., 2006, Peres et al., 2007). SIM was shown to repress the mitotic cycle in endoreplicating trichomes (Walker et al., 2000) and was suggested to function as a repressor of the G2/M transition, promoting endoreplication by inhibiting CDK activity (Churchman et al., 2006). The expression of other *SMR* genes is regulated in response to external stress conditions (Peres et al., 2007, Yi et al., 2014), suggesting that these SMRs might be important for adapting the cell cycle progression in response to external stimuli.

The activity of CDK-CYC complexes is also regulated through various post-translational modification events. Among them, the timely controlled ubiquitin-mediated protein degradation is one of the key mechanisms assuring the unidirectional progression of the cell cycle (Frescas and Pagano, 2008, Pesin and Orr-Weaver, 2008, Marrocco et al., 2010). Positive and negative cell cycle regulators are degraded in a cell cycle phase-dependent manner and in response to endogenous and exogenous stimuli (Marrocco et al., 2010). In all cases, ubiquitin E3 ligases mark target proteins for their selective proteolysis by the 26S proteasome. Poly-ubiquitinylation by specific E3 ligases is the main pathway by which cell cycle proteins are degraded (Pickart, 2001). The Anaphase-promoting complex/cyclosome (APC/C) and Skp1/Cullin/F-box (SCF) are the major E3 ubiquitin ligases involved in cell cycle control (Vodermaier, 2004). The SCF E3 ligase is mainly involved in the regulation of the G1/S transition while the APC/C E3 ligase is mostly implicated in the mid-M-phase to end of the G1 progression during the mitotic cycle (Komaki and Sugimoto, 2012). Although the APC/C complex was initially described as having a function restricted to the mitotic cycle, recent evidence suggests that the APC/C complex is not only relevant during the mitotic cycle but it is also involved in post-mitotic cell differentiation, as the different subunits of the complex are clearly expressed in mature leaves (Marrocco et al., 2009).

Another important mechanism of cell cycle control, in particular for the G1/S transition, is the E2F-RBR (E2 promoter-binding factor - Retinoblastoma-related) pathway. E2Fs are transcription factors necessary for the transcriptional activation of genes required in the cell cycle progression and DNA replication (Dyson, 1998, van den Heuvel and Dyson, 2008). E2F target genes are involved in the initiation and progression of DNA replication, DNA repair, and chromatin regulation (Ramirez-Parra et al., 2003, Vandepoele et al., 2005, Takahashi et al., 2008, Takahashi et al., 2010). E2F form heterodimers with dimerization partner (DP) proteins in order to bind to the E2F-binding sites present on the promoters of their target genes (Ramirez-Parra et al., 2003). Three typical E2F proteins (E2Fa, E2Fb and E2Fc) and two DP proteins (DPa and DPb) have been identified in *Arabidopsis*. E2Fa and E2Fb dimerize with

DPa and function as transcriptional activators (De Veylder et al., 2002, Rossignol et al., 2002, Magyar et al., 2005, Sozzani et al., 2006) while E2Fc dimerizes with DPb and acts as a transcriptional repressor (del Pozo et al., 2002, del Pozo et al., 2006). The regulation of the E2F-DP complex activity is mediated by its interactions with the negative regulator RBR (Retinoblastoma-related protein). Hypo-phosphorylation of RBR due to low activity of the CDK-CYC complex allows RBR interaction with the E2F-DP heterodimer, and thus impeding them from binding to their targets. On the other hand, CDK-mediated phosphorylation of RBR during the G1-phase releases a functional E2F-DP heterodimer that will be able to activate the key genes essential for driving the G1/S transition and S-phase progression (Dyson, 1998, Shen, 2002, Attwooll et al., 2004).

In addition to typical E2F proteins, plants also display atypical E2Fs (Lammens et al., 2009). In *Arabidopsis*, three atypical E2F factors have been identified (E2Fd/DEL2, E2Fe/DEL1 and E2Ff/DEL3, DEL stands for DP-E2F-like) (Vandepoele et al., 2002). They can bind directly to DNA without heterodimerizing with DP proteins (Kosugi and Ohashi, 2002, Mariconti et al., 2002, Lammens et al., 2009). The absence of a Rb-binding domain suggests that they are not regulated by RBR (Lammens et al., 2009). However, they can compete with typical E2Fs to transcriptionally repress their targets (Kosugi and Ohashi, 2002, Mariconti et al., 2002). E2Fe/DEL1 has been shown to inhibit endoreplication in proliferating cells through the repression of the endocycle positive regulator CELL CYCLE SWITCH PROTEIN 52 A2 (CCS52A2), which is an activator subunit of the APC/C complex (Vlieghe et al., 2005, Lammens et al., 2008). Although E2Fd/DEL2 has been shown to affect several cell cycle regulators, thus far no direct targets have been identified (Sozzani et al., 2010).

3.3. The plant endocycle

The endocycle is a cell cycle variant of the mitotic cycle in which cells duplicate their nuclear DNA content without further division in a process known as endoreplication. This results in cells with multiple copies of their DNA, which are referred as polyploids. Endoreplication is often associated will cell expansion and differentiation, therefore the switch from a mitotic cycle to an endocycle tends to correlate with the passage from cell proliferation to cell differentiation (Inagaki and Umeda, 2011, Edgar et al., 2014). Endocycles share much of the molecular machinery from the G1/S transition and S-phase progression of mitotic cycles. The main difference with the mitotic cycle resides on the lack of chromosome segregation and division. In this section, we provide a brief overview on the molecular machinery governing the onset and progression of the endocycle (Figure 6).

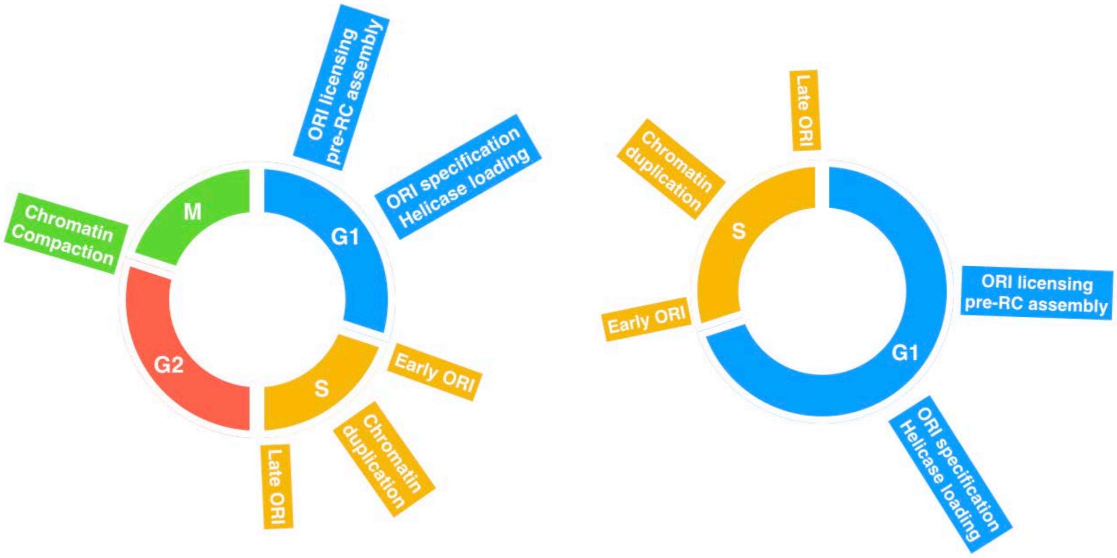
ORI licensing
pre-RC assembly
ORI specification
Helicase loading
Chromatin
Compaction
M
G1
G2
S
Early ORI
Chromatin
duplication
Late ORI
Chromatin
duplication
Late ORI
S
ORI licensing
pre-RC assembly
Early ORI
G1
ORI specification
Helicase loading

Figure 6. Highlight of the events linked to DNA replication during cell cycle progression. This simplified depiction of the mitotic cycle (left) and the endocycle (right) show the main events related to DNA replication. These are mainly situated during the G1-phase (DNA licensing and ORI specification) and the S-phase (chromatin duplication) when replication actually takes place. The general molecular mechanism behind DNA replication are the same for both variants of the plant cell cycle (Modified from Gutierrez 2016).

As mentioned above, CDKs are the main regulators of cell cycle progression. They can be classified according to their phase-specific role as mitotic CDKs (M-CDK), in charge of safeguarding the G2/M transition, and S-phase CDKs (S-CDK), in charge of securing the G1/S transition and progression. Cells undergoing endoreplication need to overcome the events linked to mitosis, without blocking DNA replication, by inhibiting M-CDKs and promoting S-CDKs activity. It was proposed that a higher threshold of CDK activity seems to be required for progression into mitosis rather than reentry into S-phase (Stern and Nurse, 1996). Endocycling cells maintain oscillatory patterns of S-CDK activity in order to allow the transition from G1 to S-phase. During the G1, low levels of CDK activity enable the assembly of the pre-RC (pre Replication Complex) at origins of replication, which will serve as DNA replication starting points. Previous studies on different eukaryotes models have described the CDK-dependent mechanisms by which M-CDKs suppress the assembly of the pre-RC during the mitotic cycle which involve mainly targeted protein phosphorylation (Remus and Diffley, 2009). However how S-CDKs accomplish this same function in endoreplicating cells is still not clear (Edgar et al., 2014).

In plants, CDKA acts as both M-CDK and S-CDK while CDKBs only as M-CDK (Boudolf et al., 2004, Nowack et al., 2012). Down-regulation of their activity can be achieved by transcriptional repression of *CYCs*. For example, repression of *CYCAs* expression suppresses M-CDKs activity leading to increase endoreplication, while over-activation of the same family of CYCs reduces endoreplication (Imai et al., 2006). Likewise, over-expression of *CYCBs* can inhibit endoreplication onset (Schnittger et al., 2002, Qi and John, 2007, Boudolf et al., 2009). Repression of M-CDK activity in order to progress into the endocycle can be also regulated by CYC protein degradation through the APC/C E3 ligase pathway. Three genes encoding for co-activator subunits of the APC/C complex have been described in plants. These are CDH1-type proteins and are known as CELL CYCLE SWITCH 52 (CCS52) or FZR90 (CCS52A1, CCS52A2 and CCS52B). All of them have been shown to promote the onset of endoreplication although it is not clear if they contribute to the progression of the endocycle itself (Tarayre et al., 2004, Larson-Rabin et al., 2009, Vanstraelen et al., 2009, Kasili et al., 2010, Roodbarkelari et al., 2010, Takahashi et al., 2013).

Besides the mechanisms involving proteolysis of CYCs, the onset and progression into the endocycle can also be achieved by down-regulation of CDK activity through the action of CDK inhibitors as KRPs. Some members of the KRP family have been shown to be involved in the transition and progression of G1/S-phase by inhibiting S-CDK activity, while others as SIM have been described as inhibiting both classes of CDKs activity throughout the cell cycle (Churchman et al., 2006, Haga et al., 2011). Interestingly, KRPs can be degraded by the SCF E3 ubiquitin ligase (Kim et al., 2008, Gusti et al., 2009, Roodbarkelari et al., 2010, Zhao et al., 2012), and in turn, the SCF substrate-specificity is conferred by CDK-dependent phosphorylation. Thus, this regulatory network suggests the possible existence of a two-oscillator model in which both components will negatively regulate each other. This mechanism could explain the inhibition of endoreplication by high levels of KRP activity (Weinl et al., 2005, Roodbarkelari et al., 2010, De Veylder et al., 2011). Despite the interest of this hypothesis, the full mechanistic details behind KRP oscillation still need to be identified.

Transcriptional regulation through the E2F-RBR pathway has also been shown to play an important role in the switch from mitotic cycle to endocycle. High levels of E2F-DP transcriptional activator complexes promote endoreplication (De Veylder et al., 2002, Rossignol et al., 2002, Magyar et al., 2005) while low levels of E2F transcriptional repressors (e.g. E2Fc) inhibit it (del Pozo et al., 2002, del Pozo et al., 2006). Atypical E2Fs can also influence the onset of endoreplication. For instance, E2Fe/DEL1 represses the expression of *CCS52A2* by direct binding to its promoter. Miss-regulation of E2Fe/DEL1 will therefore change the timing of *CCS52A2* transcription and disrupt the entry into endocycle (Lammens et al., 2008). Overall, the different studies point to a core mechanism based on the anti-phasic oscillatory pattern of CDK activity and CDK inhibitors. This can be achieved by transcriptional regulation, protein-protein interaction and targeted proteolysis.

3.4. Importance of G1/S phase transition during the plant cell cycle

Before entering the S-phase, cells need to get ready in order to meet the requirements necessary to assure the proper progression of DNA replication. The G1-phase serves to prepare the nuclei for entry into S-phase and acts as the main integrator between environmental signals and cell cycle activation and progression (Inze and De Veylder, 2006). External stimuli are determined by a wide range of signals that can be grouped into the ones promoting the G1/S transition and therefore entry into mitosis and the ones inducting arrest at the G1/S checkpoint. Plant hormones: auxin, cytokinins and brassinosteroids as well as sucrose act as growth promoting factors by inducing the expression of CDKA and CYCD and therefore the formation of the CDKA-CYCD complex that is responsible for the G1/S transition (Sauter et al., 1995, Riou-Khamlichi et al., 1999, Hu et al., 2000, Riou-Khamlichi et al., 2000, Richard et al., 2002). On the other hand, the hormone ABA (Abscisic acid) and exposure to cold inactivate the CDKA-CYCD complex through induction of KRPs expression, resulting in an arrest and accumulation of cells at G1 (Redig et al., 1996, Wang et al., 1998, Achard et al., 2008). Energy signaling plays a role in cell cycle progression too. The plant energetic status sensed by TOR1 kinase (TARGET OF RAPAMAYCIN 1) can promote G1/S phase progression by direct phosphorylation and activation of E2Fa (Xiong et al., 2013). Low energy homeostasis on the other hand, induces KRP expression, resulting in G1 arrest, most likely by the action of SnRK1 (SUCROSE NON-FERMENTING 1-RELATED KINASE1), a kinase involved in the maintenance of cellular energy homeostasis shown to phosphorylate KRP6 and KRP7 (Guerinier et al., 2013).

As stated above, the decision to enter a new round of the cell cycle in response to growth factors and hormones is made at the G1/S transition (Gutierrez et al., 2002, Inze and De Veylder, 2006). However, in the absence of these signals, it is widely accepted that the CDK-CYCLIN complexes are in charge of controlling the transition by regulating two coupled pathways: the inactivation of the RBR/E2F/DP pathway and the modulation of the pre-RC components, which are required for S-phase entry and progression (Nakagami et al., 2002, Uemukai et al., 2005, Zhao et al., 2012). Only when all the requirements have been met at the G1-phase, cells commit into the S-phase in order to allow genome duplication.

3.5. DNA replication during the S-phase

Most of the euchromatin replicates during the early and mid S-phase while the heterochromatin and the remaining euchromatin replicate during the late S-phase (Lee et al., 2010). To ensure genome integrity, the initiation, progression and finalization of genome duplication are tightly controlled. Different regulatory mechanisms are engaged to ensure that DNA replication only occurs once every cell cycle round (Susan, 2014).

The first point of control before committing into DNA replication occurs during the G1-phase when the potential origins of replication are licensed for later use during the S-phase. In plants, as in all eukaryotes, DNA replication origin sites are scattered along the genome (Mechali, 2010, Leonard and Mechali, 2013). Origins to be used are marked by the sequential and interdependent assembly of the pre-RC in a process called origin specification or licensing. This first level of regulation is essential to avoid genome instability (Arias and Walter, 2007). The pre-RC is a protein complex composed by the six sub-units of the ORIGIN RECOGNITION COMPLEX 1-6 (ORC1-6), CDC6, CDT1a (ARABIDOPSIS HOMOLOG OF YEAST CDT1A) and the six subunits of the MINICHROMOSOME MAINTENANCE complex (MCM2-7). As in other multicellular organisms, origin specification in plants is not determined by specific DNA sequences. However, it seems that epigenetic modifications as DNA methylation and histone modifications play a crucial role in this determination. The second point of control, known as origin firing, occurs at the G1/S transition and along the S-phase. During this process, only a small amount of the previously licensed origins will become active. Pre-RC firing from active replication origins relies among others on the selective proteolysis of pre-RC components, changes in subcellular localization and binding of inhibitors of the pre-RC components (Shultz et al., 2007).

The plant pre-RC and other players involved in DNA replication share high homology with those described in other eukaryotes (Caro and Gutierrez, 2007, Shultz et al., 2007). The shared underlying dynamics of their roles during the G1 and S-phases seems to indicate functional homology too. However, some studies have shown that plants have developed unique mechanisms to control replication, as for example DNA helicase (or MCM complex) release from origins of replication only during mitosis (Shultz et al., 2009) (Figure 7).

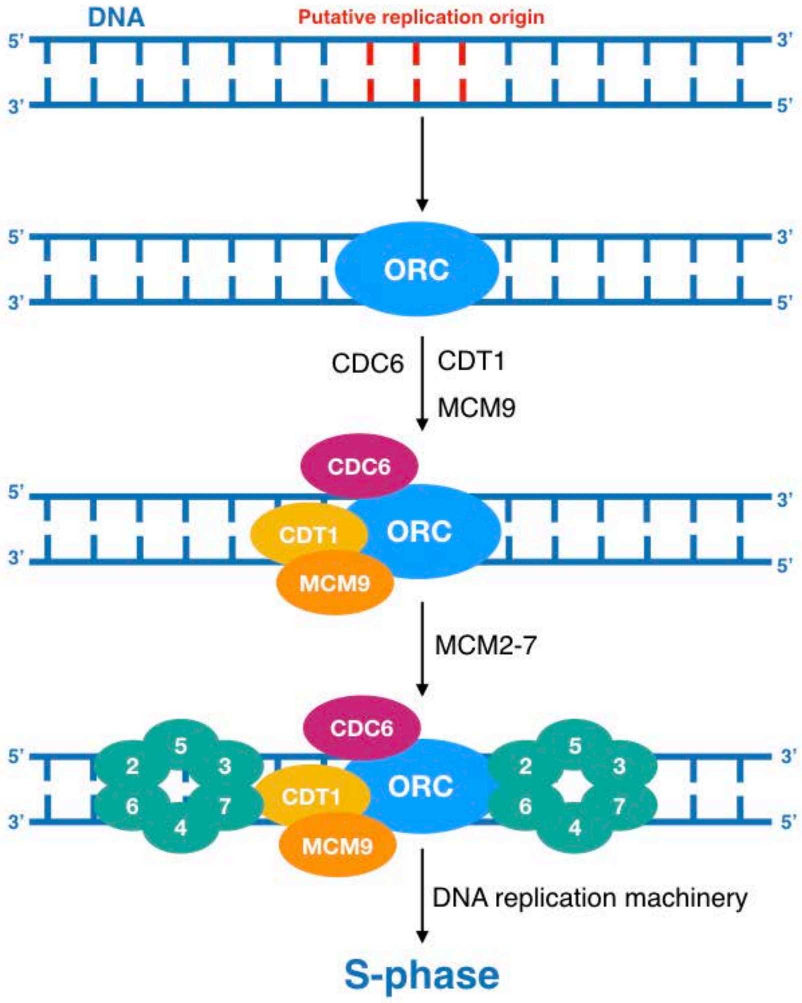

Figure 7. Assembly of the pre Replication Complex. Scheme describing the steps between DNA origin specification and entry into the S-phase. For DNA replication to take place DNA origins of replication need to be specified. In eukaryotes the assembly of the pre-RC is the first step of this process. First, ORC will determine the potential sites for DNA replication to start. The recruitment of CDC6, CDT1 and MCM9 proteins is essential for the loading of the MCM2-7 complex (helicase) in order to open the DNA double helix and start with replication spring the S-phase (Modified from Méchali 2010).

3.5.1. Role of CDC6 in the formation of the Arabidopsis pre-replication complex

CDC6 is a key component of the pre-RC, playing a central role for complex assembly and maintenance and therefore for the initiation of DNA replication. Its importance has been shown in different organisms where its association with ORC during G1 has been demonstrated to be essential for licensing origins of replication and the subsequent DNA synthesis initiation (Kelly et al., 1993, Liang et al., 1995, Piatti et al., 1995, Costas et al., 2011). CDC6 function, together with that of CDT1, is essential for the MCM complex recruitment and for the final conformation of the pre-RC (Bell and Dutta, 2002). Similar to other organisms, in the absence of CDC6, plant cells fail to initiate DNA replication (Cocker et al., 1996). In contrast, CDC6 over-expression results in extra rounds of endoreplication, therefore increasing the cell ploidy (Nishitani and Nurse, 1995, Muzi Falconi et al., 1996, Wolf et al., 1999, Bermejo et al., 2002).

Plant CDC6 shares some structural characteristics with its homologues in other species. CDC6 proteins display a conserved region corresponding to the nucleotide triphosphatases family (NTPase) with two peptide motifs (Walker-A and B) common to nucleotide binding proteins (Wang et al., 1999). The NTP binding domain is essential for its interaction with other components of the pre-RC (Wang et al., 1999, Mizushima et al., 2000, Castellano et al., 2001). Moreover, the presence of consensus CDK phosphorylation sites at the protein N-terminal region (Ramos et al., 2001) indicates that as in other eukaryotes, *Arabidopsis* CDC6 may also be regulated by phosphorylation events for targeted ubiquitinylation and proteolysis (Elsasser et al., 1999). This regulation might be important to allow just one round of DNA replication per cycle.

The similarities among CDC6 in eukaryotes suggest that the specific molecular mechanisms of CDC6 activity during DNA replication must be conserved (Masuda et al., 2004). Indeed, as in metazoans, plant CDC6 expression is cell cycle regulated. Transcripts in *Arabidopsis* cultured cells accumulate during G1 followed by a decreased in the S-phase (Castellano et al., 2001, Ramos et al., 2001). This is also supported by the fact that the levels of other pre-RC components in plants and other eukaryotes follow the same expression pattern (Kelly et al., 1993, Nishitani and Nurse, 1995, Piatti et al., 1995, Williams et al., 1997). Another common point in the regulation of S-phase components is their up-regulation at the G1/S transition by the E2F/DP pathway. In *Arabidopsis*, nearly all of the pre-RC components display a putative E2F consensus binding motif in their promoters (Masuda et al., 2004). In particular, *CDC6* showed increased accumulation in plants over-expressing the transcriptional activator E2Fa/DPa (De Veylder et al., 2002) and decreased levels by over-expression of the transcriptional repressor E2Fc (Ramirez-Parra et al., 2003).

Expression analysis performed in *Arabidopsis* showed that the activity of the *CDC6* promoter was localized in cells of rapidly proliferating tissues (e.g. root meristems, leaf primordial and young leaves). Interestingly, CDC6 activity was also seen in cells of tissues undergoing endoreplication (e.g. etiolated hypocotyls, mature leaves). This indicated that CDC6 role in DNA replication is important for both the mitotic cycle and the endocyle in plants (Castellano et al., 2001, Ramos et al., 2001). Moreover, and as mentioned before, over-expression of CDC6 in *Arabidopsis* seedlings lead to an increase of the overall ploidy level in adult tissues (Castellano et al., 2001). These results indicate that ectopic expression of CDC6 is sufficient to induce extra rounds of endoreplication in plants.

OBJECTIVES

Objectives

The main goal of this Thesis is to understand the cellular and molecular basis underlying the circadian control of cell and organ growth in *Arabidopsis*. In particular, we focused on **the functional interplay between the circadian clock and the cell cycle**. This general goal was achieved by several specific objectives:

1. **To examine the role of the circadian clock on the mitotic cycle and growth in developing leaves.** We examined leaf area, cell number and cell area in Wild-Type and TOC1 miss-expressing plants. The studies also included analyses of the average cell division rates and the duration of the G1, S and G2/M phases.

2. **To examine the role of the circadian clock in the control of endoreplication in developing leaves.** The studies were completed by analyses of ploidy distribution by flow cytometry of leaves in Wild-Type and TOC1 miss-expressing plants grown under different photoperiodic conditions. The studies also included calculation of the Endoreplication Index of the different genotypes under the different conditions.

3. **To analyze the expression profiles of core cell cycle genes during development in leaves miss-expressing TOC1.** We analyzed the expression pattern of core cell cycle genes during proliferation, expansion and leaf maturation to obtain an overview of the cell cycle gene transcriptional changes in plants over-expressing TOC1.

4. **To examine the diurnal oscillatory pattern of cell cycle genes in leaves of plants miss-expressing TOC1.** We explored the diurnal rhythms of key cell cycle genes in leaves of plants miss-expressing TOC1. We also used a battery of mutant and over-expressing plants in which the accumulation of TOC1 was altered.

5. **To elucidate the molecular mechanism coupling the circadian clock and the cell cycle.** We performed chromatin immunoprecipitation assays in order to identify cell cycle gene promoters to which TOC1 might directly bind. We used TOC1 over-expressing plants and plants expressing TOC1 under its own promoter to identify a possible rhythmic binding.

6. **To characterize the CDC6 and TOC1 genetic interaction.** We performed genetic interaction studies between the DNA replication licensing factor CDC6 and TOC1. Single and double CDC6 and TOC1 over-expressing plants were used to examine the growth phenotypes and polyploidy profiles. The effects of TOC1 over-expression on tumor progression were also examined.

RESULTS

Results

1. TOC1 regulates the timing of cell division in developing leaves

TOC1-ox plants show a dwarf phenotype, with reduced plant size (Figure 8A) and small leaves (Figure 8B). At early stages of leaf development, active cell division during the mitotic cycle controls growth. To examine the possible involvement of TOC1 in cell division, we conducted time course analyses at early time points of growth with the first pair of leaves grown under Short Days (ShD, 8h light:16h dark) (Figure 9A-C) and Long Days (LgD, 16h light:8h dark) (Figure 10A-C).

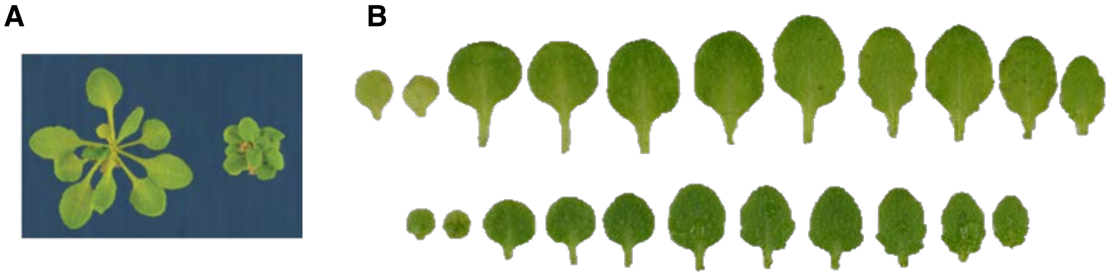

Figure 8. TOC1 over-expression affects plant growth. (A) Representative images of WT and TOC1-ox plants at 24 das and (B) rosette leaves from WT (top) and TOC1-ox (bottom) plants at 22 das. Leaves are shown from the oldest, including the two cotyledons (left) to the youngest (right). (A-B) Plants were grown under LgD.

The blade area of Wild-Type (WT) plants showed a progressive growth, consistent with the trend reported by previous studies (De Veylder et al., 2001). In contrast, leaf area was considerably reduced in TOC1-ox (Figure 9A); a phenotype that was evident at early stages (6 and 7 days after stratification, das). Although leaves continued growing over the days, the growth rate in TOC1-ox was noticeably reduced compared to WT and resulted in a 60% reduction at 9 das (Figure 9A). Leaf epidermal cell number was reduced in TOC1-ox at early stages (Figure 9B), which indicate that cell proliferation is affected by accumulation of TOC1. Cell area was also reduced in TOC1-ox (Figure 9C) suggesting that both the reduced cell number and area contribute to the reduction of leaf size. A role for TOC1 controlling the duration of the mitotic cycle was supported by the analysis of the average cell division rate, which showed a slower speed in TOC1-ox (0.032 cells cell^{-1} h^{-1}) compared to WT

(0.050 cells cell^{-1} h^{-1}) (Figure 11A). A similar reduced leaf area, cell area and cell number were observed in TOC1-ox under LgD (Figure 10A-C) which also led to a reduced average cell division rate (Figure 11B). Therefore, over-expression of TOC1 affects the speed of the cell cycle, altering cell division during the mitotic cycle.

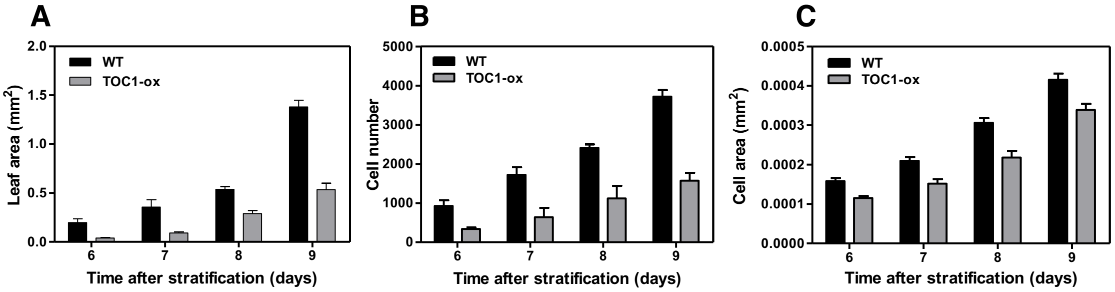

Figure 9. TOC1 modulates growth during leaf development under ShD. Early time course analyses of (A) leaf blade area, (B) cell number and (C) cell area of the first leaf pair. (A-C) Plants were grown under ShD conditions. Data are represented as the mean + SEM of n ≈ 10-20 leaves and n ≈ 100 cells. At least two biological replicates per experiment were performed.

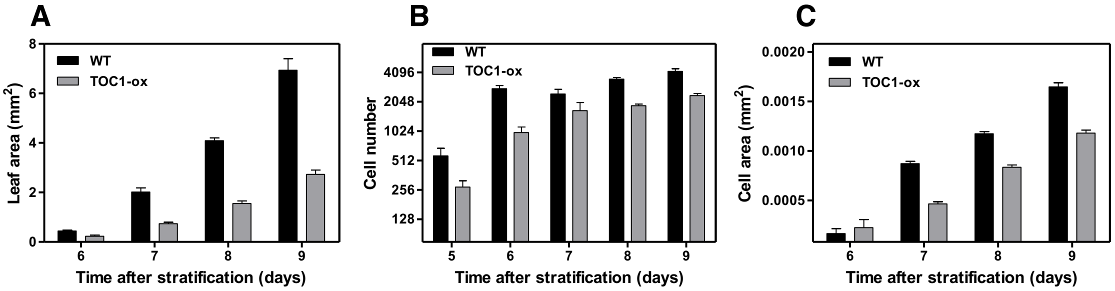

Figure 10. TOC1 modulates growth during leaf development under LgD. Early time course analyses of (A) leaf blade area, (B) cell number and (C) cell area of the first leaf pair. (A-C) Plants were grown under LgD conditions. Data are represented as the mean + SEM of n ≈ 10-20 leaves and n ≈ 100 cells. At least two biological replicates per experiment were performed.

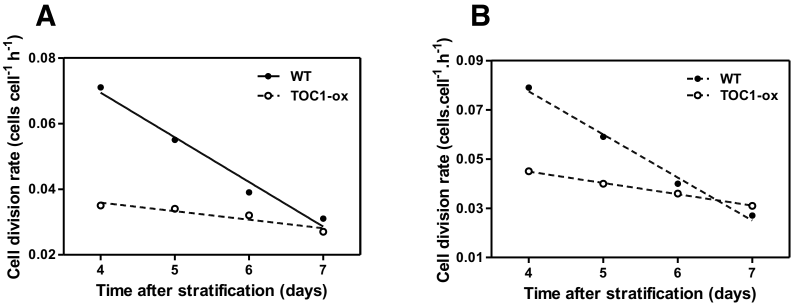

Figure 11. TOC1 modulates the cell division rate in young developing leaves. (A-B) Average cell division rates of abaxial epidermal cells and linear regression analyses of the first four points of the kinematic assay. Plants were grown under (A) ShD and (B) LgD conditions.

Analyses of *ztl-3* mutant plants, harboring a mutation in ZTL (Somers et al., 2000), the F-box protein responsible for TOC1 protein degradation (Mas et al., 2003b) showed a decreased plant size and leaf area that correlated with reduced cell number and cell size (Figure 12A and B, 14A-F), following a similar trend to that observed in TOC1-ox. Conversely, *toc1-2* mutant plants displayed increased leaf size that coincided with higher cell number at early stages of development and increased cell area at later stages (Figure 12A and B, 13A-F).

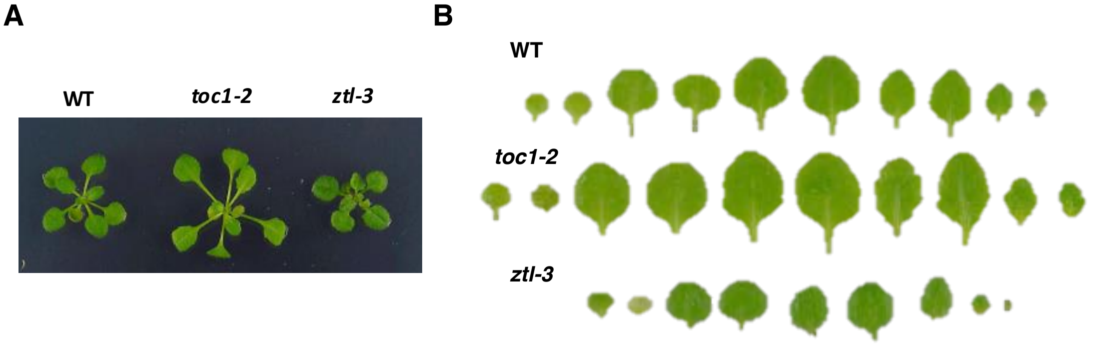

Figure 12. TOC1 miss-expression affects overall plant growth. (A) Representative images of WT, *toc1-2* and *ztl-3* plants and (B) leaves from WT (top), *toc1-2* (middle) and *ztl-3* (bottom) at 19 das. Leaves are shown from the oldest, including the two cotyledons (left) o the youngest (right). (A-B) Plant were grown under LgD.

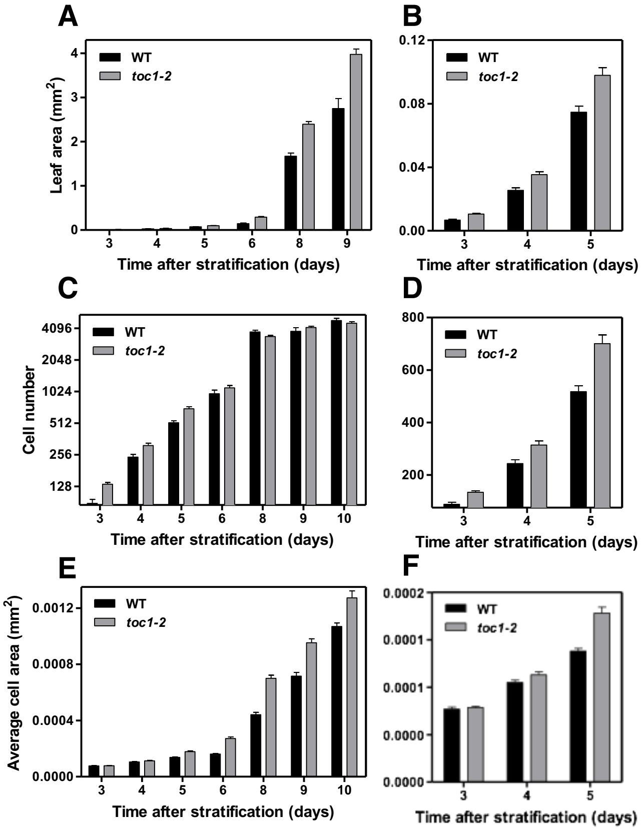

Figure 13. TOC1 mutation increases growth in *Arabidopsis* leaves during development. Time course analyses of (A-B) leaf blade area, (C-D) cell number, and (E-F) cell area of the first leaf pair in *toc1-2* mutants grown under LgD. Values of (B) leaf area, (D) cell number, and (F) cell area at early stages of development are separately represented. Data in panel (C) is graphed in log2 scale. Data are represented as the mean + SEM of n ≈ 10-20 leaves and n ≈ 100 cells. At least two biological replicates per experiment were performed.

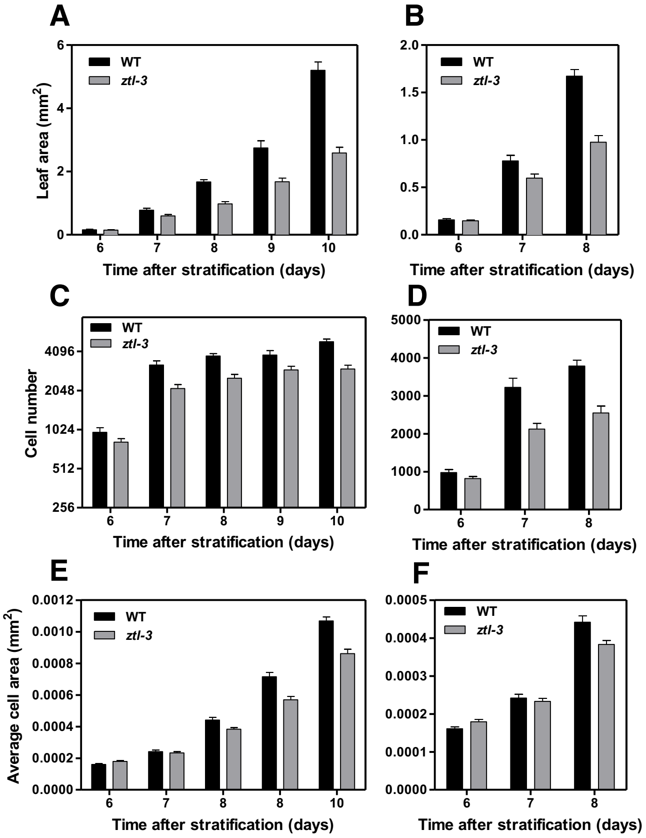

Figure 14. Mutation of ZTL reduces overall growth in *Arabidopsis* leaves during development. Time course analyses of (A-B) leaf blade area, (C-D) cell number, and (E-F) cell area of the first leaf pair in *ztl-3* mutants grown under LgD. Values of (B) leaf area, (D) cell number, and (F) cell area at early stages of development are separately represented. Data in panel (C) is graphed in log2 scale. Data are represented as the mean + SEM of n ≈ 10-20 leaves and n ≈ 100 cells. At least two biological replicates per experiment were performed.

To determine if a specific cell cycle phase is affected in TOC1-ox, we conducted flow cytometry analyses to examine ploidy profiles of leaves from plants grown at 9 das under ShD (Figure 15A) or 7 das under LgD (Figure 15D). WT and TOC1-ox mostly showed nuclear DNA content (C-values) of 2C and 4C, correlating with the high proliferation at this developmental stage (Figure 15A and D). Calculation of the relative amount of cells in the G1-, S-, and G2/M-phases revealed that TOC1-ox leaves displayed a decreased proportion of nuclei in S and G2/M phases and a clear enrichment of the G1-phase under both ShD (Figure 15B) and LgD (Figure 15E). The data indicates that the G1-phase takes much longer in TOC1-ox (aprox. 22h) than in WT (aprox. 13h) at the expense of a shorter S-phase (1.6h versus 2h in WT) (compare TOC1-ox in the outer ring with WT in the inner ring in Figure 15C). A similar trend was observed under LgD (Figure 15F). Thus, the slow circadian clock in TOC1-ox plants correlates with an extended G1-phase and reduced S-phase. The results indicate that TOC1 is important not only for controlling the pace of the clock but also the cell cycle.

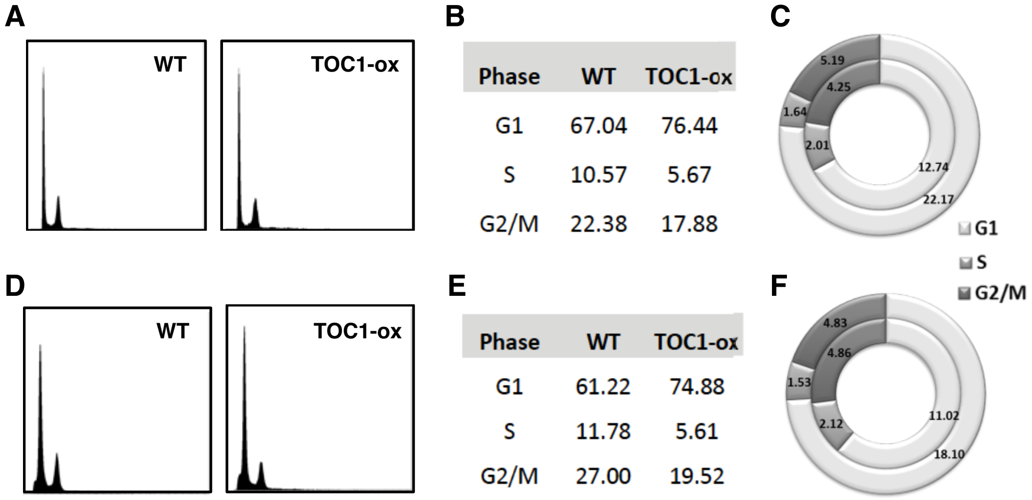

B

Phase	WT	TOC1-ox
G1	67.04	76.44
S	10.57	5.67
G2/M	22.38	17.88

E

Phase	WT	TOC1-ox
G1	61.22	74.88
S	11.78	5.61
G2/M	27.00	19.52

Figure 15. TOC1 modulates the mitotic cycle in developing leaves. Ploidy distribution by flow cytometry of WT and TOC1-ox first pair of leaves at (A) 9 das and (D) 7 das. Estimation of the relative amounts of cells in G1, S and G2/M phases in proliferating leaves analyzed by flow cytometry at (B) 9 das and (E) 7 das. Estimated duration (hours) of the G1, S and G2/M phases at (C) 9 das and (F) 7 das in WT (inner rings) and TOC1-ox (outer rings). (A-C) Plants were grown under ShD and (D-F) under LgD conditions. At least two biological replicates per experiment were performed.

2. TOC1 controls the timing of the endocycle in leaves

Our results suggest that TOC1 regulates the mitotic cycle at early stages of leaf development. However, after the mitotic cycle, cells transition to the endocycle in which endoreplication predominates at mid and late stages of leaf growth (De Veylder et al., 2011). To determine whether in addition to the mitotic cycle, TOC1 also regulates endoreplication in leaves, we conducted a time course analysis by flow cytometry to examine ploidy of leaves at later stages of development (Figure 16A and B). At 13 das, WT plants grown under ShD showed around 5% of the nuclei with 8C content, which represent cells entering the endocycle (Figure 16C). The frequency of 2C and 4C nuclei progressively decreased over time in favor of higher-order C values that can be attributed to extra rounds of endoreplication (Figure 16C). In TOC1-ox seedlings at 13 das, the 4C/2C ratio was reduced compared to WT (Figure 16D). The sharp 4C increase observed in WT was delayed and reached a peak only at 15 das in TOC1-ox (Figure 17A) while the marked reduction of the 2C content at 9 to 13 das observed in WT leaves was less pronounced in TOC1-ox (Figure 16C and D). From day 13 onward, the proportion of 8C and 16C nuclei was considerably reduced in TOC1-ox compared to WT (Figure 17B and C).

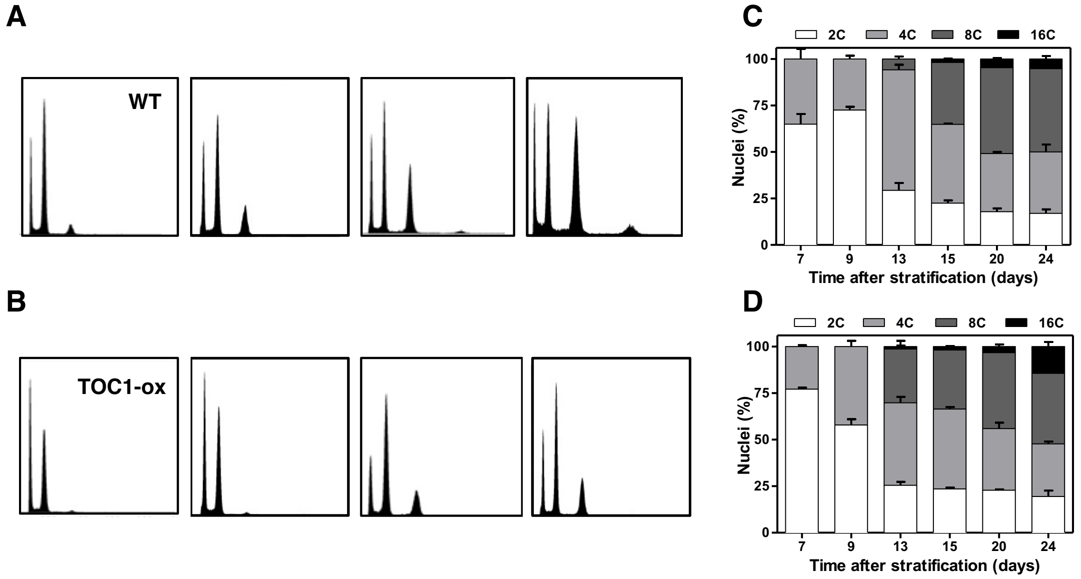

Figure 16. TOC1 modulates endoreplication in developing leaves under ShD. Ploidy distribution by flow cytometry of (A) WT and (B) TOC1-ox first leaf pair at 13, 15, 20 and 24 das. Kinematics of polyploid nuclei in (C) WT and (D) TOC1-ox. (A-D) Plants were grown under ShD conditions. Data are represented as the mean + SEM of n ≈ 10000 nuclei. At least two biological replicates per experiment were performed.

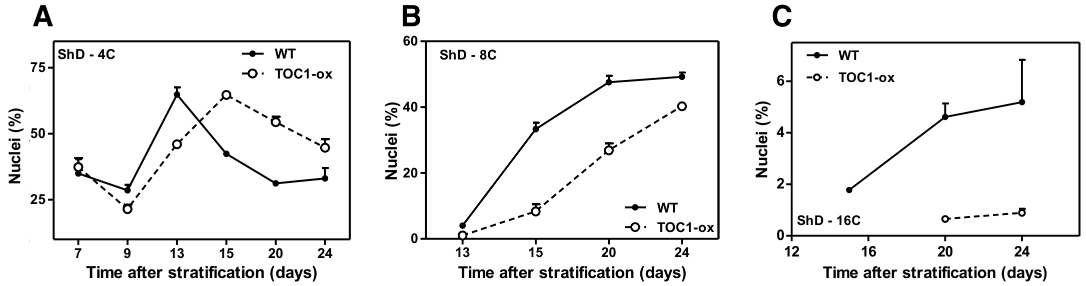

Figure 17. TOC1 over-expression alters ploidy progression in developing leaves under ShD. Relative profiles of (A) 4C, (B) 8C and (C) 16C content in WT and TOC1-ox. (A-C) Plants were grown under ShD conditions. Data are represented as the mean + SEM of n ≈ 10000 nuclei. At least two biological replicates per experiment were performed.

Leaf ploidy of plants grown under LgD also revealed a delayed enrichment of higher-order C values in TOC1-ox compared to WT (Figure 18A-D and 19A-C), suggesting that alteration of endoreplication in TOC1-ox is not dependent on a particular environmental condition. The DNA content was eventually reached but at a slower pace, suggesting a delayed progression of endoreplication. These results are noteworthy as TOC1-ox also delays the phase of the clock under diurnal conditions.

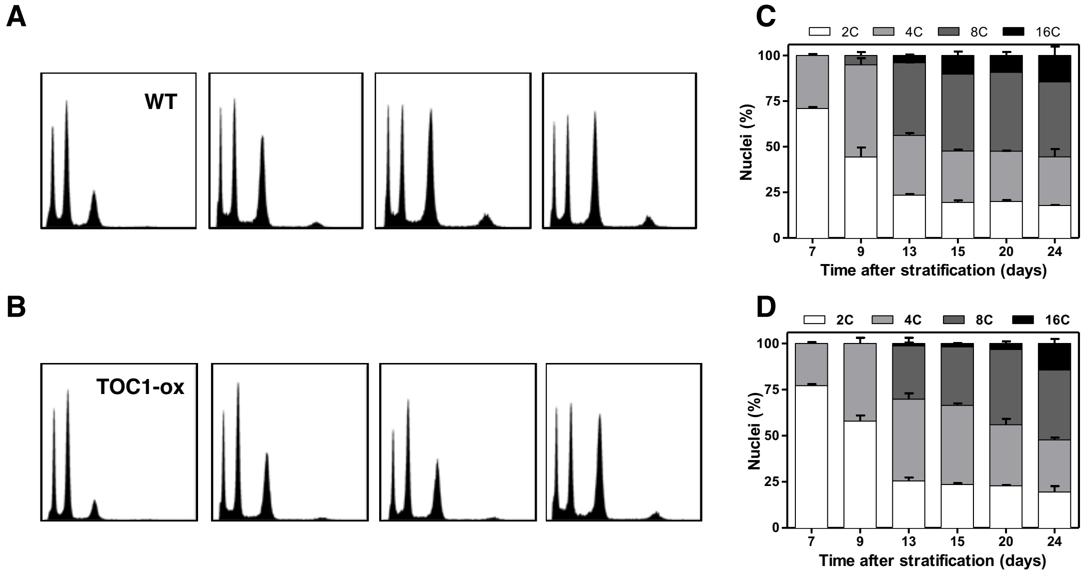

Figure 18. TOC1 modulates endoreplication in developing leaves under LgD. Ploidy distribution by flow cytometry of (A) WT and (B) TOC1-ox first leaf pair at 11, 13, 15 and 20 das. Kinematics of polyploid nuclei in (C) WT and (D) TOC1-ox. (A-D) Plants were grown under LgD conditions. Data are represented as the mean + SEM of n ≈ 10000 nuclei. At least two biological replicates per experiment were performed.

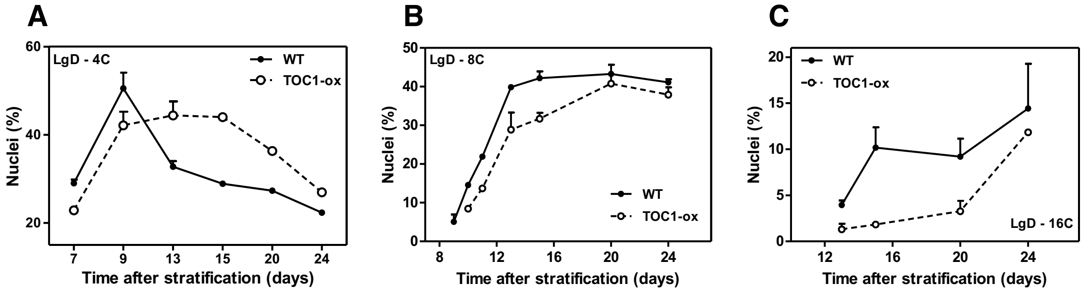

Figure 19. TOC1 over-expression alters ploidy progression in developing leaves under LgD. Relative profiles of (A) 4C, (B) 8C and (C) 16C content in WT and TOC1-ox. (A-C) Plants were grown under LgD conditions. Data are represented as the mean + SEM of n ≈ 10000 nuclei. At least two biological replicates per experiment were performed.

Calculation of the endoreplication activity, measured as the average number of endocycles per nucleus (Endoreplication Index, EI) of *ztl* mutant plants showed reduced EI (Figure 20A), which confirmed that over-accumulation of TOC1 correlates with a reduction of endoreplication. The phenotypes were not exclusive for TOC1 gain-of-function since *toc1-2* mutant and over-expression of ZTL (ZTL-ox) leaves showed enhanced endoreplication (Figure 21A-C). Calculation of the EI confirmed the reduced index in TOC1-ox (Figure 20B and C) and its increment in *toc1-2* and ZTL-ox plants (Figure 21D). Therefore, proper accumulation of TOC1 is important for endocycle activity and influences endoreplication in developing leaves.

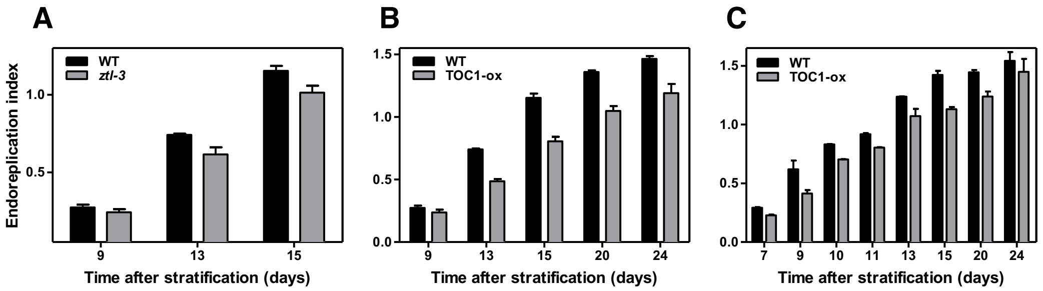

Figure 20. Increased levels of TOC1 lead to a reduction of endoreplication in developing leaves. Endoreplication index of (A) WT and *ztl-3* leaves of plants grown under ShD and of WT and TOC1-ox leaves under (B) ShD and (C) LgD. Data are represented as the mean + SEM of n ≈ 10000 nuclei. At least two biological replicates per experiment were performed.

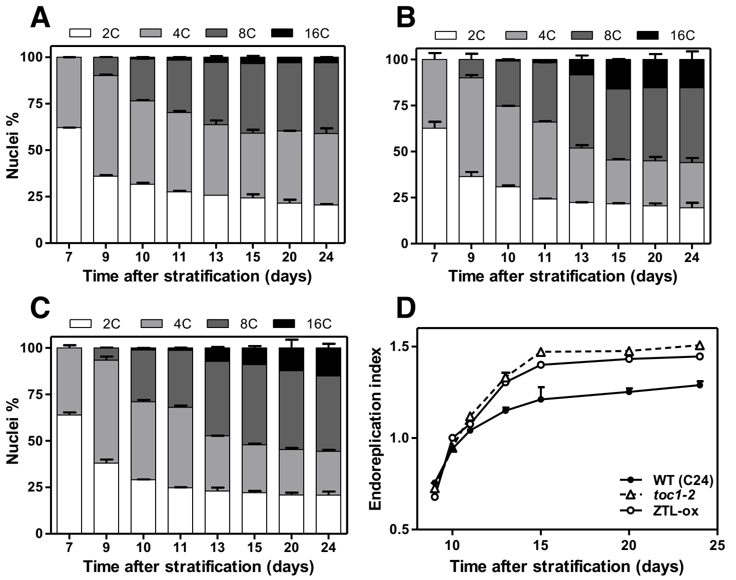

Figure 21. Loss-of-function TOC1 leads to increased endoreplication in developing leaves. Kinematics of polyploid nuclei in (A) WT (C24), (B) *toc1-2* and (C) ZTL-ox. (D) Endoreplication index of WT (C24), *toc1-2* and ZTL-ox leaves. (A-D) Plants were grown under LgD. Data are represented as the mean + SEM of n ≈ 10000 nuclei. At least two biological replicates per experiment were performed.

3. TOC1 controls the endocycle in hypocotyl cells

We next examined whether regulation of endoreplication by TOC1 was exclusive for leaves or also pervaded other organs. Hypocotyl cells are a convenient and simple system to analyze endocycle activity as the *Arabidopsis* hypocotyl epidermal and cortex cells only undergo endoreplication (Gendreau et al., 1997). We first examined hypocotyl length of TOC1-ox plants under constant white light conditions (WL, 40 μE) and found significantly shorter hypocotyls compared to WT (Figure 22A, left panel). Conversely, TOC1-RNAi plants showed longer than WT hypocotyls (Figure 22A, left panel). The trend of hypocotyl phenotypes was similar at low fluences (1 μE, WL1) (Figure 22A, right panel).

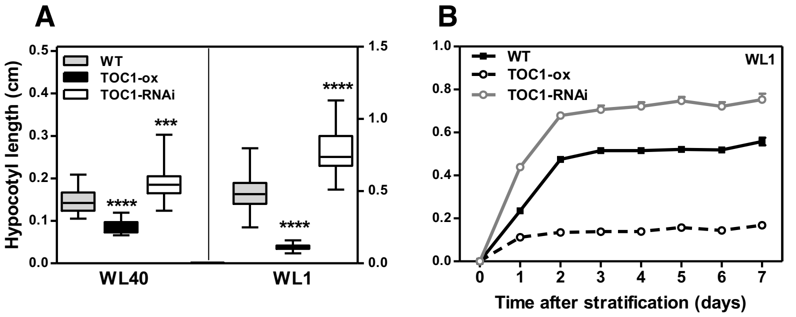

Figure 22. TOC1 miss-expression affects hypocotyl elongation. (A) Analyses of hypocotyl length at WL40 (40 μmol·quanta·m^{-2}·s^{-1}) and WL1 (1 μmol·quanta·m^{-2}·s^{-1}) and (B) growth kinetics of WT, TOC1-ox and TOC1-RNAi. Graphs represent mean + SEM of n ≈ 20 hypocotyls (per genotype and/or condition). At least two biological replicates per experiment were performed. Length under WL1 in (A) is represented on the right axe. ****P≤ 0.0001; ***P≤0.001.

Analyses of *ztl-3* mutant plants also resulted in short hypocotyls (Figure 23A and B), confirming that over-accumulation of TOC1 correlates with inhibition of hypocotyl growth. Very short hypocotyls were also observed in TOC1 minigene (TMG) seedlings, which express *TOC1* genomic fragment fused to the yellow fluorescent protein in a *ztl* mutant background (*ztl-1*/TMG) (Figure 23C). Contrarily, over-expression of ZTL resulted in long hypocotyls (Figure 23A and B) similar to TOC1-RNAi seedlings. Time course analyses of hypocotyl growth over 7 days revealed that the phenotypes were readily observed at 1 das and continued throughout the time course (Figure 22B). Thus, TOC1 engages in the control of hypocotyl elongation at early stages of post-embryonic growth.

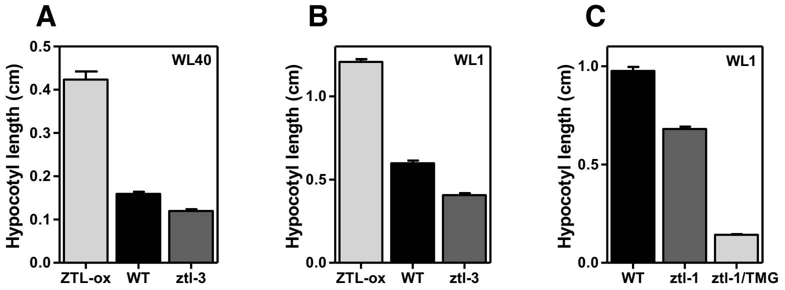

Figure 23. ZTL miss-expression modulates hypocotyl elongation. Hypocotyl length of WT, *ztl-3* and ZTL-ox seedlings under (A) WL40 (40 μmol·quanta·m^{-2}·s^{-1}) and (B) WL1 (1 μmol·quanta·m^{-2}·s^{-1}). (C) Hypocotyl length of WT, *ztl-1* and *ztl-1*/TMG seedlings under WL1. Graphs represent the mean + SEM of n ≈ 20 hypocotyls (per genotype and/or condition). At least two biological replicates per experiment were performed.

We next examined the number and size of hypocotyl epidermal cells. Cell number was not significantly altered in TOC1-ox or TOC1-RNAi compared to WT plants (Figure 24A). The results agree with the fact that hypocotyl growth is mostly regulated by cell expansion rather than cell division (Gendreau et al., 1997). Analyses of the bottom, mid or top regions of hypocotyls showed a significantly reduced cell length in TOC1-ox and conversely, and increased elongation in TOC1-RNAi (Figure 24B and C). In WT and TOC1-RNAi plants, cells were longer at the mid-region compared to the top or the bottom. This relationship was lost in TOC1-ox with a constant and reduced cell length in every region. A similar trend in cell length phenotypes was observed in *ztl-1* and *ztl-1*/TMG plants (Figure 24D). Thus, the hypocotyl phenotypes due to miss-expression of TOC1 correlate with significant changes in cell expansion.

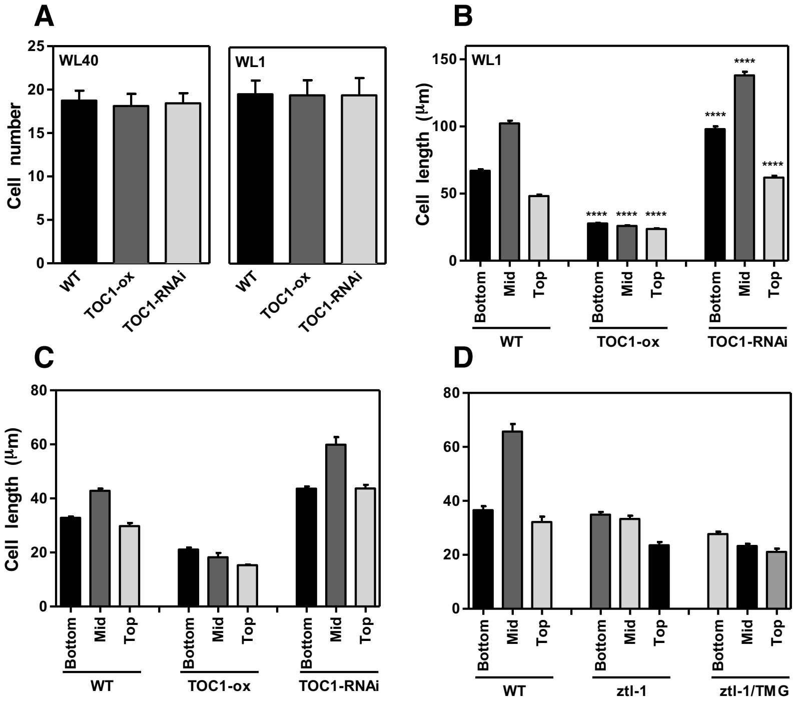

Figure 24. TOC1 modulates hypocotyl cell length. Hypocotyl epidermal (A) cell number and (B-D) cell length at the bottom, mid and top regions of (B-C) WT, TOC1-ox and TOC1-RNAi and (D) WT, *ztl-1* and *ztl-1*/TMG hypocotyls. Seedlings were grown under (A left panel, C and D) 40 $\mu mol \cdot quanta \cdot m^{-2} \cdot s^{-1}$ (WL40) and (A right panel and B) 1 $\mu mol \cdot quanta \cdot m^{-2} \cdot s^{-1}$ (WL1). Graphs represent the mean + SEM of $n \approx 20$ hypocotyls and $n \approx 100$ cells (per genotype and/or condition). At least two biological replicates per experiment were performed. ****$P \leq 0.0001$; ***$P \leq 0.001$.

Flow cytometry analyses to determine the ploidy profiles of hypocotyls revealed that WT cells showed three evident peaks corresponding to nuclear DNA content of 2C, 4C and 8C (Figure 25A-C). In TOC1-ox seedlings, the proportion of 4C nuclei was higher than in WT, with a reduction in the proportion of 8C and 16C nuclei (Figure 25A-C). In contrast, TOC1-RNAi cells showed a small but reproducible enrichment of the 8C and 16C peaks (Figure 25A-C). Thus, TOC1 over-expression decreases the 8C/4C ratio while TOC1-RNAi increases endoreplication leading to an incomplete repression of the third endoreplication round. Although polyploidy is not necessarily coupled with elongation, the Endoreplication Index (EI) showed a direct correlation with hypocotyl length in lines with decreasing amounts of TOC1 (Figure 25D). These results suggest that proper expression of TOC1 is also important for modulating the endocycle activity during hypocotyl growth.

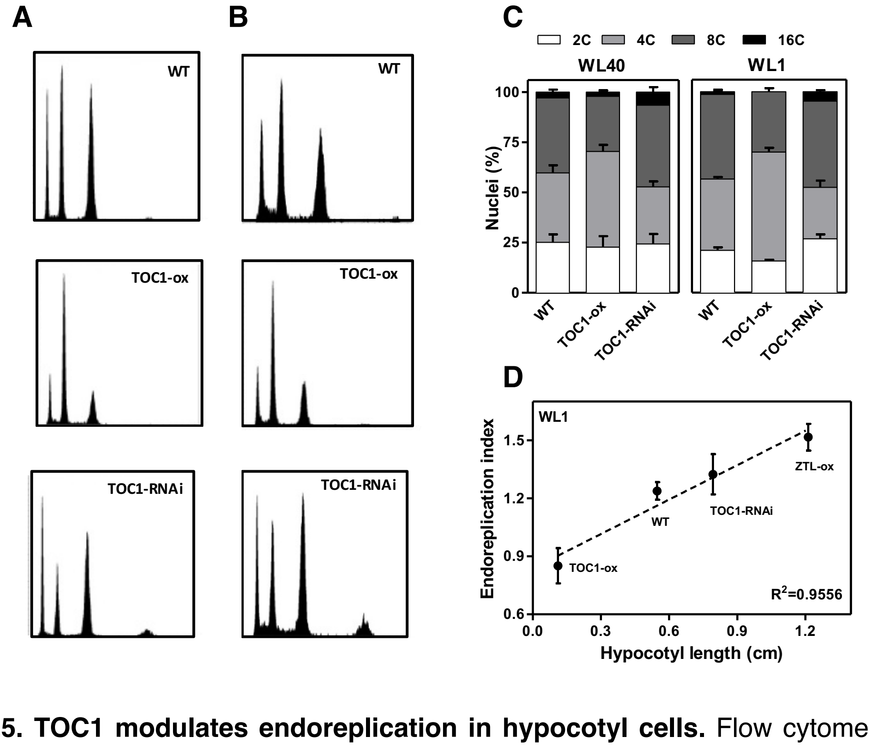

Figure 25. TOC1 modulates endoreplication in hypocotyl cells. Flow cytometry of ploidy profiles under constant white light (A) 40 µmol·quanta·m^{-2}·s^{-1}, WL40 and (B) 1 µmol·quanta·m^{-2}·s^{-1}, WL1. (C) Relative proportions of polyploid nuclei in hypocotyls of seedlings grown under WL40 and WL1 for 7 days. Data are represented as the mean + SEM of n ≈ 10000 nuclei. (I) Correlation of hypocotyl length and the endoreplication index in lines with decreasing amounts of TOC1. Graph represents the mean ± SEM of n ≈ 20 hypocotyls and n ≈ 10000 nuclei. At least two biological replicates per experiment were performed.

4. The developmental expression of cell cycle genes is altered in TOC1-ox

As TOC1 functions as a transcriptional regulator, we investigated which cell cycle genes could be transcriptionally altered in TOC1-ox. The timing of mitotic exit is different between the leaf tip and base (Donnelly et al., 1999) so that the first pair of leaves were cut in halves and the expression of selected core cell cycle genes was separately examined at the leaf tip and base. Overall, the trend of expression of cell cycle genes in WT leaves was similar to that described in previous reports and correlated with their cell cycle function. At the leaf tip, the G1-expressed D3-type cyclins showed a slight but reproducible up-regulation (Figure 26A-C) that might be consistent with the longer G1-phase and altered endoreplication in TOC1-ox, as CYCDs restrain the transition to endocycling (Dewitte et al., 2007). The slight up-regulation of *CYCD3;1* (Figure 26A) might also contribute to the delayed S-phase, as *CYCD3;1* is repressed during the S-phase (Menges et al., 2005). A down-regulation was observed for *CYCD4;1* (Menges and Murray, 2002) (Figure 26D), and *CDKA;1* (Figure 26F). For *CYCB1;1* a down-regulation was observed in TOC1-ox at the tip of the leaf while no change was observed at the base (Figure 26E).

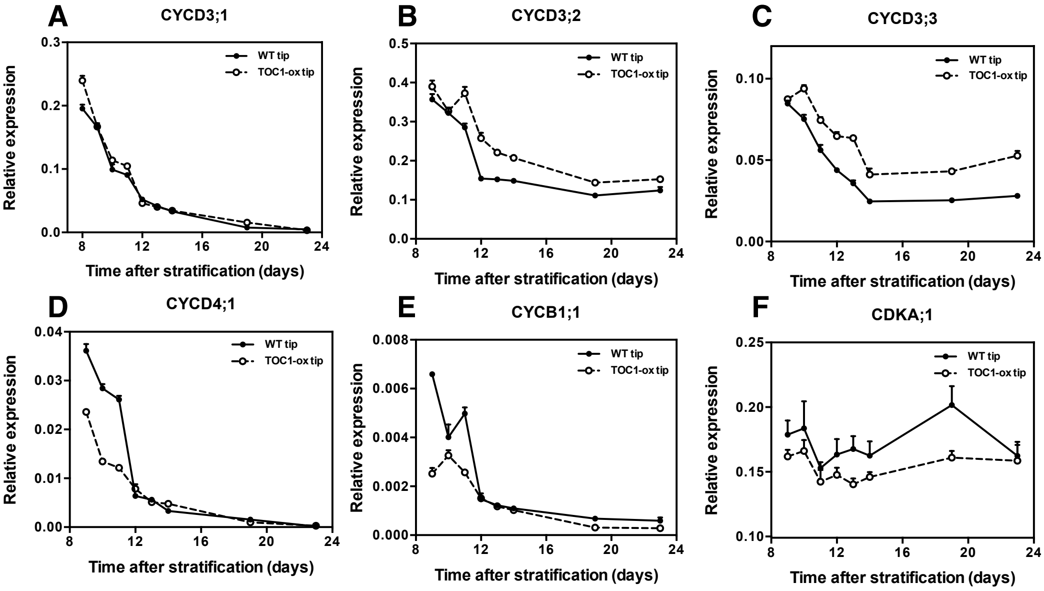

Figure 26. Miss-expression of CYCs and CDKs in TOC1-ox developing leaves. Time course analyses of cell cycle genes in WT and TOC1-ox leaves over development. Plants were grown under LgD and samples were collected at ZT7. Leaves were cut in halves and gene expression was separately examined at the tip of leaves. Expression of (A) *CYCD3;1*, (B) *CYCD3;2,* (C) *CYCD3;3,* (D) *CYCD4;1,* (E) *CYCB1;1, and* (F) *CDKA;1* at the tip of leaves. Relative expression was obtained by Quantitative real-time PCR (Q-PCR) analyses. Data represent as te mean + SEM of technical triplicates. The experiment was repeated twice, giving similar results.

The expression of CDK inhibitors such as *KRP2* shifted from up-regulated at early stages to down-regulated at late stages (Figure 27B). This pattern might reflect the mismatch in timing between proliferation and differentiation in TOC1-ox, as KRP2 not only inhibits cell proliferation but also sustains differentiation (Verkest et al., 2005). A similar pattern was observed for *KRP4* (Figure 27C) and *KRP1* (Figure 27A). In contrast, the expression of *KRP7* was clearly up-regulated mostly at late stages (Figure 27D). The expression of the inhibitors SMR (SIAMESE-RELATED) was also altered in TOC1-ox. For instance, *SMR1* and *SMR8* (Figure 28A and E) were down-regulated mostly at late stages of development while a very significant down-regulation was observed for *SMR5* and *SMR7* at all time points (Figure 28C and D). However, others as *SMR4* displayed WT expression levels throughout development (Figure 28B). The down-regulation of SMRs contrasted with the up-regulation of *SIM* (*SIAMESE*) (Figure 28F). The up-regulation of *SIM* correlates with the slow growing phenotype of plants over-expressing SIM but not with their increased DNA content. It is possible that the reduced expression of other endoreplication promoting factors in TOC1-ox might be able to overcome the over-expression of SIM.

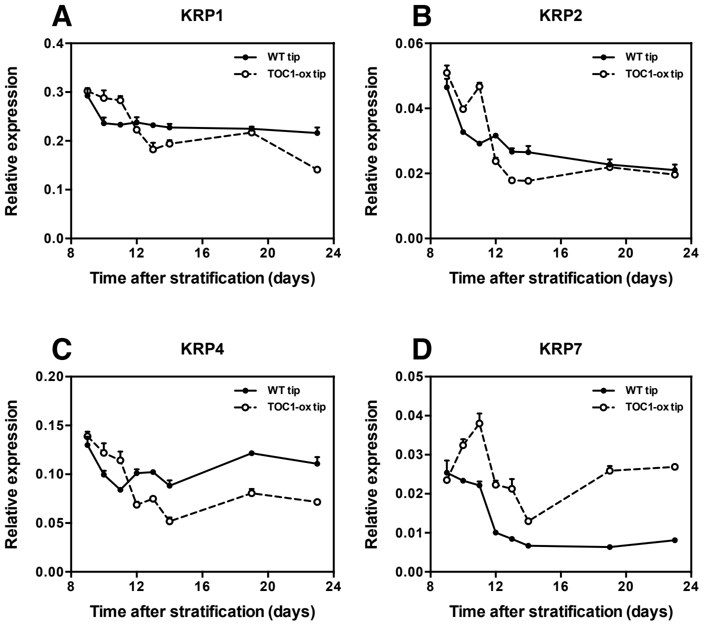

Figure 27. Miss-expression of KRPs in TOC1-ox developing leaves. Time course analyses of cell cycle genes in WT and TOC1-ox leaves over development. Plants were grown under LgD and samples were collected at ZT7. Leaves were cut in halves and gene expression was separately examined at the tip of leaves. Expression of (A) *KRP1*, (B) *KRP2,* (C) *KRP4,* and (D) *KRP7,* at the tip of leaves. Relative expression was obtained by Q-PCR analyses. Data are represented as the mean + SEM of technical triplicates. The experiment was repeated twice, giving similar results.

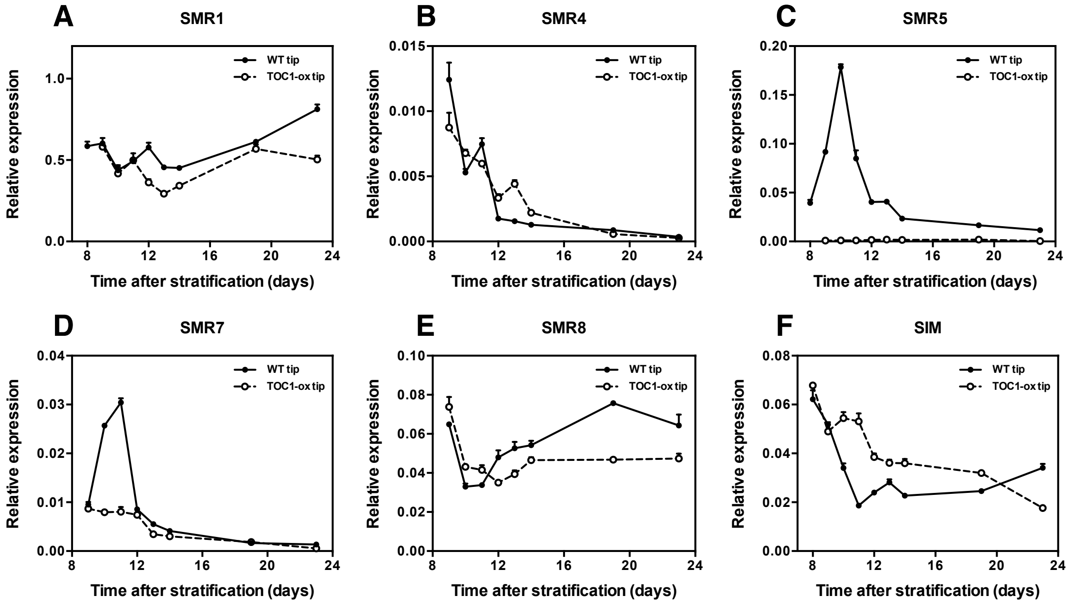

Figure 28. Miss-expression of SMRs in TOC1-ox developing leaves. Time course analyses of cell cycle genes in WT and TOC1-ox leaves over development. Plants were grown under LgD and samples were collected at ZT7. Leaves were cut in halves and gene expression was separately examined at the tip of leaves. Expression of (A) *SMR1*, (B) *SMR4,* (C) *SMR5,* (D) *SMR7,* (E) *SMR8* and (F) *SIM* at the tip of leaves. Relative expression was obtained by Q-PCR analyses. Data are represented as the mean + SEM of technical triplicates. The experiment was repeated twice, giving similar results.

In agreement with this idea, the expression of the endocycle promoting factor *CCS52A2* and the DNA replication factor *CDC6* was clearly down-regulated in TOC1-ox (Figure 29A and B). In WT, the expression decreased until day 12-13 to subsequently rise again. However, in TOC1-ox, expression failed to rise and remained lower than in WT. The expression of *CDT1a* was reduced in TOC1-ox at early stages of development (Figure 29C).

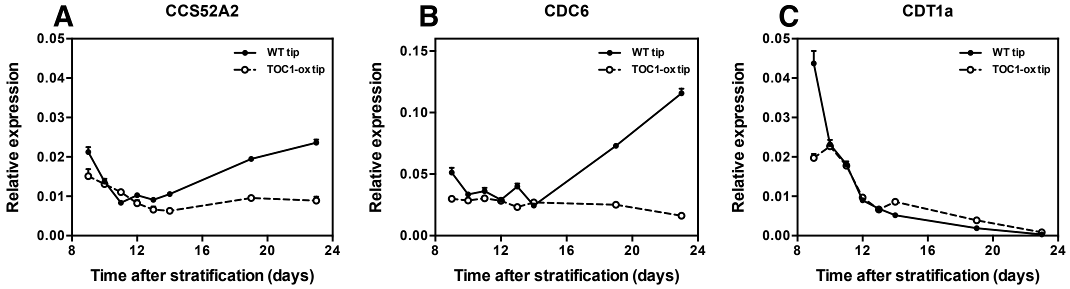

Figure 29. Miss-expression of endocycle related genes in TOC1-ox developing leaves. Time course analyses of cell cycle genes in WT and TOC1-ox leaves over development. Plants were grown under LgD and samples were collected at ZT7. Leaves were cut in halves and gene expression was separately examined at the tip of leaves. Expression of (A) *CCS52A2*, (B) *CDC6, and* (C) *CDT1a* at the tip of leaves. Relative expression was obtained by Q-PCR analyses. Data are represented as the mean + SEM of technical triplicates. The experiment was repeated twice, giving similar results.

Although values and timing varied, similar trends of gene expression were observed at the bases of leaves (Figure 30). Thus, there is considerable transcriptional miss-regulation of cell cycle genes involved in both the mitotic cycle and the endocycle. The changes in gene expression correlate with the phenotypes in cell and organ size, cell number and ploidy.

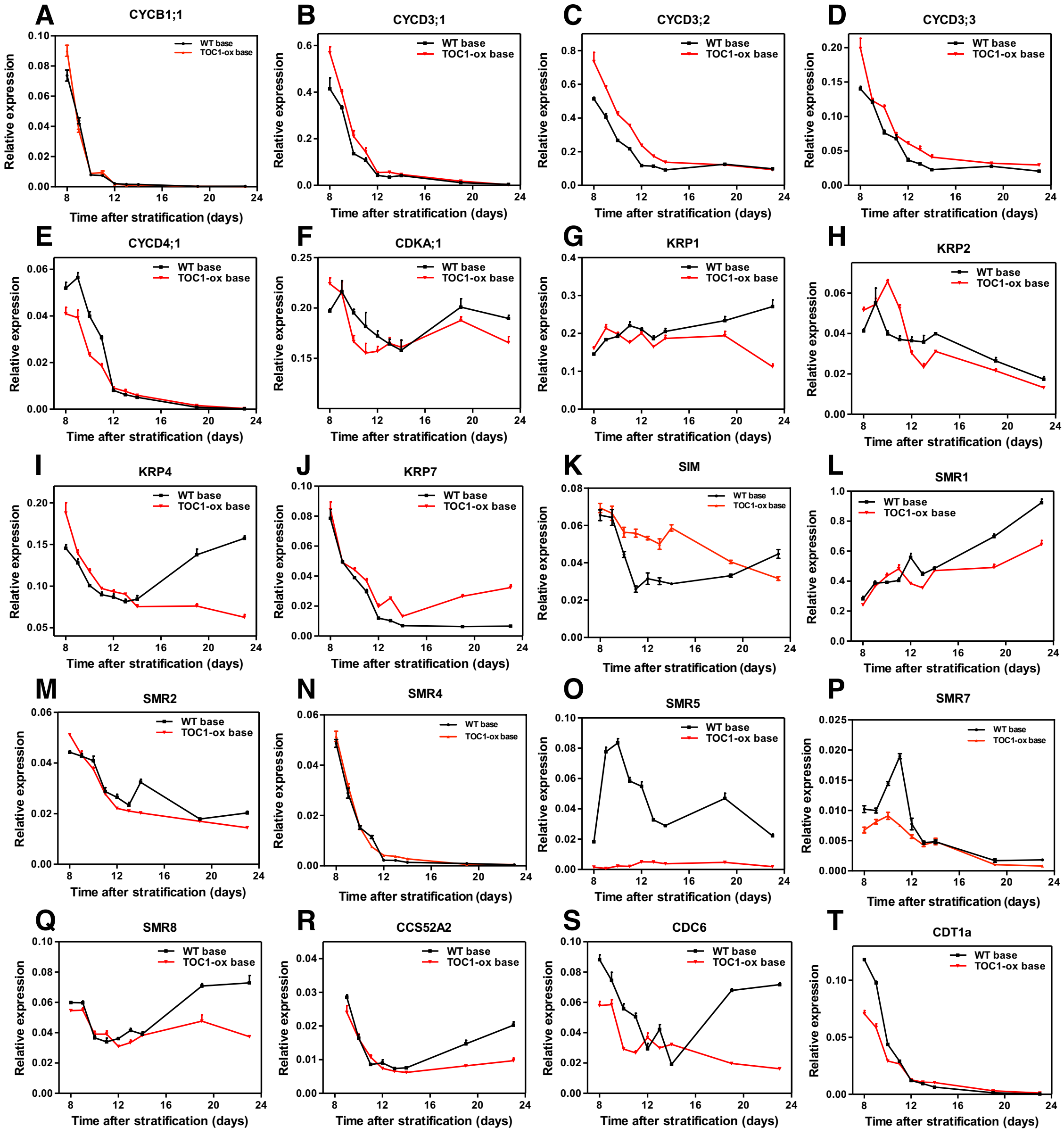

Figure 30. Miss-expression of cell cycle genes in TOC1-ox developing leaves. Time course analyses of cell cycle genes in WT and TOC1-ox leaves over development. Plants were grown under LgD and samples were collected at ZT7. Leaves were cut in halves and gene expression was separately examined at the tip of leaves. Expression of (A) *CYCB1;1*, (B) *CYCD3;1,* (C) *CYCD3;2*, (D) *CYCD3;3*, (E) *CYCD4;1*, (F) *CDKA;1*, (G) *KRP1*, (H) *KRP2*, (I) *KRP4*, (J) *KRP7*, (K) *SIM*, (L) *SMR1*, (M) *SMR2*, (N) *SMR4*, (O) *SMR5*, (P) *SMR7*, (Q) *SMR8*, (R) *CCS52A2*, (S) *CDC6* and (T) *CDT1a* at the base of leaves. Relative expression was obtained by Q-PCR analyses. Data are represented as the mean + SEM of technical triplicates. The experiment was repeated twice, giving similar results.

5. The diurnal expression of cell cycle genes is altered in TOC1-ox

We next examined whether the expression of cell cycles genes followed a diurnal oscillatory trend and whether this oscillation was affected in TOC1-ox. Analyses of clock core gene expression in plants grown under LgD conditions at 7 or 14 das confirmed the reliability of the diurnal time course showing the proper rhythmic oscillation and its decreased expression in TOC1-ox (Figure 31A-D).

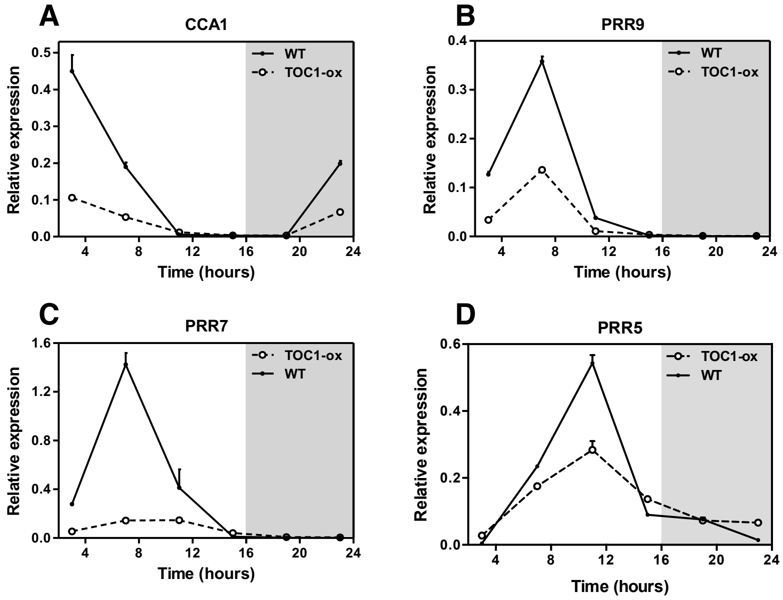

Figure 31. TOC1 acts as a repressor of the circadian clock network. Time course analyses of circadian clock genes over a diurnal cycle. Plants were grown under LgD and samples were collected at (A and B) 7 das and (C and D) 14 das every 4h over a 24h cycle. Expression of (A) *CCA1*, (B) *PRR9*, (C) *PRR7* and (D) *PRR5*. Relative expression was obtained by Q-PCR analyses. Data are represented as the mean + SEM of technical triplicates. The experiments were repeated at least twice.

For cell cycle genes, we found a slight oscillation of *CYCDs* showing higher expression during the day and lower during the night (Figure 32A-C). Consistent with an antagonistic function, *KRP2* expression followed an inversed trend with higher expression during the night (Figure 33A-C). In TOC1-ox, *CYCDs* were up-regulated, particularly close to dusk, and also before dawn for *CYCD3;2*. The up-regulation of *CYCD3;1* before dusk was not so evident at Zeitgeber Time 7 (ZT7; ZT0: lights-on), the time point of the developmental expression analyses. The results highlight the importance of full time course diurnal analyses to obtain a view of the regulatory interactions. The expression of *KRP2* in TOC1-ox showed a slight but reproducible up-regulation during the day and down-regulation during the night at 7 das (Figure 33A), 14 (Figure 33B) and 18 das (Figure 33C). *KRP7* also followed a similar trend of expression (Figure 33D). Consistent with the developmental results, the expression of *SMR5* was severely reduced in TOC1-ox at all time points (Figure 33E). For *SMR7*, the peak of expression was delayed in TOC1-ox with a clear down-regulation at ZT7, the time point used for the developmental time course (Figure 33F). The expression of other genes (e.g. *E2Fa*) was not clearly oscillating although the expression was affected in TOC1-ox (Figure 32D).

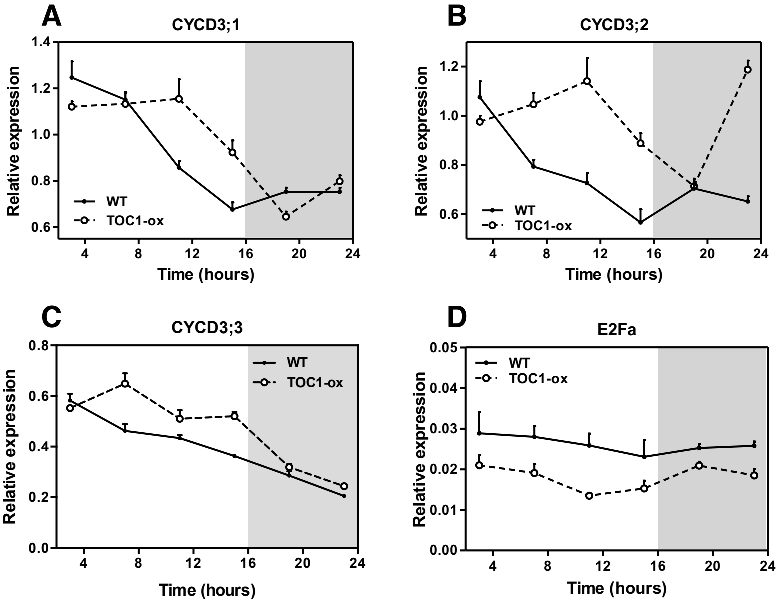

Figure 32. TOC1 regulates the diurnal expression of G1/S phase transition cell cycle genes. Time course analyses of cell cycle genes over a diurnal cycle under LgD at 7 das every 4h over a 24h cycle. Expression of (A) *CYCD3;1*, (B) *CYCD3;2*, (C) *CYCD3;3*, and (D) *E2FA*. Relative expression was obtained by Q-PCR analyses. Data are represented as the mean + SEM of technical triplicates. The experiments were repeated at least twice.

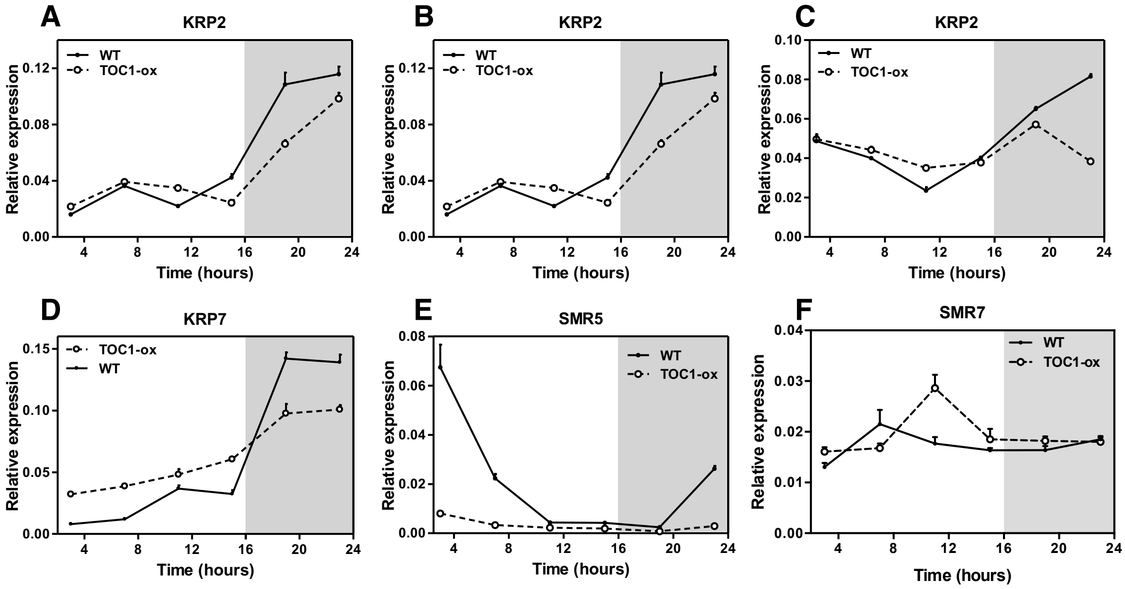

Figure 33. TOC1 regulates the diurnal transcriptional expression of CDK inhibitors. Time course analyses of cell cycle genes over a diurnal cycle under LgD at (A,D-F) 7 das, (B) 14 das and (C) 18 das every 4h over a 24h cycle. Expression of (A-C) *KRP2*, (D) *KRP7*, (E) *SMR5* and (F) *SMR7*. Relative expression was obtained by Q-PCR analyses. Data are represented as the mean + SEM of technical triplicates. The experiments were repeated at least twice.

Based on the gene expression profiles from our developmental assays, we also examined endocycle genes such as *CCS52A2* and *CDC6* at later stages of growth (18 das). Our results showed that *CCS52A2* expression was down-regulated in TOC1-ox throughout the diurnal time course (Figure 34A). We also observed an acute up-regulation of *CDC6* in WT leaves that was completely abolished in TOC1-ox (Figure 34C), suggesting that over-expression of TOC1 strongly represses this induction. A similar severe repression was observed at 14 das (Figure 34B). Compared to WT, *CDC6* expression rose at the mid-, end-of night in TOC1-ox (Figure 34B and C), which indicates that other components are able to overcome the repressive function of TOC1 after dusk. We found that the diurnal peak of *CDC6* coincided with a very low expression of *TOC1* and conversely, the high expression of *TOC1* correlated with low expression of *CDC6* (Figure 34D).

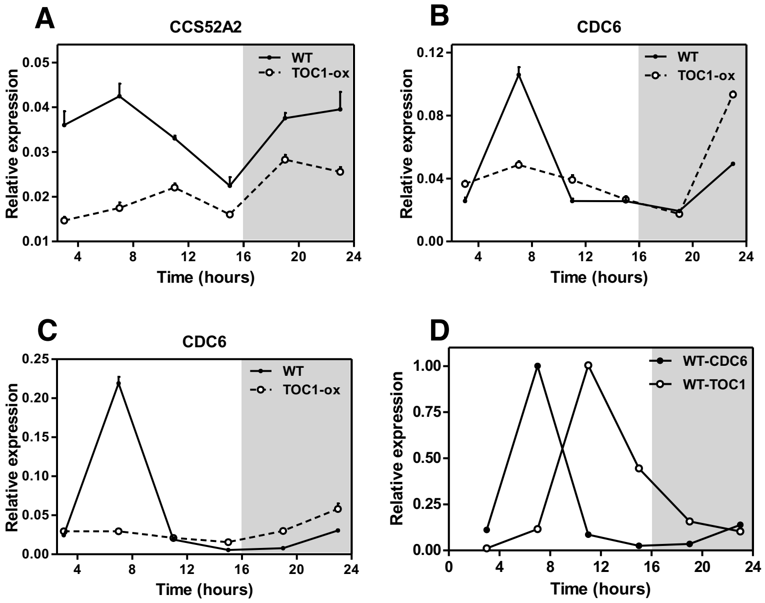

Figure 34. TOC1 regulates the diurnal expression of endocycle related genes. Time course analyses of cell cycle genes over a diurnal cycle under LgD at (B) 14 das and (A and C-D) 18 das every 4h over a 24h cycle. Expression of (A) *CCS52A2*, (B-D) *CDC6*, and (D) *TOC1*. Relative expression was obtained by Q-PCR analyses. Data are represented as the mean + SEM of technical triplicates. The experiments were repeated at least twice.

Notably, a similar oscillation was observed in the expression of the S-phase marker Histone 4 (H4) with a peak around midday that was delayed in TOC1-ox (Figure 35A). These results suggest the interesting possibility of a diurnal synchronization of the S-phase. To explore this possibility, we analyzed ploidy every 4h over a 24h LgD cycle in WT and TOC1-ox leaves. Despite the expected variation among the biological replicates, we found an interesting trend in the proportion of cells in S-phase, which accumulated during the mid-, late day in WT leaves. Notably, the oscillatory pattern of the S-phase population was clearly delayed in TOC1-ox (Figure 35B). Therefore, the S-phase follows an oscillatory trend that is controlled by the circadian clock through TOC1 repression of *CDC6* expression. This regulation might define a temporal window before dusk in which S-phase progression is favored.

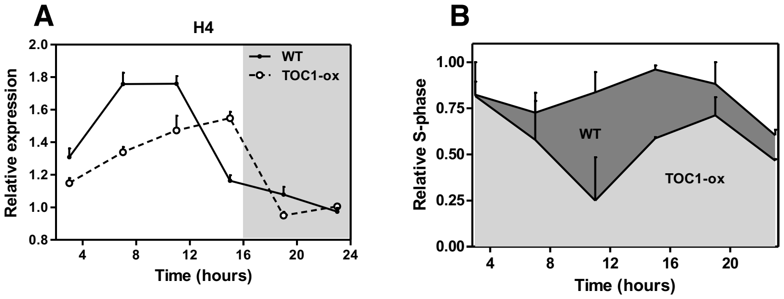

Figure 35. TOC1 controls the diurnal oscillation of the S-phase. (A) Time course analyses of *H4* over a diurnal cycle under LgD at 7 das. Relative expression was obtained by Q-PCR analyses. Data are represented as the mean + SEM of technical triplicates. (B) Estimation of S-phase occurrence by modeling with ModFit the ploidy profiles under LgD at 7 das. At least two biological replicates per experiment were performed.

6. TOC1 directly binds to the *CDC6* promoter

As TOC1 acts as a repressor that binds to the promoters of nearly all central oscillator genes, we next performed chromatin immunoprecipitation (ChIP) assays followed by Q-PCR analyses of the promoters of selected cell cycle genes. ChIP assays were performed with TOC1-ox plants (Huang et al., 2012) at 7 das using an anti-MYC antibody to immunoprecipitate the MYC-tagged TOC1 protein. Our results showed specific amplification of the promoter of *CDC6* (Figure 36A) while no amplification was observed for other promoters including for instance *CDKB1; 1*, *CYCA2;3*, *CYCB1;1, CDKA;1, ACTIN2* (*ACT2*) or when samples were incubated without antibody (-α). Analyses at later stages (14 and 22 das) also rendered amplification of the *CDC6* promoter while the promoters of other cell cycle genes were not significantly enriched (Figure 36B and C). We also monitored the possible oscillation of TOC1 binding by using ChIP assays with TMG seedlings, which express the *TOC1* genomic fragment fused to the yellow fluorescent protein in the *toc1-2* mutant background (Huang et al., 2012). Fold enrichment analyses following TOC1 immunoprecipitation with the anti-green fluorescent protein (GFP) antibody showed a clear amplification of *CDC6* promoter at ZT15 compared with ZT3 (Figure 36D).

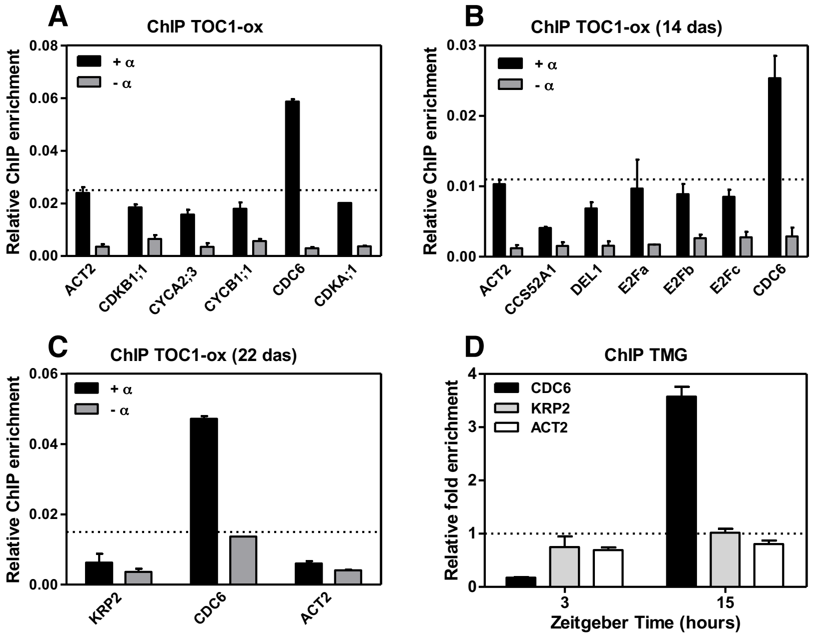

Figure 36. TOC1 binds to the *CDC6* promoter. (A-C) Chromatin immunoprecipitation (ChIP) assays with TOC1-ox plants examined at (A) 7, (B) 14, and (C) 22 das and sampled at ZT7 using an anti-MYC antibody to immunoprecipitate the MYC-tagged TOC1 protein. ChIP enrichment was calculated relative to the input. Samples were incubated with anti-MYC antibody (+α) or without antibody (-α). (D) ChIP assays with TMG plants grown under LgD and collected at ZT3 and ZT15. ChIPs were performed with an anti-GFP antibody to immunoprecipitate the GFP-tagged TOC1 protein. For comparisons of the different time points, fold enrichment was calculated relative to the input and to values without antibody (-α). At least two biological replicates per experiment were performed.

The binding to the *CDC6* locus occurs in a region containing a previously identified TOC1 binding motif (Huang et al., 2012), the so-called Evening Element (EE). Consistently, GUS (GLUCURONIDASE) activity of the *CDC6* promoter was reduced in protoplasts co-transfected with TOC1 while no effect was observed in mutated versions of the promoter lacking the EE (Figure 37A). Our results are noteworthy as CDC6 is key for both the mitotic cycle and the endocycle. The effects are not due to artifacts TOC1-ox plants as accumulation of TOC1 in *ztl-3* mutant plants also results in reduced *CDC6* expression (Figure 38A). Furthermore, if TOC1 controls the cell cycle through regulation of *CDC6* expression, down-regulation of *TOC1* should lead to the opposite phenotypes to those observed in TOC1-ox plants. Indeed, our results showed that *CDC6* expression was up-regulated in *toc1-2* and ZTL-ox compared to WT plants (Figure 38B and C).

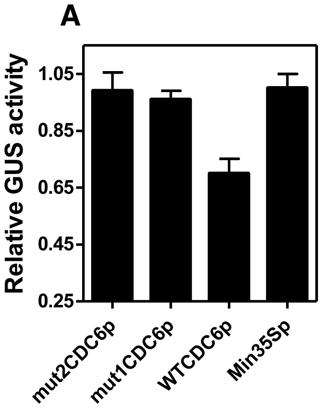

Figure 37. TOC1 binds to The Evening Element motif present at the *CDC6* promoter. (A) Relative GUS activity of WT *CDC6* promoter (WTCDC6p) and two mutated versions lacking the Evening Element (mut1CDC6p and mut2CDC6p). Activity was assayed in protoplasts co-transfected with TOC1. The Minimal 35S promoter (Min35Sp) was used as a control. Data are represented as the mean + SEM of technical triplicates. The experiments were repeated at least twice.

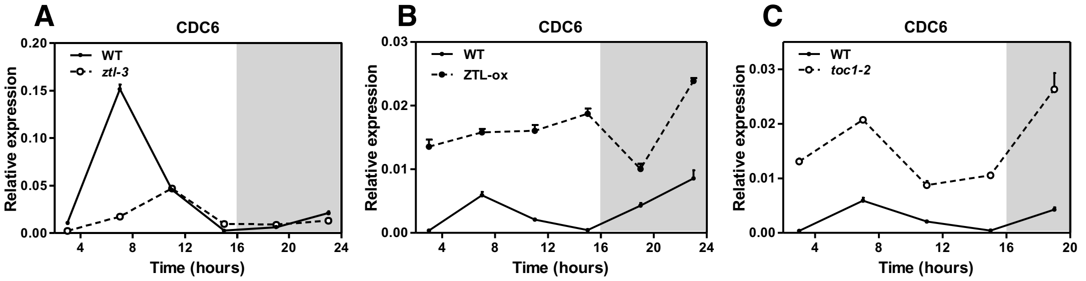

Figure 38. TOC1 and ZTL miss-regulation disrupts the oscillatory expression pattern of *CDC6*. Expression of *CDC6* in WT and (A) *ztl-3* mutant, (B) ZTL-ox and (C), *toc1-2* mutant plants. Plants were grown under LgD and samples were collected at 18 das every 4h over a 24h cycle. Relative expression was obtained by Q-PCR. Data are represented as the mean + SEM of technical triplicates. The experiments were repeated at least twice.

Previous studies have shown that over-expression of CDC6 increases somatic ploidy (Castellano et al., 2001). Our analyses confirmed the increased leaf size and ploidy of CDC6-ox plants (Figure 39A and B, 40A and B). To further confirm the direct link between TOC1 and CDC6, we performed genetic interaction studies using TOC1-ox plants transformed with the CDC6 over-expressing construct. Analyses of double over-expressing plants (ox/ox) showed that the reduced size of TOC1-ox plants was reverted by over-expression of CDC6 (Figure 41A and B). Furthermore, time course analysis by flow cytometry showed that the reduced ploidy and delayed enrichment of higher-order C values in TOC1-ox plants (Figure 42A, B, D and E) were overcome by over-expression of CDC6 (Figure 42A, C, D and F). Calculation of the Endoreplication Index also confirmed the recovery of the endoreplication activity (EI) (Figure 43A). A similar phenotypic reversion was observed in other double over-expressing lines (Figure 43B). These results suggest that the reduced expression of CDC6 contributes to the observed phenotypes in TOC1-ox. Although it is possible that TOC1 may directly regulate other checkpoint factors or regulators of cell cycle progression, our data are consistent with the direct binding of TOC1 to the *CDC6* promoter to control its developmental and diurnal transcriptional expression.

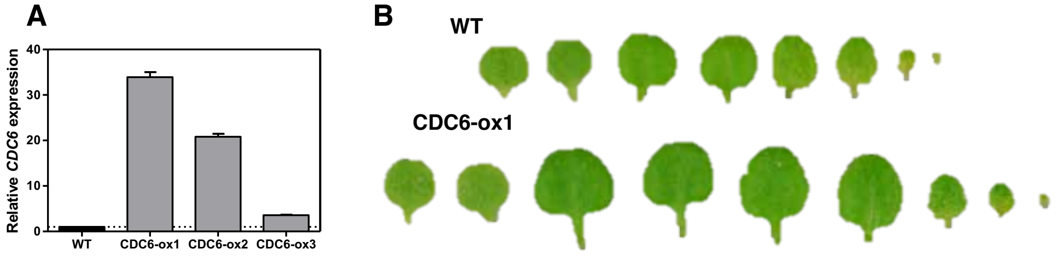

Figure 39. CDC6 over-expression leads to an increased leaf size. (A) Relative *CDC6* expression in WT and three different lines over-expressing CDC6. Samples were collected at ZT7. Relative expression was obtained by Q-PCR. Data is presented relative to WT and represented as the mean + SEM of technical triplicates. (B) Representative images of WT and CDC6-ox leaves. Plants were grown under LgD. The experiments were repeated at least twice.

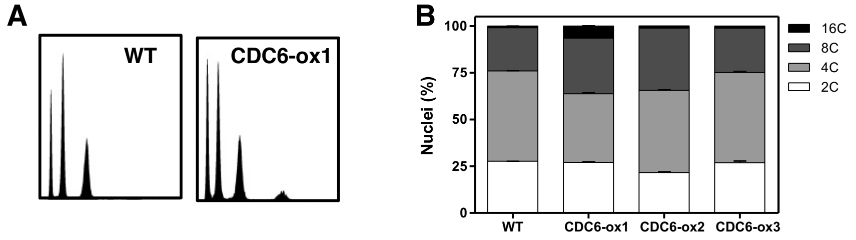

Figure 40. *CDC6* over-expression increases endoreplication in developing leaves. (A) Ploidy distribution by flow cytometry of WT and CDC6-ox line 1 of the first pair of leaves at 9 das. (B) Proportion of polyploid nuclei in WT and three different CDC6-ox lines. Data are represented as the mean + SEM of n ≈ 10000 nuclei. Plants were grown under LgD. The experiments were repeated at least twice.

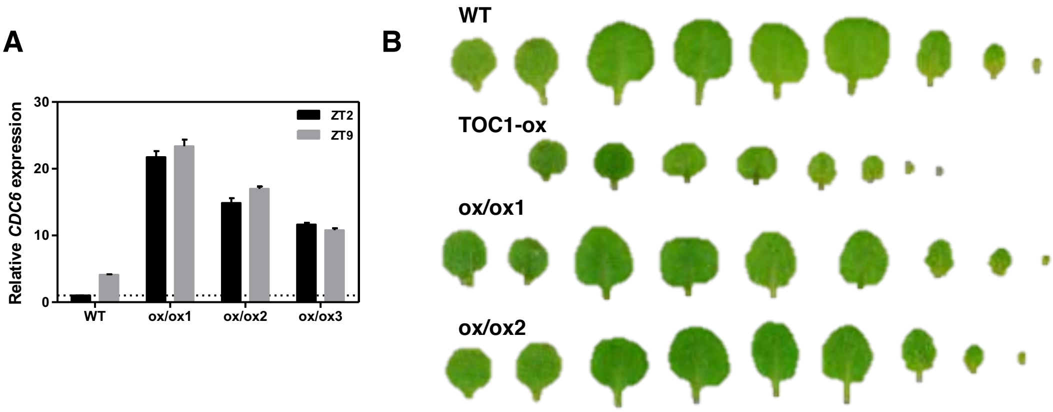

Figure 41. Over-expression of *CDC6* rescues the growth phenotype of TOC1-ox plants. (A) Relative *CDC6* expression in WT and three different double CDC6 and TOC1 over-expressing lines (ox/ox). Samples were collected at ZT2 and ZT9. Data is presented relative to WT ZT2 and represented as the mean + SEM of technical triplicates. (B) Representative images of WT, TOC1-ox and CDC6-ox/TOC1-ox leaves. Plants were grown under LgD. The experiments were repeated at least twice.

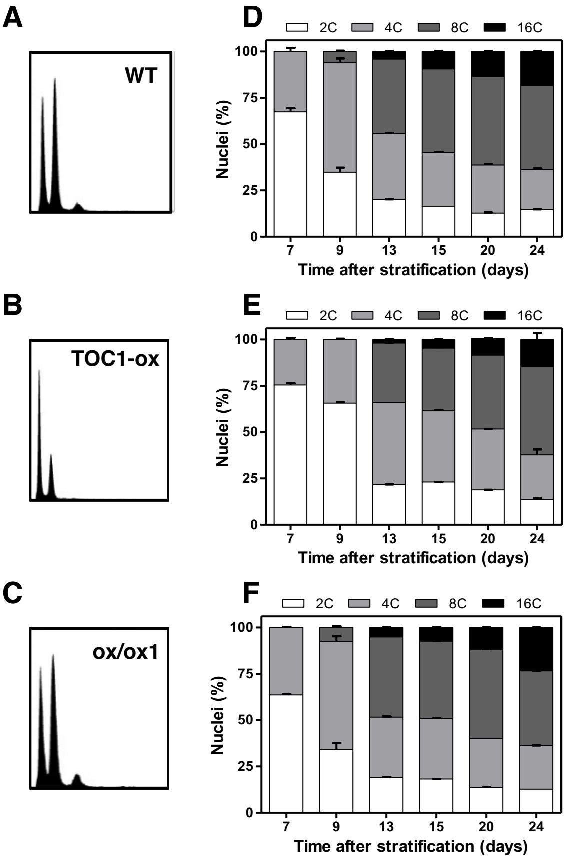

Figure 42. Over-expression of *CDC6* rescues the ploidy phenotype of TOC1-ox plants. Ploidy distribution by flow cytometry of (A) WT, (B) TOC1-ox, and (C) CDC6-ox/TOC1-ox (ox/ox1) first pair of leaves at 9 das. Kinematics of polyploid nuclei in (A) WT, (B) TOC1-ox and (C) CDC6-ox/TOC1-ox line 1 (ox/ox1). Plants were grown under LgD. Data are represented as the mean + SEM of n ≈ 10000 nuclei. At least two biological replicates per experiment were performed.

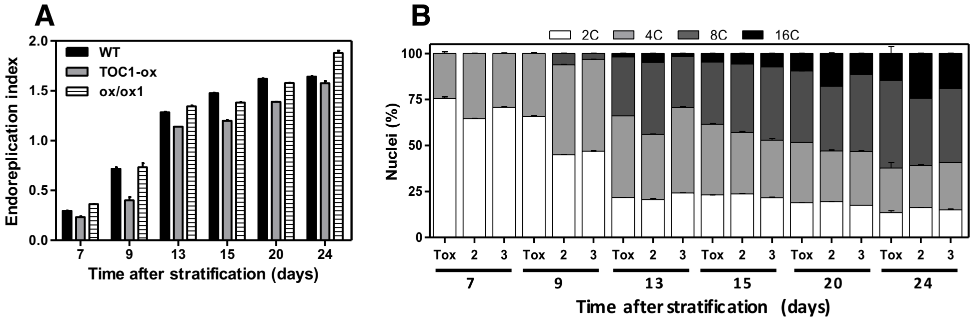

Figure 43. Over-expression of *CDC6* rescues the ploidy phenotype of TOC1-ox plants. (A) Endoreplication index in WT, TOC1-ox and CDC6-ox/TOC1-ox line 1 (ox/ox1) leaves. (B) Kinematics of polyploid nuclei in TOC1-ox (Tox) and two CDC6-ox/TOC1-ox lines (2 and 3). (A and B) Plants were grown under LgD. Data are represented as the mean + SEM of n ≈ 10000 nuclei. At least two biological replicates per experiment were performed.

7. Tumor progression is affected in TOC1-ox inflorescence stalks

If TOC1 regulates the cell cycle, then cellular systems in which the cell cycle is miss-regulated should display a differential response in WT versus TOC1-ox plants. To explore this possibility, we monitored if the slow pace of the cell cycle in TOC1-ox correlated with delayed tumor growth. To that end, we inoculated the bases and first internodes of inflorescence stalks with a virulent *Agrobacterium tumefaciens* strain (A281) (Deeken et al., 2003). The T-DNA contains the *β-glucuronidase* (*GUS*) gene so that tumor development can be followed after infection. At 5 days after inoculation (dai), staining was readily observed as small blue foci of variable sizes (Figure 44A, left two images, Figure 46A). The areas of GUS foci were considerable increased at 7 dai, forming bigger and strongly stained patches (Figure 44A, right image). The staining appeared higher in tumors at the base of the stalks than at the internodes (Figure 44A). Tumors were also observed in TOC1-ox stalks and internodes (Figure 44B and 46B). However, the small and medium size GUS foci were clearly reduced compared to WT (Figure 45A and B). Comparative analyses of the proportion of the different areas clearly showed an enrichment of bigger patches in WT compared to TOC1-ox (Figure 45C and 46C). The reduction in GUS foci area in TOC1-ox was even more evident at the first internode (Figure 45D-F). No staining or other visible phenotypes were observed when plants were inoculated with the non-tumorigenic *Agrobacterium* strain GV3101 (Figure 46A and B). Altogether, our results suggest that the slowed cell cycle and reduced S-phase duration in TOC1-ox might contribute to the observed delay in tumor progression.

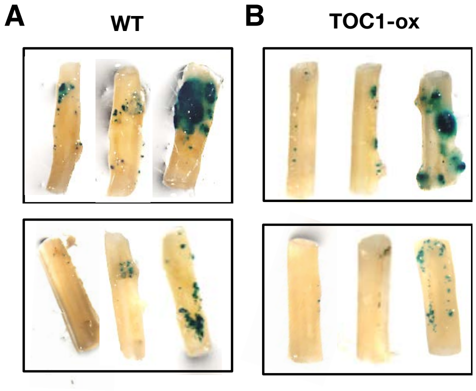

Figure 44. Tumor progression is delayed in TOC1-ox. Representative images of inflorescence stalks inoculated with the *Agrobacterium* virulent strain A281 at the base of inflorescence stalks in (A upper image) WT and (B upper image) TOC1-ox at 5 dai (left two images) and 7 dai (right images). Inoculations were also performed at the first internode of (A lower image) WT and (B lower image) TOC1-ox. At least 15 stalks per genotype were inoculated and GUS stained.

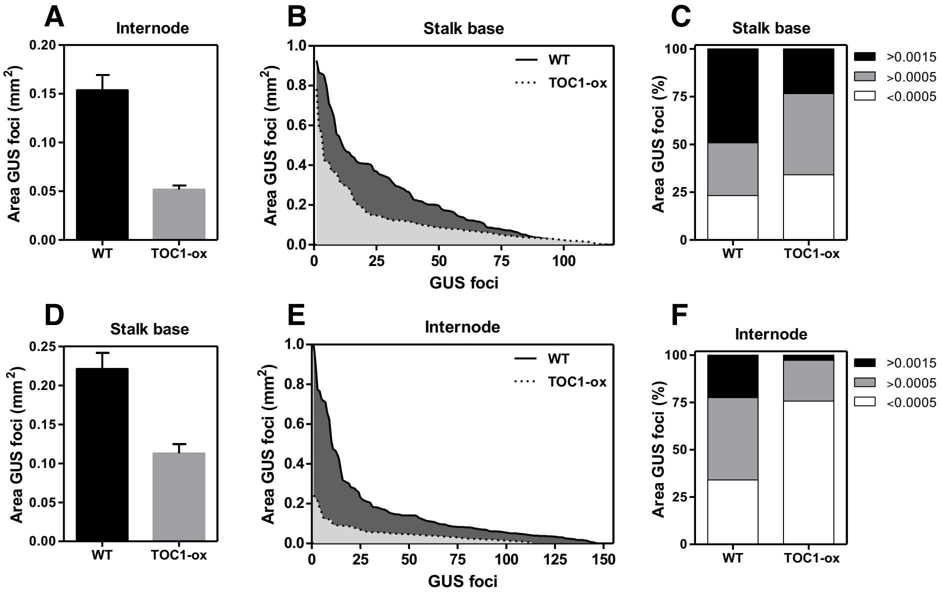

Figure 45. Quantification of the delayed tumor progression in TOC1-ox. Mean area of small and medium GUS foci at the (A) base of inflorescence stalks and in the (D) first internode. Distribution of the different GUS areas (B and E) and proportion of sizes (C and F) at the (B and C) base and at the (E and F) first internode of inflorescence stalks. Graphs represent the mean + SEM of n ≈ 110 foci. At least two biological replicates were performed.

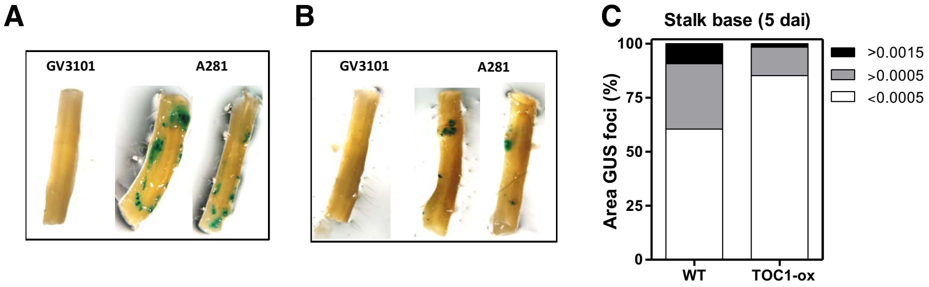

Figure 46. Tumor progression is delayed in young TOC1-ox inflorescence stalks. Representative images of inflorescence stalks inoculated with the *Agrobacterium* non-virulent strain GV3101 and virulent strain A281 at the base of inflorescence stalks in (A) WT and (B) TOC1-ox at 5 dai. (C) Distribution of the proportion of sizes of the different GUS areas at the base of inflorescence stalks at 5 dai. Graphs represent the mean +SEM of n ≈ 110 foci. At least two biological replicates were performed.

DISCUSSION

Discussion

In this Thesis we have addressed a key question regarding the circadian clock control of organ growth in *Arabidopsis*. We have found that the circadian clock, through the function of the core clock component TOC1, regulates the G1/S phase transition during the mitotic cycle in young developing leaves, as well as the progression of the endocycle during later stages of leaf development and during hypocotyl growth. This correlated with changes in the developmental and diurnal expression of key genes of the cell cycle machinery. More specifically, we have discovered that TOC1 safeguards the G1/S phase transition by direct binding and repression of the DNA replication licensing factor *CDC6*. Moreover, the role of TOC1 in the control of the cell cycle was verified by analyzing tumor progression in *Arabidopsis*. Further studies of the cell cycle in different circadian clock mutants might help to identify other possible clock components important for cell cycle progression.

Coordination of the cell cycle progression is essential for proper regulation of post-embryonic plant development. This coordination is particularly important when cells undergo cell division to form new cell types and tissues. They can also sense changes in the environment and therefore alter the rate of cell proliferation and differentiation. Many of the cell cycle regulators show differential expression patterns when subjected to diverse external cues (Peres et al., 2007). This shows that cells can integrate exogenous and endogenous signals to decide whether or not to progress from the G1 to the S-phase.

Regulation of the G1/S transition is essential for proper cell cycle progression as cells only commit to division once they have replicated their DNA (Johnson and Skotheim, 2013). Our results show that TOC1 regulates the proper timing of the G1-to-S-phase transition, as indicated by the relative duration of the G1 and S phases as well as by the delayed S-phase entrance. These results are fully consistent with the slow cell division rate and the reduced progression of cell number observed in TOC1-ox developing leaves. Inhibition of cell proliferation in leaves is often associated with cell expansion. This mechanism is known as compensation, and reduces the impact of decreased cell number on organ size (Beemster et al., 2006). In TOC1-ox, both cell number and cell size are affected and hence the overall leaf area is reduced. The reduction might be due to uncoupled cell division and cell growth in TOC1-ox. It is also possible that there is a threshold below which compensation is induced (Horiguchi et al., 2006) so that the cell number reduction in TOC1-ox does not reach such as threshold.

Similar reduction in cell number and area are observed in the *ztl-3* mutant plants. In the absence of a functional ZTL, TOC1 protein accumulates, mimicking the effect of TOC1 over-expressing plants. The opposite phenotypes are observed in *toc1-2* mutant plants, where more cells are produced at younger stages of development while displaying increased cell sizes. These phenotypes reinforce our conclusions regarding the role of TOC1 controlling proper timing of the G1/S-phase transition. The function of TOC1 in the mitotic cycle resembles that of the mammalian circadian component NONO, an interacting partner of the clock protein PERIOD that circadianly gates the S-phase in fibroblasts (Kowalska et al., 2013). It would be interesting to check whether in addition to TOC1, other clock components in plants contribute to the regulation of the cell cycle at different cell cycle phases. Studies in unicellular and multicellular algae have shown that the circadian clock regulates the growth phase and gates this process to the night (Sweeney and Hastings, 1958, Edmunds and Laval-Martin, 1984, Carre and Edmunds, 1993, Goto and Johnson, 1995, Makarov et al., 1995, Mori et al., 1996, Nikaido and Johnson, 2000, Serrano et al., 2009). Indeed, DNA replication during the cell cycle is limited to the night through circadian regulation most likely to avoid DNA damage by the UV radiation during the day (Nikaido and Johnson, 2000).

Our results opened the question about the mechanism responsible for the alteration of the cell cycle progression in plants miss-expressing TOC1. To address this question, we first focused on the pattern of expression of the core cell cycle machinery during leaf development. Although post-translational regulation of cell cycle components is crucial for cell cycle function, the transcriptional regulation of cell cycle genes is highly important for cell cycle progression (Beemster et al., 2005, Menges et al., 2005). Furthermore, there is a clear correlation between transcribed cell cycle genes and their protein accumulation in yeast and human cells. We found that during the mitotic cycle, the developmental expression of several cell cycle genes was altered in TOC1-ox plants. Genes affected include the D-type cyclins, which have essential roles for cell cycle responses to nutrients and hormones during the G1/S-phase transition (Riou-Khamlichi et al., 1999, Menges and Murray, 2002). The observed transcriptional changes correlated well with the phenotypes of the slow cycle in TOC1-ox. The phenotypes also correlated with the changes in the expression of the KRP inhibitors, which were increased at early stages and decreased at later stages of leaf development. KRP2 not only inhibits cell proliferation but its weak over-expression inhibits CDKA;1 activity and leads to increased polyploidy (Verkest et al., 2005). Therefore, the increased accumulation of KRP2 at early stages is consistent with the decreased cell number, while the decreased accumulation later in development agrees with the reduced endoreplication in TOC1-ox. The expression of *SMR5* and *SMR7* was also clearly altered in TOC1-ox. SMR5 and SMR7 are important for cell cycle checkpoint activation following DNA damage by ROS (Yi et al., 2014). Although SMR5 and SMR7 over-expression promotes endoreplication, the corresponding knock-outs display no altered ploidy (Yi et al., 2014), suggesting that the effects of TOC1-ox on their expression might rather be linked to altered ROS response.

The transcriptional miss-expression of the cell cycle core machinery was observed in the tip and bases of leaves along development. Overall, the trends of expression were similar, indicating that despite the spatio-temporal regulation of entry and exit from the mitotic cycle in proliferating leaves, TOC1 is able to ultimately regulate the cell cycle progression by altering the expression of its molecular machinery on the whole leaf. Our findings suggest that the circadian clockwork constitutes an additional layer of transcriptional regulation of the cell cycle components. Similar transcriptional regulations have been reported in other organisms such as unicellular algae (Goto and Johnson, 1995) or mammalian cells (Matsuo et al., 2003), which indicate that transcriptional cell cycle control is a common feature for the circadian regulation of the cell cycle progression.

Our gene expression analyses revealed that a disrupted clock alters not only the expression of genes involved in the mitotic cycle but also the expression of components needed for the entrance and maintenance of the endocycle. These results opened the question of the importance of the circadian clock in the regulation of endoreplication in growing organs during development. Multiple layers of endogenous and exogenous signals converge to ensure proper regulation of the endocycle. Tight control of the endocycle progression is essential for the coordinated growth of diverse plant organs and for the maintenance of cell fate (Bramsiepe et al., 2010). The physiological and molecular analyses performed in this study indicated that the circadian clock controls nuclear DNA replication in leaves through TOC1 function. TOC1-ox delays the endocycle activity and conversely, loss of TOC1 function accelerates this event. Proper regulation of endoreplication provides a means to increase gene copy number and to ensure increased protection against irradiation (Traas et al., 1998). Thus, the circadian clockwork might provide proper timing information for endoreplication to fulfill these functions.

The time between seed germination and the establishment of the first true leaves constitutes a crucial period in plant development. Right after germination, seedlings need to accurately control their overall growth in order to reach photosynthetic success. Thus, hypocotyl elongation enables buried seedlings to reach the light. Because of the embryonic origin of *Arabidopsis* hypocotyls, their growth mostly relies on cell expansion rather than cell division after germination (Gendreau et al., 1997). Miss-expression of TOC1 perturbs hypocotyl cell expansion and affects the successive rounds of DNA replication. Although polyploidy is not necessarily coupled with elongation, and endoreplication might not have the same sensitivity threshold as cell expansion (Vandenbussche et al., 2005), the inverse correlation of the endocycle activity in lines accumulating increasing amounts of TOC1 suggests an important connection of TOC1 with replication of the nuclear genome. Altering the timing of DNA synthesis by higher or lower than WT expression of *TOC1* slows-down or speeds-up the successive rounds of endoreplication, respectively. Light not only inhibits hypocotyl elongation but also reduces one round of endoreplication in comparison with dark-grown seedlings (Gendreau et al., 1997). Proper expression of TOC1 might thus regulate this repression such that TOC1-ox plants are hypersensitive to the light-dependent repression of endoreplication while reduced expression of TOC1 attenuates this response. Thus, the endocycle activity might be part of a circadianly controlled developmental program.

Our results thus indicate that proper circadian function is important for the appropriate progression of both the mitotic cycle and the endocycle. The coordinated transition of these events is essential for plant growth. They also share some molecular components, which seem to exert different roles depending on the cell cycle variant taking place. A threshold in their expression was also proposed to play a role determining which cycle variant dominates depending on the developmental stage. From our data, we conclude that the circadian clock works as a key mechanism regulating the exit of the mitotic cycle an entry of the endocycle in response to changes in the environment in order to achieve optimal growth rate.

Strict control of S-phase entry is crucial as DNA replication occurs during this phase. In our study we found that TOC1 acts as a repressor of *CDC6* expression by direct binding to its promoter. The downregulation of *CDC6* in TOC1-ox explains why both the cell division and endoreplication are affected as these factors, are required for the S-phase progression during both cycles (Castellano et al., 2001, Castellano Mdel et al., 2004). In *S. pombe*, CDC18/ CDC6 over-expression induces multiple rounds of DNA replication (Nishitani and Nurse, 1995, Jallepalli and Kelly, 1996) while extra rounds of endoreplication were observed by CDC6 over-expression in cultured megakaryocytes (Bermejo et al., 2002). TOC1-ox plants are dwarf. In humans, mutations in the genes encoding components of the pre-replication complex, including *CDC6* were linked to the Meier–Gorlin Syndrome (MGS), an autosomal recessive disorder characterized by primordial dwarfism (short-stature, microcephaly) (Bicknell et al., 2011). Ensuring that DNA replication only occurs under “safe” conditions is essential for maintaining genome integrity, and thus, TOC1 regulation of *CDC6* might allow or delay DNA licensing in consonance with external and internal cues.

Diurnal expression of other cell cycle key components showed a clear oscillation and an altered expression in plants over-expressing TOC1. It is possible that the changes in *CDC6* expression trigger a cascade of transcriptional changes in other cell cycle genes in order to accommodate the “unexpected” down-regulation of *CDC6* in TOC1-ox plants. It is also possible that the alteration of other clock components by TOC1-ox affect other cell cycle checkpoints. Regardless the additional possible clock components also regulating the cell cycle, our results clearly indicate that the circadian clockwork through TOC1 maintains the appropriate pace of the cell cycle not only during development but also during the diurnal cycle.

Previous studies in *Arabidopsis* (Castellano et al., 2001) as well as our own results have shown that over-expression of CDC6 results in bigger plants with higher somatic ploidy. CDC6 is a key component of the DNA pre-replication complex; its location on the DNA during the late G1-phase will determine the origins of DNA replication that will be activated during the S-phase (Costas et al., 2011). The observed phenotypes are likely due to an increased number of licensed, active origins of replication as a consequence of the higher abundance of functional CDC6 protein. However, in addition to CDC6 other components are necessary to complete the pre-replication complex. All these components eventually allow the docking of the DNA helicase (MCM complex) responsible for the establishment of the replication fork, which will mark the start of DNA replication during the S-phase. Two possible scenarios could explain the phenotypes observed in CDC6-ox plants. In the first one, it is possible that the higher level of CDC6 triggers the induction of the other elements needed to complete the formation of the pre-replication complex (CDT1, ORC and MCM proteins). Increased components will be therefore necessary to cover the higher number of licensed DNA origins marked by CDC6 so that they can become active and serve as initiation points of DNA replication.

It is also possible that the increased CDC6-bound-DNA regions somehow induce the accumulation of the remaining members of the pre-replication complex. In any of these two scenarios, the higher number of active DNA origins poses an induction in the amount or in the activity of the elements needed for the establishment of the replication fork and the initiation of DNA replication in order to reach higher than WT somatic ploidy levels. A more precise study of the molecular signaling cascades triggered by CDC6 over-expression will be needed in order to elucidate the mechanism of DNA replication enhancement.

Genetic interaction analyses showed that the dwarf phenotypes and reduced somatic ploidy levels displayed in TOC1-ox plants were reverted when CDC6 was also over-expressed. The restoration of the phenotypes reinforces the idea that TOC1 regulates the cell cycle by repressing *CDC6* expression. The direct binding of TOC1 to the *CDC6* promoter and the GUS activity assays with versions of the *CDC6* promoter in which the TOC1 DNA binding motif was mutated confirmed this notion. Our data indicates that the function of TOC1 is essential for the proper expression of *CDC6* and therefore the establishment of DNA origins of replication during the late G1-phase.

Human cancer is characterized by increased cell proliferation, invasion and metastasis. Among many others, several DNA replication initiation proteins are over-expressed in human cancers. We found that the reduced expression of *CDC6* in TOC1-ox correlates with the slow progression of tumors. Notably, a recent study has shown that miR26 represses replication licensing and tumorigenesis by targeting *CDC6* in lung cancer cells (Zhang et al., 2014). A similar situation might be happening in plants in which TOC1 represses *CDC6* expression. Loss of circadian function increases the susceptibility to cancer and affect anticancer treatments (Brown, 2014). In this scenario, several research lines are focusing on the possible modulation of clock-related proteins as an effective anticancer strategy. Our study opens the possibility of incorporating the circadian clockwork for the prevention of crown gall in crops. As previously proposed (Brown, 2014) and beyond cancer prevention, we envision a circadian system that moves past its canonical function as a 24h timer and serves as a flexible metronome that modulates complex cellular processes in organisms.

Altogether, we have used in this study a combination of physiological, molecular and biophysical approaches to follow the progression of the cell cycle and to show that the circadian clock controls the overall duration of the cell cycle by modulating the S-phase in *Arabidopsis*. The circadian clock component TOC1 operates by binding to the promoter of the DNA replication factor *CDC6* to repress its diurnal expression. Thus, miss-expression of TOC1 not only changes the pace of the clock but also affects cell division during the mitotic cycle and endoreplication during the endocycle. Cell size and number, somatic ploidy, organ size and the overall plant growth are coordinated and regulated by the clock in synchronization with the environment. By controlling the pace of the cell cycle, the circadian clock not only regulates normal growth but also tumor progression in *Arabidopsis* (Figure 47).

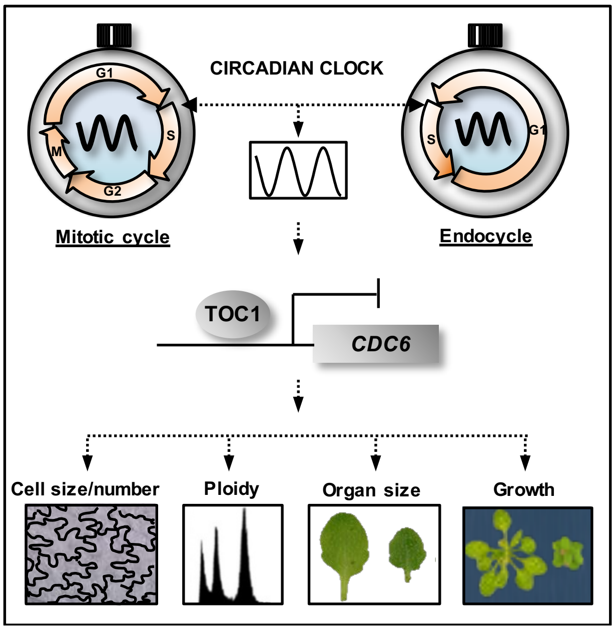

Figure 47. Schematic representation depicting the connection between the circadian clock and the cell cycle in Arabidopsis. The circadian clock modulates the timing of the cell cycle through the rhythmic binding of TOC1 to the promoter of the DNA replication factor *CDC6*. Regulation of the S-phase affects both the mitotic cycle and the endocycle so that cell size and number, somatic ploidy, organ size and overall plant growth are affected in plants miss-expressing TOC1. Ensuring that DNA replication only occurs under “safe” conditions is essential for maintaining genome integrity, and thus, TOC1 regulation of *CDC6* might allow or delay DNA licensing in consonance with external and internal cues.

CONCLUSIONS

Conclusions

In this Doctoral Thesis we found that the circadian clock sets the pace of the cell cycle, controlling both the mitotic cycle and the endocycle. The clock component TOC1 regulates the expression of the DNA replication licensing gene *CDC6* by direct binding to its promoter. We found that the concerted interplay of the clock and the cell cycle controls plant growth. More specifically, the main conclusions of our studies include:

1. **The circadian clock, through TOC1 function, modulates growth and the mitotic cycle at early stages of leaf development.** Leaf area, cell number and cell size are affected in plants miss-expressing TOC1. The cell division rate is slowed down in TOC1 over-expressing plants due to an extended G1-phase and shortened S-phase.

2. **The circadian clock, through TOC1 function, modulates endoreplication and cell expansion in hypocotyl cells and developing leaves.** Time course analyses of ploidy profiles by flow cytometry showed that somatic ploidy and the endoreplication index are clearly affected in hypocotyls and developing leaves of plants miss-expressing TOC1.

3. **TOC1 regulates the developmental expression of core cell cycle genes involved in proliferation and endoreplication.** Developmental time course analyses showed that the expression of key cell cycle genes is altered in developing leaves of TOC1 over-expressing plants.

4. **TOC1 regulates the diurnal expression of core cell cycle genes involved in proliferation and endoreplication.** Diurnal time course analyses showed that the expression of key cell cycle genes is altered in developing leaves of TOC1 over-expressing plants.

5. **TOC1 regulates the cell cycle by direct binding to the promoter of the DNA replication licensing factor CDC6.** Chromatin immunoprecipitation

assays with plants over-expressing TOC1 and with plants expressing TOC1 under its own promoter showed that TOC1 binds to *CDC6* locus and that this binding is rhythmic. Mutation of the TOC1 binding motif at the *CDC6* promoter reduces the repression.

6. **The genetic interaction between TOC1 and CDC6 confirms that the circadian clock through TOC1 function regulates the cell cycle by repressing the expression of *CDC6***. Over-expression of CDC6 in plants over-expressing TOC1 rescue the ploidy and size phenotypes observed in TOC1-ox, confirming that TOC1 indeed function through repression of *CDC6*.

RESUMEN EN CASTELLANO

Resumen en castellano

La función circadiana es esencial para el crecimiento y adaptación de las plantas a su entorno. La maquinaria molecular responsable de la generación de ritmos circadianos está basada en la expresión rítmica de genes cuyo pico de expresión oscila en diferentes fases durante el día y la noche. Los ritmos de expresión génica se traducen en oscilaciones de procesos fisiológicos y de desarrollo. El crecimiento de las plantas está regulado por una plétora de procesos que en última instancia operan a través del control de la proliferación y diferenciación celular. La proliferación celular depende de la progresión del ciclo mitótico, el cual está dividido en 4 fases: S (Síntesis del ADN), M (Mitosis) y de las interfases G1 y G2 (en inglés Gap 1 y 2) que ocurren antes de las fases S y M respectivamente. El proceso de diferenciación celular coincide con el cambio al endociclo, una variante del ciclo mitótico en la que el ADN genómico se duplica pero sin posterior división, es decir en ausencia de fase M. Aunque la regulación circadiana y el ciclo celular han sido individualmente estudiados en plantas, no se ha demostrado hasta la fecha la posible conexión de ambos ciclos en plantas. El trabajo realizado durante esta Tesis Doctoral se ha centrado en el estudio del papel del reloj circadiano en el control del ciclo celular durante la regulación del crecimiento de la planta. Los resultados obtenidos muestran que plantas con un reloj circadiano de ritmo lento desaceleran la progresión del ciclo celular, mientras que un reloj de ritmo rápido lo acelera. El componente esencial del reloj denominado en inglés TIMING OF CAB EXPRESSION 1 (TOC1) controla la transición de la fase G1 a la fase S, regulando así el ritmo del ciclo mitótico durante los estadios tempranos del desarrollo foliar. Asimismo, TOC1 también controla la ploidía somática característica del endociclo durante estadios tardíos del desarrollo foliar y en las células del hipocotilo. Utilizando técnicas de citometría de flujo y parámetros de cinéticas de crecimiento foliar se pudo determinar que en plantas que sobre-expresan TOC1 la fase S es más corta, lo que se correlaciona con la represión diurna del gen *CELL DIVISION CONTROL 6* (*CDC6*). Este gen codifica un factor esencial en la formación de los complejos de pre-replicación que determinan los orígenes de replicación del ADN. Mediante técnicas de inmunoprecipitación de cromatina encontramos que la represión de *CDC6* ocurre a través de la unión directa de TOC1 al promotor de *CDC6*. Los análisis de interacción genética demostraron que los fenotipos de crecimiento reducido y de ploidía somática alterada observados en plantas que sobre-expresan TOC1, quedaban revertidos al sobre-expresarse también CDC6. Estos resultados confirman que la función de TOC1 en el ciclo celular ocurre en gran medida a través de la represión de *CDC6*. La desaceleración de la progresión del ciclo celular en plantas que sobre-expresan TOC1 afecta no solo el desarrollo de los órganos de la planta, sino también el desarrollo tumoral en los tallos de las inflorescencias. Por lo tanto, nuestros estudios demuestran que la función de TOC1 es importante en la regulación rítmica de la maquinaria pre-replicativa del ADN para controlar el crecimiento de las plantas en resonancia con el medio ambiente.

SUMMARY IN ENGLISH

Summary in english

The circadian function is essential for plant growth and its adaptation to the environment. The molecular machinery responsible for the establishment of the circadian rhythmicity relies on the rhythmic oscillation of differentially expressed genes with different peaks of expression along the day and night. The rhythms in gene expression are translated into oscillations of physiological and developmental processes. Plant growth is controlled by a plethora of different processes that ultimately work through the control of cell proliferation and differentiation. Cell proliferation relies on the proper progression of the mitotic cycle, which is divided in 4 phases: S (DNA synthesis), M (Mitosis) and two gap phases G1 and G2, that take place before S and M phases, respectively. Cell differentiation coincides with the entry into the endocycle, a variant of the mitotic cycle in which genomic DNA duplicates without further division or mitosis. Even though the circadian clock and cell cycle as separate pathways have been well documented in plants, the possible direct interplay between these two cyclic processes has not been previously addressed. The work performed during this Thesis has focused on the characterization of the role of the circadian clock in the control of the cell cycle during plant growth. We found that plants with slower than Wild-Type circadian clocks slow down the progression of the cell cycle, while plants with faster clocks speed it up. The core clock component TIMING OF CAB EXPRESSION 1 (TOC1) controls the G1 to S-phase transition, thereby regulating the rhythm of the mitotic cycle during the early stages of leaf development. Likewise, TOC1 controls somatic ploidy during later stages of leaf development and of hypocotyl cell elongation. The use of flow cytometry analyses and of leaf growth kinetics showed that in plants over-expressing TOC1, the S-phase is shorter, which correlates with the diurnal repression of the *CELL DIVISION CONTROL 6* (*CDC6*) gene. This gene encodes an essential component of the pre-replication complex, which is responsible for the specification of DNA origins of replication. Chromatin immunoprecipitation assays showed that the diurnal repression of *CDC6* most likely relies on the direct binding of TOC1 to the *CDC6* promoter. Genetic interaction analyses showeed that the reduced growth and altered somatic ploidy phenotypes observed in plants over-expressing TOC1 were reverted when CDC6 was over-expressed. Thus, our results confirm that TOC1 regulation of the cell cycle occurs through *CDC6* repression. The slow cell cycle progression in plants over-expressing TOC1 has an impact not only in organ development but also on tumor growth in stems and inflorescences. Thus, TOC1 sets the time of the DNA pre-replicative machinery to control plant growth in resonance with the environment.

MATERIALS AND METHODS

Materials and methods

---

1. DNA constructs and plant transformation

Generation of single CDC6-ox and CDC6-ox/TOC1-ox double over-expressing plants (ox/ox) was performed by *Agrobacterium tumefaciens* (GV2260) mediated DNA transfer (Clough and Bent, 1998) of WT and TOC1-ox plants with a CDC6 over-expressing construct. The construct was generated by PCR-mediated amplification of the *CDC6* coding sequence followed by cloning into the pENTR/D-TOPO vector (Invitrogen). The coding sequence was cloned into the plant destination vector pGWB514 (35S pro, C-3xHA) (Nakagawa et al., 2007a, Nakagawa et al., 2007b) following the manufacturer's recommendations (Invitrogen). Several one insertion, T2 lines were used for the kinematic analyses of ploidy. Cloning of the *CDC6* promoter was performed by PCR amplification of 2000 base pairs (bp) of the genomic region upstream of the gene's transcription start site (TSS) (primer pairs A and D). The mutated versions of the *CDC6* promoter lacking the Evening Element (EE) (-670 bp from TSS) were obtained following two strategies. The mut1*CDC6*p was generated by just deleting the EE (-10 bp). A second mutated version (mut2*CDC6*p) was obtained by deleting the EE plus 10 nucleotides on each side flanking the motif. To generate the mutants, a PCR-based mutagenesis by overlap extension was performed (Lee et al., 2004). The WT and mutated versions of the *CDC6* promoter were then cloned into a vector derived from the pCAMBIA1305.1 vector containing the *GLUCURONIDASE* gene (GUSplus) under the control of a minimal 35S promoter (Lee et al., 2017).

2. Hypocotyl measurements

For hypocotyl length measurements, seeds were stratified on MS medium in the dark for 4 days at 4°C, exposed to white light (40 µmol·quanta·m^{-2}·s^{-1}) for 6 h and maintained in the dark for 18 h before transferring to chambers under constant white light, 40 µmol·m^{-2}·s^{-1} (WL40) or 1 µmol·quanta·m^{-2}·s^{-1} (WL1). Hypocotyl length was measured using the ImageJ software at 7 days after stratification or every day over 7 days for the growth kinetic analyses. Hypocotyl epidermal cell length and number were examined at 7 days after stratification by using a wide-field fluorescence microscope (Axiophot Zeiss) and analyzed using the ImageJ software. At least 20 hypocotyls and about 100 cells per condition and genotype were measured. Each experiment was repeated at least twice using a similar “n” number. Statistical analyses were performed by two-tailed t-tests with 99% of confidence.

For flow cytometry analyses, the apex, cotyledons and roots were removed with a razor blade, and about 10 hypocotyls were chopped in ice-cold LB01 buffer (15 mM Tris, 2 mM Na2EDTA, 0.5 mM spermine tetrahydrochloride, 80 mM KCl, 20 mM NaCl, 0.1% (vol/vol) Triton X-100, pH 7,5) (Galbraith et al., 1983, Dolezel et al., 2007). The suspension was filtered through a 30 μm nylon mesh (Sysmex CellTrics) before incubation with 50 μg mL^{-1} DNase-free RNase and 50 μg mL^{-1} propidium iodide (Sigma-Aldrich). DNA content was examined with a FACSCalibur flow cytometer (Becton Dickinson) and the BD CellQuest Pro software (Becton Dickinson). Propidium iodide was detected using the FL2 (585/42) channel. Gates were set in the fluorescence intensity (FL2)/side scatter density plot. At least 10000 nuclei were measured within a gate. Each experiment was repeated at least twice using a similar “n” number. The endoreplication index or cycle value (Barow and Meister, 2003) was calculated taking the number of nuclei of each ploidy multiplied by the number of endoreplication cycles required to reach that ploidy. The sum of the resulting products was divided by the total number of nuclei measured.

3. Kinematic analyses and flow cytometry

Approximately 30 leaves (at young stages) or 10 leaves (at old stages) were chopped with a razor blade in extraction buffer LB01 (15 mM Tris, 2 mM Na2EDTA, 0.5 mM spermine tetrahydrochloride, 80 mM KCl, 20 mM NaCl, 0.1% (vol/vol) Triton X-100, pH 7,5) (Galbraith et al., 1983, Dolezel et al., 2007). The suspension was filtered through a 30 μm nylon mesh (Sysmex CellTrics) followed by incubation with 50 μg mL^{-1} DNase-free RNase, and 50 μg mL^{-1} propidium iodide (Sigma-Aldrich). Nuclei were analyzed with a FACSCalibur flow cytometer (Becton Dickinson) and BD CellQuest Pro software (Becton Dickinson). At least 10000 nuclei were counted per sample. Analyses were performed as described for hypocotyls (see section above). Cell cycle analysis on proliferating leaves was analyzed by using the ModFit software (Verity Software House). Each experiment was repeated at least twice using a similar "n" number.

For the kinematic analysis of leaf growth (De Veylder et al., 2001), approximately 10 seedlings grown under ShD and LgD conditions were harvested at the specified days after stratification. Plants were incubated with methanol overnight to remove chlorophyll, and subsequently stored in lactic acid before microscopy analyses. Leaf blade area of the first pair of true leaves (at young stages 3-7 das) was measured using a wide-field fluorescence microscope (Axiophot Zeiss) while leaves at older stages (10-24 das) were measured with a magnifying glass (Olympus DP71). Cell area of the first pair of true leaves for all stages was measured using a wide-field fluorescence microscope (Axiophot Zeiss). Measurements were performed by drawing leaf areas containing approximately 100 cells, located 25% and 75% from the distance between the tip and the base of the leaf blade of the abaxial epidermis of each leaf. Total number of cells was estimated by dividing the leaf blade area by the average cell area of each leaf. Average cell division rates were estimated as the slope of the log 2–transformed number of cells per leaf, using a five-point differentiation formula (Fiorani and Beemster, 2006). Each experiment was repeated at least twice using a similar "n" number.

4. Real-time PCR analysis

For the developmental time course analyses, the first pair of leaves were cut in halves and the expression of selected core cell cycle genes was separately examined at the tip and base of leaves. RNA was isolated using the Maxwell 16 LEV simply RNA Tissue kit (Promega). Single strand cDNA was synthesized using iScript™ Reverse Transcription Supermix for RT-Q-PCR (BioRad) following manufacturer recommendations. For quantitative real-time gene expression analysis (Q-PCR), cDNAs were diluted 10-fold with nuclease-free water and Q-PCR was performed with the Briliant III Ultra-Fast SYBR Green QPCR Master Mix (Agilent Technologies) in a 96-well CFX96 Touch Real-Time PCR Detection System (BioRad). Each sample was run in technical triplicates. The geometric mean of *APA1* and *IPP2* expression was used as a control. Crossing point (Cp) calculation was used for quantification using the Absolute Quantification analysis by the 2nd Derivative Maximum method. Table 1 shows the specific sequences for primers used in this study. For the developmental time course analyses, samples were harvested at ZT7. For the diurnal gene expression analyses samples were harvested every 4 hours over a 24 hours cycle. Each experiment was repeated at least twice.

5. Protoplast transfection

Leaves from 3-week-old plants were cut into 0.5-mm pieces using a fresh razor blade. Twenty leaves were digested in 15 ml of enzyme solution [0.8% cellulase (Yakult), 0.2% macerozyme (Yakult), 0.4 M mannitol, 10 mM $CaCl_2$, 20 mM KCl, 0.1% bovine serum albumin, and 20 mM MES (pH 5.7)], vacuumed for 20 min, and incubated in the dark for 5 hours at 22° to 23°C. Protoplasts were then passed through 40-µm stainless mesh and collected after a gentle wash with W5 media (154 mM NaCl, 125 mM $CaCl_2$, 5 mM KCl, 2 mM MES, 5 mM glucose adjusted to pH 5.7 with KOH). For transient expression assays using *Arabidopsis* protoplasts, reporter and effector plasmids were constructed. The reporter plasmid contains a minimal 35S promoter sequence and the GUS gene. The *CDC6* promoter was inserted into the reporter plasmid. To construct effector plasmids, TOC1 cDNA was inserted into the effector vector containing the CaMV 35S promoter. Recombinant reporter and effector plasmids were co-transformed into *Arabidopsis* protoplasts by PEG-mediated transformation. The GUS activities were measured by a fluorometric method. A CaMV 35S promoter–Luc construct was also co-transformed as an internal control. The Luc assay was performed using the Luciferase Assay System kit (Promega).

6. Chromatin immunoprecipitation

Plants grown under LgD conditions (7, 14 and 22 day-old) were sampled at ZT7 for TOC1-ox and ZT3 and ZT15 for TMG. Chromatin immunoprecipitation (ChIP) assays were essentially performed as previously described (Huang et al., 2012). Samples were fixed under vacuum with 1% of formaldehyde (16% formaldehyde solution (w/v) methanol-free, Thermo Scientific) for a total of 15 min, shaking the samples every 5 min. Special care was taken with the fixation process as it was found to be crucial for successful ChIP results. Soluble chromatin was incubated overnight at 4°C with an Anti-MYC antibody (Sigma-Aldrich) for assays with TOC1-ox plants or Anti-GFP (Invitrogen by Thermo Fisher Scientific) antibody for the assays with TMG plants. Chromatin antibody conjugates were then incubated for 4 hours at 4°C with Protein G–Dynabeads beads (Invitrogen by Thermo Fisher Scientific). ChIPs were quantified by Q-PCR analysis using a 96-well CFX96 Touch Real-Time PCR Detection System (BioRad). Crossing point (Cp) calculation was used for quantification using the Absolute Quantification analysis by the 2nd Derivative Maximum method. ChIP values for each set of primers were normalized to Input values. Table 1 shows the sequences of primers used in this study.

7. Tumor induction and progression

The *Agrobacterium tumefaciens* strain A281, p35SGUSint (Van Wordragen et al., 1992) was grown on Yeast Extract Broth (YEB) medium (0.5% tryptone, 0.5% yeast extract, 0.5% sucrose, 50 mm $MgSO_4$ and 1.5% agar, pH 7.8) for 24 h at 28°C. Tumors were induced by applying the *Agrobacterium* strain at the base of slightly wounded inflorescence stalks. Seven and five days after inoculation, tissues were excised under a binocular to avoid contamination of the inflorescence stalk and stained with GUS for visualization of tumor progression. The same procedure was used while inoculating the first internodes. GUS staining was performed by incubating inflorescence stalks and internodes with GUS staining solution (1mM X-Gluc, 0.5mM potassium ferrocyanide, 0.5 mM potassium ferricyanide and 0.5% triton X-100) for 30 minutes under vacuum and then for 6 hours at 37° C in the dark. Samples were rinsed in water and cleared with 70% Ethanol. Samples were mounted in water and images were taken using an Olympus DP71 magnifying glass. The same procedure was used to inoculate the non-tumorigenic *Agrobacterium* strain GV3101. This wounded but uninfected inflorescence stalks and internodes were used as controls. Two biological replicates were performed.

8. Quantification and statistical analysis

Quantification of hypocotyl length (Figures 22 and 23), leaf blade area (Figures 9A, 10A, 13A and B, and 14A and B), hypocotyl cell length (Figure 24 B-D), leaf cell area (Figures 9C, 10C, 13E and F and 14E and F) and tumor foci area (Figures 44 and 45C) were measured using the ImageJ software. For hypocotyl measurements data are mean + SEM of n ≈ 20 hypocotyls and n ≈ 100 cells (per genotype and/or condition). Statistical analyses were performed by two-tailed t-tests with 99% of confidence. For leaf and cell area measurements data are mean + SEM of n ≈ 10-20 leaves and n ≈ 100 cells. For all flow cytometry experiments (Figures 15A and D, 16, 17, 18, 19, 20, 21, 25, 40B, 41A, 42 and 43) data are mean + SEM of n ≈ 10000 nuclei per gate. For gene expression analysis using Q-PCR (Figures 26, 27, 28, 29, 30, 31, 32, 33, 34, 35A, 38, 39A and 41A), data represent means + SEM of technical triplicates. Crossing point (Cp) calculation was used for quantification using the Absolute Quantification analysis by the 2nd Derivative Maximum method. All of the experiments were repeated at least twice using a similar "n" number.

Table 1: List of primers used in this study

Name	Sequence	Experiment
APA1_EXP_F	TCCCAAGATCCAGAGAGGTC	Expression analysis
APA1_EXP_R	CTCCAGAAGAGTATGTTCTGAAAG	Expression analysis
IPP2_EXP_F	CATGCGACACACCAACACCA	Expression analysis
IPP2_EXP_R	TGAGGCGAATCAATGGGAGA	Expression analysis
CCA1_EXP_F	TCGAAAGACGGGAAGTGGAACG	Expression analysis
CCA1_EXP_R	GTCGATCTTCATTGGCCATCTCAG	Expression analysis

PRR7_EXP_F	AAGTAGTGATGGGAGTGGCG	Expression analysis
PRR7_EXP_R	GAGATACCGCTCGTGGACTG	Expression analysis
PRR9_EXP_F	ACCAATGAGGGGATTGCTGG	Expression analysis
PRR9_EXP_R	TGCAGCTTCTCTCTGGCTTC	Expression analysis
CYCB1;1_EXP_F	CTCAAAATCCCACGCTTCTTGTGG	Expression analysis
CYCB1;1_EXP_R	CACGTCTACTACCTTTGGTTTCCC	Expression analysis
CYCD3;1_EXP_F	CCTCTCTGTAATCTCCGATTC	Expression analysis
CYCD3;1_EXP_R	AAGGACACCGAGGAGATTAG	Expression analysis
CYCD3;2_EXP_F	TCTCAGCTTGTTGCTGTGGCTTC	Expression analysis
CYCD3;2_EXP_R	TCTTGCTTCTTCCACTTGGAGGTC	Expression analysis
CYCD3;3_EXP_F	TCCGATCGGTGTGTTTGATGCG	Expression analysis
CYCD3;3_EXP_R	GCAGACACAACCCACGACTCATTC	Expression analysis
CYCD4;1_EXP_F	GAAGGAGAAGCAGCATTTGCCAAG	Expression analysis
CYCD4;1_EXP_R	ACTGGTGTACTTCACAAGCCTTCC	Expression analysis
CCS52A2_EXP_F	CGTAGATACCAACAGCCAGGTGTG	Expression analysis
CCS52A2_EXP_R	CGTGTGTGCTCACAAGCTCATTC	Expression analysis
CDC6_EXP_F	AGGCTCTATGTGTCTGCAGGAG	Expression analysis
CDC6_EXP_R	ACCACTTGACACTCTGGAACTGG	Expression analysis
CDT1a_EXP_F	AATCGCTCTTCGGAAAGTGTTTCG	Expression analysis
CDT1a_EXP_R	CCTCTGGAACTTCATCACCCTGAG	Expression analysis
CDKA;1_EXP_F	ACTGGCCAGAGCATTCGGTATC	Expression analysis
CDKA;1_EXP_R	TCGGTACCAGAGAGTAACAACCTC	Expression analysis
E2Fa_EXP_F	TAGATCGGGAGGAAGATGCTGTCG	Expression analysis
E2Fa_EXP_R	TTGTCGCCTTTCTCTTTCGTGAAG	Expression analysis
KRP1_EXP_F	ACGGAGCCGGAGAATTGTTTATG	Expression analysis
KRP1_EXP_R	CGAAACTCCATTATCACCGACGAC	Expression analysis
KRP2_EXP_F	TAGGAGATTATGGCGGCGGTTAGG	Expression analysis
KRP2_EXP_R	TTTCACCGTCGTCGTCGTAACTC	Expression analysis
KRP4_EXP_F	AAGCTTCAACAGGACCACAAGGG	Expression analysis
KRP4_EXP_R	GGGTTGTCATGATTTCAGGCCTTC	Expression analysis
KRP7_EXP_F	GAGGCTCATGAAATCTCCGAAACC	Expression analysis

KRP7_EXP_R	CCGAGTCCATTTCTGCTGTTTCTC	Expression analysis
SIM_EXP_F	AGCCATCAAGATCCGAGCCAAC	Expression analysis
SIM_EXP_R	TTGTGGTCGGAAGAAGTGGGAGTG	Expression analysis
SMR1_EXP_F	CAAAGAAGGACGAAGGTGATGACG	Expression analysis
SMR1_EXP_R	TGTTCTTGGGATGTGGGTGTGC	Expression analysis
SMR2_EXP_F	TCACAAGATTCCGGAGGTGGAGAC	Expression analysis
SMR2_EXP_R	ATCTCACGCGGTCGCTTTCTTG	Expression analysis
SMR4_EXP_F	AACGGGTACTTTCAGCCACCAG	Expression analysis
SMR4_EXP_R	TTCTCTTCGAGGCTGTGCGTAG	Expression analysis
SMR5_EXP_F	ACGCCTACACGTGATGATTGCC	Expression analysis
SMR5_EXP_R	TATCCCTTCTTCGGTGGTTCCC	Expression analysis
SMR7_EXP_F	TTCACTAAAGCCGGTGAAGACG	Expression analysis
SMR7_EXP_R	CGCCGTGGGAGTGATACAAATTC	Expression analysis
SMR8_EXP_F	GCGGTTTCCGTCAGAATTCCAAG	Expression analysis
SMR8_EXP_R	GCACTTCAACGACGGTTTACGC	Expression analysis
ACT2_CHIP_F	CGTTTCGCTTTCCTTAGTGTTAGCT	ChIP assays
ACT2_CHIP_R	AGCGAACGGATCTAGAGACTCACCTTG	ChIP assays
CCSS52A1_CHIP_F	ACGCCTGCCATCTAAGATTC	ChIP assays
CCS52A1_CHIP_R	GGCTTGAAGATGGGCCTAAA	ChIP assays
CDC6_CHIP_F	CTATATCAATGCATTGATATTTTGG	ChIP assays
CDC6_CHIP_R	AATCATTGAAGTATGAGATATCATC	ChIP assays
CDKB1;1_CHIP_F	CGTCAACTCACGCAAATCAT	ChIP assays
CDKB1;1_CHIP_R	TCGTTCGTGACAACTGCAAC	ChIP assays
CYCA2;3_CHIP_F	CAAAGCCATGACAAGAAACATC	ChIP assays
CYCA2;3_CHIP_R	CGAGTGGAGTGGTGTATGTTA	ChIP assays
CYCB1;1_CHIP_F	AGAATAAGTGGGCCGTTG	ChIP assays
CYCB1;1_CHIP_R	TTAGAGGTCGTGGGCTTG	ChIP assays
DEL_CHIP_F	TTGCTCCCTCCATCTTAATTATTTTG	ChIP assays
DEL_CHIP_R	TTGTGTGTGTGTGTATGTTAGTTTC	ChIP assays
E2Fa_CHIP_F	GCTCAAATGGGGTACACTCG	ChIP assays
E2Fa_CHIP_R	CCTGCGCCGTTAGCTTATTA	ChIP assays

E2Fb_CHIP_F	CATAGCTTTATTAACTTCGTTGACTTT	ChIP assays
E2Fb_CHIP_R	GCGCTCTTTATCTCTCTCTTTGT	ChIP assays
E2Fc_CHIP_F	TCGCGTTAGTGCACTTGAAA	ChIP assays
E2Fc_CHIP_R	TGTGACAAACAAACAAAACAAGATT	ChIP assays
KRP2_CHIP_F	TCTTTGTTCTTTTGAAGTCAACAA	ChIP assays
KRP2_CHIP_R	TCTCTCTCTTTTTTACACTCACTATA	ChIP assays
CDC6_CLN-F	CACCATGCCTGCAATCGCCGGACC	Cloning
CDC6_CLN-R	TAGAAGACAGTTGCGGAAGAATCGA	Cloning
WTCDC6p(A)_CLN_F	CACCAACCAAACGCTAAATGTCCAAA	Cloning
WTCDC6p(D)_CLN_R	TGTAGGTTATCAGAAGGAGGCAGAAAAA	Cloning
Mut1CDC6p(B)_CLN_R	ACGACGTGGCATGTATATCTGGTTCAT	Cloning
Mut1CDC6p(C)_CLN_F	ATATACATGCCACGTCGTCTTTATATG	Cloning
Mut2CDC6p(B)_CLN_R	ACATATAAATGGTTCATAAAAGGTTTT	Cloning
Mut2CDC6p(C)_CLN_F	TATGAACCATTTATATGTTGATATGAT	Cloning

Table 2: List of reagents and materials used in this study

REAGENT or RESOURCE	SOURCE	IDENTIFIER
Antibodies		
Mouse monoclonal anti-c-MYC antibody	Sigma – Aldrich	Cat#M4439-100uL
Rabbit polyclonal anti-GFP antibody (Anti-GFP, IgG)	Invitrogen by Thermo Fisher Scientific	Cat#A-11122-100uL
Bacterial Strains		
One Shot TOP10 Chemically Competent E. coli	Life Technologies	Cat#C404010
Agrobacterium tumefaciens (strain GV2260)	N/A	N/A
Agrobacterium tumefaciens (strain GV3101)	N/A	N/A
Agrobacterium tumefaciens (strain A281, p35SGUSint)	(Van Wordragen et al., 1992)	N/A

Chemicals

Propidium iodide solution (1.0 mg/ml in water)	Sigma – Aldrich	Cat#P4864-10 ML
DL-Lactic acid	Sigma – Aldrich	Cat#69785-1L
Pierce 16% Formaldehyde (w/v), Methanol-free	Thermo Scientific	Cat#28908
Protein G Dynabeads® for Immunoprecipitation	Life Technologies	Cat#10004D
Protease Inhibitor Cocktail	Sigma – Aldrich	Cat#P9599
MG-132 (powder, 20mg)	Calbiochem	Cat#474790
Antipain	Sigma – Aldrich	Cat#10791
Chymostatin	Calbiochem	Cat#230790
Cellulase	Yakult	“Onozuka” R-10
Macerozyme (Macerating enzyme)	Yakult	Macerozyme R-10
Poly(ethylene glycol) (PEG)	Sigma – Aldrich	Cat#82240

Critical Commercial Assays

pENTR/D-TOPO Cloning Kit	Life Technologies	Cat#K240020
Gateway LR Clonase® II enzyme mix	Life Technologies	Cat#11791019
Phusion high fidelity DNA polymerase	New England Biolabs	Cat#M0530L
Maxwell® 16 LEV simplyRNA Tissue Kit	Promega	Cat#AS1280
iScript™ Reverse Transcription Supermix for RT-qPC	BioRad	Cat#1708841
Brilliant III Ultra-Fast SYBR green QPCR Master Mix	Agilent Technologies	Cat#600883
Luciferase assay system kit	Promega	Cat#E1500

Experimental Models: Organisms/Strains

Arabidopsis thaliana: WT Col-0	N/A	N/A
Arabidopsis thaliana: WT C24	N/A	N/A
Arabidopsis thaliana: TOC1-MYC-ox	(Huang et al., 2012)	N/A
Arabidopsis thaliana:TOC1-RNAi	(Más et al., 2003)	N/A
Arabidopsis thaliana: toc1-2 (C24)	(Strayer et al., 2000)	N/A
Arabidopsis thaliana: toc1-2 (Col-0)	NASC	N2107710
Arabidopsis thaliana: TMG-YFP/toc1-2	(Huang et al., 2012)	N/A

Arabidopsis thaliana: ztl-1	(Somers et al., 2000)	N/A
Arabidopsis thaliana: ztl-3	(Somers et al., 2000)	N/A
Arabidopsis thaliana: ZTL-ox	(Mas et al., 2003)	N/A
Arabidopsis thaliana: ztl-1/TMG	(Mas et al., 2003)	N/A
Arabidopsis thaliana: CDC6-HA-ox	This study	N/A
Arabidopsis thaliana: CDC6-HA-ox/TOC1-MYC-ox	This study	N/A
Oligonucleotides		
Primers for plasmid construction	This study Table1	N/A
Primers for Q-PCR	This study Table1	N/A
Primers for ChIP-PCR	This study Table1	N/A
Primers for promoter cloning	This study Table1	N/A
Recombinant DNA		
35S::CDC6-HA (pGWB514)	This study	N/A
WTCDC6p::GUS (pMIN35S/pCAMBIA1305)	This study	N/A
Mut1CDC6p::GUS (pMIN35S/pCAMBIA1305)	This study	N/A
Mut2CDC6p::GUS (pMIN35S/pCAMBIA1305)	This study	N/A
Software and Algorithms		
ImageJ	ImageJ	https://imagej.nih.gov/ij/
BD CellQuest Pro software	Becton Dickinson	https://www.bd.com
ModFit software	Verity Software House	http://www.vsh.com/products/mflt/index.asp
GraphPad Prism	GraphPad Software	https://www.graphpad.com/scientific-software/prism/

BIBLIOGRAPHY

Bibliography

ACHARD, P., GONG, F., CHEMINANT, S., ALIOUA, M., HEDDEN, P. & GENSCHIK, P. 2008. The cold-inducible CBF1 factor-dependent signaling pathway modulates the accumulation of the growth-repressing DELLA proteins via its effect on gibberellin metabolism. *Plant Cell,* 20**,** 2117-29.

ADAMS, S., MANFIELD, I., STOCKLEY, P. & CARRE, I. A. 2015. Revised Morning Loops of the Arabidopsis Circadian Clock Based on Analyses of Direct Regulatory Interactions. *PLoS One,* 10**,** e0143943.

AHMAD, M. & CASHMORE, A. R. 1993. HY4 gene of A. thaliana encodes a protein with characteristics of a blue-light photoreceptor. *Nature,* 366**,** 162-6.

ALABADI, D., OYAMA, T., YANOVSKY, M. J., HARMON, F. G., MAS, P. & KAY, S. A. 2001. Reciprocal regulation between TOC1 and LHY/CCA1 within the Arabidopsis circadian clock. *Science,* 293**,** 880-3.

ALABADI, D., YANOVSKY, M. J., MAS, P., HARMER, S. L. & KAY, S. A. 2002. Critical role for CCA1 and LHY in maintaining circadian rhythmicity in Arabidopsis. *Curr Biol,* 12**,** 757-61.

ANDERSEN, S. U., BUECHEL, S., ZHAO, Z., LJUNG, K., NOVAK, O., BUSCH, W., SCHUSTER, C. & LOHMANN, J. U. 2008. Requirement of B2-type cyclin-dependent kinases for meristem integrity in Arabidopsis thaliana. *Plant Cell,* 20**,** 88-100.

ANDRIANKAJA, M., DHONDT, S., DE BODT, S., VANHAEREN, H., COPPENS, F., DE MILDE, L., MUHLENBOCK, P., SKIRYCZ, A., GONZALEZ, N., BEEMSTER, G. T. & INZE, D. 2012. Exit from proliferation during leaf development in Arabidopsis thaliana: a not-so-gradual process. *Dev Cell,* 22**,** 64-78.

ARIAS, E. E. & WALTER, J. C. 2007. Strength in numbers: preventing rereplication via multiple mechanisms in eukaryotic cells. *Genes Dev,* 21**,** 497-518.

ATTWOOLL, C., LAZZERINI DENCHI, E. & HELIN, K. 2004. The E2F family: specific functions and overlapping interests. *EMBO J,* 23**,** 4709-16.

BARBER, J. 2009. Photosynthetic energy conversion: natural and artificial. *Chem Soc Rev,* 38**,** 185-96.

BAROW, M. & MEISTER, A. 2003. Endopolyploidy in seed plants is differently correlated to systematics, organ, life strategy and genome size. *Plant, Cell & Environment,* 26**,** 571-584.

BAUDRY, A., ITO, S., SONG, Y. H., STRAIT, A. A., KIBA, T., LU, S., HENRIQUES, R., PRUNEDA-PAZ, J. L., CHUA, N. H., TOBIN, E. M., KAY, S. A. & IMAIZUMI, T. 2010. F-box proteins FKF1 and LKP2 act in concert with ZEITLUPE to control Arabidopsis clock progression. *Plant Cell,* 22**,** 606-22.

BEEMSTER, G. T., DE VEYLDER, L., VERCRUYSSE, S., WEST, G., ROMBAUT, D., VAN HUMMELEN, P., GALICHET, A., GRUISSEM, W., INZE, D. & VUYLSTEKE, M. 2005. Genome-wide analysis of gene expression profiles associated with cell cycle transitions in growing organs of Arabidopsis. *Plant Physiol,* 138**,** 734-43.

BEEMSTER, G. T., FIORANI, F. & INZE, D. 2003. Cell cycle: the key to plant growth control? *Trends Plant Sci,* 8**,** 154-8.

BEEMSTER, G. T., VERCRUYSSE, S., DE VEYLDER, L., KUIPER, M. & INZE, D. 2006. The Arabidopsis leaf as a model system for investigating the role of cell cycle regulation in organ growth. *J Plant Res,* 119**,** 43-50.

BELL, S. P. & DUTTA, A. 2002. DNA replication in eukaryotic cells. *Annu Rev Biochem,* 71**,** 333-74.

BELL-PEDERSEN, D., CASSONE, V. M., EARNEST, D. J., GOLDEN, S. S., HARDIN, P. E., THOMAS, T. L. & ZORAN, M. J. 2005. Circadian rhythms from multiple oscillators: lessons from diverse organisms. *Nat Rev Genet,* 6**,** 544-56.

BERMEJO, R., VILABOA, N. & CALES, C. 2002. Regulation of CDC6, geminin, and CDT1 in human cells that undergo polyploidization. *Mol Biol Cell,* 13**,** 3989-4000.

BICKNELL, L. S., BONGERS, E. M., LEITCH, A., BROWN, S., SCHOOTS, J., HARLEY, M. E., AFTIMOS, S., AL-AAMA, J. Y., BOBER, M., BROWN, P. A., VAN BOKHOVEN, H., DEAN, J., EDREES, A. Y., FEINGOLD, M., FRYER, A., HOEFSLOOT, L. H., KAU, N., KNOERS, N. V., MACKENZIE, J., OPITZ, J. M., SARDA, P., ROSS, A., TEMPLE, I. K., TOUTAIN, A., WISE, C. A., WRIGHT, M. & JACKSON, A. P. 2011. Mutations in the pre-replication complex cause Meier-Gorlin syndrome. *Nat Genet,* 43**,** 356-9.

BORDAGE, S., SULLIVAN, S., LAIRD, J., MILLAR, A. J. & NIMMO, H. G. 2016. Organ specificity in the plant circadian system is explained by different light inputs to the shoot and root clocks. *New Phytol,* 212**,** 136-49.

BOUDOLF, V., LAMMENS, T., BORUC, J., VAN LEENE, J., VAN DEN DAELE, H., MAES, S., VAN ISTERDAEL, G., RUSSINOVA, E., KONDOROSI, E., WITTERS, E., DE JAEGER, G., INZE, D. & DE VEYLDER, L. 2009. CDKB1;1 forms a functional complex with CYCA2;3 to suppress endocycle onset. *Plant Physiol,* 150**,** 1482-93.

BOUDOLF, V., VLIEGHE, K., BEEMSTER, G. T., MAGYAR, Z., TORRES ACOSTA, J. A., MAES, S., VAN DER SCHUEREN, E., INZE, D. & DE VEYLDER, L. 2004. The plant-specific cyclin-dependent kinase CDKB1;1 and transcription factor E2Fa-DPa control the balance of mitotically dividing and endoreduplicating cells in Arabidopsis. *Plant Cell,* 16**,** 2683-92.

BRAMSIEPE, J., WESTER, K., WEINL, C., ROODBARKELARI, F., KASILI, R., LARKIN, J. C., HULSKAMP, M. & SCHNITTGER, A. 2010. Endoreplication controls cell fate maintenance. *PLoS Genet,* 6**,** e1000996.

BREUNINGER, H. & LENHARD, M. 2010. Control of tissue and organ growth in plants. *Curr Top Dev Biol,* 91**,** 185-220.

BROWN, S. A. 2014. Circadian clock-mediated control of stem cell division and differentiation: beyond night and day. *Development,* 141**,** 3105-11.

CARO, E. & GUTIERREZ, C. 2007. A green GEM: intriguing analogies with animal geminin. *Trends Cell Biol,* 17**,** 580-5.

CARRE, I. A. & EDMUNDS, L. N., JR. 1993. Oscillator control of cell division in Euglena: cyclic AMP oscillations mediate the phasing of the cell division cycle by the circadian clock. *J Cell Sci,* 104 (Pt 4)**,** 1163-73.

CASTELLANO MDEL, M., BONIOTTI, M. B., CARO, E., SCHNITTGER, A. & GUTIERREZ, C. 2004. DNA replication licensing affects cell proliferation or endoreplication in a cell type-specific manner. *Plant Cell,* 16**,** 2380-93.

CASTELLANO, M. M., DEL POZO, J. C., RAMIREZ-PARRA, E., BROWN, S. & GUTIERREZ, C. 2001. Expression and stability of Arabidopsis CDC6 are associated with endoreplication. *Plant Cell,* 13**,** 2671-86.

CHOW, B. Y., HELFER, A., NUSINOW, D. A. & KAY, S. A. 2012. ELF3 recruitment to the PRR9 promoter requires other Evening Complex members in the Arabidopsis circadian clock. *Plant Signal Behav,* 7**,** 170-3.

CHOW, B. Y., SANCHEZ, S. E., BRETON, G., PRUNEDA-PAZ, J. L., KROGAN, N. T. & KAY, S. A. 2014. Transcriptional regulation of LUX by CBF1 mediates cold input to the circadian clock in Arabidopsis. *Curr Biol,* 24**,** 1518-24.

CHURCHMAN, M. L., BROWN, M. L., KATO, N., KIRIK, V., HULSKAMP, M., INZE, D., DE VEYLDER, L., WALKER, J. D., ZHENG, Z., OPPENHEIMER, D. G., GWIN, T., CHURCHMAN, J. & LARKIN, J. C. 2006. SIAMESE, a plant-specific cell cycle regulator, controls endoreplication onset in Arabidopsis thaliana. *Plant Cell,* 18**,** 3145-57.

CLACK, T., MATHEWS, S. & SHARROCK, R. A. 1994. The phytochrome apoprotein family in Arabidopsis is encoded by five genes: the sequences and expression of PHYD and PHYE. *Plant Mol Biol,* 25**,** 413-27.

CLOUGH, S. J. & BENT, A. F. 1998. Floral dip: a simplified method for Agrobacterium-mediated transformation of Arabidopsis thaliana. *Plant J,* 16**,** 735-43.

COCKER, J. H., PIATTI, S., SANTOCANALE, C., NASMYTH, K. & DIFFLEY, J. F. 1996. An essential role for the Cdc6 protein in forming the pre-replicative complexes of budding yeast. *Nature,* 379**,** 180-2.

COSGROVE, D. J. 2005. Growth of the plant cell wall. *Nat Rev Mol Cell Biol,* 6**,** 850-61.

COSTAS, C., DE LA PAZ SANCHEZ, M., STROUD, H., YU, Y., OLIVEROS, J. C., FENG, S., BENGURIA, A., LOPEZ-VIDRIERO, I., ZHANG, X., SOLANO, R., JACOBSEN, S. E. & GUTIERREZ, C. 2011. Genome-wide mapping of Arabidopsis thaliana origins of DNA replication and their associated epigenetic marks. *Nat Struct Mol Biol,* 18**,** 395-400.

DE CLERCQ, A. & INZE, D. 2006. Cyclin-dependent kinase inhibitors in yeast, animals, and plants: a functional comparison. *Crit Rev Biochem Mol Biol,* 41**,** 293-313.

DE VEYLDER, L., BEECKMAN, T., BEEMSTER, G. T., DE ALMEIDA ENGLER, J., ORMENESE, S., MAES, S., NAUDTS, M., VAN DER SCHUEREN, E., JACQMARD, A., ENGLER, G. & INZE, D. 2002. Control of proliferation, endoreduplication and differentiation by the Arabidopsis E2Fa-DPa transcription factor. *EMBO J,* 21**,** 1360-8.

DE VEYLDER, L., BEECKMAN, T., BEEMSTER, G. T., KROLS, L., TERRAS, F., LANDRIEU, I., VAN DER SCHUEREN, E., MAES, S., NAUDTS, M. & INZE, D. 2001. Functional analysis of cyclin-dependent kinase inhibitors of Arabidopsis. *Plant Cell,* 13**,** 1653-68.

DE VEYLDER, L., LARKIN, J. C. & SCHNITTGER, A. 2011. Molecular control and function of endoreplication in development and physiology. *Trends Plant Sci,* 16**,** 624-34.

DEEKEN, R., IVASHIKINA, N., CZIRJAK, T., PHILIPPAR, K., BECKER, D., ACHE, P. & HEDRICH, R. 2003. Tumour development in Arabidopsis thaliana involves the Shaker-like K+ channels AKT1 and AKT2/3. *Plant J,* 34**,** 778-87.

DEL POZO, J. C., BONIOTTI, M. B. & GUTIERREZ, C. 2002. Arabidopsis E2Fc functions in cell division and is degraded by the ubiquitin-SCF(AtSKP2) pathway in response to light. *Plant Cell,* 14**,** 3057-71.

DEL POZO, J. C., DIAZ-TRIVINO, S., CISNEROS, N. & GUTIERREZ, C.

2006. The balance between cell division and endoreplication depends on E2FC-DPB, transcription factors regulated by the ubiquitin-SCFSKP2A pathway in Arabidopsis. *Plant Cell,* 18, 2224-35.

DEVLIN, P. F. & KAY, S. A. 2000. Cryptochromes are required for phytochrome signaling to the circadian clock but not for rhythmicity. *Plant Cell,* 12, 2499-2510.

DEWITTE, W., SCOFIELD, S., ALCASABAS, A. A., MAUGHAN, S. C., MENGES, M., BRAUN, N., COLLINS, C., NIEUWLAND, J., PRINSEN, E., SUNDARESAN, V. & MURRAY, J. A. 2007. Arabidopsis CYCD3 D-type cyclins link cell proliferation and endocycles and are rate-limiting for cytokinin responses. *Proc Natl Acad Sci U S A,* 104, 14537-42.

DIBNER, C., SCHIBLER, U. & ALBRECHT, U. 2010. The mammalian circadian timing system: organization and coordination of central and peripheral clocks. *Annu Rev Physiol,* 72, 517-49.

DIXON, L. E., KNOX, K., KOZMA-BOGNAR, L., SOUTHERN, M. M., POKHILKO, A. & MILLAR, A. J. 2011. Temporal repression of core circadian genes is mediated through EARLY FLOWERING 3 in Arabidopsis. *Curr Biol,* 21, 120-5.

DOLEZEL, J., GREILHUBER, J. & SUDA, J. 2007. Estimation of nuclear DNA content in plants using flow cytometry. *Nat Protoc,* 2, 2233-44.

DONNELLY, P. M., BONETTA, D., TSUKAYA, H., DENGLER, R. E. & DENGLER, N. G. 1999. Cell cycling and cell enlargement in developing leaves of Arabidopsis. *Dev Biol,* 215, 407-19.

DORNBUSCH, T., MICHAUD, O., XENARIOS, I. & FANKHAUSER, C. 2014. Differentially phased leaf growth and movements in Arabidopsis depend on coordinated circadian and light regulation. *Plant Cell,* 26, 3911-21.

DOWSON-DAY, M. J. & MILLAR, A. J. 1999. Circadian dysfunction causes aberrant hypocotyl elongation patterns in Arabidopsis. *Plant J,* 17, 63-71.

DOYLE, M. R., DAVIS, S. J., BASTOW, R. M., MCWATTERS, H. G., KOZMA-BOGNAR, L., NAGY, F., MILLAR, A. J. & AMASINO, R. M. 2002. The ELF4 gene controls circadian rhythms and flowering time in Arabidopsis thaliana. *Nature,* 419, 74-7.

DUDITS, D., CSERHATI, M., MISKOLCZI, P. & HORVATH, G. 2007. The Growing Family of Plant Cyclin-Dependent Kinases with Multiple Functions in Cellular and Developmental Regulation. *Annual Plant Reviews Volume 32: Cell Cycle Control and Plant Development.*

DUNLAP, J. C. & LOROS, J. J. 2017. Making Time: Conservation of Biological Clocks from Fungi to Animals. *Microbiol Spectr,* 5.

DYSON, N. 1998. The regulation of E2F by pRB-family proteins. *Genes Dev,* 12, 2245-62.

EDGAR, B. A., ZIELKE, N. & GUTIERREZ, C. 2014. Endocycles: a recurrent evolutionary innovation for post-mitotic cell growth. *Nat Rev Mol Cell Biol,* 15, 197-210.

EDMUNDS, L. N., JR. & LAVAL-MARTIN, D. L. 1984. Cell division cycles and circadian oscillators in Euglena. *Chronobiol Int,* 1, 1-9.

EFRONI, I., ESHED, Y. & LIFSCHITZ, E. 2010. Morphogenesis of simple and compound leaves: a critical review. *Plant Cell,* 22, 1019-32.

ELSASSER, S., CHI, Y., YANG, P. & CAMPBELL, J. L. 1999. Phosphorylation controls timing of Cdc6p destruction: A biochemical analysis. *Mol Biol Cell,* 10, 3263-77.

ENDO, M., SHIMIZU, H., NOHALES, M. A., ARAKI, T. & KAY, S. A. 2014. Tissue-specific clocks in Arabidopsis show asymmetric coupling. *Nature,* 515**,** 419-22.

EZER, D., JUNG, J. H., LAN, H., BISWAS, S., GREGOIRE, L., BOX, M. S., CHAROENSAWAN, V., CORTIJO, S., LAI, X., STOCKLE, D., ZUBIETA, C., JAEGER, K. E. & WIGGE, P. A. 2017. The evening complex coordinates environmental and endogenous signals in Arabidopsis. *Nat Plants,* 3**,** 17087.

FANKHAUSER, C. & STAIGER, D. 2002. Photoreceptors in Arabidopsis thaliana: light perception, signal transduction and entrainment of the endogenous clock. *Planta,* 216**,** 1-16.

FARINAS, B. & MAS, P. 2011. Functional implication of the MYB transcription factor RVE8/LCL5 in the circadian control of histone acetylation. *Plant J,* 66**,** 318-29.

FARRE, E. M., HARMER, S. L., HARMON, F. G., YANOVSKY, M. J. & KAY, S. A. 2005. Overlapping and distinct roles of PRR7 and PRR9 in the Arabidopsis circadian clock. *Curr Biol,* 15**,** 47-54.

FILO, J., WU, A., ELIASON, E., RICHARDSON, T., THINES, B. C. & HARMON, F. G. 2015. Gibberellin driven growth in elf3 mutants requires PIF4 and PIF5. *Plant Signal Behav,* 10**,** e992707.

FIORANI, F. & BEEMSTER, G. T. 2006. Quantitative analyses of cell division in plants. *Plant Mol Biol,* 60**,** 963-79.

FRANCIS, D. 2007. The plant cell cycle--15 years on. *New Phytol,* 174**,** 261-78.

FRESCAS, D. & PAGANO, M. 2008. Deregulated proteolysis by the F-box proteins SKP2 and beta-TrCP: tipping the scales of cancer. *Nat Rev Cancer,* 8**,** 438-49.

FUJIWARA, S., WANG, L., HAN, L., SUH, S. S., SALOME, P. A., MCCLUNG, C. R. & SOMERS, D. E. 2008. Post-translational regulation of the Arabidopsis circadian clock through selective proteolysis and phosphorylation of pseudo-response regulator proteins. *J Biol Chem,* 283**,** 23073-83.

GALBRAITH, D. W., HARKINS, K. R., MADDOX, J. M., AYRES, N. M., SHARMA, D. P. & FIROOZABADY, E. 1983. Rapid flow cytometric analysis of the cell cycle in intact plant tissues. *Science,* 220**,** 1049-51.

GENDREAU, E., TRAAS, J., DESNOS, T., GRANDJEAN, O., CABOCHE, M. & HOFTE, H. 1997. Cellular basis of hypocotyl growth in Arabidopsis thaliana. *Plant Physiol,* 114**,** 295-305.

GENDRON, J. M., PRUNEDA-PAZ, J. L., DOHERTY, C. J., GROSS, A. M., KANG, S. E. & KAY, S. A. 2012. Arabidopsis circadian clock protein, TOC1, is a DNA-binding transcription factor. *Proc Natl Acad Sci U S A,* 109**,** 3167-72.

GOTO, K. & JOHNSON, C. H. 1995. Is the cell division cycle gated by a circadian clock? The case of Chlamydomonas reinhardtii. *J Cell Biol,* 129**,** 1061-9.

GOULD, P. D., LOCKE, J. C., LARUE, C., SOUTHERN, M. M., DAVIS, S. J., HANANO, S., MOYLE, R., MILICH, R., PUTTERILL, J., MILLAR, A. J. & HALL, A. 2006. The molecular basis of temperature compensation in the Arabidopsis circadian clock. *Plant Cell,* 18**,** 1177-87.

GUERINIER, T., MILLAN, L., CROZET, P., OURY, C., REY, F., VALOT, B., MATHIEU, C., VIDAL, J., HODGES, M., THOMAS, M. & GLAB, N. 2013. Phosphorylation of p27(KIP1) homologs KRP6 and 7 by SNF1-related protein kinase-1 links plant energy homeostasis and cell proliferation. *Plant J,* 75**,** 515-25.

GUSTI, A., BAUMBERGER, N., NOWACK, M., PUSCH, S., EISLER, H., POTUSCHAK, T., DE VEYLDER, L., SCHNITTGER, A. & GENSCHIK, P. 2009. The Arabidopsis thaliana F-box protein FBL17 is essential for progression through the second mitosis during pollen development. *PLoS One,* 4**,** e4780.

GUTIERREZ, C., RAMIREZ-PARRA, E., CASTELLANO, M. M. & DEL POZO, J. C. 2002. G(1) to S transition: more than a cell cycle engine switch. *Curr Opin Plant Biol,* 5**,** 480-6.

HAGA, N., KOBAYASHI, K., SUZUKI, T., MAEO, K., KUBO, M., OHTANI, M., MITSUDA, N., DEMURA, T., NAKAMURA, K., JURGENS, G. & ITO, M. 2011. Mutations in MYB3R1 and MYB3R4 cause pleiotropic developmental defects and preferential down-regulation of multiple G2/M-specific genes in Arabidopsis. *Plant Physiol,* 157**,** 706-17.

HAYDON, M. J., MIELCZAREK, O., ROBERTSON, F. C., HUBBARD, K. E. & WEBB, A. A. 2013. Photosynthetic entrainment of the Arabidopsis thaliana circadian clock. *Nature,* 502**,** 689-92.

HAZEN, S. P., SCHULTZ, T. F., PRUNEDA-PAZ, J. L., BOREVITZ, J. O., ECKER, J. R. & KAY, S. A. 2005. LUX ARRHYTHMO encodes a Myb domain protein essential for circadian rhythms. *Proc Natl Acad Sci U S A,* 102**,** 10387-92.

HELFER, A., NUSINOW, D. A., CHOW, B. Y., GEHRKE, A. R., BULYK, M. L. & KAY, S. A. 2011. LUX ARRHYTHMO encodes a nighttime repressor of circadian gene expression in the Arabidopsis core clock. *Curr Biol,* 21**,** 126-33.

HERRERO, E., KOLMOS, E., BUJDOSO, N., YUAN, Y., WANG, M., BERNS, M. C., UHLWORM, H., COUPLAND, G., SAINI, R., JASKOLSKI, M., WEBB, A., GONCALVES, J. & DAVIS, S. J. 2012. EARLY FLOWERING4 recruitment of EARLY FLOWERING3 in the nucleus sustains the Arabidopsis circadian clock. *Plant Cell,* 24**,** 428-43.

HORIGUCHI, G., FERJANI, A., FUJIKURA, U. & TSUKAYA, H. 2006. Coordination of cell proliferation and cell expansion in the control of leaf size in Arabidopsis thaliana. *J Plant Res,* 119**,** 37-42.

HSU, P. Y., DEVISETTY, U. K. & HARMER, S. L. 2013. Accurate timekeeping is controlled by a cycling activator in Arabidopsis. *Elife,* 2**,** e00473.

HU, W., FRANKLIN, K. A., SHARROCK, R. A., JONES, M. A., HARMER, S. L. & LAGARIAS, J. C. 2013. Unanticipated regulatory roles for Arabidopsis phytochromes revealed by null mutant analysis. *Proc Natl Acad Sci U S A,* 110**,** 1542-7.

HU, Y., BAO, F. & LI, J. 2000. Promotive effect of brassinosteroids on cell division involves a distinct CycD3-induction pathway in Arabidopsis. *Plant J,* 24**,** 693-701.

HUALA, E., OELLER, P. W., LISCUM, E., HAN, I. S., LARSEN, E. & BRIGGS, W. R. 1997. Arabidopsis NPH1: a protein kinase with a putative redox-sensing domain. *Science,* 278**,** 2120-3.

HUANG, H., ALVAREZ, S., BINDBEUTEL, R., SHEN, Z., NALDRETT, M. J., EVANS, B. S., BRIGGS, S. P., HICKS, L. M., KAY, S. A. & NUSINOW, D. A. 2016. Identification of Evening Complex Associated Proteins in Arabidopsis by Affinity Purification and Mass Spectrometry. *Mol Cell Proteomics,* 15**,** 201-17.

HUANG, W., PEREZ-GARCIA, P., POKHILKO, A., MILLAR, A. J., ANTOSHECHKIN, I., RIECHMANN, J. L. & MAS, P. 2012. Mapping the core of the Arabidopsis circadian clock defines the network structure of the oscillator. *Science,* 336**,** 75-9.

HUSSE, J., EICHELE, G. & OSTER, H. 2015. Synchronization of the mammalian circadian timing system: Light can control peripheral clocks independently of the SCN clock: alternate routes of entrainment optimize the alignment of the body's circadian clock network with external time. *Bioessays,* 37**,** 1119-28.

IMAI, K. K., OHASHI, Y., TSUGE, T., YOSHIZUMI, T., MATSUI, M., OKA, A. & AOYAMA, T. 2006. The A-type cyclin CYCA2;3 is a key regulator of ploidy levels in Arabidopsis endoreduplication. *Plant Cell,* 18**,** 382-96.

INAGAKI, S. & UMEDA, M. 2011. Cell-cycle control and plant development. *Int Rev Cell Mol Biol,* 291**,** 227-61.

INZE, D. & DE VEYLDER, L. 2006. Cell cycle regulation in plant development. *Annu Rev Genet,* 40**,** 77-105.

JALLEPALLI, P. V. & KELLY, T. J. 1996. Rum1 and Cdc18 link inhibition of cyclin-dependent kinase to the initiation of DNA replication in Schizosaccharomyces pombe. *Genes Dev,* 10**,** 541-52.

JAMES, A. B., SYED, N. H., BORDAGE, S., MARSHALL, J., NIMMO, G. A., JENKINS, G. I., HERZYK, P., BROWN, J. W. & NIMMO, H. G. 2012. Alternative splicing mediates responses of the Arabidopsis circadian clock to temperature changes. *Plant Cell,* 24**,** 961-81.

JOHNSON, A. & SKOTHEIM, J. M. 2013. Start and the restriction point. *Curr Opin Cell Biol,* 25**,** 717-23.

JONES, M. A., HU, W., LITTHAUER, S., LAGARIAS, J. C. & HARMER, S. L. 2015. A Constitutively Active Allele of Phytochrome B Maintains Circadian Robustness in the Absence of Light. *Plant Physiol,* 169**,** 814-25.

KAGAWA, T., SAKAI, T., SUETSUGU, N., OIKAWA, K., ISHIGURO, S., KATO, T., TABATA, S., OKADA, K. & WADA, M. 2001. Arabidopsis NPL1: a phototropin homolog controlling the chloroplast high-light avoidance response. *Science,* 291**,** 2138-41.

KAMI, C., LORRAIN, S., HORNITSCHEK, P. & FANKHAUSER, C. 2010. Light-regulated plant growth and development. *Curr Top Dev Biol,* 91**,** 29-66.

KAMIOKA, M., TAKAO, S., SUZUKI, T., TAKI, K., HIGASHIYAMA, T., KINOSHITA, T. & NAKAMICHI, N. 2016. Direct Repression of Evening Genes by CIRCADIAN CLOCK-ASSOCIATED1 in the Arabidopsis Circadian Clock. *Plant Cell,* 28**,** 696-711.

KASILI, R., WALKER, J. D., SIMMONS, L. A., ZHOU, J., DE VEYLDER, L. & LARKIN, J. C. 2010. SIAMESE cooperates with the CDH1-like protein CCS52A1 to establish endoreplication in Arabidopsis thaliana trichomes. *Genetics,* 185**,** 257-68.

KELLY, T. J., MARTIN, G. S., FORSBURG, S. L., STEPHEN, R. J., RUSSO, A. & NURSE, P. 1993. The fission yeast cdc18+ gene product couples S phase to START and mitosis. *Cell,* 74**,** 371-82.

KIDOKORO, S., MARUYAMA, K., NAKASHIMA, K., IMURA, Y., NARUSAKA, Y., SHINWARI, Z. K., OSAKABE, Y., FUJITA, Y., MIZOI, J., SHINOZAKI, K. & YAMAGUCHI-SHINOZAKI, K. 2009. The phytochrome-interacting factor PIF7 negatively regulates DREB1 expression under circadian control in Arabidopsis. *Plant Physiol,* 151**,** 2046-57.

KIM, H. J., OH, S. A., BROWNFIELD, L., HONG, S. H., RYU, H., HWANG, I., TWELL, D. & NAM, H. G. 2008. Control of plant germline proliferation by SCF(FBL17) degradation of cell cycle inhibitors. *Nature,* 455**,** 1134-7.

KIM, J. Y., SONG, H. R., TAYLOR, B. L. & CARRE, I. A. 2003. Light-regulated translation mediates gated induction of the Arabidopsis clock protein LHY. *EMBO J,* 22, 935-44.

KIM, W. Y., FUJIWARA, S., SUH, S. S., KIM, J., KIM, Y., HAN, L., DAVID, K., PUTTERILL, J., NAM, H. G. & SOMERS, D. E. 2007. ZEITLUPE is a circadian photoreceptor stabilized by GIGANTEA in blue light. *Nature,* 449, 356-60.

KOLMOS, E., CHOW, B. Y., PRUNEDA-PAZ, J. L. & KAY, S. A. 2014. HsfB2b-mediated repression of PRR7 directs abiotic stress responses of the circadian clock. *Proc Natl Acad Sci U S A,* 111, 16172-7.

KOMAKI, S. & SUGIMOTO, K. 2012. Control of the plant cell cycle by developmental and environmental cues. *Plant Cell Physiol,* 53, 953-64.

KOSUGI, S. & OHASHI, Y. 2002. E2Ls, E2F-like repressors of Arabidopsis that bind to E2F sites in a monomeric form. *J Biol Chem,* 277, 16553-8.

KOWALSKA, E., RIPPERGER, J. A., HOEGGER, D. C., BRUEGGER, P., BUCH, T., BIRCHLER, T., MUELLER, A., ALBRECHT, U., CONTALDO, C. & BROWN, S. A. 2013. NONO couples the circadian clock to the cell cycle. *Proc Natl Acad Sci U S A,* 110, 1592-9.

KWON, Y. J., PARK, M. J., KIM, S. G., BALDWIN, I. T. & PARK, C. M. 2014. Alternative splicing and nonsense-mediated decay of circadian clock genes under environmental stress conditions in Arabidopsis. *BMC Plant Biol,* 14, 136.

LAMMENS, T., BOUDOLF, V., KHEIBARSHEKAN, L., ZALMAS, L. P., GAAMOUCHE, T., MAES, S., VANSTRAELEN, M., KONDOROSI, E., LA THANGUE, N. B., GOVAERTS, W., INZE, D. & DE VEYLDER, L. 2008. Atypical E2F activity restrains APC/CCCS52A2 function obligatory for endocycle onset. *Proc Natl Acad Sci U S A,* 105, 14721-6.

LAMMENS, T., LI, J., LEONE, G. & DE VEYLDER, L. 2009. Atypical E2Fs: new players in the E2F transcription factor family. *Trends Cell Biol,* 19, 111-8.

LARSON-RABIN, Z., LI, Z., MASSON, P. H. & DAY, C. D. 2009. FZR2/CCS52A1 expression is a determinant of endoreduplication and cell expansion in Arabidopsis. *Plant Physiol,* 149, 874-84.

LEE, J., LEE, H. J., SHIN, M. K. & RYU, W. S. 2004. Versatile PCR-mediated insertion or deletion mutagenesis. *Biotechniques,* 36, 398-400.

LEE, K., PARK, O. S. & SEO, P. J. 2017. Arabidopsis ATXR2 deposits H3K36me3 at the promoters of LBD genes to facilitate cellular dedifferentiation. *Sci Signal,* 10.

LEE, T. J., PASCUZZI, P. E., SETTLAGE, S. B., SHULTZ, R. W., TANURDZIC, M., RABINOWICZ, P. D., MENGES, M., ZHENG, P., MAIN, D., MURRAY, J. A., SOSINSKI, B., ALLEN, G. C., MARTIENSSEN, R. A., HANLEY-BOWDOIN, L., VAUGHN, M. W. & THOMPSON, W. F. 2010. Arabidopsis thaliana chromosome 4 replicates in two phases that correlate with chromatin state. *PLoS Genet,* 6, e1000982.

LEIVAR, P. & QUAIL, P. H. 2011. PIFs: pivotal components in a cellular signaling hub. *Trends Plant Sci,* 16, 19-28.

LEONARD, A. C. & MECHALI, M. 2013. DNA replication origins. *Cold Spring Harb Perspect Biol,* 5, a010116.

LI, B., CAREY, M. & WORKMAN, J. L. 2007. The role of chromatin during transcription. *Cell,* 128, 707-19.

LI, G., SIDDIQUI, H., TENG, Y., LIN, R., WAN, X. Y., LI, J., LAU, O. S., OUYANG, X., DAI, M., WAN, J., DEVLIN, P. F., DENG, X. W. & WANG,

H. 2011. Coordinated transcriptional regulation underlying the circadian clock in Arabidopsis. *Nat Cell Biol,* 13**,** 616-22.

LIANG, C., WEINREICH, M. & STILLMAN, B. 1995. ORC and Cdc6p interact and determine the frequency of initiation of DNA replication in the genome. *Cell,* 81**,** 667-76.

LIN, C., AHMAD, M. & CASHMORE, A. R. 1996. Arabidopsis cryptochrome 1 is a soluble protein mediating blue light-dependent regulation of plant growth and development. *Plant J,* 10**,** 893-902.

LIU, X. L., COVINGTON, M. F., FANKHAUSER, C., CHORY, J. & WAGNER, D. R. 2001. ELF3 encodes a circadian clock-regulated nuclear protein that functions in an Arabidopsis PHYB signal transduction pathway. *Plant Cell,* 13**,** 1293-304.

LU, S. X., KNOWLES, S. M., ANDRONIS, C., ONG, M. S. & TOBIN, E. M. 2009. CIRCADIAN CLOCK ASSOCIATED1 and LATE ELONGATED HYPOCOTYL function synergistically in the circadian clock of Arabidopsis. *Plant Physiol,* 150**,** 834-43.

LU, S. X., WEBB, C. J., KNOWLES, S. M., KIM, S. H., WANG, Z. & TOBIN, E. M. 2012. CCA1 and ELF3 Interact in the control of hypocotyl length and flowering time in Arabidopsis. *Plant Physiol,* 158**,** 1079-88.

MA, Y., GIL, S., GRASSER, K. D. & MAS, P. 2018. Targeted Recruitment of the Basal Transcriptional Machinery by LNK Clock Components Controls the Circadian Rhythms of Nascent RNAs in Arabidopsis. *Plant Cell,* 30**,** 907-924.

MAGYAR, Z., DE VEYLDER, L., ATANASSOVA, A., BAKO, L., INZE, D. & BOGRE, L. 2005. The role of the Arabidopsis E2FB transcription factor in regulating auxin-dependent cell division. *Plant Cell,* 17**,** 2527-41.

MAKAROV, V. N., SCHOSCHINA, E. V. & LÜNING, K. 1995. Diurnal and circadian periodicity of mitosis and growth in marine macroalgae. I. Juvenile sporophytes of Laminariales (Phaeophyta). *European Journal of Phycology,* 30**,** 261-266.

MAKINO, S., MATSUSHIKA, A., KOJIMA, M., ODA, Y. & MIZUNO, T. 2001. Light response of the circadian waves of the APRR1/TOC1 quintet: when does the quintet start singing rhythmically in Arabidopsis? *Plant Cell Physiol,* 42**,** 334-9.

MAKINO, S., MATSUSHIKA, A., KOJIMA, M., YAMASHINO, T. & MIZUNO, T. 2002. The APRR1/TOC1 quintet implicated in circadian rhythms of Arabidopsis thaliana: I. Characterization with APRR1-overexpressing plants. *Plant Cell Physiol,* 43**,** 58-69.

MALAPEIRA, J., KHAITOVA, L. C. & MAS, P. 2012. Ordered changes in histone modifications at the core of the Arabidopsis circadian clock. *Proc Natl Acad Sci U S A,* 109**,** 21540-5.

MANCINI, E., SANCHEZ, S. E., ROMANOWSKI, A., SCHLAEN, R. G., SANCHEZ-LAMAS, M., CERDAN, P. D. & YANOVSKY, M. J. 2016. Acute Effects of Light on Alternative Splicing in Light-Grown Plants. *Photochem Photobiol,* 92**,** 126-33.

MARICONTI, L., PELLEGRINI, B., CANTONI, R., STEVENS, R., BERGOUNIOUX, C., CELLA, R. & ALBANI, D. 2002. The E2F family of transcription factors from Arabidopsis thaliana. Novel and conserved components of the retinoblastoma/E2F pathway in plants. *J Biol Chem,* 277**,** 9911-9.

MARROCCO, K., BERGDOLL, M., ACHARD, P., CRIQUI, M. C. & GENSCHIK, P. 2010. Selective proteolysis sets the tempo of the cell cycle. *Curr Opin Plant Biol,* 13**,** 631-9.

MARROCCO, K., THOMANN, A., PARMENTIER, Y., GENSCHIK, P. & CRIQUI, M. C. 2009. The APC/C E3 ligase remains active in most post-mitotic Arabidopsis cells and is required for proper vasculature development and organization. *Development,* 136**,** 1475-85.

MARTIN, G., ROVIRA, A., VECIANA, N., SOY, J., TOLEDO-ORTIZ, G., GOMMERS, C. M. M., BOIX, M., HENRIQUES, R., MINGUET, E. G., ALABADI, D., HALLIDAY, K. J., LEIVAR, P. & MONTE, E. 2018. Circadian Waves of Transcriptional Repression Shape PIF-Regulated Photoperiod-Responsive Growth in Arabidopsis. *Curr Biol,* 28**,** 311-318 e5.

MAS, P., ALABADI, D., YANOVSKY, M. J., OYAMA, T. & KAY, S. A. 2003a. Dual role of TOC1 in the control of circadian and photomorphogenic responses in Arabidopsis. *Plant Cell,* 15**,** 223-36.

MAS, P., KIM, W. Y., SOMERS, D. E. & KAY, S. A. 2003b. Targeted degradation of TOC1 by ZTL modulates circadian function in Arabidopsis thaliana. *Nature,* 426**,** 567-70.

MASRI, S., ZOCCHI, L., KATADA, S., MORA, E. & SASSONE-CORSI, P. 2012. The circadian clock transcriptional complex: metabolic feedback intersects with epigenetic control. *Ann N Y Acad Sci,* 1264**,** 103-9.

MASUDA, H. P., RAMOS, G. B., DE ALMEIDA-ENGLER, J., CABRAL, L. M., COQUEIRO, V. M., MACRINI, C. M., FERREIRA, P. C. & HEMERLY, A. S. 2004. Genome based identification and analysis of the pre-replicative complex of Arabidopsis thaliana. *FEBS Lett,* 574**,** 192-202.

MATSUO, T., YAMAGUCHI, S., MITSUI, S., EMI, A., SHIMODA, F. & OKAMURA, H. 2003. Control mechanism of the circadian clock for timing of cell division in vivo. *Science,* 302**,** 255-9.

MATSUSHIKA, A., MAKINO, S., KOJIMA, M. & MIZUNO, T. 2000. Circadian waves of expression of the APRR1/TOC1 family of pseudo-response regulators in Arabidopsis thaliana: insight into the plant circadian clock. *Plant Cell Physiol,* 41**,** 1002-12.

MCWATTERS, H. G., BASTOW, R. M., HALL, A. & MILLAR, A. J. 2000. The ELF3 zeitnehmer regulates light signalling to the circadian clock. *Nature,* 408**,** 716-20.

MECHALI, M. 2010. Eukaryotic DNA replication origins: many choices for appropriate answers. *Nat Rev Mol Cell Biol,* 11**,** 728-38.

MENDOZA-VIVEROS, L., BOUCHARD-CANNON, P., HEGAZI, S., CHENG, A. H., PASTORE, S. & CHENG, H. M. 2017. Molecular modulators of the circadian clock: lessons from flies and mice. *Cell Mol Life Sci,* 74**,** 1035-1059.

MENGES, M., DE JAGER, S. M., GRUISSEM, W. & MURRAY, J. A. 2005. Global analysis of the core cell cycle regulators of Arabidopsis identifies novel genes, reveals multiple and highly specific profiles of expression and provides a coherent model for plant cell cycle control. *Plant J,* 41**,** 546-66.

MENGES, M. & MURRAY, J. A. 2002. Synchronous Arabidopsis suspension cultures for analysis of cell-cycle gene activity. *Plant J,* 30**,** 203-12.

MENGES, M., SAMLAND, A. K., PLANCHAIS, S. & MURRAY, J. A. 2006. The D-type cyclin CYCD3;1 is limiting for the G1-to-S-phase transition in Arabidopsis. *Plant Cell,* 18**,** 893-906.

MILLAR, A. J. 2016. The Intracellular Dynamics of Circadian Clocks Reach for the Light of Ecology and Evolution. *Annu Rev Plant Biol,* 67**,** 595-618.

MILLAR, A. J., CARRE, I. A., STRAYER, C. A., CHUA, N. H. & KAY, S. A. 1995. Circadian clock mutants in Arabidopsis identified by luciferase imaging. *Science,* 267**,** 1161-3.

MIZOGUCHI, T., WHEATLEY, K., HANZAWA, Y., WRIGHT, L., MIZOGUCHI, M., SONG, H. R., CARRE, I. A. & COUPLAND, G. 2002. LHY and CCA1 are partially redundant genes required to maintain circadian rhythms in Arabidopsis. *Dev Cell,* 2**,** 629-41.

MIZUSHIMA, T., TAKAHASHI, N. & STILLMAN, B. 2000. Cdc6p modulates the structure and DNA binding activity of the origin recognition complex in vitro. *Genes Dev,* 14**,** 1631-41.

MORGAN, D. O. 1997. Cyclin-dependent kinases: engines, clocks, and microprocessors. *Annu Rev Cell Dev Biol,* 13**,** 261-91.

MORI, T., BINDER, B. & JOHNSON, C. H. 1996. Circadian gating of cell division in cyanobacteria growing with average doubling times of less than 24 hours. *Proc Natl Acad Sci U S A,* 93**,** 10183-8.

MUZI FALCONI, M., BROWN, G. W. & KELLY, T. J. 1996. cdc18+ regulates initiation of DNA replication in Schizosaccharomyces pombe. *Proc Natl Acad Sci U S A,* 93**,** 1566-70.

NAGEL, D. H., PRUNEDA-PAZ, J. L. & KAY, S. A. 2014. FBH1 affects warm temperature responses in the Arabidopsis circadian clock. *Proc Natl Acad Sci U S A,* 111**,** 14595-600.

NAKAGAMI, H., KAWAMURA, K., SUGISAKA, K., SEKINE, M. & SHINMYO, A. 2002. Phosphorylation of retinoblastoma-related protein by the cyclin D/cyclin-dependent kinase complex is activated at the G1/S-phase transition in tobacco. *Plant Cell,* 14**,** 1847-57.

NAKAGAWA, T., KUROSE, T., HINO, T., TANAKA, K., KAWAMUKAI, M., NIWA, Y., TOYOOKA, K., MATSUOKA, K., JINBO, T. & KIMURA, T. 2007a. Development of series of gateway binary vectors, pGWBs, for realizing efficient construction of fusion genes for plant transformation. *J Biosci Bioeng,* 104**,** 34-41.

NAKAGAWA, T., SUZUKI, T., MURATA, S., NAKAMURA, S., HINO, T., MAEO, K., TABATA, R., KAWAI, T., TANAKA, K., NIWA, Y., WATANABE, Y., NAKAMURA, K., KIMURA, T. & ISHIGURO, S. 2007b. Improved Gateway binary vectors: high-performance vectors for creation of fusion constructs in transgenic analysis of plants. *Biosci Biotechnol Biochem,* 71**,** 2095-100.

NAKAMICHI, N., KIBA, T., HENRIQUES, R., MIZUNO, T., CHUA, N. H. & SAKAKIBARA, H. 2010. PSEUDO-RESPONSE REGULATORS 9, 7, and 5 are transcriptional repressors in the Arabidopsis circadian clock. *Plant Cell,* 22**,** 594-605.

NAKAMICHI, N., KIBA, T., KAMIOKA, M., SUZUKI, T., YAMASHINO, T., HIGASHIYAMA, T., SAKAKIBARA, H. & MIZUNO, T. 2012. Transcriptional repressor PRR5 directly regulates clock-output pathways. *Proc Natl Acad Sci U S A,* 109**,** 17123-8.

NAKAMICHI, N., KITA, M., ITO, S., YAMASHINO, T. & MIZUNO, T. 2005. PSEUDO-RESPONSE REGULATORS, PRR9, PRR7 and PRR5, together play essential roles close to the circadian clock of Arabidopsis thaliana. *Plant Cell Physiol,* 46**,** 686-98.

NAKAYAMA, K. & NAKAYAMA, K. 1998. Cip/Kip cyclin-dependent kinase inhibitors: brakes of the cell cycle engine during development. *Bioessays,* 20**,** 1020-9.

NATH, U., CRAWFORD, B. C., CARPENTER, R. & COEN, E. 2003. Genetic control of surface curvature. *Science,* 299**,** 1404-7.

NELSON, D. C., LASSWELL, J., ROGG, L. E., COHEN, M. A. & BARTEL, B. 2000. FKF1, a clock-controlled gene that regulates the transition to flowering in Arabidopsis. *Cell,* 101**,** 331-40.

NI, Z., KIM, E. D., HA, M., LACKEY, E., LIU, J., ZHANG, Y., SUN, Q. & CHEN, Z. J. 2009. Altered circadian rhythms regulate growth vigour in hybrids and allopolyploids. *Nature,* 457**,** 327-31.

NIETO, C., LOPEZ-SALMERON, V., DAVIERE, J. M. & PRAT, S. 2015. ELF3-PIF4 interaction regulates plant growth independently of the Evening Complex. *Curr Biol,* 25**,** 187-93.

NIKAIDO, S. S. & JOHNSON, C. H. 2000. Daily and circadian variation in survival from ultraviolet radiation in Chlamydomonas reinhardtii. *Photochem Photobiol,* 71**,** 758-65.

NISHITANI, H. & NURSE, P. 1995. p65cdc18 plays a major role controlling the initiation of DNA replication in fission yeast. *Cell,* 83**,** 397-405.

NIWA, Y., YAMASHINO, T. & MIZUNO, T. 2009. The circadian clock regulates the photoperiodic response of hypocotyl elongation through a coincidence mechanism in Arabidopsis thaliana. *Plant Cell Physiol,* 50**,** 838-54.

NOHALES, M. A. & KAY, S. A. 2016. Molecular mechanisms at the core of the plant circadian oscillator. *Nat Struct Mol Biol,* 23**,** 1061-1069.

NOWACK, M. K., HARASHIMA, H., DISSMEYER, N., ZHAO, X., BOUYER, D., WEIMER, A. K., DE WINTER, F., YANG, F. & SCHNITTGER, A. 2012. Genetic framework of cyclin-dependent kinase function in Arabidopsis. *Dev Cell,* 22**,** 1030-40.

NOZUE, K., COVINGTON, M. F., DUEK, P. D., LORRAIN, S., FANKHAUSER, C., HARMER, S. L. & MALOOF, J. N. 2007. Rhythmic growth explained by coincidence between internal and external cues. *Nature,* 448**,** 358-61.

NUSINOW, D. A., HELFER, A., HAMILTON, E. E., KING, J. J., IMAIZUMI, T., SCHULTZ, T. F., FARRE, E. M. & KAY, S. A. 2011. The ELF4-ELF3-LUX complex links the circadian clock to diurnal control of hypocotyl growth. *Nature,* 475**,** 398-402.

ONAI, K. & ISHIURA, M. 2005. PHYTOCLOCK 1 encoding a novel GARP protein essential for the Arabidopsis circadian clock. *Genes Cells,* 10**,** 963-72.

PANDA, S. 2016. Circadian physiology of metabolism. *Science,* 354**,** 1008-1015.

PANTIN, F., SIMONNEAU, T., ROLLAND, G., DAUZAT, M. & MULLER, B. 2011. Control of leaf expansion: a developmental switch from metabolics to hydraulics. *Plant Physiol,* 156**,** 803-15.

PARA, A., FARRE, E. M., IMAIZUMI, T., PRUNEDA-PAZ, J. L., HARMON, F. G. & KAY, S. A. 2007. PRR3 Is a vascular regulator of TOC1 stability in the Arabidopsis circadian clock. *Plant Cell,* 19**,** 3462-73.

PARTCH, C. L., GREEN, C. B. & TAKAHASHI, J. S. 2014. Molecular architecture of the mammalian circadian clock. *Trends Cell Biol,* 24**,** 90-9.

PERALES, M. & MAS, P. 2007. A functional link between rhythmic changes in chromatin structure and the Arabidopsis biological clock. *Plant Cell,* 19**,** 2111-23.

PERES, A., CHURCHMAN, M. L., HARIHARAN, S., HIMANEN, K., VERKEST, A., VANDEPOELE, K., MAGYAR, Z., HATZFELD, Y., VAN DER SCHUEREN, E., BEEMSTER, G. T., FRANKARD, V., LARKIN, J. C., INZE, D. & DE VEYLDER, L. 2007. Novel plant-specific cyclin-dependent kinase inhibitors induced by biotic and abiotic stresses. *J Biol Chem,* 282**,** 25588-96.

PEREZ-GARCIA, P., MA, Y., YANOVSKY, M. J. & MAS, P. 2015. Time-dependent sequestration of RVE8 by LNK proteins shapes the diurnal oscillation of anthocyanin biosynthesis. *Proc Natl Acad Sci U S A,* 112**,** 5249-53.

PESIN, J. A. & ORR-WEAVER, T. L. 2008. Regulation of APC/C activators in mitosis and meiosis. *Annu Rev Cell Dev Biol,* 24**,** 475-99.

PIATTI, S., LENGAUER, C. & NASMYTH, K. 1995. Cdc6 is an unstable protein whose de novo synthesis in G1 is important for the onset of S phase and for preventing a 'reductional' anaphase in the budding yeast Saccharomyces cerevisiae. *EMBO J,* 14**,** 3788-99.

PICKART, C. M. 2001. Mechanisms underlying ubiquitination. *Annu Rev Biochem,* 70**,** 503-33.

PILORZ, V., HELFRICH-FORSTER, C. & OSTER, H. 2018. The role of the circadian clock system in physiology. *Pflugers Arch,* 470**,** 227-239.

POIRE, R., WIESE-KLINKENBERG, A., PARENT, B., MIELEWCZIK, M., SCHURR, U., TARDIEU, F. & WALTER, A. 2010. Diel time-courses of leaf growth in monocot and dicot species: endogenous rhythms and temperature effects. *J Exp Bot,* 61**,** 1751-9.

POKHILKO, A., FERNANDEZ, A. P., EDWARDS, K. D., SOUTHERN, M. M., HALLIDAY, K. J. & MILLAR, A. J. 2012. The clock gene circuit in Arabidopsis includes a repressilator with additional feedback loops. *Mol Syst Biol,* 8**,** 574.

PORTOLES, S. & MAS, P. 2010. The functional interplay between protein kinase CK2 and CCA1 transcriptional activity is essential for clock temperature compensation in Arabidopsis. *PLoS Genet,* 6**,** e1001201.

PRUNEDA-PAZ, J. L., BRETON, G., PARA, A. & KAY, S. A. 2009. A functional genomics approach reveals CHE as a component of the Arabidopsis circadian clock. *Science,* 323**,** 1481-5.

QI, R. & JOHN, P. C. 2007. Expression of genomic AtCYCD2;1 in Arabidopsis induces cell division at smaller cell sizes: implications for the control of plant growth. *Plant Physiol,* 144**,** 1587-97.

RAMIREZ-PARRA, E., FRUNDT, C. & GUTIERREZ, C. 2003. A genome-wide identification of E2F-regulated genes in Arabidopsis. *Plant J,* 33**,** 801-11.

RAMOS, G. B., DE ALMEIDA ENGLER, J., FERREIRA, P. C. & HEMERLY, A. S. 2001. DNA replication in plants: characterization of a cdc6 homologue from Arabidopsis thaliana. *J Exp Bot,* 52**,** 2239-40.

RAWAT, R., TAKAHASHI, N., HSU, P. Y., JONES, M. A., SCHWARTZ, J., SALEMI, M. R., PHINNEY, B. S. & HARMER, S. L. 2011. REVEILLE8 and PSEUDO-REPONSE REGULATOR5 form a negative feedback loop within the Arabidopsis circadian clock. *PLoS Genet,* 7**,** e1001350.

REDIG, P., SHAUL, O., INZE, D., VAN MONTAGU, M. & VAN ONCKELEN, H. 1996. Levels of endogenous cytokinins, indole-3-acetic acid and abscisic acid during the cell cycle of synchronized tobacco BY-2 cells. *FEBS Lett,* 391**,** 175-80.

REMUS, D. & DIFFLEY, J. F. 2009. Eukaryotic DNA replication control: lock and load, then fire. *Curr Opin Cell Biol,* 21**,** 771-7.

RICHARD, C., LESCOT, M., INZÉ, D. & DE VEYLDER, L. 2002. Effect of auxin, cytokinin, and sucrose on cell cycle gene expression in Arabidopsis thaliana cell suspension cultures. *Plant Cell, Tissue and Organ Culture,* 69**,** 167-176.

RIOU-KHAMLICHI, C., HUNTLEY, R., JACQMARD, A. & MURRAY, J. A. 1999. Cytokinin activation of Arabidopsis cell division through a D-type cyclin. *Science,* 283**,** 1541-4.

RIOU-KHAMLICHI, C., MENGES, M., HEALY, J. M. & MURRAY, J. A. 2000. Sugar control of the plant cell cycle: differential regulation of Arabidopsis D-type cyclin gene expression. *Mol Cell Biol,* 20**,** 4513-21.

RIZZINI, L., FAVORY, J. J., CLOIX, C., FAGGIONATO, D., O'HARA, A., KAISERLI, E., BAUMEISTER, R., SCHAFER, E., NAGY, F., JENKINS, G. I. & ULM, R. 2011. Perception of UV-B by the Arabidopsis UVR8 protein. *Science,* 332**,** 103-6.

ROCKWELL, N. C., SU, Y. S. & LAGARIAS, J. C. 2006. Phytochrome structure and signaling mechanisms. *Annu Rev Plant Biol,* 57**,** 837-58.

ROODBARKELARI, F., BRAMSIEPE, J., WEINL, C., MARQUARDT, S., NOVAK, B., JAKOBY, M. J., LECHNER, E., GENSCHIK, P. & SCHNITTGER, A. 2010. Cullin 4-ring finger-ligase plays a key role in the control of endoreplication cycles in Arabidopsis trichomes. *Proc Natl Acad Sci U S A,* 107**,** 15275-80.

ROSSIGNOL, P., STEVENS, R., PERENNES, C., JASINSKI, S., CELLA, R., TREMOUSAYGUE, D. & BERGOUNIOUX, C. 2002. AtE2F-a and AtDP-a, members of the E2F family of transcription factors, induce Arabidopsis leaf cells to re-enter S phase. *Mol Genet Genomics,* 266**,** 995-1003.

RUGNONE, M. L., FAIGON SOVERNA, A., SANCHEZ, S. E., SCHLAEN, R. G., HERNANDO, C. E., SEYMOUR, D. K., MANCINI, E., CHERNOMORETZ, A., WEIGEL, D., MAS, P. & YANOVSKY, M. J. 2013. LNK genes integrate light and clock signaling networks at the core of the Arabidopsis oscillator. *Proc Natl Acad Sci U S A,* 110**,** 12120-5.

SALOME, P. A. & MCCLUNG, C. R. 2005. PSEUDO-RESPONSE REGULATOR 7 and 9 are partially redundant genes essential for the temperature responsiveness of the Arabidopsis circadian clock. *Plant Cell,* 17**,** 791-803.

SALOME, P. A., WEIGEL, D. & MCCLUNG, C. R. 2010. The role of the Arabidopsis morning loop components CCA1, LHY, PRR7, and PRR9 in temperature compensation. *Plant Cell,* 22**,** 3650-61.

SAUTER, M., MEKHEDOV, S. L. & KENDE, H. 1995. Gibberellin promotes histone H1 kinase activity and the expression of cdc2 and cyclin genes during the induction of rapid growth in deepwater rice internodes. *Plant J,* 7**,** 623-32.

SCHAFFER, R., RAMSAY, N., SAMACH, A., CORDEN, S., PUTTERILL, J., CARRE, I. A. & COUPLAND, G. 1998. The late elongated hypocotyl mutation of Arabidopsis disrupts circadian rhythms and the photoperiodic control of flowering. *Cell,* 93**,** 1219-29.

SCHNITTGER, A., SCHOBINGER, U., STIERHOF, Y. D. & HULSKAMP, M. 2002. Ectopic B-type cyclin expression induces mitotic cycles in endoreduplicating Arabidopsis trichomes. *Curr Biol,* 12**,** 415-20.

SCHULTZ, T. F., KIYOSUE, T., YANOVSKY, M., WADA, M. & KAY, S. A. 2001. A role for LKP2 in the circadian clock of Arabidopsis. *Plant Cell,* 13**,** 2659-70.

SEO, P. J., PARK, M. J., LIM, M. H., KIM, S. G., LEE, M., BALDWIN, I. T. & PARK, C. M. 2012. A self-regulatory circuit of CIRCADIAN CLOCK-ASSOCIATED1 underlies the circadian clock regulation of temperature responses in Arabidopsis. *Plant Cell,* 24**,** 2427-42.

SEQUEIRA-MENDES, J., ARAGUEZ, I., PEIRO, R., MENDEZ-GIRALDEZ, R., ZHANG, X., JACOBSEN, S. E., BASTOLLA, U. & GUTIERREZ, C. 2014. The Functional Topography of the Arabidopsis Genome Is Organized in a Reduced Number of Linear Motifs of Chromatin States. *Plant Cell,* 26**,** 2351-2366.

SERRANO, G., HERRERA-PALAU, R., ROMERO, J. M., SERRANO, A., COUPLAND, G. & VALVERDE, F. 2009. Chlamydomonas CONSTANS and the evolution of plant photoperiodic signaling. *Curr Biol,* 19**,** 359-68.

SHARROCK, R. A. & QUAIL, P. H. 1989. Novel phytochrome sequences in Arabidopsis thaliana: structure, evolution, and differential expression of a plant regulatory photoreceptor family. *Genes Dev,* 3**,** 1745-57.

SHEN, W. H. 2002. The plant E2F-Rb pathway and epigenetic control. *Trends Plant Sci,* 7**,** 505-11.

SHULTZ, R. W., LEE, T. J., ALLEN, G. C., THOMPSON, W. F. & HANLEY-BOWDOIN, L. 2009. Dynamic localization of the DNA replication proteins MCM5 and MCM7 in plants. *Plant Physiol,* 150**,** 658-69.

SHULTZ, R. W., TATINENI, V. M., HANLEY-BOWDOIN, L. & THOMPSON, W. F. 2007. Genome-wide analysis of the core DNA replication machinery in the higher plants Arabidopsis and rice. *Plant Physiol,* 144**,** 1697-714.

SOMERS, D. E., SCHULTZ, T. F., MILNAMOW, M. & KAY, S. A. 2000. ZEITLUPE encodes a novel clock-associated PAS protein from Arabidopsis. *Cell,* 101**,** 319-29.

SOMERS, D. E., WEBB, A. A., PEARSON, M. & KAY, S. A. 1998. The short-period mutant, toc1-1, alters circadian clock regulation of multiple outputs throughout development in Arabidopsis thaliana. *Development,* 125**,** 485-94.

SONG, H. R. & NOH, Y. S. 2012. Rhythmic oscillation of histone acetylation and methylation at the Arabidopsis central clock loci. *Mol Cells,* 34**,** 279-87.

SOY, J., LEIVAR, P., GONZALEZ-SCHAIN, N., MARTIN, G., DIAZ, C., SENTANDREU, M., AL-SADY, B., QUAIL, P. H. & MONTE, E. 2016. Molecular convergence of clock and photosensory pathways through PIF3-TOC1 interaction and co-occupancy of target promoters. *Proc Natl Acad Sci U S A,* 113**,** 4870-5.

SOZZANI, R., MAGGIO, C., GIORDO, R., UMANA, E., ASCENCIO-IBANEZ, J. T., HANLEY-BOWDOIN, L., BERGOUNIOUX, C., CELLA, R. & ALBANI, D. 2010. The E2FD/DEL2 factor is a component of a regulatory network controlling cell proliferation and development in Arabidopsis. *Plant Mol Biol,* 72**,** 381-95.

SOZZANI, R., MAGGIO, C., VAROTTO, S., CANOVA, S., BERGOUNIOUX, C., ALBANI, D. & CELLA, R. 2006. Interplay between Arabidopsis activating factors E2Fb and E2Fa in cell cycle progression and development. *Plant Physiol,* 140**,** 1355-66.

STERN, B. & NURSE, P. 1996. A quantitative model for the cdc2 control of S phase and mitosis in fission yeast. *Trends Genet,* 12**,** 345-50.

STEVENSON, T. J. 2017. Epigenetic Regulation of Biological Rhythms: An

Evolutionary Ancient Molecular Timer. *Trends Genet*.

STRATMANN, M. & SCHIBLER, U. 2006. Properties, entrainment, and physiological functions of mammalian peripheral oscillators. *J Biol Rhythms,* 21**,** 494-506.

STRAYER, C., OYAMA, T., SCHULTZ, T. F., RAMAN, R., SOMERS, D. E., MAS, P., PANDA, S., KREPS, J. A. & KAY, S. A. 2000. Cloning of the Arabidopsis clock gene TOC1, an autoregulatory response regulator homolog. *Science,* 289**,** 768-71.

SUSAN, W. 2014. Genome Duplication: Concepts, Mechanisms, Evolution, and Disease. Melvin L. DePamphilis and Stephen D. Bell, Garland Science, 2011, 450 pp., ISBN 978-0-4154–4206-0 (paperback, $162.00). *Biochemistry and Molecular Biology Education,* 42**,** 281-281.

SWEENEY, B. M. & HASTINGS, J. W. 1958. Rhythmic Cell Division in Populations of Gonyaulax polyedra*†‡. *The Journal of Protozoology,* 5**,** 217-224.

TAKAHASHI, N., HIRATA, Y., AIHARA, K. & MAS, P. 2015. A hierarchical multi-oscillator network orchestrates the Arabidopsis circadian system. *Cell,* 163**,** 148-59.

TAKAHASHI, N., KAJIHARA, T., OKAMURA, C., KIM, Y., KATAGIRI, Y., OKUSHIMA, Y., MATSUNAGA, S., HWANG, I. & UMEDA, M. 2013. Cytokinins control endocycle onset by promoting the expression of an APC/C activator in Arabidopsis roots. *Curr Biol,* 23**,** 1812-7.

TAKAHASHI, N., LAMMENS, T., BOUDOLF, V., MAES, S., YOSHIZUMI, T., DE JAEGER, G., WITTERS, E., INZE, D. & DE VEYLDER, L. 2008. The DNA replication checkpoint aids survival of plants deficient in the novel replisome factor ETG1. *EMBO J,* 27**,** 1840-51.

TAKAHASHI, N., QUIMBAYA, M., SCHUBERT, V., LAMMENS, T., VANDEPOELE, K., SCHUBERT, I., MATSUI, M., INZE, D., BERX, G. & DE VEYLDER, L. 2010. The MCM-binding protein ETG1 aids sister chromatid cohesion required for postreplicative homologous recombination repair. *PLoS Genet,* 6**,** e1000817.

TARAYRE, S., VINARDELL, J. M., CEBOLLA, A., KONDOROSI, A. & KONDOROSI, E. 2004. Two classes of the CDh1-type activators of the anaphase-promoting complex in plants: novel functional domains and distinct regulation. *Plant Cell,* 16**,** 422-34.

TERZIBASI-TOZZINI, E., MARTINEZ-NICOLAS, A. & LUCAS-SANCHEZ, A. 2017. The clock is ticking. Ageing of the circadian system: From physiology to cell cycle. *Semin Cell Dev Biol,* 70**,** 164-176.

THAIN, S. C., HALL, A. & MILLAR, A. J. 2000. Functional independence of circadian clocks that regulate plant gene expression. *Curr Biol,* 10**,** 951-6.

THINES, B. & HARMON, F. G. 2010. Ambient temperature response establishes ELF3 as a required component of the core Arabidopsis circadian clock. *Proc Natl Acad Sci U S A,* 107**,** 3257-62.

TRAAS, J., HULSKAMP, M., GENDREAU, E. & HOFTE, H. 1998. Endoreduplication and development: rule without dividing? *Curr Opin Plant Biol,* 1**,** 498-503.

TRAAS, J. & MONEGER, F. 2010. Systems biology of organ initiation at the shoot apex. *Plant Physiol,* 152**,** 420-7.

TSUKAYA, H. 2002. Interpretation of mutants in leaf morphology: genetic evidence for a compensatory system in leaf morphogenesis that provides a new link between cell and organismal theories. *Int Rev Cytol,* 217**,** 1-39.

TSUKAYA, H. 2003. Organ shape and size: a lesson from studies of leaf morphogenesis. *Curr Opin Plant Biol,* 6**,** 57-62.

UEMUKAI, K., IWAKAWA, H., KOSUGI, S., DE UEMUKAI, S., KATO, K., KONDOROSI, E., MURRAY, J. A., ITO, M., SHINMYO, A. & SEKINE, M. 2005. Transcriptional activation of tobacco E2F is repressed by co-transfection with the retinoblastoma-related protein: cyclin D expression overcomes this repressor activity. *Plant Mol Biol,* 57**,** 83-100.

VAN DEN HEUVEL, S. & DYSON, N. J. 2008. Conserved functions of the pRB and E2F families. *Nat Rev Mol Cell Biol,* 9**,** 713-24.

VAN DER VEEN, D. R., RIEDE, S. J., HEIDEMAN, P. D., HAU, M., VAN DER VINNE, V. & HUT, R. A. 2017. Flexible clock systems: adjusting the temporal programme. *Philos Trans R Soc Lond B Biol Sci,* 372.

VAN WORDRAGEN, M. F., DE JONG, J., SCHORNAGEL, M. J. & DONS, H. J. M. 1992. Rapid screening for host-bacterium interactions in Agrobacterium-mediated gene transfer to chrysanthemum, by using the GUS-intron gene. *Plant Science,* 81**,** 207-214.

VANDENBUSSCHE, F., VERBELEN, J. P. & VAN DER STRAETEN, D. 2005. Of light and length: regulation of hypocotyl growth in Arabidopsis. *Bioessays,* 27**,** 275-84.

VANDEPOELE, K., RAES, J., DE VEYLDER, L., ROUZE, P., ROMBAUTS, S. & INZE, D. 2002. Genome-wide analysis of core cell cycle genes in Arabidopsis. *Plant Cell,* 14**,** 903-16.

VANDEPOELE, K., VLIEGHE, K., FLORQUIN, K., HENNIG, L., BEEMSTER, G. T., GRUISSEM, W., VAN DE PEER, Y., INZE, D. & DE VEYLDER, L. 2005. Genome-wide identification of potential plant E2F target genes. *Plant Physiol,* 139**,** 316-28.

VANSTRAELEN, M., BALOBAN, M., DA INES, O., CULTRONE, A., LAMMENS, T., BOUDOLF, V., BROWN, S. C., DE VEYLDER, L., MERGAERT, P. & KONDOROSI, E. 2009. APC/C-CCS52A complexes control meristem maintenance in the Arabidopsis root. *Proc Natl Acad Sci U S A,* 106**,** 11806-11.

VERKEST, A., MANES, C. L., VERCRUYSSE, S., MAES, S., VAN DER SCHUEREN, E., BEECKMAN, T., GENSCHIK, P., KUIPER, M., INZE, D. & DE VEYLDER, L. 2005. The cyclin-dependent kinase inhibitor KRP2 controls the onset of the endoreduplication cycle during Arabidopsis leaf development through inhibition of mitotic CDKA;1 kinase complexes. *Plant Cell,* 17**,** 1723-36.

VLIEGHE, K., BOUDOLF, V., BEEMSTER, G. T., MAES, S., MAGYAR, Z., ATANASSOVA, A., DE ALMEIDA ENGLER, J., DE GROODT, R., INZE, D. & DE VEYLDER, L. 2005. The DP-E2F-like gene DEL1 controls the endocycle in Arabidopsis thaliana. *Curr Biol,* 15**,** 59-63.

VODERMAIER, H. C. 2004. APC/C and SCF: controlling each other and the cell cycle. *Curr Biol,* 14**,** R787-96.

WALKER, J. D., OPPENHEIMER, D. G., CONCIENNE, J. & LARKIN, J. C. 2000. SIAMESE, a gene controlling the endoreduplication cell cycle in Arabidopsis thaliana trichomes. *Development,* 127**,** 3931-40.

WALTER, A., SILK, W. K. & SCHURR, U. 2009. Environmental effects on spatial and temporal patterns of leaf and root growth. *Annu Rev Plant Biol,* 60**,** 279-304.

WANG, B., FENG, L., HU, Y., HUANG, S. H., REYNOLDS, C. P., WU, L. & JONG, A. Y. 1999. The essential role of Saccharomyces cerevisiae CDC6 nucleotide-binding site in cell growth, DNA synthesis, and Orc1 association. *J Biol Chem,* 274**,** 8291-8.

WANG, H., QI, Q., SCHORR, P., CUTLER, A. J., CROSBY, W. L. & FOWKE, L. C. 1998. ICK1, a cyclin-dependent protein kinase inhibitor from Arabidopsis thaliana interacts with both Cdc2a and CycD3, and its expression is induced by abscisic acid. *Plant J,* 15**,** 501-10.

WANG, H., ZHOU, Y., GILMER, S., WHITWILL, S. & FOWKE, L. C. 2000. Expression of the plant cyclin-dependent kinase inhibitor ICK1 affects cell division, plant growth and morphology. *Plant J,* 24**,** 613-23.

WANG, L., FUJIWARA, S. & SOMERS, D. E. 2010. PRR5 regulates phosphorylation, nuclear import and subnuclear localization of TOC1 in the Arabidopsis circadian clock. *EMBO J,* 29**,** 1903-15.

WANG, X., WU, F., XIE, Q., WANG, H., WANG, Y., YUE, Y., GAHURA, O., MA, S., LIU, L., CAO, Y., JIAO, Y., PUTA, F., MCCLUNG, C. R., XU, X. & MA, L. 2012. SKIP is a component of the spliceosome linking alternative splicing and the circadian clock in Arabidopsis. *Plant Cell,* 24**,** 3278-95.

WANG, Y., WU, J. F., NAKAMICHI, N., SAKAKIBARA, H., NAM, H. G. & WU, S. H. 2011. LIGHT-REGULATED WD1 and PSEUDO-RESPONSE REGULATOR9 form a positive feedback regulatory loop in the Arabidopsis circadian clock. *Plant Cell,* 23**,** 486-98.

WANG, Z. Y. & TOBIN, E. M. 1998. Constitutive expression of the CIRCADIAN CLOCK ASSOCIATED 1 (CCA1) gene disrupts circadian rhythms and suppresses its own expression. *Cell,* 93**,** 1207-17.

WEINL, C., MARQUARDT, S., KUIJT, S. J., NOWACK, M. K., JAKOBY, M. J., HULSKAMP, M. & SCHNITTGER, A. 2005. Novel functions of plant cyclin-dependent kinase inhibitors, ICK1/KRP1, can act non-cell-autonomously and inhibit entry into mitosis. *Plant Cell,* 17**,** 1704-22.

WELSH, D. K., TAKAHASHI, J. S. & KAY, S. A. 2010. Suprachiasmatic nucleus: cell autonomy and network properties. *Annu Rev Physiol,* 72**,** 551-77.

WENDEN, B., KOZMA-BOGNAR, L., EDWARDS, K. D., HALL, A. J., LOCKE, J. C. & MILLAR, A. J. 2011. Light inputs shape the Arabidopsis circadian system. *Plant J,* 66**,** 480-91.

WENDEN, B., TONER, D. L., HODGE, S. K., GRIMA, R. & MILLAR, A. J. 2012. Spontaneous spatiotemporal waves of gene expression from biological clocks in the leaf. *Proc Natl Acad Sci U S A,* 109**,** 6757-62.

WILLIAMS, R. S., SHOHET, R. V. & STILLMAN, B. 1997. A human protein related to yeast Cdc6p. *Proc Natl Acad Sci U S A,* 94**,** 142-7.

WOLF, D. A., MCKEON, F. & JACKSON, P. K. 1999. Budding yeast Cdc6p induces re-replication in fission yeast by inhibition of SCF(Pop)-mediated proteolysis. *Mol Gen Genet,* 262**,** 473-80.

WU, J. F., TSAI, H. L., JOANITO, I., WU, Y. C., CHANG, C. W., LI, Y. H., WANG, Y., HONG, J. C., CHU, J. W., HSU, C. P. & WU, S. H. 2016. LWD-TCP complex activates the morning gene CCA1 in Arabidopsis. *Nat Commun,* 7**,** 13181.

XIE, Q., WANG, P., LIU, X., YUAN, L., WANG, L., ZHANG, C., LI, Y., XING, H., ZHI, L., YUE, Z., ZHAO, C., MCCLUNG, C. R. & XU, X. 2014. LNK1 and LNK2 are transcriptional coactivators in the Arabidopsis circadian oscillator. *Plant Cell,* 26**,** 2843-57.

XIONG, Y., MCCORMACK, M., LI, L., HALL, Q., XIANG, C. & SHEEN, J. 2013. Glucose-TOR signalling reprograms the transcriptome and activates meristems. *Nature,* 496, 181-6.

YAKIR, E., HASSIDIM, M., MELAMED-BOOK, N., HILMAN, D., KRON, I. & GREEN, R. M. 2011. Cell autonomous and cell-type specific circadian rhythms in Arabidopsis. *Plant J,* 68, 520-31.

YAKIR, E., HILMAN, D., HASSIDIM, M. & GREEN, R. M. 2007. CIRCADIAN CLOCK ASSOCIATED1 transcript stability and the entrainment of the circadian clock in Arabidopsis. *Plant Physiol,* 145, 925-32.

YAMASHINO, T., MATSUSHIKA, A., FUJIMORI, T., SATO, S., KATO, T., TABATA, S. & MIZUNO, T. 2003. A Link between circadian-controlled bHLH factors and the APRR1/TOC1 quintet in Arabidopsis thaliana. *Plant Cell Physiol,* 44, 619-29.

YEOM, M., KIM, H., LIM, J., SHIN, A. Y., HONG, S., KIM, J. I. & NAM, H. G. 2014. How do phytochromes transmit the light quality information to the circadian clock in Arabidopsis? *Mol Plant,* 7, 1701-4.

YI, D., ALVIM KAMEI, C. L., COOLS, T., VANDERAUWERA, S., TAKAHASHI, N., OKUSHIMA, Y., EEKHOUT, T., YOSHIYAMA, K. O., LARKIN, J., VAN DEN DAELE, H., CONKLIN, P., BRITT, A., UMEDA, M. & DE VEYLDER, L. 2014. The Arabidopsis SIAMESE-RELATED cyclin-dependent kinase inhibitors SMR5 and SMR7 regulate the DNA damage checkpoint in response to reactive oxygen species. *Plant Cell,* 26, 296-309.

YU, J. W., RUBIO, V., LEE, N. Y., BAI, S., LEE, S. Y., KIM, S. S., LIU, L., ZHANG, Y., IRIGOYEN, M. L., SULLIVAN, J. A., ZHANG, Y., LEE, I., XIE, Q., PAEK, N. C. & DENG, X. W. 2008. COP1 and ELF3 control circadian function and photoperiodic flowering by regulating GI stability. *Mol Cell,* 32, 617-30.

ZHANG, X., XIAO, D., WANG, Z., ZOU, Y., HUANG, L., LIN, W., DENG, Q., PAN, H., ZHOU, J., LIANG, C. & HE, J. 2014. MicroRNA-26a/b regulate DNA replication licensing, tumorigenesis, and prognosis by targeting CDC6 in lung cancer. *Mol Cancer Res,* 12, 1535-46.

ZHAO, X., HARASHIMA, H., DISSMEYER, N., PUSCH, S., WEIMER, A. K., BRAMSIEPE, J., BOUYER, D., RADEMACHER, S., NOWACK, M. K., NOVAK, B., SPRUNCK, S. & SCHNITTGER, A. 2012. A general G1/S-phase cell-cycle control module in the flowering plant Arabidopsis thaliana. *PLoS Genet,* 8, e1002847.

ZHOU, Y., WANG, H., GILMER, S., WHITWILL, S. & FOWKE, L. C. 2003. Effects of co-expressing the plant CDK inhibitor ICK1 and D-type cyclin genes on plant growth, cell size and ploidy in Arabidopsis thaliana. *Planta,* 216, 604-13.

ZHU, J. Y., OH, E., WANG, T. & WANG, Z. Y. 2016. TOC1-PIF4 interaction mediates the circadian gating of thermoresponsive growth in Arabidopsis. *Nat Commun,* 7, 13692.

ZHU, X. G., LONG, S. P. & ORT, D. R. 2010. Improving photosynthetic efficiency for greater yield. *Annu Rev Plant Biol,* 61, 235-61.

ANNEXES

Annexes

Annex I

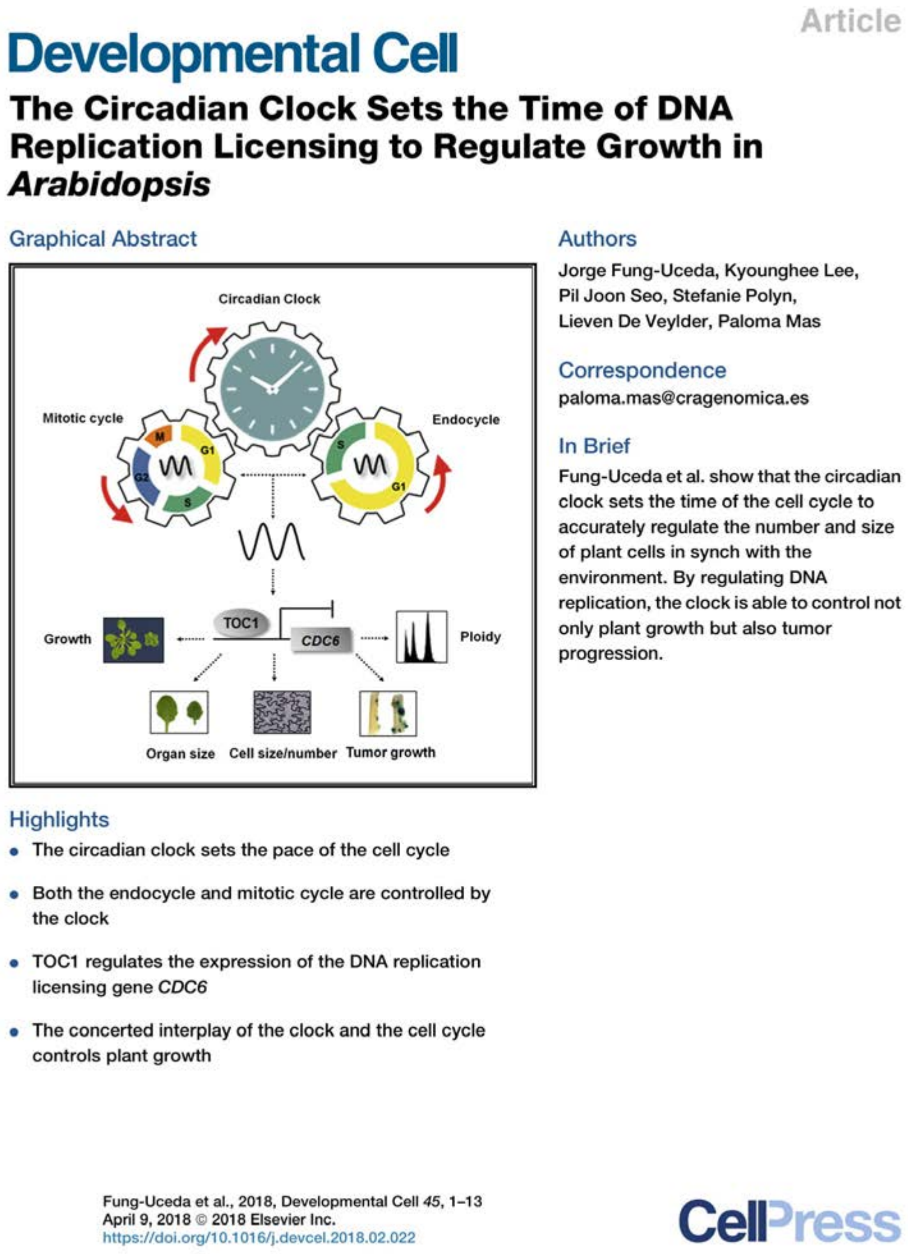

Developmental Cell

Article

The Circadian Clock Sets the Time of DNA Replication Licensing to Regulate Growth in *Arabidopsis*

Graphical Abstract

Circadian Clock
Mitotic cycle
Endocycle
M
G1
G2
S
S
G1
TOC1
CDC6
Growth
Ploidy
Organ size
Cell size/number
Tumor growth

Authors

Jorge Fung-Uceda, Kyounghee Lee, Pil Joon Seo, Stefanie Polyn, Lieven De Veylder, Paloma Mas

Correspondence

paloma.mas@cragenomica.es

In Brief

Fung-Uceda et al. show that the circadian clock sets the time of the cell cycle to accurately regulate the number and size of plant cells in synch with the environment. By regulating DNA replication, the clock is able to control not only plant growth but also tumor progression.

Highlights

- The circadian clock sets the pace of the cell cycle
- Both the endocycle and mitotic cycle are controlled by the clock
- TOC1 regulates the expression of the DNA replication licensing gene *CDC6*
- The concerted interplay of the clock and the cell cycle controls plant growth

Fung-Uceda et al., 2018, Developmental Cell *45*, 1–13
April 9, 2018 © 2018 Elsevier Inc.
https://doi.org/10.1016/j.devcel.2018.02.022

Please cite this article in press as: Fung-Uceda et al., The Circadian Clock Sets the Time of DNA Replication Licensing to Regulate Growth in *Arabidopsis*, Developmental Cell (2018), https://doi.org/10.1016/j.devcel.2018.02.022

Developmental Cell

Article

The Circadian Clock Sets the Time of DNA Replication Licensing to Regulate Growth in *Arabidopsis*

Jorge Fung-Uceda,[1] Kyounghee Lee,[2] Pil Joon Seo,[2] Stefanie Polyn,[3,4] Lieven De Veylder,[3,4] and Paloma Mas[1,5,6,*]

[1] Plant Development and Signal Transduction, Centre for Research in Agricultural Genomics (CRAG), CSIC-IRTA-UAB-UB, Campus UAB, Bellaterra, 08193 Barcelona, Spain

[2] Department of Biological Sciences, Sungkyunkwan University, Suwon 16419, Republic of Korea

[3] Ghent University, Department of Plant Biotechnology and Bioinformatics, Technologiepark 927, 9052 Ghent, Belgium

[4] VIB Center for Plant Systems Biology, Technologiepark 927, 9052 Ghent, Belgium

[5] Consejo Superior de Investigaciones Científicas (CSIC), 08028 Barcelona, Spain

[6] Lead Contact

*Correspondence: paloma.mas@cragenomica.es

https://doi.org/10.1016/j.devcel.2018.02.022

SUMMARY

The circadian clock and cell cycle as separate pathways have been well documented in plants. Elucidating whether these two oscillators are connected is critical for understanding plant growth. We found that a slow-running circadian clock decelerates the cell cycle and, conversely, a fast clock speeds it up. The clock component TOC1 safeguards the G_1-to-S transition and controls the timing of the mitotic cycle at early stages of leaf development. TOC1 also regulates somatic ploidy at later stages of leaf development and in hypocotyl cells. The S-phase is shorter and delayed in TOC1 overexpressing plants, which correlates with the diurnal repression of the DNA replication licensing gene *CDC6* through binding of TOC1 to the *CDC6* promoter. The slow cell-cycle pace in TOC1-ox also results in delayed tumor progression in inflorescence stalks. Thus, TOC1 sets the time of the DNA pre-replicative machinery to control plant growth in resonance with the environment.

INTRODUCTION

Biological rhythms are ubiquitous in nature, from the heart ventricle depolarization with subsecond periods to the flowering of Chinese bamboo every 100–120 years. Within a cell, distinct rhythmic activities are coordinated by metabolic and environmental cues to ultimately sustain cellular homeostasis. Both the circadian clock and the cell cycle exhibit rhythmic phases of activation and repression, operated by interlocked feedback loops. Evolution might have favored the interplay between two such oscillators, providing circadian timing information to cell division and differentiation. Despite its biological relevance, the possible connection between the circadian clock and the cell cycle in plants has remained elusive.

The circadian function is crucial for adaptation to the environment. In *Arabidopsis thaliana*, virtually every cell contains a clock displaying different degrees of circadian coupling depending on the organ and the environmental conditions (e.g., Bordage et al., 2016; Endo et al., 2014; Takahashi et al., 2015; Thain et al., 2000; Wenden et al., 2012; Yakir et al., 2011). The molecular architecture responsible for the generation of rhythms relies on regulatory waves of clock core gene expression that oscillate at different phases during the day and night (Nohales and Kay, 2016). The rhythms in gene expression are translated into oscillations of physiological and developmental outputs.

One key component of the *Arabidopsis* circadian system is the pseudo-response regulator TOC1/PRR1 (TIMING OF CAB EXPRESSION1/PSEUDO RESPONSE REGULATOR1) (Makino et al., 2002; Strayer et al., 2000). TOC1 belongs to a family composed of five members sequentially expressed from dawn to dusk (Matsushika et al., 2000). TOC1 overexpression (TOC1-ox) slows down the pace of the clock under diurnal conditions and leads to arrhythmia under constant light conditions (Makino et al., 2002; Más et al., 2003a). Conversely, the clock runs faster in TOC1 mutant or silenced plants (Más et al., 2003a; Somers et al., 1998; Strayer et al., 2000). TOC1 also represses the expression of nearly all clock core genes (Gendron et al., 2012; Huang et al., 2012; Pokhilko et al., 2012). Misexpression of TOC1 also affects rhythmic outputs including among others hypocotyl growth, flowering time (Más et al., 2003a; Niwa et al., 2007; Somers et al., 1998), and responses to drought (Legnaioli et al., 2009). TOC1 also contributes to clock resonance with the environment for proper growth (Más et al., 2003a; Yamashino et al., 2008).

Plant growth is regulated by a plethora of pathways that eventually operate through the control of cell proliferation and differentiation (Inzé and De Veylder, 2006). Broadly speaking, changes in the rate and duration of the cell cycle determine the cell number and size that correlate with organ growth during development (Gonzalez et al., 2012; Sablowski and Carnier Dornelas, 2014). Cell proliferation through progression of the mitotic cycle is governed by the activation of cyclin-dependent kinases (CDKs), which associate with specific cyclins (CYCs) to control the G_1 (Gap 1) to S (DNA Synthesis) and the G_2 (Gap 2) to M (Mitotic) transition phases (Gutierrez, 2009). Critical checkpoints at the transitions ensure proper control of the cell cycle. After proliferation, differentiation often coincides with the switch to the endocycle (or endoreplication), an alternative

Please cite this article in press as: Fung-Uceda et al., The Circadian Clock Sets the Time of DNA Replication Licensing to Regulate Growth in *Arabidopsis*, Developmental Cell (2018), https://doi.org/10.1016/j.devcel.2018.02.022

mode of the cell cycle in which the mitotic CYC-CDK complex activity decreases. During this cell-cycle variant, cells duplicate their genomic DNA without mitoses, which is characteristic of polyploid cells (Edgar et al., 2014).

Control of the plant cell cycle at the G_1-S-phase transition is exerted by D-type CYCs (CYCD) and A-type CDKs (CDKA) (Nowack et al., 2012) that also contributes to M-phase entry (De Veylder et al., 2007). A key regulatory event for cell-cycle progression is licensing DNA for replication, which allows cells to progress into S-phase. Origin licensing relies on the sequential formation of pre-replicative complexes composed of a number of proteins including the Origin Recognition Complex (ORC), CELL DIVISION CONTROL 6 (CDC6), ARABIDOPSIS HOMOLOG OF YEAST CDT1 (CDT1a), and Minichromosome maintenance (MCM). In *Arabidopsis*, *CDC6* is upregulated at the G_1-S transition, reaching a peak early in S-phase (Castellano et al., 2001). CDC6 and CDT1a are active in dividing and endoreplicating cells, and their overexpression induces endoreplication (Castellano et al., 2001, 2004). The S-phase relies on a balance between the inhibition of the E2F/DP transcriptional activity by the hypophosphorylated retinoblastoma-related (RBR) protein and RBR phosphorylation by the CDKA-CYCD kinase activity, which relieves the repression (De Veylder et al., 2007). E2Fa/b activate the expression of genes involved in DNA synthesis and replication including *CDC6* and *CDT1* (de Jager et al., 2005). Their transcriptional and post-transcriptional regulation are key for sustaining the balance between cell proliferation and differentiation (Gutierrez, 2009).

Gating of cell division by the clock has been reported in unicellular organisms (Johnson, 2010; Pando and van Oudenaarden, 2010). However, studying the circadian regulation of the cell cycle in the context of a growing multicellular organism adds numerous layers of complexity that highly complicates the studies (Brown, 2014; Hunt and Sassone-Corsi, 2007). For instance, the circadian gating of cell division has been described in mammals (e.g., Kowalska et al., 2013; Matsuo et al., 2003; Nagoshi et al., 2004). However, other studies have reported the lack of such circadian regulation (e.g., Pendergast et al., 2010; Yeom et al., 2010). Another open question concerns the unidirectional versus bidirectional regulation between the cell cycle and the circadian clock (Feillet et al., 2015).

The role of the circadian clock in controlling plant growth and nearly every aspect of development raises the appealing idea of a connection between the circadian clock and the cell cycle. Despite its biological relevance, the interplay of these two oscillators remains to be fully explored in higher plants. Here we tackle this question to demonstrate that the circadian clock, through TOC1 function, drives the speed of the cell cycle in *Arabidopsis*. By regulating the DNA pre-replicative machinery, the circadian clock modulates cell division during proliferation and somatic ploidy during differentiation and thus controls not only normal growth but also tumor development.

RESULTS

TOC1 Regulates the Timing of Cell Division in Developing Leaves

TOC1-ox plants show a dwarf phenotype, with reduced plant size (Figure 1A) and small leaves (Figure 1B). At early stages of leaf development, active cell division during the mitotic cycle controls growth. To examine the possible involvement of TOC1 in cell division, we conducted time-course analyses at early time points of growth with the first pair of leaves grown under short days (ShD; 8 hr light,16 hr dark) and long days (LgD; 16 hr light, 8 hr dark). The blade area of wild-type (WT) plants showed a progressive growth, consistent with the trend reported by previous studies (De Veylder et al., 2001). In contrast, leaf area was considerably reduced in TOC1-ox (Figure 1C), a phenotype that was evident at early stages (6 and 7 days after stratification [das]). Although leaves continued growing over the days, the growth rate in TOC1-ox was noticeably reduced compared with WT and resulted in a 60% reduction at 9 das (Figure 1C). Leaf epidermal cell number was reduced in TOC1-ox at early stages (Figure 1D), which indicates that cell proliferation is affected by accumulation of TOC1. Cell area was also reduced in TOC1-ox (Figure 1E), suggesting that both the reduced cell number and area contribute to the reduction of leaf size. A role for TOC1 controlling the duration of the mitotic cycle was supported by the analysis of the average cell division rate, which showed a slower speed in TOC1-ox (0.032 cells $\text{cell}^{-1}\ \text{hr}^{-1}$) compared with WT (0.050 cells $\text{cell}^{-1}\ \text{hr}^{-1}$) (Figure 1F). A similar reduced leaf area, cell area, and cell number were observed in TOC1-ox under LgD (Figure S1), which also led to a reduced average cell division rate (Figure S1). Therefore, overexpression of TOC1 affects the speed of the cell cycle, altering cell division during the mitotic cycle. Analyses of *ztl-3* mutant plants, harboring a mutation in ZTL (ZEITLUPE) (Somers et al., 2000), the F-box protein responsible for TOC1 protein degradation (Más et al., 2003b), showed a decreased plant size and leaf area that correlated with reduced cell number and cell size (Figure S1), following a similar trend to that observed in TOC1-ox. Conversely, *toc1-2* mutant plants displayed increased leaf size that coincided with higher cell number at early stages of development and increased cell area at later stages (Figure S1).

To determine whether a specific cell-cycle phase is affected in TOC1-ox, we conducted flow-cytometry analyses to examine ploidy profiles of leaves from plants grown at 9 das under ShD or 7 das under LgD. WT and TOC1-ox mostly showed nuclear DNA content (C values) of 2C and 4C, correlating with the high proliferation at this developmental stage (Figure S1). Calculation of the relative amount of cells in the G_1, S, and G_2/M phases revealed that TOC1-ox leaves displayed a decreased proportion of nuclei in S and G_2/M phases and a clear enrichment of the G_1 phase under both ShD (Figure 1G) and LgD (Figure S1). The data indicate that the G_1 phase takes longer in TOC1-ox (approx. 22 hr) than in WT (approx. 13 hr) at the expense of a shorter S-phase (1.6 hr versus 2 hr in WT) (compare TOC1-ox in the outer ring with WT in the inner ring in Figure 1H). A similar trend was observed under LgD (Figure S1). Thus, the slow circadian clock in TOC1-ox plants correlates with an extended G_1 phase and reduced S-phase. The results indicate that TOC1 is important not only for controlling the pace of the clock but also the cell cycle.

TOC1 Controls the Timing of the Endocycle in Leaves

Our results suggest that TOC1 regulates the mitotic cycle at early stages of leaf development. However, after the mitotic cycle, cells transition to the endocycle in which endoreplication

Please cite this article in press as: Fung-Uceda et al., The Circadian Clock Sets the Time of DNA Replication Licensing to Regulate Growth in *Arabidopsis*, Developmental Cell (2018), https://doi.org/10.1016/j.devcel.2018.02.022

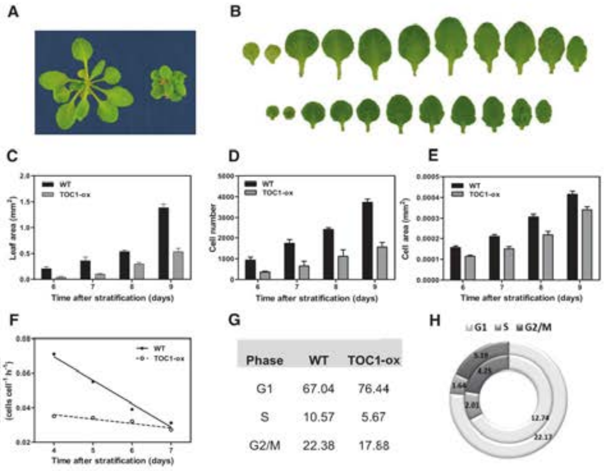

Figure 1. TOC1 Modulates Growth and the Mitotic Cycle in Developing Leaves

(A–E) Representative images of (A) WT and TOC1-ox plants at 24 das and (B) leaves from WT (top) and TOC1-ox (bottom) plants at 22 das under LgD. Leaves are shown from the oldest, including the two cotyledons (left) to the youngest (right). Early time-course analyses of (C) leaf blade area, (D) cell number, and (E) cell area of the first leaf pair. Data are mean + SEM of n ≈ 10–20 leaves and n ≈ 100 cells.

(F) Average cell division rates of abaxial epidermal cells and linear regression analyses of the first four points of the kinematic assay.

(G) Estimation of the relative amounts of cells in G_1, S, and G_2/M phases in proliferating first pair of leaves analyzed by flow cytometry at 9 das.

(H) Estimated duration (hr) of the G_1, S, and G_2/M phases at 9 das in WT (inner rings) and TOC1-ox (outer rings). Plants were grown under ShD. At least two biological replicates per experiment were performed.

See also Figure S1.

predominates at mid and late stages of leaf growth (De Veylder et al., 2011). To determine whether in addition to the mitotic cycle TOC1 also regulates endoreplication in leaves, we conducted a time-course analysis by flow cytometry to examine ploidy of leaves at later stages of development (Figure 2A). At 13 das, WT plants grown under ShD showed around 5% of the nuclei with 8C content, which represent cells entering the endocycle (Figures 2B and S2). The frequency of 2C and 4C nuclei progressively decreased over time in favor of higher-order C values that can be attributed to extra rounds of endoreplication (Figures 2B and S2). In TOC1-ox seedlings at 13 das, the 4C/2C ratio was reduced compared with WT (Figure 2C). The sharp 4C increase observed in WT was delayed and reached a peak only at 15 das in TOC1-ox (Figure 2D) while the marked reduction of the 2C content at 9 to 13 das observed in WT leaves was less pronounced in TOC1-ox (Figures 2B and 2C). From day 13 onward, the proportion of 8C and 16C nuclei was considerably reduced in TOC1-ox compared with WT (Figures 2B, 2C, and S2).

Leaf ploidy of plants grown under LgD also revealed a delayed enrichment of higher-order C values in TOC1-ox compared with WT (Figure S2), suggesting that alteration of endoreplication in TOC1-ox is not dependent on a particular environmental condition. The DNA content was eventually reached but at a slower pace, suggesting a delayed progression of endoreplication. These results are noteworthy as TOC1-ox also delays the phase of the clock under diurnal conditions. Calculation of the endoreplication activity, measured as the average number of endocycles per nucleus (Endoreplication Index [EI]) of *ztl* mutant plants showed reduced EI (Figure S2), which confirmed that overaccumulation of TOC1 correlates with a reduction of endoreplication. The phenotypes were not exclusive for TOC1 gain of function since *toc1-2* mutant and overexpression of ZTL (ZTL-ox) leaves showed enhanced endoreplication (Figures 2E–2G). Calculation of the EI confirmed the reduced index in TOC1-ox (Figures 2H and 2I) and its increment in *toc1-2* and ZTL-ox plants (Figure 2J). Therefore, proper accumulation of TOC1 is important for endocycle activity and influences endoreplication in developing leaves.

TOC1 Controls the Endocycle in Hypocotyl Cells

We next examined whether regulation of endoreplication by TOC1 was exclusive for leaves or also pervaded other organs. Hypocotyl cells are a convenient and simple system for analysis of endocycle activity, as the *Arabidopsis* hypocotyl epidermal and cortex cells only undergo endoreplication (Gendreau et al., 1997). We first examined hypocotyl length of TOC1-ox plants under constant white light conditions (40 μE, WL40) and found significantly shorter hypocotyls compared

Please cite this article in press as: Fung-Uceda et al., The Circadian Clock Sets the Time of DNA Replication Licensing to Regulate Growth in *Arabidopsis*, Developmental Cell (2018), https://doi.org/10.1016/j.devcel.2018.02.022

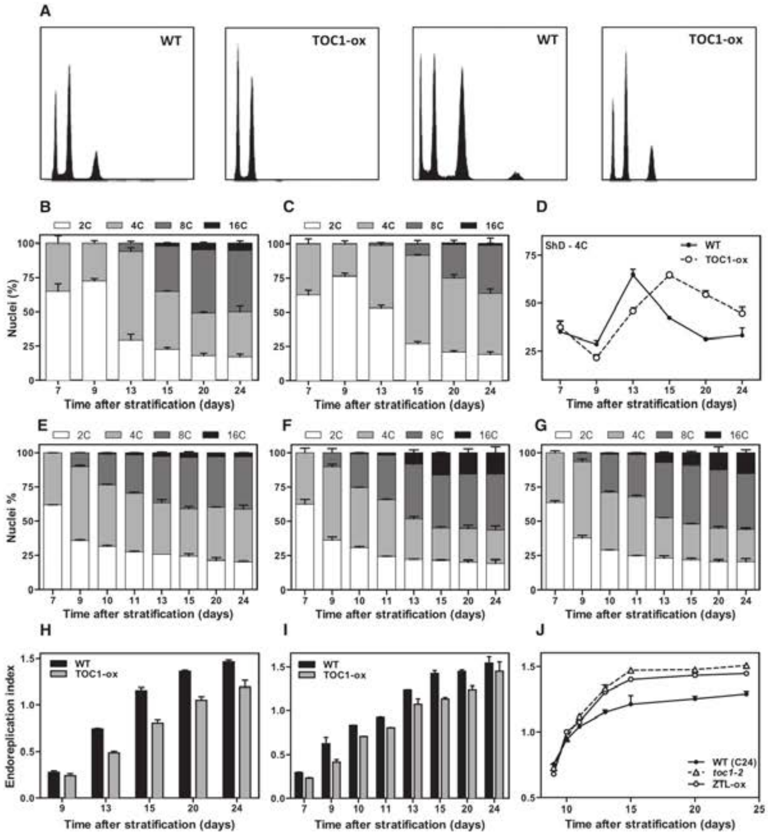

Figure 2. TOC1 Modulates Endoreplication in Developing Leaves

(A–I) Ploidy distribution by flow cytometry (A) of WT and TOC1-ox first pair of leaves at 15 das (left two panels) and 24 das (right two panels). Kinematics of polyploidy nuclei in (B) WT and (C) TOC1-ox. (D) Relative profiles of 4C content in WT and TOC1-ox. Plants were grown under ShD in (A) to (D). Kinematics of polyploid nuclei in (E) WT, (F) *toc1-2*, and (G) ZTL-ox under LgD. Endoreplication Index in WT and TOC1-ox leaves under (H) ShD and (I) LgD.

(J) Endoreplication Index of WT, *toc1-2* and ZTL-ox leaves under LgD. Data are mean + SEM of n ≈ 10,000 nuclei. At least two biological replicates per experiment were performed.

See also Figure S2.

with WT (Figure 3A, left panel). Conversely, *TOC1-RNAi* plants showed longer hypocotyls than WT (Figure 3A, left panel). The trend of hypocotyl phenotypes was similar at low fluences (1 μE, WL1) (Figure 3A, right panel). Analyses of *ztl-3* mutant plants also resulted in short hypocotyls (Figure S3), confirming that overaccumulation of TOC1 correlates with inhibition of hypocotyl growth. Very short hypocotyls were also observed in TOC1 minigene (TMG) seedlings, which express *TOC1* genomic fragment fused to the YFP in a *ztl* mutant background (*ztl-1*/TMG) (Figure S3). Contrarily, overexpression of ZTL resulted in long hypocotyls (Figure S3) similar to *TOC1-RNAi* seedlings. Time-course analyses of hypocotyl growth over 7 days revealed that the phenotypes were readily observed at 1 das and continued throughout the time course (Figure 3B). Thus, TOC1 engages in the control of hypocotyl elongation at early stages of post-embryonic growth.

Please cite this article in press as: Fung-Uceda et al., The Circadian Clock Sets the Time of DNA Replication Licensing to Regulate Growth in *Arabidopsis*, Developmental Cell (2018), https://doi.org/10.1016/j.devcel.2018.02.022

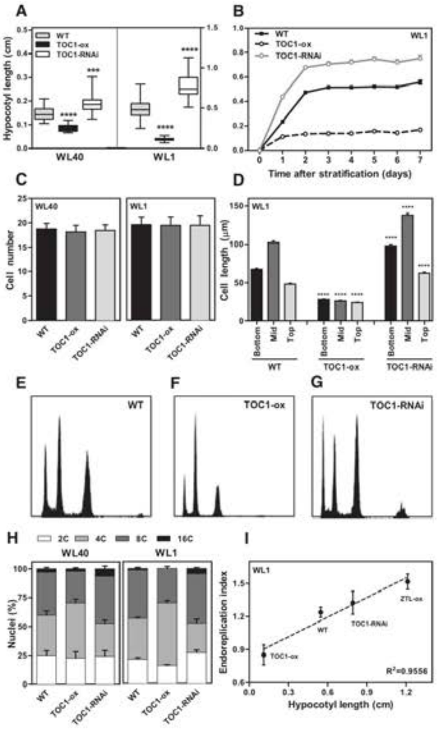

Figure 3. TOC1 Modulates Hypocotyl Cell Expansion and Endoreplication

(A–D) Hypocotyl length (A), growth kinetics (B), epidermal cell number (C), and cell length (D) at the bottom, mid, and top regions of hypocotyls. Graphs represent mean + SEM of n ≈ 20 hypocotyls and n ≈ 100 cells (per genotype and/or condition).

(E–H) Flow cytometry of ploidy profiles under constant white light (40 µmol·quanta·m^{-2}·s^{-1}, WL40; E–G) and (H) relative proportions of polyploid nuclei in hypocotyls of seedlings grown under WL40 and 1 µmol·quanta·m^{-2}·s^{-1} (WL1) for 7 days. Data are mean + SEM of n ≈ 10,000 nuclei.

(I) Correlation of hypocotyl length and the Endoreplication Index in lines with decreasing amounts of TOC1. Graph represents mean ± SEM of n ≈ 20 hypocotyls and n = 10,000 nuclei.

Length under WL1 in (A) is represented on the right axis. $^{****}p \leq 0.0001$, $^{***}p \leq 0.001$. At least two biological replicates per experiment were performed. See also Figure S3.

We next examined the number and size of hypocotyl epidermal cells. Cell number was not significantly altered in TOC1-ox or *TOC1-RNAi* compared with WT plants (Figure 3C). The results agree with the fact that hypocotyl growth is mostly regulated by cell expansion rather than cell division (Gendreau et al., 1997). Analyses of the bottom, mid, or top regions of hypocotyls showed a significantly reduced cell length in TOC1-ox and, conversely, increased elongation in *TOC1-RNAi* (Figures 3D and S3). In WT and *TOC1-RNAi* plants, cells were longer at the mid region compared with the top or the bottom. This relationship was lost in TOC1-ox, with a constant and reduced cell length in every region. A similar trend in cell length phenotypes was observed in *ztl-1* and *ztl-1*/TMG plants (Figure S3). Thus, the hypocotyl phenotypes due to misexpression of TOC1 correlate with significant changes in cell expansion.

Flow-cytometry analyses to determine the ploidy profiles of hypocotyls revealed that WT cells showed three evident peaks corresponding to nuclear DNA content of 2C, 4C, and 8C (Figures 3E, 3H, and S3). In TOC1-ox seedlings the proportion of 4C nuclei was higher than in WT, with a reduction in the proportion of 8C and 16C nuclei (Figures 3F, 3H, and S3). In contrast, *TOC1-RNAi* cells showed a small but reproducible enrichment of the 8C and 16C peaks (Figures 3G, 3H, and S3). Thus, TOC1 overexpression decreases the 8C/4C ratio while *TOC1-RNAi* increases endoreplication, leading to an incomplete repression of the third endoreplication round. Although polyploidy is not necessarily coupled with elongation, the EI showed a direct correlation with hypocotyl length in lines with decreasing amounts of TOC1 (Figure 3I). These results suggest that proper expression of TOC1 is also important for modulating the endocycle activity during hypocotyl growth.

The Developmental Expression of Cell-Cycle Genes Is Altered in TOC1-ox

As TOC1 functions as a transcriptional regulator, we investigated which cell-cycle genes could be transcriptionally altered in TOC1-ox. The timing of mitotic exit is different between the leaf tip and base (Donnelly et al., 1999) so that the first pair of leaves were cut in halves and the expression of selected core cell-cycle genes was separately examined at the leaf tip (Figure 4) and base (Figure S4). Overall, the trend of expression of cell-cycle genes in WT leaves was similar to that described in previous reports and correlated with their cell-cycle function. At the leaf tip, the G$_1$-expressed D3-type cyclins showed a slight but reproducible upregulation (Figures 4A and 4B) that might be consistent with the longer G$_1$ phase and altered endoreplication in TOC1-ox, as CYCDs restrain the transition to endocycling (Dewitte et al., 2007). The slight upregulation of *CYCD3;1* (Figures S4 and 5A) might also contribute to the delayed S-phase, as *CYCD3;1* is repressed during the S-phase (Menges et al., 2005). Downregulation was observed for *CYCD4;1* (Menges and Murray, 2002) (Figure 4C) and *CDKA;1* (Figure 4D).

The expression of CDK inhibitors (CKIs) such as *KRP2* (Interactors of CDK/Kip-Related Protein) shifted from upregulated at early stages to downregulated at late stages (Figure 4E). This pattern might reflect the mismatch in timing between proliferation and differentiation in TOC1-ox, as KRP2 not only inhibits cell proliferation but also sustains differentiation (Verkest et al., 2005). A similar pattern was observed for *KRP4* (Figure 4F) and *KRP1* (Figure S4). In contrast, the expression of *KRP7* was clearly upregulated, mostly at late stages (Figure S4). The expression of the inhibitors *SMR* (*SIAMESE-RELATED*) was also altered in TOC1-ox. For instance, *SMR1*, *SMR2*, and *SMR8* (Figures 4G, 4H, and S4) were downregulated mostly at

Please cite this article in press as: Fung-Uceda et al., The Circadian Clock Sets the Time of DNA Replication Licensing to Regulate Growth in *Arabidopsis*, Developmental Cell (2018), https://doi.org/10.1016/j.devcel.2018.02.022

late stages of development while a very significant downregulation was observed for *SMR5* at all time points (Figure S4). The downregulation of *SMRs* contrasted with the upregulation of *SIM* (*SIAMESE*) (Figure 4I). The upregulation of *SIM* correlates with the slow-growing phenotype of plants overexpressing *SIM* but not with their increased DNA content. It is possible that the reduced expression of other endoreplication-promoting factors in TOC1-ox might be able to overcome the overexpression of *SIM*. Indeed, the expression of the endocycle-promoting factor *CELL CYCLE SWITCH PROTEIN 52 A2/FIZZY-RELATED 1* (*CCS52A2*) and the DNA replication factor *CDC6* was clearly downregulated in TOC1-ox (Figures 4J and 4K). In WT, the expression decreased until day 12–13 only to subsequently rise again. However, in TOC1-ox, expression failed to rise and remained lower than in WT. The expression of *CDT1a* was reduced in TOC1-ox at early stages of development (Figure 4L). Although values and timing varied, similar trends of gene expression were observed at the bases of leaves (Figure S4). Thus, there is considerable transcriptional misregulation of cell-cycle genes involved in both the mitotic cycle and the endocycle. The changes in gene expression correlate with the phenotypes in cell and organ size, cell number, and ploidy.

The Diurnal Expression of Cell-Cycle Genes Is Altered in TOC1-ox

We next examined whether the expression of cell-cycle genes followed a diurnal oscillatory trend and whether this oscillation was affected in TOC1-ox. Analyses of clock core gene expression in plants grown under LgD conditions at 7 or 14 das confirmed the reliability of the diurnal time course showing the proper rhythmic oscillation and its decreased expression in TOC1-ox (Figure S5). For cell-cycle genes, we found a slight oscillation for *CYCDs* showing higher expression during the day and lower expression during the night (Figures 5A and 5B). Consistent with an antagonistic function, *KRP2* expression followed an inverse trend with higher expression during the night (Figure 5C). In TOC1-ox, *CYCDs* were upregulated, particularly close to dusk, and also before dawn for *CYCD3;2*. The upregulation of *CYCD3;1* before dusk was not so evident at zeitgeber time 7 (ZT7; ZT0 = lights on), the time point of the developmental expression analyses. The results highlight the importance of full time-course diurnal analyses to obtain a view of the regulatory interactions. The expression of *KRP2* in TOC1-ox showed a slight but reproducible upregulation during the day and downregulation during the night at 7 das (Figure 5C), 14 das, and 18 das (Figure S5). *KRP7* also followed a similar trend of expression (Figure 5D). Consistent with the developmental results, the expression of *SMR5* was severely reduced in TOC1-ox at all time points (Figure 5E). The expression of other genes (e.g., *E2Fa*) was not clearly oscillating although the expression was affected in TOC1-ox (Figure 5F).

Based on the gene expression profiles from our developmental assays, we also examined endocycle genes such as *CCS52A2* and *CDC6* at later stages of growth (18 das). Our results showed that *CCS52A2* expression was downregulated in TOC1-ox throughout the diurnal time course (Figure S5). We also observed an acute upregulation of *CDC6* in WT leaves that was completely abolished in TOC1-ox (Figure 5G), suggesting that overexpression of TOC1 strongly represses this induction. A similar severe repression was observed at 14 das (Figure S5). Compared with WT, *CDC6* expression rose at the mid to end of night in TOC1-ox (Figures 5G and S5), which indicates that other components are able to overcome the repressive function of TOC1 after dusk. We found that the diurnal peak of *CDC6* coincided with a very low expression of *TOC1* and conversely, the high expression of *TOC1* correlated with low expression of *CDC6* (Figure 5H). Notably, a similar oscillation was observed in the expression of the S-phase marker *Histone 4* (*H4*) with a peak around midday that was delayed in TOC1-ox (Figure 5I). These results suggest the interesting possibility of a diurnal synchronization of the S-phase. To explore this possibility, we analyzed ploidy every 4 hr over a 24-hr LgD cycle in WT and TOC1-ox leaves. Despite the expected variation among the biological replicates, we found an interesting trend in the proportion of cells in S-phase, which accumulated during the mid to late day in WT leaves. Notably, the oscillatory pattern of the S-phase population was clearly delayed in TOC1-ox (Figure 5J). Therefore, the S-phase follows an oscillatory trend that is controlled by the circadian clock through TOC1 repression of *CDC6* expression. This regulation might define a temporal window before dusk in which S-phase progression is favored.

TOC1 Directly Binds to the *CDC6* Promoter

As TOC1 acts as a repressor that binds to the promoters of nearly all central oscillator genes, we next performed chromatin immunoprecipitation (ChIP) assays followed by qPCR analyses of the promoters of selected cell-cycle genes. ChIP assays were performed with TOC1-ox plants (Huang et al., 2012) at 7 das using an anti-MYC antibody to immunoprecipitate the MYC-tagged TOC1 protein. Our results showed specific amplification of the promoter of *CDC6* (Figure 5K) while no amplification was observed for other promoters including, for instance, *CDKB1;1*, *CYCA2;3*, *CYCB1;1*, *CDKA;1*, and *ACTIN2* (*ACT2*), or when samples were incubated without antibody ($-\alpha$). Analyses at later stages (14 and 22 das) also rendered amplification of the *CDC6* promoter while the promoters of other cell-cycle genes were not significantly enriched (Figure S5). We also monitored the possible oscillation of TOC1 binding by using ChIP assays with TMG seedlings, which express the *TOC1* genomic fragment fused to the YFP in the *toc1-2* mutant background (Huang et al., 2012). Fold-enrichment analyses following TOC1 immunoprecipitation with the anti-GFP antibody showed a clear amplification of *CDC6* promoter at ZT15 compared with ZT3 (Figure 5L). The binding to the *CDC6* locus occurs in a region containing a previously identified TOC1 binding motif (Huang et al., 2012), the so-called Evening Element (EE). Consistently, GUS (GLUCURONIDASE) activity of the *CDC6* promoter was reduced in protoplasts co-transfected with TOC1 while no effect was observed in mutated versions of the promoter lacking the EE (Figure S5). Our results are noteworthy, as CDC6 is key for both the mitotic cycle and the endocycle. The effects are not due to artifacts TOC1-ox plants, as accumulation of TOC1 in *ztl-3* mutant plants also results in reduced *CDC6* expression (Figure S5). Furthermore, if TOC1 controls the cell cycle through regulation of *CDC6* expression, downregulation of *TOC1* should lead to the opposite phenotypes to those observed in TOC1-ox plants. Indeed, our results showed that *CDC6* expression was

Please cite this article in press as: Fung-Uceda et al., The Circadian Clock Sets the Time of DNA Replication Licensing to Regulate Growth in *Arabidopsis*, Developmental Cell (2018), https://doi.org/10.1016/j.devcel.2018.02.022

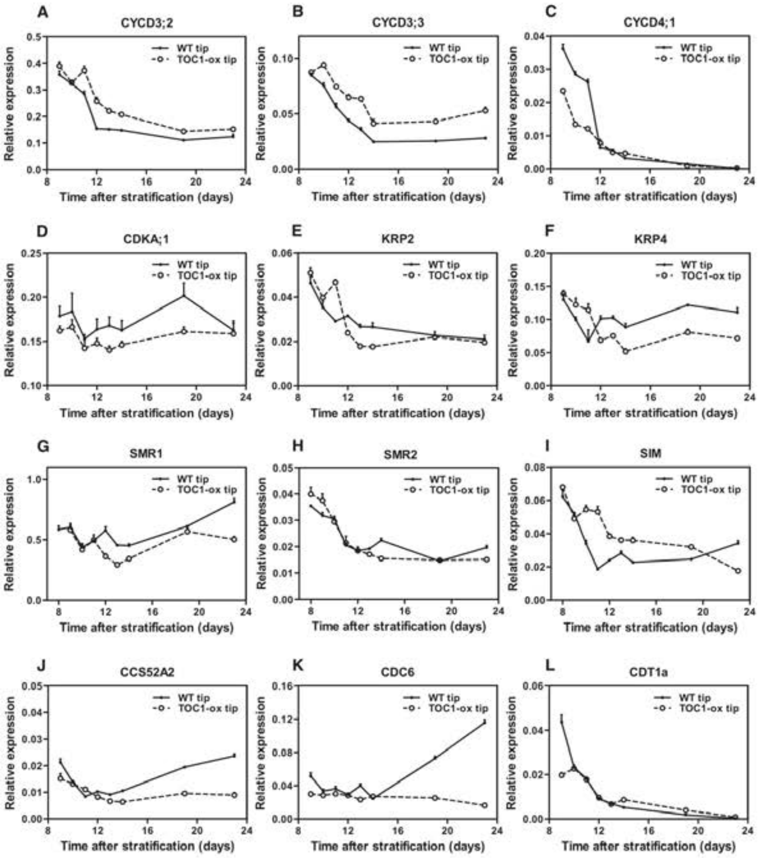

Figure 4. Cell-Cycle Gene Expression Is Affected in TOC1-ox Developing Leaves

Time-course analyses of cell-cycle genes in WT and TOC1-ox leaves over development. Plants were grown under LgD and samples were collected at ZT7. Leaves were cut in halves and gene expression was examined at the tip and base of leaves. *CYCD3;2* (A), *CYCD3;3* (B), *CYCD4;1* (C), *CDKA;1* (D), *KRP2* (E), *KRP4* (F), *SMR1* (G), *SMR2* (H), *SIM* (I), *CCS52A2* (J), *CDC6* (K), and *CDT1a* (L) expression at the tip of leaves. Relative expression was obtained by real-time qPCR analyses. Data represent means + SEM of technical triplicates. The experiment was repeated twice. See also Figure S4.

upregulated in *toc1-2* and ZTL-ox compared with WT plants (Figure S5).

Previous studies have shown that overexpression of *CDC6* increases somatic ploidy (Castellano et al., 2001). Our analyses confirmed the increased leaf size and ploidy of CDC6-ox plants (Figure S6). To further confirm the direct link between TOC1 and *CDC6*, we performed genetic interaction studies using TOC1-ox plants transformed with the *CDC6*-overexpressing construct. Analyses of double overexpressing plants (ox/ox) showed that the reduced size of TOC1-ox plants was reverted by overexpression of *CDC6* (Figure S6). Furthermore, time-course analysis by flow cytometry showed that the reduced ploidy and delayed enrichment of higher-order C values in TOC1-ox plants (Figures 5M and 5N) were overcome by overexpression of *CDC6* (Figures 5O and S6). Calculation of the EI also confirmed the recovery of the endoreplication activity (Figure 5P). A similar phenotypic reversion was observed in other double overexpressing lines (Figure S6). These results suggest that the reduced expression

Please cite this article in press as: Fung-Uceda et al., The Circadian Clock Sets the Time of DNA Replication Licensing to Regulate Growth in *Arabidopsis*, Developmental Cell (2018), https://doi.org/10.1016/j.devcel.2018.02.022

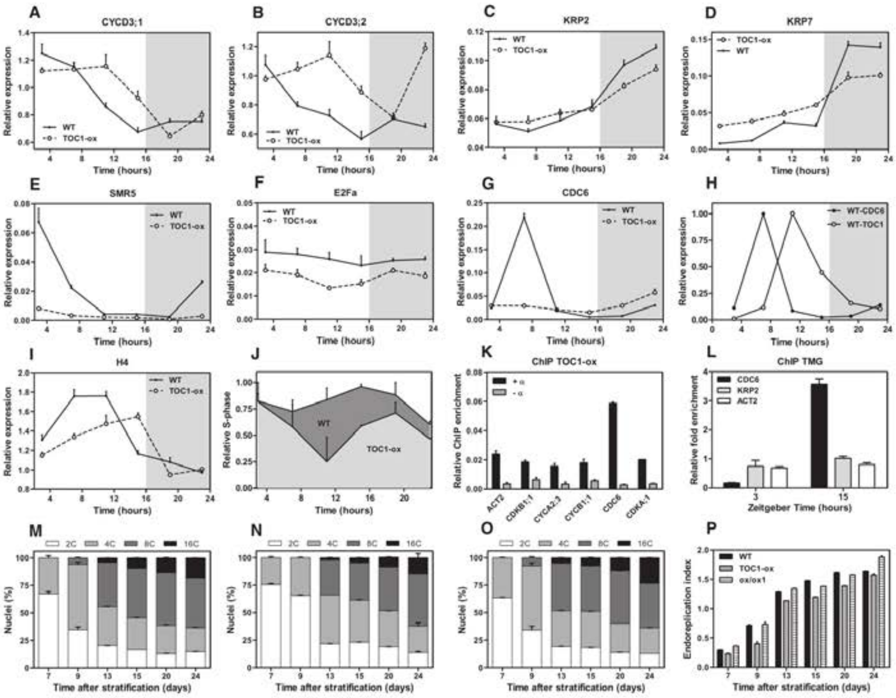

Figure 5. TOC1 Regulates the Diurnal Expression of Cell-Cycle Genes and Binds to the *CDC6* Promoter

Time-course analyses of cell-cycle genes over a diurnal cycle under LgD at 7 das (A–F) or 18 das (G and H).

(A–I) Expression of *CYCD3;1* (A), *CYCD3;2* (B), *KRP2* (C), *KRP7* (D), *SMR5* (E), *E2FA* (F), *CDC6* (G), *CDC6* and *TOC1* (H), and *H4* (I). Relative expression was obtained by real-time qPCR analyses. Data represent means + SEM of technical triplicates.

(J) Estimation of S-phase occurrence by modeling with ModFit the ploidy profiles under LgD at 7 das.

(K) ChIP assays were performed with TOC1-ox plants at ZT7 using an anti-MYC antibody to immunoprecipitate the MYC-tagged TOC1 protein. ChIP enrichment was calculated relative to the input. Samples were incubated with anti-MYC antibody (+α) or without antibody (−α).

(L) ChIP assays with TMG plants grown under LgD and collected at ZT3 and ZT15. ChIPs were performed with an anti-GFP antibody to immunoprecipitate the GFP-tagged TOC1 protein. For comparisons of the different time points, fold enrichment was calculated relative to the input and to values without antibody (−α).

(M–O) Kinematics of polyploidy nuclei in (M) WT, (N) TOC1-ox, and (O) CDC6-ox/TOC1-ox line 1 (ox/ox1). Plants were grown under LgD.

(P) Endoreplication Index in WT, TOC1-ox, and CDC6-ox/TOC1-ox line 1 (ox/ox1) leaves of plants grown under LgD.

Data are mean + SEM of n ≈ 10,000 nuclei. At least two biological replicates per experiment were performed. See also Figures S5 and S6.

of *CDC6* contributes to the observed phenotypes in TOC1-ox. Although it is possible that TOC1 may directly regulate other checkpoint factors or regulators of cell-cycle progression, our data are consistent with the direct binding of TOC1 to the *CDC6* promoter to control its developmental and diurnal transcriptional expression.

Tumor Progression Is Affected in TOC1-ox Inflorescence Stalks

If TOC1 regulates the cell cycle, cellular systems in which the cell cycle is misregulated should display a differential response in WT versus TOC1-ox plants. To explore this possibility, we monitored whether the slow pace of the cell cycle in TOC1-ox correlated with delayed tumor growth. To this end, we inoculated the bases and first internodes of inflorescence stalks with a virulent *Agrobacterium tumefaciens* strain (A281) (Deeken et al., 2003). The transfer DNA contains the *β-glucuronidase* (*GUS*) gene so that tumor development can be followed after infection. At 5 days after inoculation (dai), staining was readily observed as small blue foci of variable sizes (Figure 6A, left two images; Figure S7). The areas of GUS foci were considerably increased at 7 dai, forming bigger and strongly stained patches (Figure 6A, right

Please cite this article in press as: Fung-Uceda et al., The Circadian Clock Sets the Time of DNA Replication Licensing to Regulate Growth in *Arabidopsis*, Developmental Cell (2018), https://doi.org/10.1016/j.devcel.2018.02.022

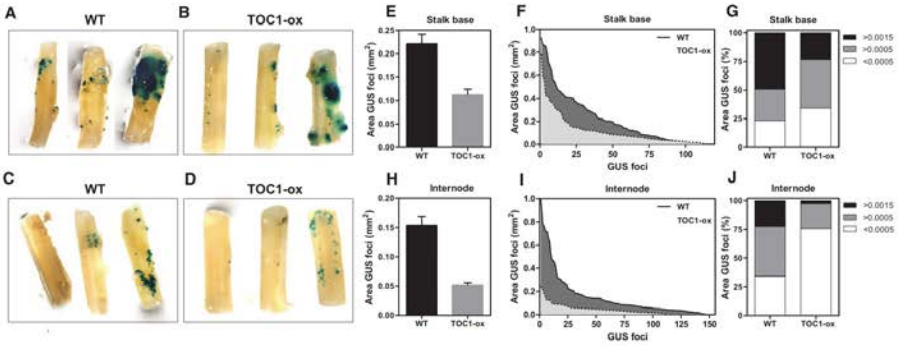

Figure 6. Tumor Progression Is Delayed in TOC1-ox

Representative images of inflorescence stalks inoculated with the *Agrobacterium* virulent strain A281 at the base of inflorescence stalks in (A) WT and (B) TOC1-ox at 5 dai (left two images) and 7 dai (right images). Inoculations were also performed at the first internode of (C) WT and (D) TOC1-ox. Mean area of small and medium GUS foci at the base of (E) inflorescence stalks and (H) in the first internode. Graphs represent mean + SEM of n ≈ 110 foci. (F and I) Distribution of the different GUS areas, and (G and J) proportion of sizes at the base (F, G) and at the first internode of inflorescence stalks (I, J). At least two biological replicates were performed. See also Figure S7.

image). The staining appeared higher in tumors at the base of the stalks than at the internodes (Figures 6A and 6C). Tumors were also observed in TOC1-ox stalks and internodes (Figures 6B–6D). However, the small and medium-sized GUS foci were clearly reduced compared with WT (Figures 6E and 6F). Comparative analyses of the proportion of the different areas clearly showed an enrichment of bigger patches in WT compared with TOC1-ox (Figure 6G). The reduction in GUS foci area in TOC1-ox was even more evident at the first internode (Figures 6H–6J). No staining or other visible phenotypes were observed when plants were inoculated with the non-tumorigenic *Agrobacterium* strain GV3101 (Figure S7). Altogether, our results suggest that the slowed cell cycle and reduced S-phase duration in TOC1-ox might contribute to the observed delay in tumor progression.

DISCUSSION

Cells integrate exogenous and endogenous signals to decide whether or not to progress from the G_1 to the S-phase. We found that the circadian clock controls the overall duration of the cell cycle by modulating the S-phase in *Arabidopsis*. The circadian clock component TOC1 operates by binding to the promoter of the DNA replication factor *CDC6* to repress its diurnal expression. Thus, misexpression of TOC1 not only changes the pace of the clock but also affects cell division during the mitotic cycle and endoreplication during the endocycle. Cell size and number, somatic ploidy, organ size, and the overall plant growth are coordinately regulated by the clock in synchronization with the environment (Figure 7). By controlling the pace of the cell cycle, the circadian clock not only regulates normal growth but also tumor progression in *Arabidopsis*.

Regulation of the G_1-S transition is essential for proper cell-cycle progression, as cells only commit to division once they have replicated their DNA (Johnson and Skotheim, 2013). TOC1 regulates the proper timing of the G_1- to S-phase transition, as indicated by the relative duration of the G_1 and S-phases as well as by the delayed S-phase entrance. These results are fully consistent with the slow cell division rate and the reduced progression of cell number observed in TOC1-ox developing leaves. Inhibition of cell proliferation in leaves is often associated with cell expansion. This mechanism is known as compensation, and reduces the impact of decreased cell number on organ size (Beemster et al., 2006). In TOC1-ox, both cell number and cell size are affected and hence the overall leaf area is reduced. The reduction might be due to uncoupled cell division and cell growth in TOC1-ox. It is also possible that there is a threshold below which compensation is induced (Horiguchi et al., 2006) so that the cell number reduction in TOC1-ox does not reach such a threshold. The function of TOC1 in the mitotic cycle resembles that of the mammalian circadian component NONO, an interacting partner of the clock protein PERIOD that circadianly gates the S-phase in fibroblasts (Kowalska et al., 2013). It would be interesting to check whether in addition to TOC1, other clock components in plants contribute to the regulation of the cell cycle at different cell-cycle phases.

Although post-translational regulation of cell-cycle components is crucial for cell-cycle function, the expression of key cell-cycle genes clearly oscillates during the cycle (Beemster et al., 2005; Menges et al., 2005), suggesting that transcriptional regulation is also important for cell-cycle progression. Furthermore, there is a clear correlation between periodically transcribed cell-cycle genes and their protein accumulations in yeast and human cells. We found that during the mitotic cycle, the expression of various cell-cycle genes was altered in TOC1-ox. Genes affected include the D-type cyclins, which have essential roles for cell-cycle responses to nutrients and

Please cite this article in press as: Fung-Uceda et al., The Circadian Clock Sets the Time of DNA Replication Licensing to Regulate Growth in *Arabidopsis*, Developmental Cell (2018), https://doi.org/10.1016/j.devcel.2018.02.022

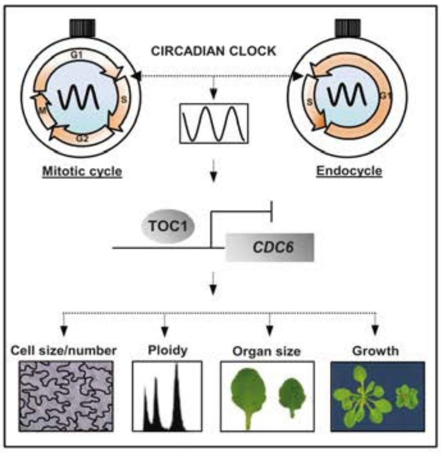

Figure 7. Schematic Representation Depicting the Connection between the Circadian Clock and the Cell Cycle in *Arabidopsis*

The circadian clock modulates the timing of the cell cycle through the rhythmic binding of TOC1 to the promoter of the DNA replication factor *CDC6*. Regulation of the S-phase affects both the mitotic cycle and the endocycle so that cell size and number, somatic ploidy, organ size, and overall plant growth are affected in plants misexpressing TOC1. Ensuring that DNA replication only occurs under "safe" conditions is essential for maintaining genome integrity, and thus TOC1 regulation of *CDC6* might allow or delay DNA licensing in consonance with external and internal cues.

hormones during the G_1-S-phase transition (Menges and Murray, 2002; Riou-Khamlichi et al., 1999). The observed transcriptional changes correlate with the slow cycle in TOC1-ox that alters the timing of expression compared with WT. This idea is in agreement with the expression of the KRP inhibitors, which are increased at early stages and decreased later during development. KRP2 not only inhibits cell proliferation but its weak overexpression inhibits CDKA;1 activity and leads to increased polyploidy (Verkest et al., 2005). Therefore, the increased accumulation of *KRP2* at early stages is consistent with the decreased cell number, while the decreased accumulation later in development agrees with the reduced endoreplication in TOC1-ox. The expression of *SMR5* was also clearly altered in TOC1-ox. SMR5 is important for cell-cycle checkpoint activation following DNA damage by reactive oxygen species (ROS) (Yi et al., 2014). Although *SMR5* overexpression promotes endoreplication, the corresponding knockouts display no altered ploidy (Yi et al., 2014), suggesting that the effects of TOC1-ox on their expression might rather be linked to an altered ROS response.

Multiple layers of endogenous and exogenous signals converge to ensure proper regulation of the endocycle. The circadian clock also controls nuclear DNA replication in leaves. TOC1-ox delays the endocycle activity and, conversely, loss of TOC1 function accelerates this event. Proper regulation of endoreplication provides a means to increase gene copy number and to ensure increased protection against irradiation (Traas et al., 1998). Thus, the circadian clockwork might provide proper timing information for endoreplication to fulfill these functions. Misexpression of TOC1 also perturbs hypocotyl cell expansion and affects the successive rounds of DNA replication. Post-embryonic hypocotyl growth primarily relies on cell expansion rather than on cell division, which makes this organ amenable for studies of cell elongation (Gendreau et al., 1997). Although polyploidy is not necessarily coupled with elongation, and endoreplication might not have the same sensitivity threshold as cell expansion (Vandenbussche et al., 2005), the inverse correlation of the endocycle activity in lines accumulating increasing amounts of TOC1 suggests an important connection of TOC1 with replication of the nuclear genome. Altering the timing of DNA synthesis by higher or lower than WT expression of *TOC1* slows down or speeds up the successive rounds of endoreplication, respectively. Light not only inhibits hypocotyl elongation but also reduces one round of endoreplication in comparison with dark-grown seedlings (Gendreau et al., 1997). Proper expression of TOC1 might thus regulate this repression such that TOC1-ox plants are hypersensitive to the light-dependent repression of endoreplication while reduced expression of TOC1 attenuates this response. Thus, the endocycle activity might be part of a circadianly controlled developmental program.

Strict control of S-phase entry is crucial, as DNA replication occurs during this phase. Here we found that TOC1 acts as a repressor of *CDC6* expression by direct binding to its promoter. The downregulation of *CDC6* in TOC1-ox explains why both the cell division and endoreplication are affected, as this factor is required for the S-phase progression during both cycles (Castellano et al., 2001, 2004). In *Schizosaccharomyces pombe*, CDC18/CDC6 overexpression induces multiple rounds of DNA replication (Jallepalli and Kelly, 1996; Nishitani and Nurse, 1995) while extra rounds of endoreplication were observed by CDC6 overexpression in cultured megakaryocytes (Bermejo et al., 2002). TOC1-ox plants are dwarf. In humans, mutations in the genes encoding components of the pre-replication complex, including *CDC6*, were linked to the Meier-Gorlin syndrome, an autosomal recessive disorder characterized by primordial dwarfism (short stature, microcephaly) (Bicknell et al., 2011). Ensuring that DNA replication only occurs under "safe" conditions is essential for maintaining genome integrity, and thus, TOC1 regulation of *CDC6* might allow or delay DNA licensing in consonance with external and internal cues.

Human cancer is characterized by increased cell proliferation, invasion, and metastasis. Among many others, several DNA replication initiation proteins are overexpressed in human cancers. We found that the reduced expression of *CDC6* in TOC1-ox correlates with the slow progression of tumors. Notably, a recent study has shown that miR26 represses replication licensing and tumorigenesis by targeting *CDC6* in lung cancer cells (Zhang et al., 2014). A similar situation might be happening in plants in which TOC1 represses *CDC6* expression. Loss of circadian function increases the susceptibility to cancer and affects anticancer treatments (Brown, 2014). In this

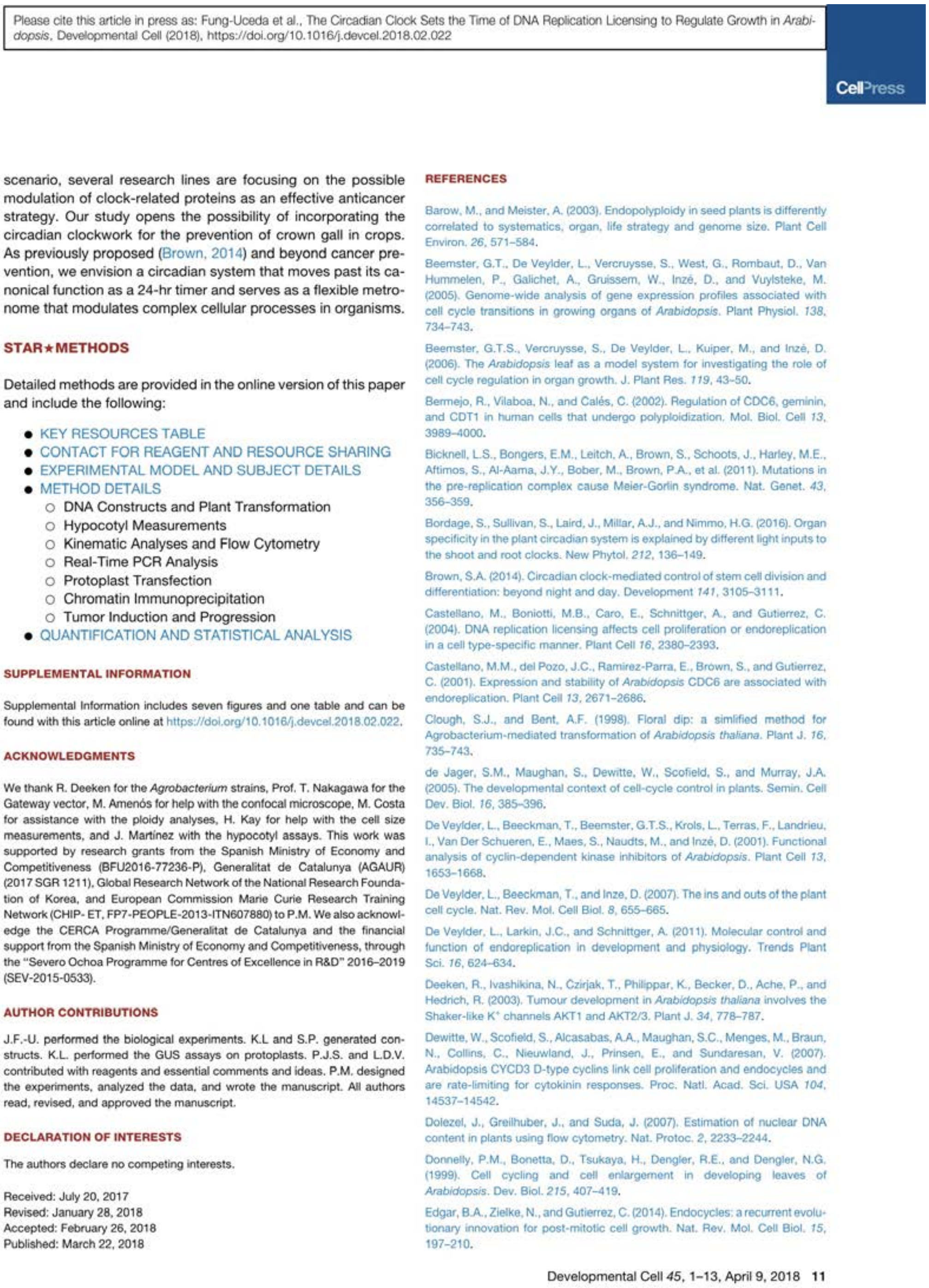

Please cite this article in press as: Fung-Uceda et al., The Circadian Clock Sets the Time of DNA Replication Licensing to Regulate Growth in *Arabidopsis*, Developmental Cell (2018), https://doi.org/10.1016/j.devcel.2018.02.022

scenario, several research lines are focusing on the possible modulation of clock-related proteins as an effective anticancer strategy. Our study opens the possibility of incorporating the circadian clockwork for the prevention of crown gall in crops. As previously proposed (Brown, 2014) and beyond cancer prevention, we envision a circadian system that moves past its canonical function as a 24-hr timer and serves as a flexible metronome that modulates complex cellular processes in organisms.

STAR★METHODS

Detailed methods are provided in the online version of this paper and include the following:

- KEY RESOURCES TABLE
- CONTACT FOR REAGENT AND RESOURCE SHARING
- EXPERIMENTAL MODEL AND SUBJECT DETAILS
- METHOD DETAILS
  - ○ DNA Constructs and Plant Transformation
  - ○ Hypocotyl Measurements
  - ○ Kinematic Analyses and Flow Cytometry
  - ○ Real-Time PCR Analysis
  - ○ Protoplast Transfection
  - ○ Chromatin Immunoprecipitation
  - ○ Tumor Induction and Progression
- QUANTIFICATION AND STATISTICAL ANALYSIS

SUPPLEMENTAL INFORMATION

Supplemental Information includes seven figures and one table and can be found with this article online at https://doi.org/10.1016/j.devcel.2018.02.022.

ACKNOWLEDGMENTS

We thank R. Deeken for the *Agrobacterium* strains, Prof. T. Nakagawa for the Gateway vector, M. Amenós for help with the confocal microscope, M. Costa for assistance with the ploidy analyses, H. Kay for help with the cell size measurements, and J. Martínez with the hypocotyl assays. This work was supported by research grants from the Spanish Ministry of Economy and Competitiveness (BFU2016-77236-P), Generalitat de Catalunya (AGAUR) (2017 SGR 1211), Global Research Network of the National Research Foundation of Korea, and European Commission Marie Curie Research Training Network (CHIP- ET, FP7-PEOPLE-2013-ITN607880) to P.M. We also acknowledge the CERCA Programme/Generalitat de Catalunya and the financial support from the Spanish Ministry of Economy and Competitiveness, through the "Severo Ochoa Programme for Centres of Excellence in R&D" 2016–2019 (SEV-2015-0533).

AUTHOR CONTRIBUTIONS

J.F.-U. performed the biological experiments. K.L and S.P. generated constructs. K.L. performed the GUS assays on protoplasts. P.J.S. and L.D.V. contributed with reagents and essential comments and ideas. P.M. designed the experiments, analyzed the data, and wrote the manuscript. All authors read, revised, and approved the manuscript.

DECLARATION OF INTERESTS

The authors declare no competing interests.

Received: July 20, 2017
Revised: January 28, 2018
Accepted: February 26, 2018
Published: March 22, 2018

REFERENCES

Barow, M., and Meister, A. (2003). Endopolyploidy in seed plants is differently correlated to systematics, organ, life strategy and genome size. Plant Cell Environ. *26*, 571–584.

Beemster, G.T., De Veylder, L., Vercruysse, S., West, G., Rombaut, D., Van Hummelen, P., Galichet, A., Gruissem, W., Inzé, D., and Vuylsteke, M. (2005). Genome-wide analysis of gene expression profiles associated with cell cycle transitions in growing organs of *Arabidopsis*. Plant Physiol. *138*, 734–743.

Beemster, G.T.S., Vercruysse, S., De Veylder, L., Kuiper, M., and Inzé, D. (2006). The *Arabidopsis* leaf as a model system for investigating the role of cell cycle regulation in organ growth. J. Plant Res. *119*, 43–50.

Bermejo, R., Vilaboa, N., and Calés, C. (2002). Regulation of CDC6, geminin, and CDT1 in human cells that undergo polyploidization. Mol. Biol. Cell *13*, 3989–4000.

Bicknell, L.S., Bongers, E.M., Leitch, A., Brown, S., Schoots, J., Harley, M.E., Aftimos, S., Al-Aama, J.Y., Bober, M., Brown, P.A., et al. (2011). Mutations in the pre-replication complex cause Meier-Gorlin syndrome. Nat. Genet. *43*, 356–359.

Bordage, S., Sullivan, S., Laird, J., Millar, A.J., and Nimmo, H.G. (2016). Organ specificity in the plant circadian system is explained by different light inputs to the shoot and root clocks. New Phytol. *212*, 136–149.

Brown, S.A. (2014). Circadian clock-mediated control of stem cell division and differentiation: beyond night and day. Development *141*, 3105–3111.

Castellano, M., Boniotti, M.B., Caro, E., Schnittger, A., and Gutierrez, C. (2004). DNA replication licensing affects cell proliferation or endoreplication in a cell type-specific manner. Plant Cell *16*, 2380–2393.

Castellano, M.M., del Pozo, J.C., Ramirez-Parra, E., Brown, S., and Gutierrez, C. (2001). Expression and stability of *Arabidopsis* CDC6 are associated with endoreplication. Plant Cell *13*, 2671–2686.

Clough, S.J., and Bent, A.F. (1998). Floral dip: a simlified method for Agrobacterium-mediated transformation of *Arabidopsis thaliana*. Plant J. *16*, 735–743.

de Jager, S.M., Maughan, S., Dewitte, W., Scofield, S., and Murray, J.A. (2005). The developmental context of cell-cycle control in plants. Semin. Cell Dev. Biol. *16*, 385–396.

De Veylder, L., Beeckman, T., Beemster, G.T.S., Krols, L., Terras, F., Landrieu, I., Van Der Schueren, E., Maes, S., Naudts, M., and Inzé, D. (2001). Functional analysis of cyclin-dependent kinase inhibitors of *Arabidopsis*. Plant Cell *13*, 1653–1668.

De Veylder, L., Beeckman, T., and Inze, D. (2007). The ins and outs of the plant cell cycle. Nat. Rev. Mol. Cell Biol. *8*, 655–665.

De Veylder, L., Larkin, J.C., and Schnittger, A. (2011). Molecular control and function of endoreplication in development and physiology. Trends Plant Sci. *16*, 624–634.

Deeken, R., Ivashikina, N., Czirjak, T., Philippar, K., Becker, D., Ache, P., and Hedrich, R. (2003). Tumour development in *Arabidopsis thaliana* involves the Shaker-like K^+ channels AKT1 and AKT2/3. Plant J. *34*, 778–787.

Dewitte, W., Scofield, S., Alcasabas, A.A., Maughan, S.C., Menges, M., Braun, N., Collins, C., Nieuwland, J., Prinsen, E., and Sundaresan, V. (2007). Arabidopsis CYCD3 D-type cyclins link cell proliferation and endocycles and are rate-limiting for cytokinin responses. Proc. Natl. Acad. Sci. USA *104*, 14537–14542.

Dolezel, J., Greilhuber, J., and Suda, J. (2007). Estimation of nuclear DNA content in plants using flow cytometry. Nat. Protoc. *2*, 2233–2244.

Donnelly, P.M., Bonetta, D., Tsukaya, H., Dengler, R.E., and Dengler, N.G. (1999). Cell cycling and cell enlargement in developing leaves of *Arabidopsis*. Dev. Biol. *215*, 407–419.

Edgar, B.A., Zielke, N., and Gutierrez, C. (2014). Endocycles: a recurrent evolutionary innovation for post-mitotic cell growth. Nat. Rev. Mol. Cell Biol. *15*, 197–210.

Please cite this article in press as: Fung-Uceda et al., The Circadian Clock Sets the Time of DNA Replication Licensing to Regulate Growth in *Arabidopsis*, Developmental Cell (2018), https://doi.org/10.1016/j.devcel.2018.02.022

Endo, M., Shimizu, H., Nohales, M.A., Araki, T., and Kay, S.A. (2014). Tissue-specific clocks in *Arabidopsis* show asymmetric coupling. Nature *515*, 419–422.

Feillet, C., van der Horst, G.T., Levi, F., Rand, D.A., and Delaunay, F. (2015). Coupling between the circadian clock and cell cycle oscillators: implication for healthy cells and malignant growth. Front. Neurol. *6*, 96.

Fiorani, F., and Beemster, G.T.S. (2006). Quantitative analyses of cell division in plants. Plant Mol. Biol. *60*, 963–979.

Galbraith, D.W., Harkins, K.R., Maddox, J.M., Ayres, N.M., Sharma, D.P., and Firoozabady, E. (1983). Rapid flow cytometric analysis of the cell cycle in intact plant tissues. Science *220*, 1049–1051.

Gendreau, E., Traas, J., Desnos, T., Grandjean, O., Caboche, M., and Hofte, H. (1997). Cellular basis of hypocotyl growth in *Arabidopsis thaliana*. Plant Physiol. *114*, 295–305.

Gendron, J.M., Pruneda-Paz, J.L., Doherty, C.J., Gross, A.M., Kang, S.E., and Kay, S.A. (2012). *Arabidopsis* circadian clock protein, TOC1, is a DNA-binding transcription factor. Proc. Natl. Acad. Sci. USA *109*, 3167–3172.

Gonzalez, N., Vanhaeren, H., and Inzé, D. (2012). Leaf size control: complex coordination of cell division and expansion. Trends Plant Sci. *17*, 332–340.

Gutierrez, C. (2009). The *Arabidopsis* cell division cycle. Arabidopsis Book *7*, e0120.

Horiguchi, G., Ferjani, A., Fujikura, U., and Tsukaya, H. (2006). Coordination of cell proliferation and cell expansion in the control of leaf size in *Arabidopsis thaliana*. J. Plant Res. *119*, 37–42.

Huang, W., Perez-Garcia, P., Pokhilko, A., Millar, A.J., Antoshechkin, I., Riechmann, J.L., and Más, P. (2012). Mapping the core of the *Arabidopsis* circadian clock defines the network structure of the oscillator. Science *336*, 75–79.

Hunt, T., and Sassone-Corsi, P. (2007). Riding tandem: circadian clocks and the cell cycle. Cell *129*, 461–464.

Inzé, D., and De Veylder, L. (2006). Cell cycle regulation in plant development. Annu. Rev. Genet. *40*, 77–105.

Jallepalli, P.V., and Kelly, T.J. (1996). Rum1 and Cdc18 link inhibition of cyclin-dependent kinase to the initiation of DNA replication in *Schizosaccharomyces pombe*. Genes Dev. *10*, 541–552.

Johnson, A., and Skotheim, J.M. (2013). Start and the restriction point. Curr. Opin. Cell Biol. *25*, 717–723.

Johnson, C.H. (2010). Circadian clocks and cell division. Cell Cycle *9*, 3864–3873.

Kowalska, E., Ripperger, J.A., Hoegger, D.C., Bruegger, P., Buch, T., Birchler, T., Mueller, A., Albrecht, U., Contaldo, C., and Brown, S.A. (2013). NONO couples the circadian clock to the cell cycle. Proc. Natl. Acad. Sci. USA *110*, 1592–1599.

Lee, J., Lee, H.J., Shin, M.K., and Ryu, W.S. (2004). Versatile PCR-mediated insertion or deletion mutagenesis. Biotechniques *36*, 398–400.

Lee, K., Park, O.S., and Seo, P.J. (2017). *Arabidopsis* ATXR2 deposits H3K36me3 at the promoters of LBD genes to facilitate cellular dedifferentiation. Sci. Signal. *10*, https://doi.org/10.1126/scisignal.aan0316.

Legnaioli, T., Cuevas, J., and Más, P. (2009). TOC1 functions as a molecular switch connecting the circadian clock with plant responses to drought. EMBO J. *28*, 3745–3757.

Makino, S., Matsushika, A., Kojima, M., Yamashino, T., and Mizuno, T. (2002). The APRR1/TOC1 quintet implicated in circadian rhythms of *Arabidopsis thaliana*: characterization with APRR1-overexpressing plants. Plant Cell Physiol. *43*, 58–69.

Más, P., Alabadi, D., Yanovsky, M.J., Oyama, T., and Kay, S.A. (2003a). Dual role of TOC1 in the control of circadian and photomorphogenic responses in *Arabidopsis*. Plant Cell *15*, 223–236.

Más, P., Kim, W.J., Somers, D.E., and Kay, S.A. (2003b). Targeted degradation of TOC1 by ZTL modulates circadian function in *Arabidopsis*. Nature *426*, 567–570.

Matsuo, T., Yamaguchi, S., Mitsui, S., Emi, A., Shimoda, F., and Okamura, H. (2003). Control mechanism of the circadian clock for timing of cell division in vivo. Science *302*, 255–259.

Matsushika, A., Makino, S., Kojima, M., and Mizuno, T. (2000). Circadian waves of expression of the APRR1/TOC1 family of pseudo-response regulators in *Arabidopsis thaliana*: insight into the plant circadian clock. Plant Cell Physiol. *41*, 1002–1012.

Menges, M., De Jager, S.M., Gruissem, W., and Murray, J.A. (2005). Global analysis of the core cell cycle regulators of *Arabidopsis* identifies novel genes, reveals multiple and highly specific profiles of expression and provides a coherent model for plant cell cycle control. Plant J. *41*, 546–566.

Menges, M., and Murray, J.A. (2002). Synchronous *Arabidopsis* suspension cultures for analysis of cell-cycle gene activity. Plant J. *30*, 203–212.

Nagoshi, E., Saini, C., Bauer, C., Laroche, T., Naef, F., and Schibler, U. (2004). Circadian gene expression in individual fibroblasts: cell-autonomous and self-sustained oscillators pass time to daughter cells. Cell *119*, 693–705.

Nakagawa, T., Kurose, T., Hino, T., Tanaka, K., Kawamukai, M., Niwa, Y., Toyooka, K., Matsuoka, K., Jinbo, T., and Kimura, T. (2007a). Development of series of gateway binary vectors, pGWBs, for realizing efficient construction of fusion genes for plant transformation. J. Biosci. Bioeng. *104*, 34–41.

Nakagawa, T., Suzuki, T., Murata, S., Nakamura, S., Hino, T., Maeo, K., Tabata, R., Kawai, T., Tanaka, K., Niwa, Y., et al. (2007b). Improved gateway binary vectors: high-performance vectors for creation of fusion constructs in transgenic analysis of plants. Biosci. Biotechnol. Biochem. *71*, 2095–2100.

Nishitani, H., and Nurse, P. (1995). p65cdc18 plays a major role controlling the initiation of DNA replication in fission yeast. Cell *83*, 397–405.

Niwa, Y., Ito, S., Nakamichi, N., Mizoguchi, T., Niinuma, K., Yamashino, T., and Mizuno, T. (2007). Genetic linkages of the circadian clock-associated genes, TOC1, CCA1 and LHY, in the photoperiodic control of flowering time in *Arabidopsis thaliana*. Plant Cell Physiol. *48*, 925–937.

Nohales, M.A., and Kay, S.A. (2016). Molecular mechanisms at the core of the plant circadian oscillator. Nat. Struct. Mol. Biol. *23*, 1061–1069.

Nowack, M.K., Harashima, H., Dissmeyer, N., Zhao, X., Bouyer, D., Weimer, A.K., De Winter, F., Yang, F., and Schnittger, A. (2012). Genetic framework of cyclin-dependent kinase function in *Arabidopsis*. Dev. Cell *22*, 1030–1040.

Pando, B.F., and van Oudenaarden, A. (2010). Coupling cellular oscillators—circadian and cell division cycles in cyanobacteria. Curr. Opin. Genet. Dev. *20*, 613–618.

Pendergast, J.S., Yeom, M., Reyes, B.A., Ohmiya, Y., and Yamazaki, S. (2010). Disconnected circadian and cell cycles in a tumor-driven cell line. Commun. Integr. Biol. *3*, 536–539.

Pokhilko, A., Fernández, A.P., Edwards, K.D., Southern, M.M., Halliday, K.J., and Millar, A.J. (2012). The clock gene circuit in *Arabidopsis* includes a repressilator with additional feedback loops. Mol. Syst. Biol. *8*, 574.

Riou-Khamlichi, C., Huntley, R., Jacqmard, A., and Murray, J.A. (1999). Cytokinin activation of *Arabidopsis* cell division through a D-type cyclin. Science *283*, 1541–1544.

Sablowski, R., and Carnier Dornelas, M. (2014). Interplay between cell growth and cell cycle in plants. J. Exp. Bot. *65*, 2703–2714.

Somers, D.E., Schultz, T.F., Milnamow, M., and Kay, S.A. (2000). *ZEITLUPE* encodes a novel clock-associated PAS protein from *Arabidopsis*. Cell *101*, 319–329.

Somers, D.E., Webb, A.A., Pearson, M., and Kay, S.A. (1998). The short-period mutant *toc1-1*, alters circadian clock regulation of multiple outputs throughout development in *Arabidopsis thaliana*. Development *125*, 485–494.

Strayer, C.A., Oyama, T., Schultz, T.F., Raman, R., Somers, D.E., Más, P., Panda, S., Kreps, J.A., and Kay, S.A. (2000). Cloning of the *Arabidopsis* clock gene *TOC1*, an autoregulatory response regulator homolog. Science *289*, 768–771.

Takahashi, N., Hirata, Y., Aihara, K., and Más, P. (2015). A hierarchical multi-oscillator network orchestrates the *Arabidopsis* circadian system. Cell *163*, 148–159.

Thain, S.C., Hall, A., and Millar, A.J. (2000). Functional independence of circadian clocks that regulate plant gene expression. Curr. Biol. *10*, 951–956.

Please cite this article in press as: Fung-Uceda et al., The Circadian Clock Sets the Time of DNA Replication Licensing to Regulate Growth in *Arabidopsis*, Developmental Cell (2018), https://doi.org/10.1016/j.devcel.2018.02.022

Traas, J., Hulskamp, M., Gendreau, E., and Hofte, H. (1998). Endoreduplication and development: rule without dividing? Curr. Opin. Plant Biol. *1*, 498–503.

Van Wordragen, M.F., De Jong, J., Schornagel, M.J., and Dons, H.J.M. (1992). Rapid screening for host-bacterium interactions in *Agrobacterium*-mediated gene transfer to chrysanthemum, by using the GUS-intron gene. Plant Sci. *81*, 207–214.

Vandenbussche, F., Verbelen, J.-P., and Van Der Straeten, D. (2005). Of light and length: regulation of hypocotyl growth in *Arabidopsis*. Bioessays *27*, 275–284.

Verkest, A., Weinl, C., Inze, D., De Veylder, L., and Schnittger, A. (2005). Switching the cell cycle. Kip-related proteins in plant cell cycle control. Plant Physiol. *139*, 1099–1106.

Wenden, B., Toner, D.L., Hodge, S.K., Grima, R., and Millar, A.J. (2012). Spontaneous spatiotemporal waves of gene expression from biological clocks in the leaf. Proc. Natl. Acad. Sci. USA *109*, 6757–6762.

Yakir, E., Hassidim, M., Melamed-Book, N., Hilman, D., Kron, I., and Green, R.M. (2011). Cell autonomous and cell-type specific circadian rhythms in *Arabidopsis*. Plant J. *68*, 520–531.

Yamashino, T., Ito, S., Niwa, Y., Kunihiro, A., Nakamichi, N., and Mizuno, T. (2008). Involvement of *Arabidopsis* clock-associated pseudo-response regulators in diurnal oscillations of gene expression in the presence of environmental time cues. Plant Cell Physiol. *49*, 1839–1850.

Yeom, M., Pendergast, J.S., Ohmiya, Y., and Yamazaki, S. (2010). Circadian-independent cell mitosis in immortalized fibroblasts. Proc. Natl. Acad. Sci. USA *107*, 9665–9670.

Yi, D., Alvim Kamei, C.L., Cools, T., Vanderauwera, S., Takahashi, N., Okushima, Y., Eekhout, T., Yoshiyama, K.O., Larkin, J., Van den Daele, H., et al. (2014). The *Arabidopsis* SIAMESE-RELATED cyclin-dependent kinase inhibitors SMR5 and SMR7 regulate the DNA damage checkpoint in response to reactive oxygen species. Plant Cell *26*, 296–309.

Zhang, X., Xiao, D., Wang, Z., Zou, Y., Huang, L., Lin, W., Deng, Q., Pan, H., Zhou, J., Liang, C., et al. (2014). MicroRNA-26a/b regulate DNA replication licensing, tumorigenesis, and prognosis by targeting CDC6 in lung cancer. Mol. Cancer Res. *12*, 1535–1546.

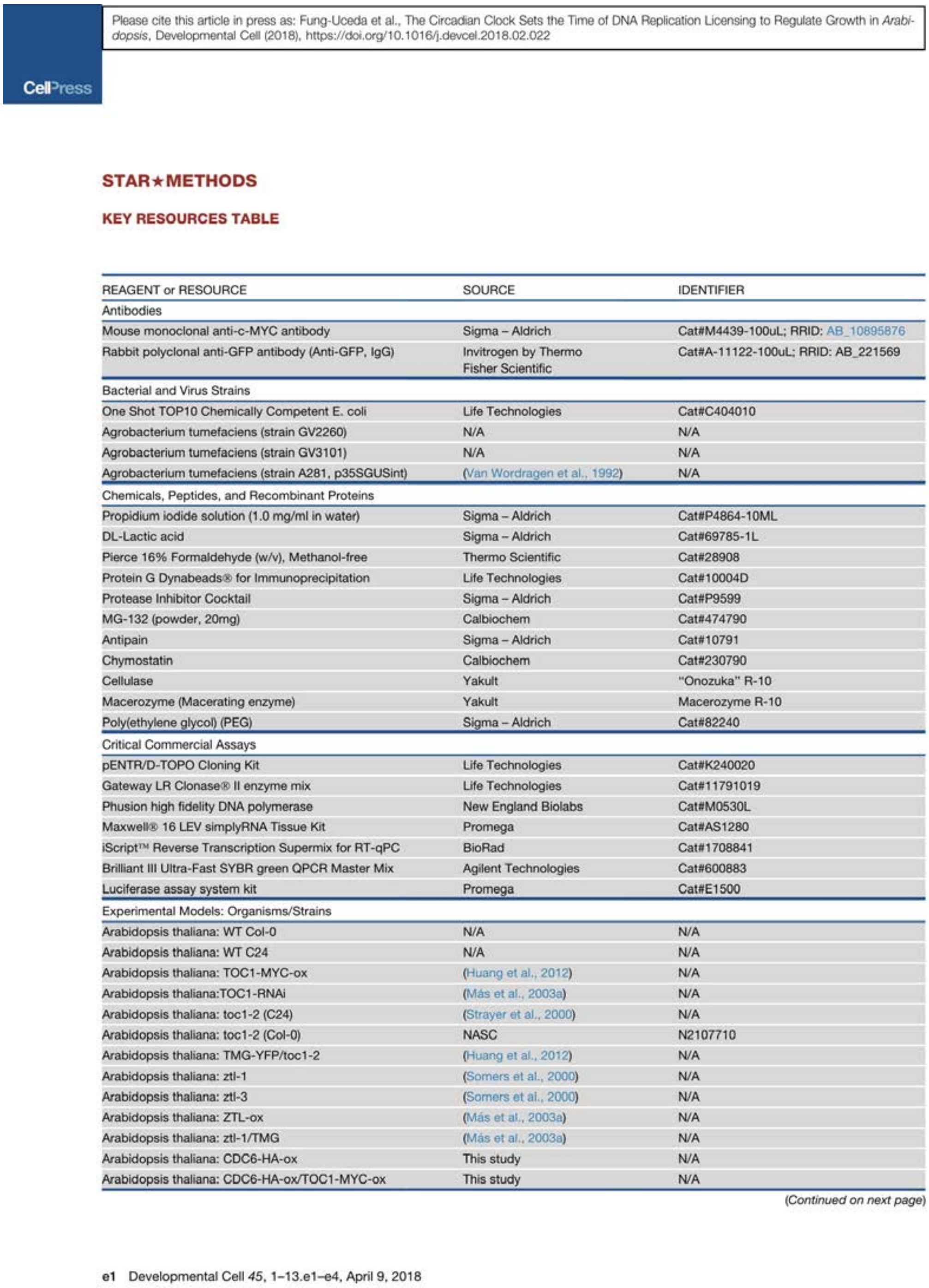

Please cite this article in press as: Fung-Uceda et al., The Circadian Clock Sets the Time of DNA Replication Licensing to Regulate Growth in *Arabidopsis*, Developmental Cell (2018), https://doi.org/10.1016/j.devcel.2018.02.022

STAR★METHODS

KEY RESOURCES TABLE

REAGENT or RESOURCE	SOURCE	IDENTIFIER
Antibodies		
Mouse monoclonal anti-c-MYC antibody	Sigma – Aldrich	Cat#M4439-100uL; RRID: AB_10895876
Rabbit polyclonal anti-GFP antibody (Anti-GFP, IgG)	Invitrogen by Thermo Fisher Scientific	Cat#A-11122-100uL; RRID: AB_221569
Bacterial and Virus Strains		
One Shot TOP10 Chemically Competent E. coli	Life Technologies	Cat#C404010
Agrobacterium tumefaciens (strain GV2260)	N/A	N/A
Agrobacterium tumefaciens (strain GV3101)	N/A	N/A
Agrobacterium tumefaciens (strain A281, p35SGUSint)	(Van Wordragen et al., 1992)	N/A
Chemicals, Peptides, and Recombinant Proteins		
Propidium iodide solution (1.0 mg/ml in water)	Sigma – Aldrich	Cat#P4864-10ML
DL-Lactic acid	Sigma – Aldrich	Cat#69785-1L
Pierce 16% Formaldehyde (w/v), Methanol-free	Thermo Scientific	Cat#28908
Protein G Dynabeads® for Immunoprecipitation	Life Technologies	Cat#10004D
Protease Inhibitor Cocktail	Sigma – Aldrich	Cat#P9599
MG-132 (powder, 20mg)	Calbiochem	Cat#474790
Antipain	Sigma – Aldrich	Cat#10791
Chymostatin	Calbiochem	Cat#230790
Cellulase	Yakult	"Onozuka" R-10
Macerozyme (Macerating enzyme)	Yakult	Macerozyme R-10
Poly(ethylene glycol) (PEG)	Sigma – Aldrich	Cat#82240
Critical Commercial Assays		
pENTR/D-TOPO Cloning Kit	Life Technologies	Cat#K240020
Gateway LR Clonase® II enzyme mix	Life Technologies	Cat#11791019
Phusion high fidelity DNA polymerase	New England Biolabs	Cat#M0530L
Maxwell® 16 LEV simplyRNA Tissue Kit	Promega	Cat#AS1280
iScript™ Reverse Transcription Supermix for RT-qPC	BioRad	Cat#1708841
Brilliant III Ultra-Fast SYBR green QPCR Master Mix	Agilent Technologies	Cat#600883
Luciferase assay system kit	Promega	Cat#E1500
Experimental Models: Organisms/Strains		
Arabidopsis thaliana: WT Col-0	N/A	N/A
Arabidopsis thaliana: WT C24	N/A	N/A
Arabidopsis thaliana: TOC1-MYC-ox	(Huang et al., 2012)	N/A
Arabidopsis thaliana:TOC1-RNAi	(Más et al., 2003a)	N/A
Arabidopsis thaliana: toc1-2 (C24)	(Strayer et al., 2000)	N/A
Arabidopsis thaliana: toc1-2 (Col-0)	NASC	N2107710
Arabidopsis thaliana: TMG-YFP/toc1-2	(Huang et al., 2012)	N/A
Arabidopsis thaliana: ztl-1	(Somers et al., 2000)	N/A
Arabidopsis thaliana: ztl-3	(Somers et al., 2000)	N/A
Arabidopsis thaliana: ZTL-ox	(Más et al., 2003a)	N/A
Arabidopsis thaliana: ztl-1/TMG	(Más et al., 2003a)	N/A
Arabidopsis thaliana: CDC6-HA-ox	This study	N/A
Arabidopsis thaliana: CDC6-HA-ox/TOC1-MYC-ox	This study	N/A

(*Continued on next page*)

Please cite this article in press as: Fung-Uceda et al., The Circadian Clock Sets the Time of DNA Replication Licensing to Regulate Growth in *Arabidopsis*, Developmental Cell (2018), https://doi.org/10.1016/j.devcel.2018.02.022

Continued

REAGENT or RESOURCE	SOURCE	IDENTIFIER
Oligonucleotides		
Primers for plasmid construction	This study Table S1	N/A
Primers for qRT-PCR	This study Table S1	N/A
Primers for ChIP-PCR	This study Table S1	N/A
Primers for promoter cloning	This study Table S1	N/A
Recombinant DNA		
35S::CDC6-HA (pGWB514)	This study	N/A
WTCDC6p::GUS (pMIN35S/pCAMBIA1305)	This study	N/A
Mut1CDC6p::GUS (pMIN35S/pCAMBIA1305)	This study	N/A
Mut2CDC6p::GUS (pMIN35S/pCAMBIA1305)	This study	N/A
Software and Algorithms		
ImageJ	ImageJ	https://imagej.nih.gov/ij/
BD CellQuest Pro software	Becton Dickinson	https://www.bd.com
ModFit software	Verity Software House	http://www.vsh.com/products/mflt/index.asp
GraphPad Prism	GraphPad Software	https://www.graphpad.com/scientific-software/prism/

CONTACT FOR REAGENT AND RESOURCE SHARING

Further information and requests for resources and reagents should be directed to and will be fulfilled by the Lead Contact, Paloma Mas (paloma.mas@cragenomica.es).

EXPERIMENTAL MODEL AND SUBJECT DETAILS

Arabidopsis thaliana seedlings were grown on Murashige and Skoog (MS) agar medium. Seedlings were synchronized under Light:Dark cycles, ShD (8h light:16h dark), LD (12h light:12h dark), LgD (16h light:8h dark) as specified in each experiment, with 50-100 μmol $m^{-2}s^{-1}$ of cool white fluorescent light at 22°C. WT Columbia (Col-0) or C24, TOC1-MYC-ox (Huang et al., 2012), TOC1-RNAi (Más et al., 2003a), *toc1-2* (Strayer et al., 2000), TMG-YFP/*toc1-2* (Huang et al., 2012), *ztl-1*, *ztl-3*, (Somers et al., 2000) ZTL-ox, *ztl-1*/TMG (Más et al., 2003b) were described elsewhere. Transgenic CDC6-HA over-expressing plants (CDC6-HA-ox) in Wild-Type and TOC1-MYC-ox backgrounds were generated by *Agrobacterium tumefaciens* (GV2260) mediated DNA transfer of the CDC6-HA-ox construct specified below.

METHOD DETAILS

DNA Constructs and Plant Transformation

Generation of single CDC6-ox and CDC6-ox/TOC1-ox double over-expressing plants (ox/ox) was performed by *Agrobacterium tumefaciens* (GV2260) mediated DNA transfer (Clough and Bent, 1998) of WT and TOC1-ox plants with a CDC6 over-expressing construct. The construct was generated by PCR-mediated amplification of the *CDC6* coding sequence followed by cloning into the pENTR/D-TOPO vector (Invitrogen). The coding sequence was cloned into the plant destination vector pGWB514 (35S pro, C-3xHA) (Nakagawa et al., 2007a, 2007b) following the manufacturer's recommendations (Invitrogen). Several one insertion, T2 lines were used for the kinematic analyses of ploidy. Cloning of the *CDC6* promoter was performed by PCR amplification of 2000 base pairs (bp) of the genomic region upstream of the gene's transcription start site (TSS) (primer pairs A and D). The mutated versions of the *CDC6* promoter lacking the Evening Element (EE) (-670 bp from TSS) were obtained following two strategies. The mut1*CDC6*p was generated by just deleting the EE (-10 bp). A second mutated version (mut2*CDC6*p) was obtained by deleting the EE plus 10 nucleotides on each side flanking the motif. To generate the mutants, a PCR-based mutagenesis by overlap extension was performed (Lee et al., 2004). The WT and mutated versions of the *CDC6* promoter were then cloned into a vector derived from the pCAMBIA1305.1 vector containing the *GLUCURONIDASE* gene (GUSplus) under the control of a minimal 35S promoter (Lee et al., 2017).

Hypocotyl Measurements

For hypocotyl length measurements, seeds were stratified on MS medium in the dark for 4 days at 4°C, exposed to white light (40 μmol·quanta·$m^{-2}·s^{-1}$) for 6 h and maintained in the dark for 18 h before transferring to chambers under constant white light, 40 μmol·$m^{-2}·s^{-1}$ (WL40) or 1 μmol·quanta·$m^{-2}·s^{-1}$ (WL1). Hypocotyl length was measured using the ImageJ software at 7 days

Please cite this article in press as: Fung-Uceda et al., The Circadian Clock Sets the Time of DNA Replication Licensing to Regulate Growth in *Arabidopsis*, Developmental Cell (2018), https://doi.org/10.1016/j.devcel.2018.02.022

after stratification or every day over 7 days for the growth kinetic analyses. Hypocotyl epidermal cell length and number were examined at 7 days after stratification by using a wide-field fluorescence microscope (Axiophot Zeiss) and analyzed using the ImageJ software. At least 20 hypocotyls and about 100 cells per condition and genotype were measured. Each experiment was repeated at least twice using a similar "n" number. Statistical analyses were performed by two-tailed t-tests with 99% of confidence.

For flow cytometry analyses, the apex, cotyledons and roots were removed with a razor blade, and about 10 hypocotyls were chopped in ice-cold LB01 buffer (15 mM Tris, 2 mM Na2EDTA, 0.5 mM spermine tetrahydrochloride, 80 mM KCl, 20 mM NaCl, 0.1% (vol/vol) Triton X-100, pH 7,5 (Dolezel et al., 2007; Galbraith et al., 1983). The suspension was filtered through a 30 μm nylon mesh (Sysmex CellTrics) before incubation with 50 μg mL^{-1} DNase-free RNase and 50 μg mL^{-1} propidium iodide (Sigma-Aldrich). DNA content was examined with a FACSCalibur flow cytometer (Becton Dickinson) and the BD CellQuest Pro software (Becton Dickinson). Propidium iodide was detected using the FL2 (585/42) channel. Gates were set in the fluorescence intensity (FL2)/side scatter density plot. At least 10000 nuclei were measured within a gate. Each experiment was repeated at least twice using a similar "n" number. The endoreplication index or cycle value (Barow and Meister, 2003) was calculated taking the number of nuclei of each ploidy multiplied by the number of endoreplication cycles required to reach that ploidy. The sum of the resulting products was divided by the total number of nuclei measured.

Kinematic Analyses and Flow Cytometry

Approximately 30 leaves (at young stages) or 10 leaves (at old stages) were chopped with a razor blade in extraction buffer LB01 (15 mM Tris, 2 mM Na2EDTA, 0.5 mM spermine tetrahydrochloride, 80 mM KCl, 20 mM NaCl, 0.1% (vol/vol) Triton X-100, pH 7,5) (Dolezel et al., 2007; Galbraith et al., 1983). The suspension was filtered through a 30 μm nylon mesh (Sysmex CellTrics) followed by incubation with 50 μg mL^{-1} DNase-free RNase, and 50 μg mL^{-1} propidium iodide (Sigma-Aldrich). Nuclei were analyzed with a FACSCalibur flow cytometer (Becton Dickinson) and BD CellQuest Pro software (Becton Dickinson). At least 10000 nuclei were counted per sample. Analyses were performed as described for hypocotyls (see section above). Cell cycle analysis on proliferating leaves was analyzed by using the ModFit software (Verity Software House). Each experiment was repeated at least twice using a similar "n" number.

For the kinematic analysis of leaf growth (De Veylder et al., 2001), approximately 10 seedlings grown under ShD and LgD conditions were harvested at the specified days after stratification. Plants were incubated with methanol overnight to remove chlorophyll, and subsequently stored in lactic acid before microscopy analyses. Leaf blade area of the first pair of true leaves (at young stages 3-7 das) was measured using a wide-field fluorescence microscope (Axiophot Zeiss) while leaves at older stages (10-24 das) were measured with a magnifying glass (Olympus DP71). Cell area of the first pair of true leaves for all stages was measured using a wide-field fluorescence microscope (Axiophot Zeiss). Measurements were performed by drawing leaf areas containing approximately 100 cells, located 25% and 75% from the distance between the tip and the base of the leaf blade of the abaxial epidermis of each leaf. Total number of cells was estimated by dividing the leaf blade area by the average cell area of each leaf. Average cell division rates were estimated as the slope of the log 2–transformed number of cells per leaf, using a five-point differentiation formula (Fiorani and Beemster, 2006). Each experiment was repeated at least twice using a similar "n" number.

Real-Time PCR Analysis

For the developmental time course analyses, the first pair of leaves were cut in halves and the expression of selected core cell cycle genes was separately examined at the tip and base of leaves. RNA was isolated using the Maxwell 16 LEV simply RNA Tissue kit (Promega). Single strand cDNA was synthesized using iScript™ Reverse Transcription Supermix for RT-qPCR (BioRad) following manufacturer recommendations. For quantitative real-time gene expression analysis (qPCR), cDNAs were diluted 10-fold with nuclease-free water and qPCR was performed with the Briliant III Ultra-Fast SYBR Green qPCR Master Mix (Agilent Technologies) in a 96-well CFX96 Touch Real-Time PCR Detection System (BioRad). Each sample was run in technical triplicates. The geometric mean of *APA1* and *IPP2* expression was used as a control. Crossing point (Cp) calculation was used for quantification using the Absolute Quantification analysis by the 2nd Derivative Maximun method. Table S1 shows the specific sequences for primers used in this study. For the developmental time course analyses, samples were harvested at ZT7. For the diurnal gene expression analyses samples were harvested every 4 hours over a 24 hours cycle. Each experiment was repeated at least twice.

Protoplast Transfection

Leaves from 3-week-old plants were cut into 0.5-mm pieces using a fresh razor blade. Twenty leaves were digested in 15 ml of enzyme solution [0.8% cellulase (Yakult), 0.2% macerozyme (Yakult), 0.4 M mannitol, 10 mM $CaCl_2$, 20 mM KCl, 0.1% bovine serum albumin, and 20 mM MES (pH 5.7)], vacuumed for 20 min, and incubated in the dark for 5 hours at 22° to 23°C. Protoplasts were then passed through 40-μm stainless mesh and collected after a gentle wash with W5 media (154 mM NaCl, 125 mM $CaCl_2$, 5 mM KCl, 2 mM MES, 5 mM glucose adjusted to pH 5.7 with KOH). For transient expression assays using Arabidopsis protoplasts, reporter and effector plasmids were constructed. The reporter plasmid contains a minimal 35S promoter sequence and the GUS gene. The *CDC6* promoter was inserted into the reporter plasmid. To construct effector plasmids, TOC1 cDNA was inserted into the effector vector containing the CaMV 35S promoter. Recombinant reporter and effector plasmids were co-transformed into Arabidopsis protoplasts by PEG-mediated transformation. The GUS activities were measured by a fluorometric method. A CaMV 35S promoter–Luc construct was also co-transformed as an internal control. The Luc assay was performed using the Luciferase Assay System kit (Promega).

Please cite this article in press as: Fung-Uceda et al., The Circadian Clock Sets the Time of DNA Replication Licensing to Regulate Growth in *Arabidopsis*, Developmental Cell (2018), https://doi.org/10.1016/j.devcel.2018.02.022

Chromatin Immunoprecipitation

Plants grown under LgD conditions (22 day-old) were sampled at ZT7 for TOC1-ox and ZT3 and ZT15 for TMG. Chromatin immunoprecipitation (ChIP) assays were essentially performed as previously described (Huang et al., 2012). Samples were fixed under vacuum with 1% of formaldehyde (16% formaldehyde solution (w/v) methanol-free, Thermo Scientific) for a total of 15 min, shaking the samples every 5 min. Special care was taken with the fixation process as it was found to be crucial for successful ChIP results. Soluble chromatin was incubated overnight at 4°C with an Anti-MYC antibody (Sigma-Aldrich) for assays with TOC1-ox plants or Anti-GFP (Invitrogen by Thermo Fisher Scientific) antibody for the assays with TMG plants. Chromatin antibody conjugates were then incubated for 4 hours at 4°C with Protein G–Dynabeads beads (Invitrogen by Thermo Fisher Scientific). ChIPs were quantified by qPCR analysis using a 96-well CFX96 Touch Real-Time PCR Detection System (BioRad). Crossing point (Cp) calculation was used for quantification using the Absolute Quantification analysis by the 2nd Derivative Maximun method. ChIP values for each set of primers were normalized to Input values. Table S1 shows the sequences of primers used in this study.

Tumor Induction and Progression

The *Agrobacterium tumefaciens* strain A281, p35SGUSint (Van Wordragen et al., 1992) was grown on Yeast Extract Broth (YEB) medium (0.5% tryptone, 0.5% yeast extract, 0.5% sucrose, 50 mm $MgSO_4$ and 1.5% agar, pH 7.8) for 24 h at 28°C. Tumors were induced by applying the Agrobacterium strain at the base of slightly wounded inflorescence stalks. Seven and five days after inoculation, tissues were excised under a binocular to avoid contamination of the inflorescence stalk and stained with GUS for visualization of tumor progression. The same procedure was used while inoculating the first internodes. GUS staining was performed by incubating inflorescence stalks and internodes with GUS staining solution (1mM X-Gluc, 0.5mM potassium ferrocyanide, 0.5 mM potassium ferricyanide and 0.5% triton X-100) for 30 minutes under vacuum and then for 6 hours at 37°C in the dark. Samples were rinsed in water and cleared with 70% Ethanol. Samples were mounted in water and images were taken using an Olympus DP71 magnifying glass. The same procedure was used to inoculate the non-tumorigenic Agrobacterium strain GV3101. This wounded but uninfected inflorescence stalks and internodes were used as controls. Two biological replicates were performed.

QUANTIFICATION AND STATISTICAL ANALYSIS

Quantification of hypocotyl length (Figures 3A, 3B, 3I, and S3A–S3C), leaf blade area (Figures 1C, S1A, S1J, S1M, and S1N), hypocotyl cell length (Figures 3D, S3D, and S3E), leaf cell area (Figures 1E, S1C, S1L, and S1Q) and tumor area (Figures 6A–6J and S7A–S7C) were measured using the ImageJ software. For hypocotyl measurements data are mean + SEM of $n \approx 20$ hypocotyls and $n \approx 100$ cells (per genotype and/or condition). Statistical analyses were performed by two-tailed t-tests with 99% of confidence. For leaf and cell area measurements data are mean + SEM of $n \approx$ 10-20 leaves and $n \approx 100$ cells. For all flow cytometry experiments (Figures 1G, 2A–2J, 3E–3I, 5M–5P, S1E, S1F, S2A–S2I, S3F–S3H, S6C, S6D, S6G, and S6H) data are mean + SEM of $n \approx 10000$ nuclei per gate. For gene expression analysis using qPCR (Figures 4A–4L, 5A–5I, 5K, 5L, S4A–S4P, S5A–S5I, S5K, S5L, S6A, and S6E), data represent means + SEM of technical triplicates. Crossing point (Cp) calculation was used for quantification using the Absolute Quantification analysis by the 2nd Derivative Maximun method. All of the experiments were repeated at least twice using a similar "n" number.

Developmental Cell, Volume *45*

Supplemental Information

The Circadian Clock Sets the Time of DNA Replication Licensing to Regulate Growth in *Arabidopsis*

Jorge Fung-Uceda, Kyounghee Lee, Pil Joon Seo, Stefanie Polyn, Lieven De Veylder, and Paloma Mas

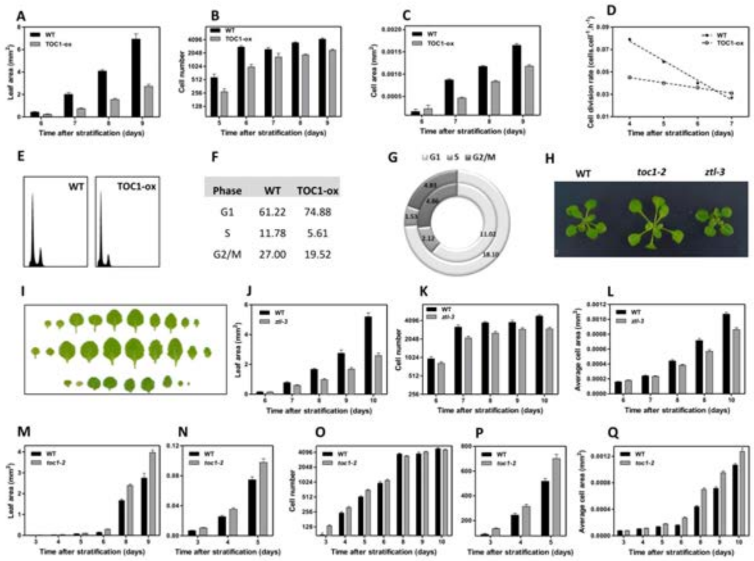

Phase	WT	TOC1-ox
G1	61.22	74.88
S	11.78	5.61
G2/M	27.00	19.52

Figure S1. TOC1 modulates growth and the mitotic cycle in developing leaves, related to Figure 1. Early time course analyses of (A) leaf blade area, (B) cell number and (C) cell area of the first leaf pair of plants grown under LgD. Data are mean + SEM of n ≈ 10-20 leaves and n=100 cells. (D) Average cell division rates of abaxial epidermal cells and linear regression analyses of the first four points of the kinematic assay. (E) Ploidy distribution by flow cytometry of WT and TOC1-ox first pair of leaves at 7 das under LgD. (F) Estimation of the relative amounts of cells in G1, S and G2/M phases in proliferating first pair of leaves analyzed by flow cytometry at 7 das. (G) Estimated duration (hours) of the G1, S and G2/M phases at 7 das under LgD in WT (inner rings) and TOC1-ox (outer rings). Representative images of (H) WT, *toc1-2* and *ztl-3* plants and (I) leaves from WT (top), *toc1-2* (middle) and *ztl-3* (bottom) plants at 19 das under LgD. Time course analyses of leaf blade area in (J) *ztl-3* and (M, N) *toc1-2* mutants. Cell number of the first leaf pair in (K) *ztl-3* and (O, P) *toc1-2* mutants. Cell area in (L) *ztl-3* and (Q) *toc1-2* mutants grown under LgD. Values of (N) leaf area and (P) cell number at early stages of development are separately represented. Data in panels (B), (K) and (O) are graphed in log2 scale. Data are mean + SEM of n ≈ 10-20 leaves and n=100 cells. At least two biological replicates per experiment were performed.

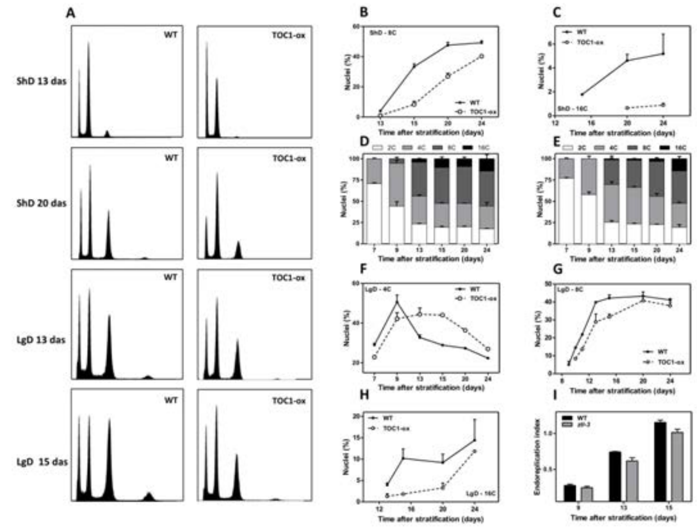

Figure S2. TOC1 modulates endoreplication in developing leaves, related to Figure 2. (A) Ploidy distribution by flow cytometry of WT and TOC1-ox first pair of leaves at 13 and 20 das under ShD and 13 and 15 das under LgD. Relative profiles of (B) 8C and (C) 16C content under ShD. Kinematics of polyploid nuclei in (D) WT and (E) TOC1-ox in plants grown under LgD. Relative profiles of (F) 4C, (G) 8C and (H) 16C content under LgD in WT and TOC1-ox leaves. (I) Endoreduplication index of WT and *ztl-3* leaves of plants grown under ShD. Data are mean + SEM of n ≈ 10000 nuclei. At least two biological replicates per experiment were performed.

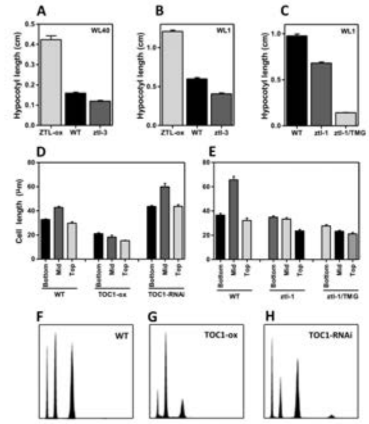

Figure S3. Proper accumulation of TOC1 is important for cell expansion and endocycle activity during hypocotyl growth, related to Figure 3. Hypocotyl length of WT , *ztl-3* and ZTL-ox seedlings under (A) WL40 and (B) WL1. (C) Hypocotyl length of WT, *ztl-1* and *ztl-1*/TMG seedlings under WL1. (D) Epidermal cell length at the bottom, mid or top sections of hypocotyls from WT, TOC1-ox and TOC1-RNAi and (E) WT, *ztl-1* and *ztl-1*/TMG seedlings under WL40. (F, G, H) Ploidy profiles by flow cytometry of WT, TOC1-ox and TOC1-RNAi hypocotyls of seedlings grown under WL1. Data are mean + SEM of n ≈ 20 hypocotyls and n=100 cells. At least two biological replicates per experiment were performed.

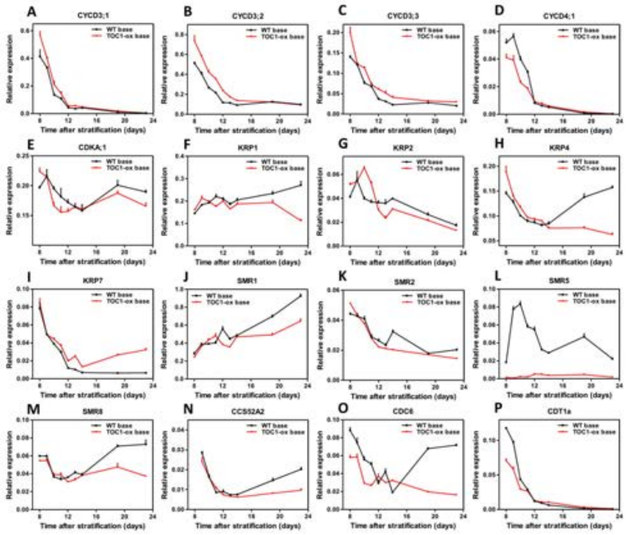

Figure S4. Miss-expression of cell cycle genes in TOC1-ox developing leaves, related to Figure 4. Time course analyses of cell cycle genes in WT and TOC1-ox leaves over development. Plants were grown under LgD and samples were collected at ZT7. Leaves were cut in halves and gene expression was separately examined at the base of leaves. Expression of (A) *CYCD3;1*, (B) *CYCD3;2,* (C) *CYCD3;3,* (D) *CYCD4;1,* (E) *CDKA;1,* (F) *KRP1*, (G) *KRP2*, (H) *KRP4,* (I) *KRP7* (J) *SMR1,* (K) *SMR2,* (L) *SMR5,* (M) *SMR8,* (N) *CCS52A2,* (O) *CDC6*, (P) *CDT1a* at the base of leaves. Relative expression was obtained by Quantitative real-time PCR (Q-PCR) analyses. Data represent means + SEM of technical triplicates. The experiment was repeated twice, giving similar results to those shown here.

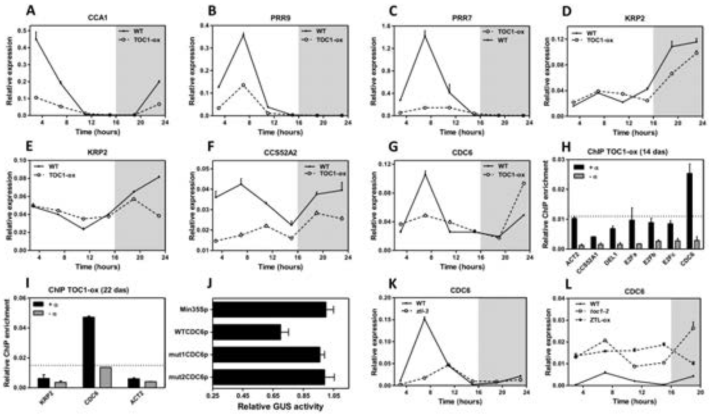

Figure S5. TOC1 regulates the diurnal expression of cell cycle genes, related to Figure 5. Time course analyses of gene expression over a diurnal cycle. Plants were grown under LgD and samples were collected at (A-B) 7 das, (C-D, G) 14 das or (E, F) 18 das every 4h over a 24h cycle. Expression of (A) *CCA1*, (B) *PRR9*, (C) *PRR7*, (D) *KRP2* at 14 das and (E) 18 das, (F) *CCS52A2* and (G) *CDC6* in WT and TOC1-ox plants. Relative expression was obtained by Quantitative real-time PCR (Q-PCR) analyses. Data represent means + SEM of technical triplicates. ChIP assays with TOC1-ox plants sampled examined at (H) 14 das and (I) 22 das. ChIP enrichment was calculated relative to the input. Samples were incubated with an anti-MYC antibody (+α) or without antibody (-α). (J) Relative GUS activity of WT *CDC6* promoter (WTCDC6p) and two mutated versions lacking the Evening Element (mut1CDC6p and mut2CDC6p). Activity was assayed in protoplasts co-transfected with TOC1. The Minimal 35S promoter (Min35Sp) was used as a control. Expression of *CDC6* in (K) WT and *ztl-3* and in (L) WT, *toc1-2* mutant and ZTL-ox plants. Plants were grown under LgD and samples were collected at 18 das. Relative expression was obtained by Q-PCR. Data represent means + SEM of technical triplicates. The experiments were repeated at least twice.

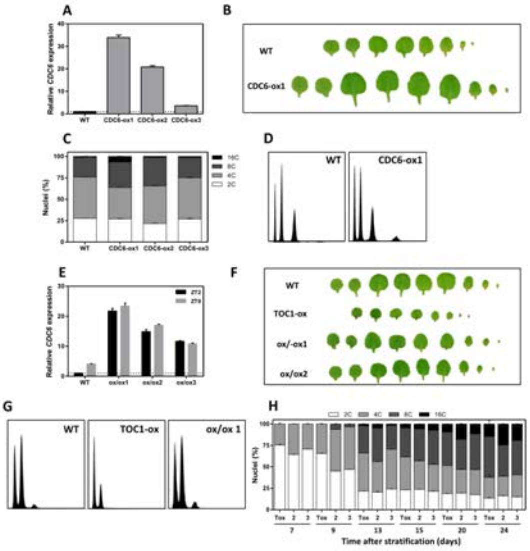

Figure S6. Analyses of CDC6 and TOC1 genetic interaction, related to Figure 5. (A) Relative *CDC6* expression in WT and three different lines over-expressing CDC6. Plants were grown under LgD and samples were collected at ZT7. Relative expression was obtained by RT-Q-PCR. Data is presented relative to WT and represent means + SEM of technical triplicates. (B) Representative images of WT and CDC6-ox leaves of plants grown under LgD. (C) Proportion of polyploidy nuclei in WT and three different CDC6-ox lines. Plants were grown under LgD. (D) Ploidy distribution by flow cytometry of WT and CDC6-ox line 1 of the first pair of leaves at 9 das under LgD. (E) Relative *CDC6* expression in WT and three different double CDC6 and TOC1 over-expressing lines (ox/ox). Plants were grown under LgD and samples were collected at ZT2 and ZT9. Relative expression was obtained by RT-Q-PCR. Data is presented relative to WT ZT2 and represent means + SEM of technical triplicates. (F) Representative images of WT, TOC1-ox and CDC6-ox/TOC1-ox leaves of plants grown under LgD. Ploidy distribution by flow cytometry of WT, TOC1-ox, and CDC6-ox/TOC1-ox (ox/ox1) plants of the first pair of leaves at 9 das under LgD. (H) Kinematics of polyploidy nuclei in TOC1-ox (Tox) and two CDC6-ox/TOC1-ox lines (2 and 3). Plants were grown under LgD. Data are mean + SEM of n=10000 nuclei. The experiments were repeated at least twice.

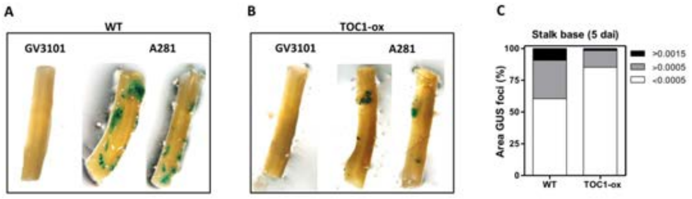
A
WT
GV3101
A281
B
TOC1-ox
GV3101
A281
C
Stalk base (5 dai)
Area GUS foci (%)
100
75
50
25
0
WT
TOC1-ox
>0.0015
>0.0005
<0.0005

Figure S7. Tumor progression is delayed in TOC1-ox, related to Figure 6. Representative images of inflorescence stalks inoculated with the Agrobacterium non-virulent strain GV3101 and virulent strain A281 at the base of inflorescence stalks in WT (A) and TOC1-ox (B) at 5 dai. (C) Distribution of the proportion of sizes of the different GUS areas at the base of inflorescence stalks at 5 dai. At least two biological replicates per experiment were performed.

Table S1. List of primers used in this study, related to STAR Methods.

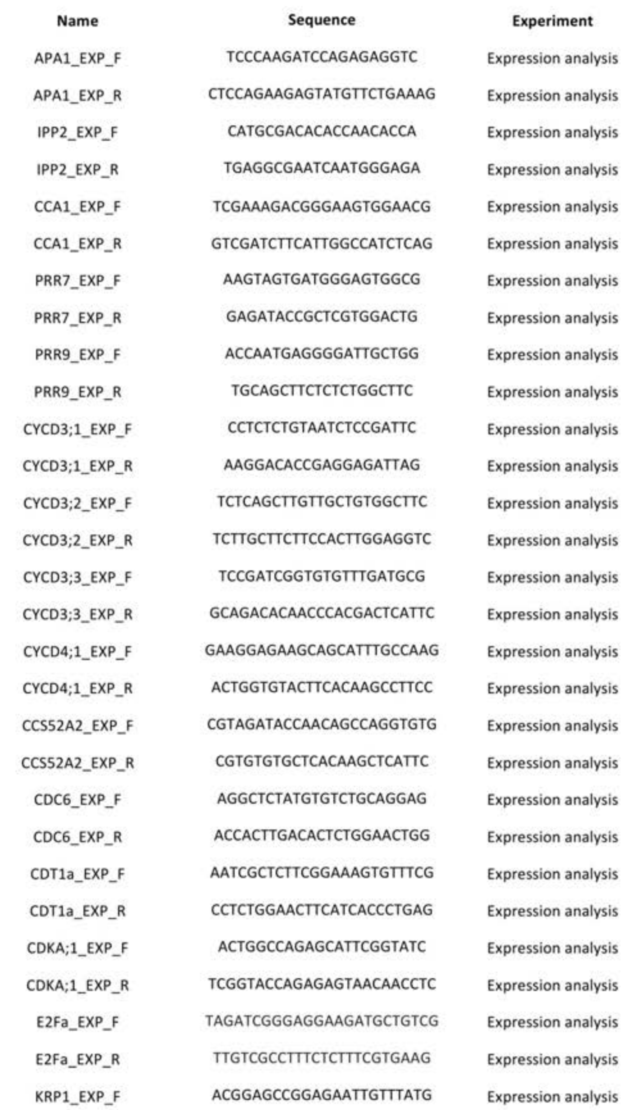

Name	Sequence	Experiment
APA1_EXP_F	TCCCAAGATCCAGAGAGGTC	Expression analysis
APA1_EXP_R	CTCCAGAAGAGTATGTTCTGAAAG	Expression analysis
IPP2_EXP_F	CATGCGACACACCAACACCA	Expression analysis
IPP2_EXP_R	TGAGGCGAATCAATGGGAGA	Expression analysis
CCA1_EXP_F	TCGAAAGACGGGAAGTGGAACG	Expression analysis
CCA1_EXP_R	GTCGATCTTCATTGGCCATCTCAG	Expression analysis
PRR7_EXP_F	AAGTAGTGATGGGAGTGGCG	Expression analysis
PRR7_EXP_R	GAGATACCGCTCGTGGACTG	Expression analysis
PRR9_EXP_F	ACCAATGAGGGGATTGCTGG	Expression analysis
PRR9_EXP_R	TGCAGCTTCTCTCTGGCTTC	Expression analysis
CYCD3;1_EXP_F	CCTCTCTGTAATCTCCGATTC	Expression analysis
CYCD3;1_EXP_R	AAGGACACCGAGGAGATTAG	Expression analysis
CYCD3;2_EXP_F	TCTCAGCTTGTTGCTGTGGCTTC	Expression analysis
CYCD3;2_EXP_R	TCTTGCTTCTTCCACTTGGAGGTC	Expression analysis
CYCD3;3_EXP_F	TCCGATCGGTGTGTTTGATGCG	Expression analysis
CYCD3;3_EXP_R	GCAGACACAACCCACGACTCATTC	Expression analysis
CYCD4;1_EXP_F	GAAGGAGAAGCAGCATTTGCCAAG	Expression analysis
CYCD4;1_EXP_R	ACTGGTGTACTTCACAAGCCTTCC	Expression analysis
CCS52A2_EXP_F	CGTAGATACCAACAGCCAGGTGTG	Expression analysis
CCS52A2_EXP_R	CGTGTGTGCTCACAAGCTCATTC	Expression analysis
CDC6_EXP_F	AGGCTCTATGTGTCTGCAGGAG	Expression analysis
CDC6_EXP_R	ACCACTTGACACTCTGGAACTGG	Expression analysis
CDT1a_EXP_F	AATCGCTCTTCGGAAAGTGTTTCG	Expression analysis
CDT1a_EXP_R	CCTCTGGAACTTCATCACCCTGAG	Expression analysis
CDKA;1_EXP_F	ACTGGCCAGAGCATTCGGTATC	Expression analysis
CDKA;1_EXP_R	TCGGTACCAGAGAGTAACAACCTC	Expression analysis
E2Fa_EXP_F	TAGATCGGGAGGAAGATGCTGTCG	Expression analysis
E2Fa_EXP_R	TTGTCGCCTTTCTCTTTCGTGAAG	Expression analysis
KRP1_EXP_F	ACGGAGCCGGAGAATTGTTTATG	Expression analysis

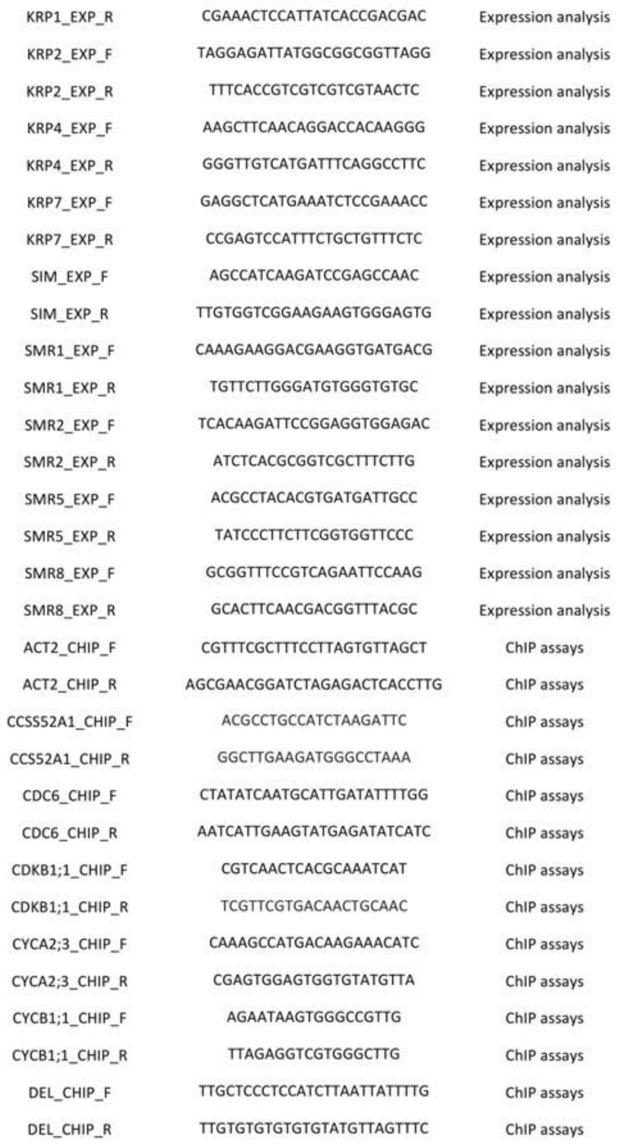

KRP1_EXP_R	CGAAACTCCATTATCACCGACGAC	Expression analysis
KRP2_EXP_F	TAGGAGATTATGGCGGCGGTTAGG	Expression analysis
KRP2_EXP_R	TTTCACCGTCGTCGTCGTAACTC	Expression analysis
KRP4_EXP_F	AAGCTTCAACAGGACCACAAGGG	Expression analysis
KRP4_EXP_R	GGGTTGTCATGATTTCAGGCCTTC	Expression analysis
KRP7_EXP_F	GAGGCTCATGAAATCTCCGAAACC	Expression analysis
KRP7_EXP_R	CCGAGTCCATTTCTGCTGTTTCTC	Expression analysis
SIM_EXP_F	AGCCATCAAGATCCGAGCCAAC	Expression analysis
SIM_EXP_R	TTGTGGTCGGAAGAAGTGGGAGTG	Expression analysis
SMR1_EXP_F	CAAAGAAGGACGAAGGTGATGACG	Expression analysis
SMR1_EXP_R	TGTTCTTGGGATGTGGGTGTGC	Expression analysis
SMR2_EXP_F	TCACAAGATTCCGGAGGTGGAGAC	Expression analysis
SMR2_EXP_R	ATCTCACGCGGTCGCTTTCTTG	Expression analysis
SMR5_EXP_F	ACGCCTACACGTGATGATTGCC	Expression analysis
SMR5_EXP_R	TATCCCTTCTTCGGTGGTTCCC	Expression analysis
SMR8_EXP_F	GCGGTTTCCGTCAGAATTCCAAG	Expression analysis
SMR8_EXP_R	GCACTTCAACGACGGTTTACGC	Expression analysis
ACT2_CHIP_F	CGTTTCGCTTTCCTTAGTGTTAGCT	ChIP assays
ACT2_CHIP_R	AGCGAACGGATCTAGAGACTCACCTTG	ChIP assays
CCSS52A1_CHIP_F	ACGCCTGCCATCTAAGATTC	ChIP assays
CCS52A1_CHIP_R	GGCTTGAAGATGGGCCTAAA	ChIP assays
CDC6_CHIP_F	CTATATCAATGCATTGATATTTTGG	ChIP assays
CDC6_CHIP_R	AATCATTGAAGTATGAGATATCATC	ChIP assays
CDKB1;1_CHIP_F	CGTCAACTCACGCAAATCAT	ChIP assays
CDKB1;1_CHIP_R	TCGTTCGTGACAACTGCAAC	ChIP assays
CYCA2;3_CHIP_F	CAAAGCCATGACAAGAAACATC	ChIP assays
CYCA2;3_CHIP_R	CGAGTGGAGTGGTGTATGTTA	ChIP assays
CYCB1;1_CHIP_F	AGAATAAGTGGGCCGTTG	ChIP assays
CYCB1;1_CHIP_R	TTAGAGGTCGTGGGCTTG	ChIP assays
DEL_CHIP_F	TTGCTCCCTCCATCTTAATTATTTTG	ChIP assays
DEL_CHIP_R	TTGTGTGTGTGTGTATGTTAGTTTC	ChIP assays

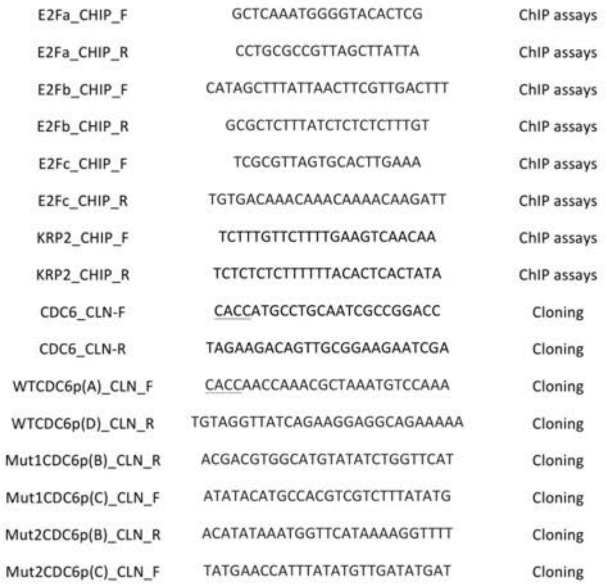

E2Fa_CHIP_F	GCTCAAATGGGGTACACTCG	ChIP assays
E2Fa_CHIP_R	CCTGCGCCGTTAGCTTATTA	ChIP assays
E2Fb_CHIP_F	CATAGCTTTATTAACTTCGTTGACTTT	ChIP assays
E2Fb_CHIP_R	GCGCTCTTTATCTCTCTCTTTGT	ChIP assays
E2Fc_CHIP_F	TCGCGTTAGTGCACTTGAAA	ChIP assays
E2Fc_CHIP_R	TGTGACAAACAAACAAAACAAGATT	ChIP assays
KRP2_CHIP_F	TCTTTGTTCTTTTGAAGTCAACAA	ChIP assays
KRP2_CHIP_R	TCTCTCTCTTTTTTACACTCACTATA	ChIP assays
CDC6_CLN-F	CACCATGCCTGCAATCGCCGGACC	Cloning
CDC6_CLN-R	TAGAAGACAGTTGCGGAAGAATCGA	Cloning
WTCDC6p(A)_CLN_F	CACCAACCAAACGCTAAATGTCCAAA	Cloning
WTCDC6p(D)_CLN_R	TGTAGGTTATCAGAAGGAGGCAGAAAAA	Cloning
Mut1CDC6p(B)_CLN_R	ACGACGTGGCATGTATATCTGGTTCAT	Cloning
Mut1CDC6p(C)_CLN_F	ATATACATGCCACGTCGTCTTTATATG	Cloning
Mut2CDC6p(B)_CLN_R	ACATATAAATGGTTCATAAAAGGTTTT	Cloning
Mut2CDC6p(C)_CLN_F	TATGAACCATTTATATGTTGATATGAT	Cloning

Annex II

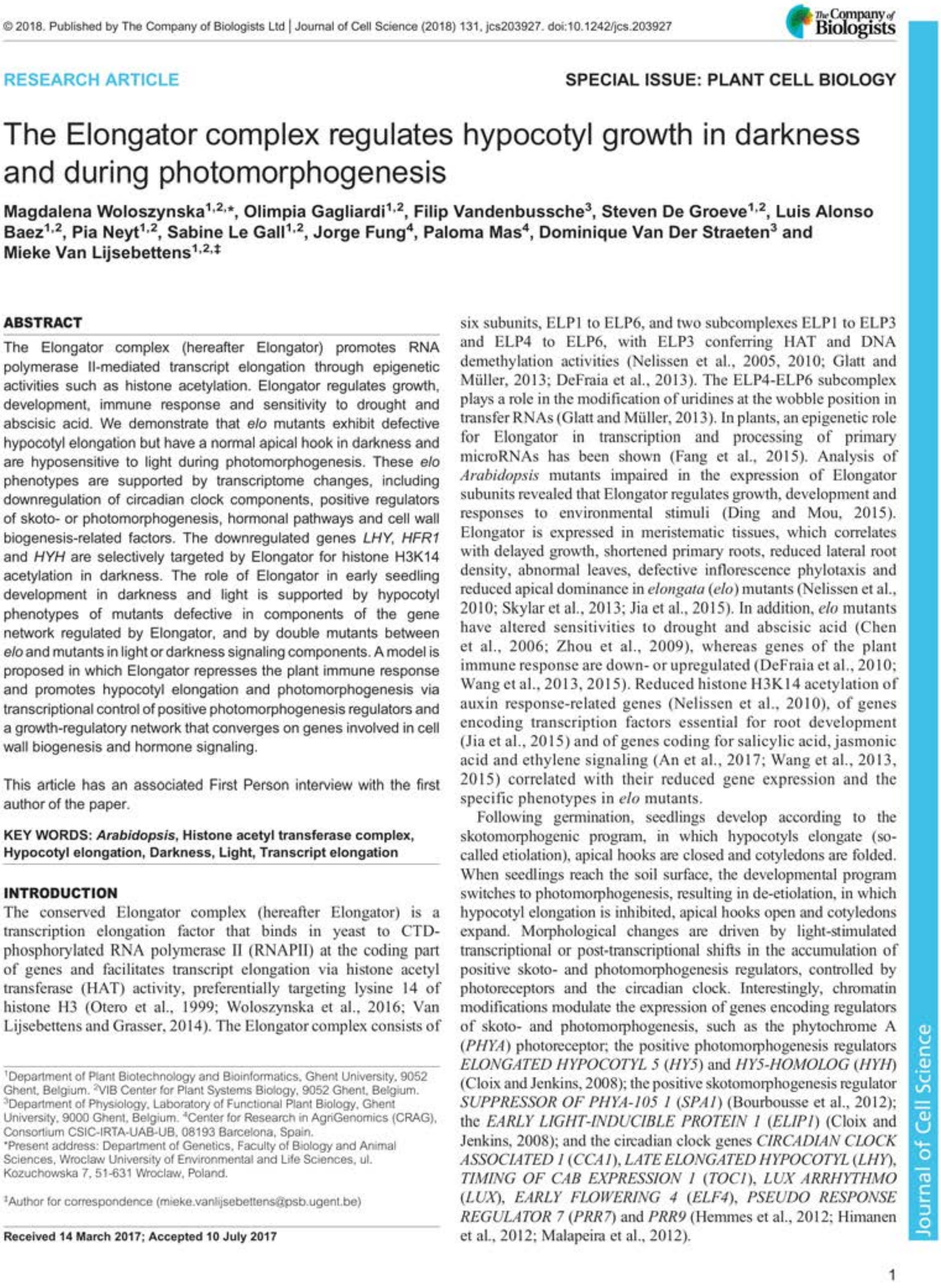

© 2018. Published by The Company of Biologists Ltd | Journal of Cell Science (2018) 131, jcs203927. doi:10.1242/jcs.203927

RESEARCH ARTICLE

SPECIAL ISSUE: PLANT CELL BIOLOGY

The Elongator complex regulates hypocotyl growth in darkness and during photomorphogenesis

Magdalena Woloszynska[1,2,*], Olimpia Gagliardi[1,2], Filip Vandenbussche[3], Steven De Groeve[1,2], Luis Alonso Baez[1,2], Pia Neyt[1,2], Sabine Le Gall[1,2], Jorge Fung[4], Paloma Mas[4], Dominique Van Der Straeten[3] and Mieke Van Lijsebettens[1,2,‡]

ABSTRACT

The Elongator complex (hereafter Elongator) promotes RNA polymerase II-mediated transcript elongation through epigenetic activities such as histone acetylation. Elongator regulates growth, development, immune response and sensitivity to drought and abscisic acid. We demonstrate that *elo* mutants exhibit defective hypocotyl elongation but have a normal apical hook in darkness and are hyposensitive to light during photomorphogenesis. These *elo* phenotypes are supported by transcriptome changes, including downregulation of circadian clock components, positive regulators of skoto- or photomorphogenesis, hormonal pathways and cell wall biogenesis-related factors. The downregulated genes *LHY*, *HFR1* and *HYH* are selectively targeted by Elongator for histone H3K14 acetylation in darkness. The role of Elongator in early seedling development in darkness and light is supported by hypocotyl phenotypes of mutants defective in components of the gene network regulated by Elongator, and by double mutants between *elo* and mutants in light or darkness signaling components. A model is proposed in which Elongator represses the plant immune response and promotes hypocotyl elongation and photomorphogenesis via transcriptional control of positive photomorphogenesis regulators and a growth-regulatory network that converges on genes involved in cell wall biogenesis and hormone signaling.

This article has an associated First Person interview with the first author of the paper.

KEY WORDS: *Arabidopsis*, Histone acetyl transferase complex, Hypocotyl elongation, Darkness, Light, Transcript elongation

INTRODUCTION

The conserved Elongator complex (hereafter Elongator) is a transcription elongation factor that binds in yeast to CTD-phosphorylated RNA polymerase II (RNAPII) at the coding part of genes and facilitates transcript elongation via histone acetyl transferase (HAT) activity, preferentially targeting lysine 14 of histone H3 (Otero et al., 1999; Woloszynska et al., 2016; Van Lijsebettens and Grasser, 2014). The Elongator complex consists of six subunits, ELP1 to ELP6, and two subcomplexes ELP1 to ELP3 and ELP4 to ELP6, with ELP3 conferring HAT and DNA demethylation activities (Nelissen et al., 2005, 2010; Glatt and Müller, 2013; DeFraia et al., 2013). The ELP4-ELP6 subcomplex plays a role in the modification of uridines at the wobble position in transfer RNAs (Glatt and Müller, 2013). In plants, an epigenetic role for Elongator in transcription and processing of primary microRNAs has been shown (Fang et al., 2015). Analysis of *Arabidopsis* mutants impaired in the expression of Elongator subunits revealed that Elongator regulates growth, development and responses to environmental stimuli (Ding and Mou, 2015). Elongator is expressed in meristematic tissues, which correlates with delayed growth, shortened primary roots, reduced lateral root density, abnormal leaves, defective inflorescence phylotaxis and reduced apical dominance in *elongata* (*elo*) mutants (Nelissen et al., 2010; Skylar et al., 2013; Jia et al., 2015). In addition, *elo* mutants have altered sensitivities to drought and abscisic acid (Chen et al., 2006; Zhou et al., 2009), whereas genes of the plant immune response are down- or upregulated (DeFraia et al., 2010; Wang et al., 2013, 2015). Reduced histone H3K14 acetylation of auxin response-related genes (Nelissen et al., 2010), of genes encoding transcription factors essential for root development (Jia et al., 2015) and of genes coding for salicylic acid, jasmonic acid and ethylene signaling (An et al., 2017; Wang et al., 2013, 2015) correlated with their reduced gene expression and the specific phenotypes in *elo* mutants.

Following germination, seedlings develop according to the skotomorphogenic program, in which hypocotyls elongate (so-called etiolation), apical hooks are closed and cotyledons are folded. When seedlings reach the soil surface, the developmental program switches to photomorphogenesis, resulting in de-etiolation, in which hypocotyl elongation is inhibited, apical hooks open and cotyledons expand. Morphological changes are driven by light-stimulated transcriptional or post-transcriptional shifts in the accumulation of positive skoto- and photomorphogenesis regulators, controlled by photoreceptors and the circadian clock. Interestingly, chromatin modifications modulate the expression of genes encoding regulators of skoto- and photomorphogenesis, such as the phytochrome A (*PHYA*) photoreceptor; the positive photomorphogenesis regulators *ELONGATED HYPOCOTYL 5* (*HY5*) and *HY5-HOMOLOG* (*HYH*) (Cloix and Jenkins, 2008); the positive skotomorphogenesis regulator *SUPPRESSOR OF PHYA-105 1* (*SPA1*) (Bourbousse et al., 2012); the *EARLY LIGHT-INDUCIBLE PROTEIN 1* (*ELIP1*) (Cloix and Jenkins, 2008); and the circadian clock genes *CIRCADIAN CLOCK ASSOCIATED 1* (*CCA1*), *LATE ELONGATED HYPOCOTYL* (*LHY*), *TIMING OF CAB EXPRESSION 1* (*TOC1*), *LUX ARRHYTHMO* (*LUX*), *EARLY FLOWERING 4* (*ELF4*), *PSEUDO RESPONSE REGULATOR 7* (*PRR7*) and *PRR9* (Hemmes et al., 2012; Himanen et al., 2012; Malapeira et al., 2012).

---

[1]Department of Plant Biotechnology and Bioinformatics, Ghent University, 9052 Ghent, Belgium. [2]VIB Center for Plant Systems Biology, 9052 Ghent, Belgium. [3]Department of Physiology, Laboratory of Functional Plant Biology, Ghent University, 9000 Ghent, Belgium. [4]Center for Research in AgriGenomics (CRAG), Consortium CSIC-IRTA-UAB-UB, 08193 Barcelona, Spain.
[*]Present address: Department of Genetics, Faculty of Biology and Animal Sciences, Wroclaw University of Environmental and Life Sciences, ul. Kozuchowska 7, 51-631 Wroclaw, Poland.

[‡]Author for correspondence (mieke.vanlijsebettens@psb.ugent.be)

Received 14 March 2017; Accepted 10 July 2017

Here, we show that Elongator regulates seedling development in darkness and light via a growth-regulatory network of genes that converge on cell wall biogenesis and positive photomorphogenesis factors, some of which are targeted by Elongator HAT activity specifically in darkness, suggesting target gene selection.

RESULTS

Phenotypes of the *elo* seedlings in darkness and light

Narrow, elongated and hyponastic leaves and petioles of *elo* mutants resemble those of photoreceptor mutants (Fig. S1A), suggesting that Elongator plays a role in the light response. Therefore, we investigated the role of Elongator in early *Arabidopsis* development in darkness or light (during etiolation or de-etiolation, respectively) by scoring hypocotyl elongation and apical hook formation, two characteristics of seedling growth that differ between the skoto- and photomorphogenetic developmental programs. Seeds of *elo3-6* and Col-0 (wild type) were sown, stratified for 48 h, illuminated for 6 h in white light to induce germination, and transferred either to darkness or to red, far-red or blue light. Representative seedling phenotypes are shown at 4 days after germination (DAG) (Fig. 1A). The hypocotyl length and seedling morphology was compared between the *elo3-6* mutant and Col-0 control every day between 3 and 7 DAG (Fig. 1A,B; Fig. S1B). Darkness-grown *elo3-6* seedlings had shorter hypocotyls than Col-0 seedlings (Fig. 1B), but cotyledons and apical hooks were similar (Fig. 1A; Fig. S1B), indicating that the mutation affected only hypocotyl growth. The hypocotyl length difference between Col-0 and *elo3-6* seedlings was maximal at 3 DAG (0.55 cm and 0.33 cm, respectively) (Fig. 1B). At 5 DAG, hypocotyl elongation nearly stopped for Col-0, whereas *elo3-6* hypocotyls still elongated, ultimately reaching lengths similar to those of the wild types at 7 DAG (Fig. 1B).

The *elo3-6* seedlings grown in red, far-red or blue light had reduced de-etiolation, visible as longer hypocotyls between 3 and 7 DAG (Fig. 1B), reduced cotyledon expansion and hyponastic

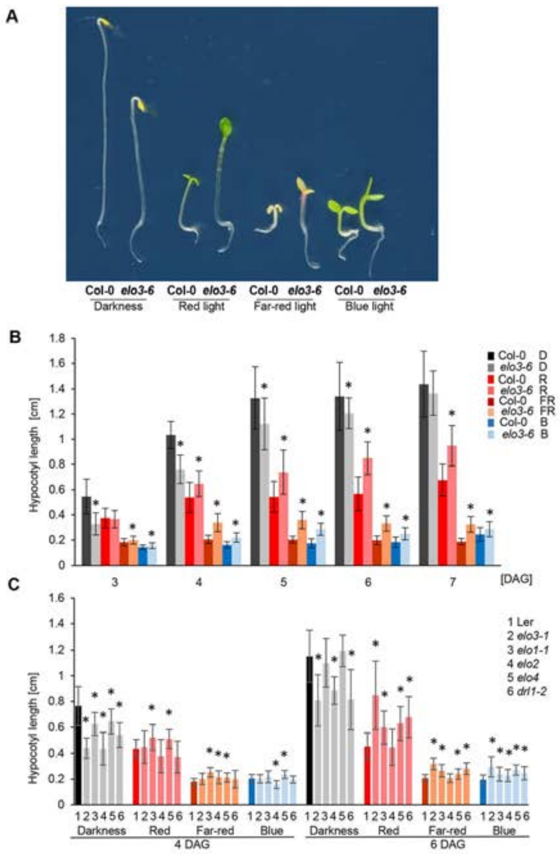

Fig. 1. Phenotypes of *elo* seedlings grown in darkness or under different light conditions. (A) Representative seedlings germinated and grown on half-strength MS medium for 4 days in darkness or under continuous monochromatic light of different wavelengths. (B) Hypocotyl lengths of Col-0 and *elo3-6* seedlings grown in darkness (D) or under continuous red (R), far-red (FR) and blue (B) light. (C) Hypocotyl lengths of mutants of different Elongator subunits grown on half-strength MS medium in darkness or under continuous monochromatic light of different wavelengths. Bars represent mean hypocotyl length of 25 seedlings (mean±s.d.). Differences between mutant and wild type were statistically analyzed with an unpaired two-tailed Student's *t*-test; $^{*}P<0.05$.

growth of the cotyledons (Fig. 1A; Fig. S1B), showing that the mutant is hyposensitive to all light qualities. Light inhibited hypocotyl elongation in the Col-0 seedlings already at 3 or 4 DAG, whereas hypocotyls elongated until 5 to 7 DAG in the *elo3-6* mutant, depending on the light quality (Fig. 1B).

The seedling phenotypes of the *elo3-1* Landsberg *erecta* (Ler) mutant grown in darkness, red, far-red or blue light were assessed at 4 and 6 DAG relative to the Ler control. Alterations were comparable to those of the *elo3-6* Col-0 allele (Fig. 1C), confirming that ELP3 regulates hypocotyl growth in darkness and in light. Hypocotyl lengths of the *elo1-1* (mutation in the accessory subunit *ELP4* gene), *elo2* (the core subunit *ELP1* gene), *elo4/drl1-4* and *drl1-2* (the Elongator interactor *DRL1/ELO4* gene) mutants, and the wild-type Ler were assayed at 4 and 6 DAG. Results were similar to those obtained for the *elo3-1* and *elo3-6* mutants (Fig. 1C), suggesting that the Elongator as an integral complex regulates hypocotyl elongation in darkness and in different light conditions in *Arabidopsis*.

Genetic interactions between Elongator and light-dependent receptors and regulators for hypocotyl growth

To examine the role of Elongator in the regulation of hypocotyl growth, the *elo3-1* (Ler) or *elo3-6* (Col-0) mutants were used as proxy for the Elongator complex and combined with the *phyB-1*, *phyA-201*, *hfr1-101* and *pif3-3 pif4-1* mutants in light-dependent receptors and regulators. Hypocotyl length was compared between the control, the parental lines and their double or triple mutant combinations grown in darkness or in red or far-red light at 4 and 6 DAG (Fig. 2).

The *phyB-1* (Fig. 2A) and *phyA-201* (Fig. 2B) mutants had significantly longer hypocotyls than the Ler control in darkness and light, because a decrease in active phytochrome molecules results in increased levels of PHYTOCHROME INTERACTING FACTORS (PIFs), which stimulate cell elongation (Leivar et al., 2008a,b). Hypocotyl lengths of double mutants combining *phyB-1* or *phyA-201* with *elo3-1* were significantly longer than those of *elo3-1*, but shorter than those of *phy* single mutants (Fig. 2A,B). This intermediate phenotype probably results from the additive effect of the *phyB-1* or *phyA-201* mutations, leading to increased hypocotyl elongation (comparable to the effect of darkness on the wild type), and the *elo3-1* mutation that disables hypocotyl elongation under such conditions. Therefore, the deficit of Elongator results in two defects leading to opposite changes in hypocotyl growth. First, the *elo3-1* mutant has decreased light sensitivity, resulting in longer hypocotyls in light-grown seedlings and, second, it grows more slowly in conditions of strongly enhanced cell elongation, such as darkness or the *phy* background. These results confirm that Elongator is indispensable for the light response and for the fast growth stimulation that occurs in darkness or upon *phy* mutation.

The hypocotyl length of the *elo3-6* mutant grown in darkness was reduced more than that of the *pif3-3 pif4-2* mutant compared to the Col-0 control (Fig. 2C), indicating that Elongator regulates hypocotyl growth via factors different or additional to PIF3 and PIF4. The combination of *elo3-6* and *pif3-3 pif4-2* mutations in the triple mutant resulted in only slightly shorter hypocotyls than *elo3-6*, suggesting that the PIF pathway positively regulating hypocotyl elongation could already have been downregulated in *elo3-6* in darkness. Therefore, in darkness, Elongator might control hypocotyl elongation via PIFs and other pathways. In red light, the hypocotyl length of *pif3-3 pif4-2* was significantly shorter than that of the Col-0 control, whereas it was intermediate in the *elo3-6 pif3-3 pif4-2* triple mutant compared with its parental lines. This effect was a result of the additive effect of mutations inversely regulating hypocotyl length in red light. These findings suggest that the PIF pathway is not affected by Elongator during growth in red light.

The *hfr1-101* mutant had significantly longer hypocotyls than the Col-0 control in darkness, indicating that HFR1 (LONG

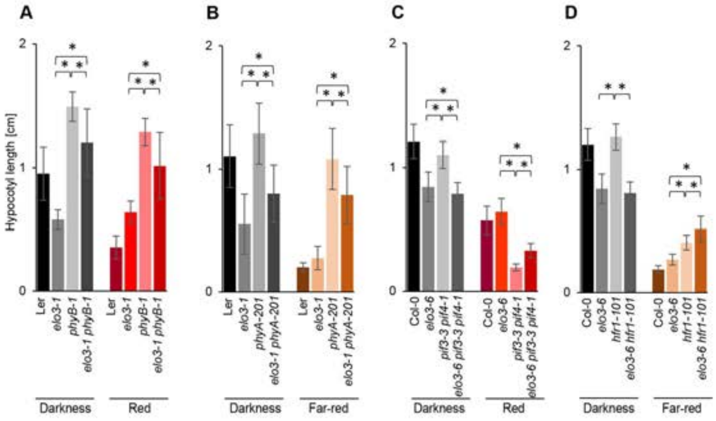

Fig. 2. Genetic interactions for hypocotyl growth between Elongator and phyA, phyB, PIF or HFR1. (A–D) Seedlings of *Arabidopsis* Ler (A,B) or Col-0 (C,D) wild types, and *elo3-1* (A,B), *elo3-6* (C,D), *phyB1* and *elo3-1 phyB-1* (A), *phyA-201* and *elo3-1 phyA-201* (B), *pif3-3 pif4-1* and *elo3-6 pif3-3 pif4-1* (C), and *hfr1-101* and *elo3-6 hfr1-101* (D) mutants were grown for 4 days on half-strength MS medium without sucrose in darkness, continuous red or far-red light. Hypocotyl lengths were quantified. Error bars represent mean values of hypocotyl length of 25 seedlings with standard deviation (mean±s.d.). Differences between genotypes were statistically analyzed with an unpaired two-tailed Student's *t*-test; **P*<0.05. Differences in hypocotyl length between single, double or triple mutants and their respective wild types were always statistically significant and therefore not indicated in the graphs. The experiment was repeated twice.

HYPOCOTYL IN FAR-RED 1, a positive photomorphogenesis regulator and suppressor of PIF action) is active in the absence of light and counteracts exaggerated hypocotyl elongation (Fig. 2D). The *hfr1-101* mutation did not increase the hypocotyl elongation of *elo3-6* in the *elo3-6 hfr1-101* double mutant in darkness, indicating that Elongator and HFR1 are involved in the same pathway regulating hypocotyl elongation in darkness and that Elongator is located upstream of HFR1. In far-red light, hypocotyls of the *elo3-6* and *hfr1-101* mutants were longer than those of Col-0, and the *elo3-6 hfr1-101* double mutant had hypocotyls longer than those of both parents, indicating a synergistic interaction between Elongator and HFR1 in hypocotyl elongation. This result suggests that in far-red light, in contrast to darkness, the ELO3 and HFR1 activities converge on the same process of hypocotyl elongation, leading to a dramatic elongation of the double-mutant hypocotyl.

In conclusion, double-mutant analyses show that Elongator is required for fast hypocotyl elongation in darkness and that this Elongator function is involved in growth-stimulating mechanisms other than the PIF pathway. Under light conditions, Elongator promotes inhibition of hypocotyl growth by acting in far-red light via an HFR1-interacting pathway.

The *elo3-6* mutant transcriptome in darkness

The gene regulatory network underlying the hypocotyl elongation phenotype of *elo3-6* was compared with that of Col-0 in the microarray dataset of 4-day-old darkness-grown seedlings: 2489 genes were downregulated and 2533 genes were upregulated in the mutant, at $-0.5 \geq \log2\mathrm{FC} \geq 0.5$, $P<0.05$ (NCBI, Gene Expression Omnibus, accession number GSE42053).

Upregulated genes in *elo3-6* clustered in two large Gene Ontology (GO) categories (Table S1), i.e. 'Response to stimuli' (defense response genes and genes induced by light, cold, osmotic stress, oxidative stress, water, desiccation, salt, carbohydrates, metal ions, hormones and other organisms) and 'Metabolic process' (genes related to catabolism of carbohydrate, coding for enzymes driving glycolysis, pentose phosphate pathway, TCA cycle, starch breakdown, photorespiration and Calvin cycle, and genes involved in biosynthesis of amino acids, lipids, nucleotides, gibberellins and flavones). The GO category 'Defense response' contains 140 genes, including those encoding important defense regulators and showing moderate (maximally two- to threefold) upregulation. phytoalexin-deficient 4 (PAD4) is a component of basal immunity against virulent pathogens and also contributes to effector-triggered immunity and systemic acquired resistance (Louis et al., 2012). PAD3/CYP71B15 catalyzes biosynthesis of camalexin, determining elicitor-induced resistance against fungal pathogens (Ferrari et al., 2007); its upregulated transcripts are markers for camalexin biosynthesis (Prince et al., 2014). Cytochrome P450s (CYP79B2 and CYP79B3) are involved in tryptophan metabolism and biosynthesis of pathogen defense components. PENETRATION 3 (PEN3) plays a role in the focal immune response and response to fungal and bacterial pathogens and is a marker of plant–pathogen interaction (Xin et al., 2013). Two ELICITOR PEPTIDE PRECURSORs (PROPEP2 and 3) are massively upregulated following pathogen challenges and recognized by PERP1/PERP2 receptors of defense signaling. Upregulation of GLYCERALDEHYDE-3-PHOSPHATE DEHYDROGENASE C SUBUNIT 1 (GAPC1) enhances glycolysis, providing ATP and pyruvate (reactive oxygen species scavenger) for plants undergoing immune response (Henry et al., 2015). Other genes with a confirmed positive effect on plant immunity were also upregulated in *elo3-6*: *AZELAIC ACID INDUCED 1* (*AZI1*), *LONG-CHAIN ACYL-COA SYNTHETASE 2* (*LACS2*), *ENHANCED DISEASE SUSCEPTIBILITY 5* (*EDS5*), *GRETCHEN HAGEN 3.12* (*GH3.12*), *ARABIDOPSIS THALIANA SULFOTRANSFERASE 1* (*ATSOT1*), *ACTIVATED DISEASE RESISTANCE 1* (*ADR1*) and *ADR1-LIKE 1*. Some of the genes involved in carbohydrates catabolism together with genes coding for subunits of the mitochondrial electron transport chain and ATP synthase were grouped in the overrepresented GO category 'Energy derivation by oxidation of organic compounds'. Two smaller GO categories of upregulated genes were identified: 'Cell wall organization or biogenesis', containing genes related to defense and/or cell wall firmness (chitinases, pectin methylesterases), and 'Localization', including the genes coding for transporters of sugars, amino acids, proteins, lipids and metal ions.

In summary, the set of genes upregulated in the *elo3-6* mutant in darkness matches transcriptome profiles typical for the plant response to pathogens (Rojas et al., 2014). The upregulation of defense-related pathways is followed by the upregulation of primary metabolism genes involved in energy production (carbohydrates catabolism, mitochondrial electron transport, nucleotides and amino acid biosynthesis) or synthesis of signaling molecules (carbohydrates and lipids). The upregulation of defense-related genes results in energy deprivation, which activates compensatory downregulation of other pathways and ultimately leads to growth deceleration, as observed in the *elo3-6* mutant in darkness.

GO categories with significantly downregulated genes were 'Response to light stimulus', 'Response to hormone stimulus', 'Cell wall biogenesis', 'Regulation of transcription', 'Regulation of developmental processes' and 'Regulation of cell cycle', with a large proportion of transcription factors within each GO category. From the downregulated GO categories, a growth-controlling network was deduced that consisted of four main hubs: circadian clock, regulators of skoto- and photomorphogenesis, different hormone response pathways, and primary and secondary cell wall biogenesis (Table S2). Downregulated genes encoded both positive upstream regulators and direct downstream effectors of growth, in line with the delayed hypocotyl elongation observed for *elo3-6* seedlings grown in darkness. Some of these pathways were functionally analyzed by means of reporter gene constructs or hypocotyl growth experiments upon treatment.

Circadian clock

The circadian clock is one of the four main hubs of the growth-regulatory network downregulated in *elo3-6* in darkness. Seven genes from this hub (*LHY*, *CCA1*, *RVE8*, *CIR1*, *LCL1/RVE4*, *RVE2* and *PRR8*) showed decreased expression levels in *elo3-6* in darkness (Table S2; Fig. 3A). To check whether downregulation of two key circadian clock components (CCA1 and LHY) contribute to the *elo* phenotype, we assayed the hypocotyl length of the *lhy-21 cca1-11*, *cca1-1lhy RNAi* and *lhy-21* mutants together with their wild type, Wassilewskija (Ws). In darkness, similarly to the *elo* mutants, the hypocotyls of the circadian clock-regulatory mutants were significantly shorter than those of the wild type at 2 and 4 DAG, but the apical hooks remained closed and cotyledons did not expand (Fig. 3B). The effects in the *lhy-21 cca1-11* double and the *lhy-21* single mutants were comparable, indicating that mutation of *LHY* is sufficient to cause decreased hypocotyl length; therefore, lowered expression of the *LHY* gene in the *elo* mutant might contribute to the observed short hypocotyl phenotype in darkness.

Next, the diurnal expression profiles of the *CCA1* and *LHY* genes were examined in wild-type and *elo3-6* mutant plants synchronized under short-day conditions. Samples were taken every 4 h during

Journal of Cell Science (2018) 131, jcs203927. doi:10.1242/jcs.203927

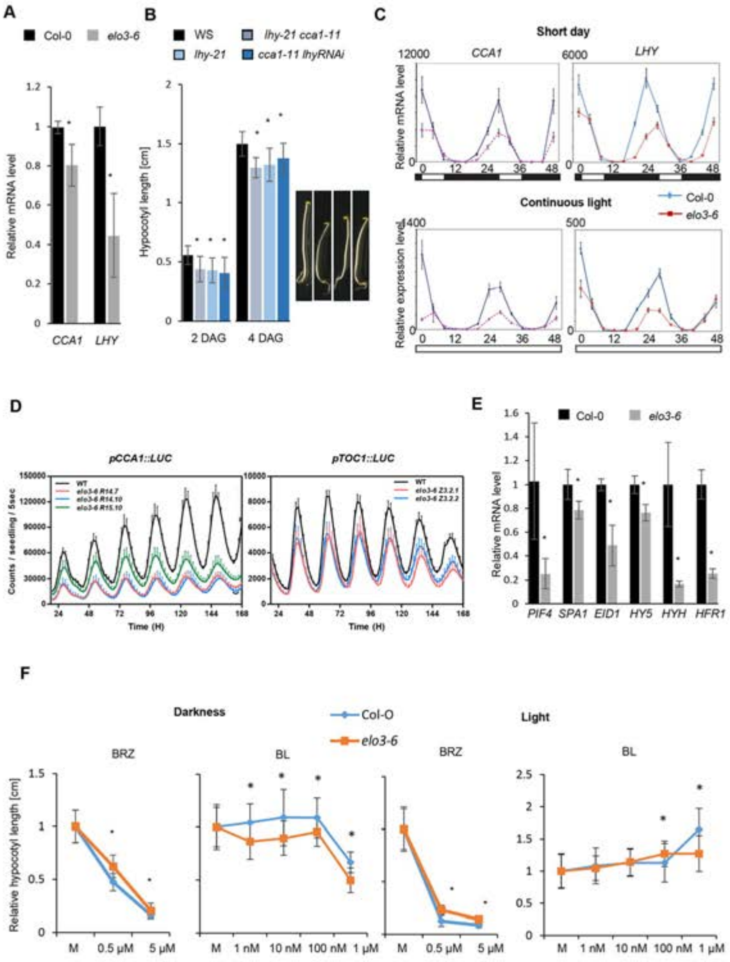

Fig. 3. Expression of circadian clock and skoto- and photomorphogenesis regulatory genes, circadian clock assays and response to BL and BRZ of the *elo3-6* mutant. (A) Relative expression levels of *CCA1* and *LHY* genes in seedlings of *elo3-6* and Col-0 wild type. (B) Hypocotyl length of single and double mutants of *CCA1* and *LHY* genes (*lhy-21*, *lhy-21 cca1-11* and *cca1-11 lhyRNAi*) compared with Ws wild type in darkness. Thirty seedlings were photographed and hypocotyls were measured with ImageJ software. (C) qPCR assessing relative expression levels of *CCA1* and *LHY* genes in the Col-0 and *elo3-6* seedlings grown for 12 days in a short-day photoperiod and analyzed for 48 h in short-day conditions or continuous white light with samples taken every 4 h. White and black boxes below the graphs indicate alternation of light and dark, respectively. (D) Bioluminescence of *pCCA1::LUC* and *pTOC1::LUC* reporter lines measured in the Col-0 wild type and *elo3-6* mutant (R14.7, R14.10 and R15.10 lines for *pCCA1*; Z3.2.1 and Z3.2.2 lines for *pTOC1*) in a time-course analysis under constant white light conditions. (E) Relative expression levels of positive regulators of skotomorphogenesis (*PIF4*, *SPA1* and *EID1*) and positive regulators of photomorphogenesis (*HY5*, *HYH* and *HFR1*) in darkness. (F) Relative hypocotyl lengths of the Col-0 wild type and *elo3-6* seedlings grown in constant darkness or white light in the absence (mock control M) or presence of indicated concentrations of BL or BRZ. In A, E and F, 4-day-old seedlings grown on half-strength MS medium were analyzed. In A and E, the relative expression levels were detected by qPCR with six biological replicates and *PP2A* and *SAND* genes as reference genes (Czechowski et al., 2005). The experiments were repeated twice. Bars represent mean±s.d. In B and F, mean values of hypocotyl length of at least 25 seedlings are presented. Differences between mutant and wild type were statistically analyzed with an unpaired two-tailed Student's *t*-test; **P*<0.05. BRZ, brassinazole; BL, brassinolide.

48 h under short-day or under continuous light conditions following the synchronization. The diurnal fluctuations of the *CCA1* and *LHY* transcripts in the *elo3-6* mutant followed a similar oscillatory trend to that observed in wild-type plants, but mRNA accumulation was clearly reduced in the *elo3-6* mutant under both conditions (Fig. 3C). These results indicate that functionality of ELO3 is important for proper amplitude of *CCA1* and *LHY* expression.

The downregulation of circadian clock components was further examined by monitoring bioluminescence of reporter lines expressing the *LUCIFERASE* (*LUC*) gene fused to the *CCA1* or *TOC1* promoters (*pCCA1::LUC* or *pTOC1::LUC*) in *elo3-6*. Our results show that the amplitude of the circadian activity for both promoters was decreased in the *elo3-6* mutant compared with the wild type and that the circadian period was not affected by the *elo3-6* mutation (Fig. 3D). These results are consistent with the decreased *CCA1* and *LHY* expression observed by quantitative polymerase chain reaction (qPCR) analysis (Fig. 3C) and suggest that altered clock function by mis-expression of oscillator components might contribute to the *elo3* hypocotyl phenotype.

Regulators of skoto- and photomorphogenesis

PHYTOCHROME INTERACTING FACTOR 4 (*PIF4*) and genes encoding other positive skotomorphogenesis regulators, such as *SPA1* and *EMPFINDLICHER IM DUNKELROTEN LICHT 1* (*EID1*) (Fig. 3E), and B-box zinc finger proteins *BBX24* and *BBX25* (Table S2) showed significantly lower expression in the *elo3-6* mutant. Downregulation of such factors reduced hypocotyl elongation, as shown in *pif4* and multiple *pif* mutants (Leivar et al., 2012), *spa1 det1-1* (Nixdorf and Hoecker, 2010), *bbx24 cop1-4* and *bbx25 cop1-4* (Gangappa et al., 2013), and might contribute to the reduced hypocotyl elongation in *elo3-6* in darkness. PIF4 is the key player among factors positively regulating hypocotyl growth. A reduced relative mRNA level of *PIF4* in *elo3-6* in darkness is in line with genetic interactions between PIF4 and Elongator observed in the triple *elo3-6 pif3-3 pif4-2* mutant. Indeed, the genes downregulated in the *elo3-6* transcriptome in darkness largely overlapped with PIF4 targets identified by chromatin immunoprecipitation-sequencing (ChIP-seq) in 5-day-old etiolated seedlings (Oh et al., 2014). There was 41% overlap in the GO category ‘Response to hormones’, 38% in ‘Response to light’, 36% in ‘Secondary cell wall biogenesis’ and 23% in ‘Regulation of transcription’.

In addition to genes of positive skotomorphogenesis regulators (including *PIF4*), the positive photomorphogenesis regulator genes *HY5*, *HYH*, *HFR1* (Fig. 3E) and *HY1* (Table S2) were also downregulated in the *elo3-6* mutant in darkness. Decreased expression of these regulators leads to hypocotyl elongation and prevents opening of the apical hook and cotyledon expansion. Considering that positive regulators of skoto- and photomorphogenesis are known to interact and suppress each other's phenotypes (Ang and Deng, 1994; Xu et al., 2014; Srivastava et al., 2015), coincidental downregulation of positive regulators of both skoto- and photomorphogenesis in the *elo3-6* mutant could blend into the combinatorial phenotype of a moderately shorter hypocotyl and a closed apical hook. This mechanism is supported by the hypocotyl length of the *elo3-6 hfr1-101* double mutant, which is the same as in *elo3-6*, indicating that introduction of the *hfr1* mutation into *elo3-6* does not result in additional hypocotyl elongation because *hfr1* expression is decreased by the *elo3-6* mutation.

Hormone response

Downregulated genes of the growth-regulatory network are related to hormonal pathways (Table S2), in particular those encoding the brassinosteroid (BR) pathway components. These genes were well represented and included three enzymes crucial for BR synthesis (*CPD*, *DWF4* and *CYP90D1*), the signaling component *BSU1*, and five genes (*VH1*, *MERI5*, *THE1*, *TCH4*, and *IBH1*) encoding response proteins related to control of cell elongation via cell wall modification. To check whether a defective BR pathway contributes to the reduced hypocotyl elongation in *elo3-6*, we tested mutant sensitivity to the BR biosynthesis inhibitor brassinazole (BRZ) and exogenous brassinolide (BL) by means of the hypocotyl elongation assay in darkness. Both Col-0 and *elo3-6* responded with reduced hypocotyl elongation to 0.5 and 5 µM BRZ, but the decrease in hypocotyl length was smaller in the mutant (Fig. 3F). This result hints at BRZ hyposensitivity and reduced activity of BR biosynthesis enzymes, in line with their decreased expression in *elo3*-6 compared with Col-0. BL treatment did not reverse the short hypocotyl phenotype of *elo3-6*, indicating that BR deficiency caused by reduced biosynthesis gene expression is not the primary reason for the short hypocotyl mutant phenotype. This *elo3-6* mutant showed moderate hypersensitivity to BL, with a decreased hypocotyl length even at the lowest BL concentration (1 nM). In the wild type, only the highest concentration of BL (1 µM) decreased the hypocotyl length (Fig. 3F). BRZ hyposensitivity and BL hypersensitivity of *elo3-6* resembled those of the *bzr1-1D* mutant, which contains increased amounts of the BRASSINAZOLE-RESISTANT 1 (BZR1) transcription factor, activated by BRs, which dimerizes with PIF4 to promote cell elongation in etiolated hypocotyls (Wang et al., 2002). Like the *bzr1-1D* mutant, *elo3-6* might also have increased levels of free BZR1 caused by downregulation of PIF4 and, hence, a reduced amount of PIF4-BZR1 dimers and retarded cell elongation. High BZR1 levels in *elo3-6* were suggested by fewer transcripts of BR biosynthesis enzymes, implying feedback inhibition as also detected in *bzr1-1D* (Wang et al., 2002). BRZ and BL sensitivities were modestly affected in *elo3-6*, suggesting that malfunction of the BR pathway contributes only partially to the short *elo3-6* hypocotyls. As indicated by the transcriptome, other growth-related hormonal pathways that might contribute to defective hypocotyl elongation are downregulated in *elo3-6*. For example, downregulation of *PIF4* could affect the auxin responses, because PIF4 stimulates expression of the auxin biosynthetic gene *YUCCA8* (Sun et al., 2012), whose expression is reduced in *elo3-6* (Table S2).

Cell wall biogenesis

Hormone pathways regulate growth by convergence to the cell wall biogenesis pathways. In the *elo3-6* mutant, more than 40 genes related to cell wall formation were downregulated in darkness; these included three genes (*IRX9*, *IRX10*, *IRX14-L*) encoding enzymes of xylan biosynthesis, which are involved in the generation of both primary and secondary cell walls. The *irx9*, *irx10* and *irx14-L* mutants are similar to *elo3-6* in that they have moderately shorter hypocotyls than the wild type in darkness and no opened cotyledons (Faik et al., 2014). In the *elo3-6* mutant, genes regulating secondary cell wall biogenesis are downregulated. These genes include xylem differentiation factors (*ATHB15*, *REV*, *PHV*); NAC and MYB factors (*AtC3H14*, *AtC3H15*, *BLH6*, *MYB42*, *MYB43*, *MYB46*, *MYB52*, *MYB54*, *MYB83*, *MYB85*, *MYB103*, *NAC075*, *XND1*, *SND2*, *VND2* to *VND6*), representing all three tiers of the transcription factor cascade (Hussey et al., 2013); and enzymes of cellulose (*CESA4*, *CESA7*, *CESA8* and *IRX6*/*COBL4*), hemicellulose (*IRX8*, *IRX9*, *IRX10*, *IRX14L*, *FRA8* and *GUX1*) and lignin (*LAC4*, *LAC10* and *LAC17*) synthesis (Table S2).

H3K14 acetylation activity of Elongator at *LHY*, *HYH* and *HFR1* in darkness

Expression of *CCA1* and *LHY* correlates with the level of the histone H3 modifications, H3K4Me2 and H3K9Ac (Ni et al., 2009). Similarly, some of the light- and/or darkness-related regulatory genes are controlled by histone modifications, suggesting that they might also be direct targets of Elongator HAT activity. Hence, ChIP-qPCR was carried out on chromatin of *elo3-6* and Col-0 4-day-old seedlings germinated in darkness. The analysis used antibodies against acetylated histone H3K14 and primers for promoter and coding regions of the circadian clock genes *CCA1* and *LHY* (Fig. 4A,B), and of the regulatory genes *PIF4* (Fig. 4C), *HYH*, *HFR1* (Fig. 4D,E), *SPA1*, *EID1* and *HY5*. Results were normalized versus both input and the *ACTIN2* gene. To check whether Elongator targets downstream transcription factors related to hormone and cell wall pathways, ChIP-qPCR was done on the *CPD*, *DWF4*, *CYP90D1* and *BSU1* genes from the BR pathway; the *CGA* and *GNC* cytokinin response genes; the secondary cell wall regulator-encoding genes *PHAV*, *REV*, *VND4*, *MYB46*, *MYB83* and *MYB103*; and the structural genes *CESA4*, *CESA7* and *CESA8* (Table S2).

Of the 20 analyzed genes, H3K14 acetylation was only significantly decreased in the coding regions of the *LHY*, *HYH* and *HFR1* genes in *elo3-6* seedlings. The results show that *LHY*, *HYH* and *HFR1* are direct targets of Elongator HAT activity in darkness (Fig. 4B,D,E) and suggest that Elongator provides selective epigenetic control to a few of the highest order transcription factors. Identification of *LHY* as a target for the histone H3K14 acetylating activity of Elongator, together with decreased expression of *LHY* in *elo3-6* and similar hypocotyl phenotypes of *lhy* and *elo3-6* mutants in darkness, indicate that epigenetic control of *LHY* expression via Elongator HAT activity might contribute to hypocotyl growth regulation. Targeting of *HYH* and *HFR1* by Elongator in darkness suggests a fine-tuning mechanism of hypocotyl growth regulation, whereby positive regulators of photomorphogenesis prevent exaggerated elongation. None of the positive skotomorphogenesis regulators showing decreased expression in *elo3-6* was targeted by Elongator HAT activity, as illustrated for *PIF4* (Fig. 4C). These factors might be regulated via other activities of Elongator or via HAT regulation of the higher-order regulators. For example, because *PIF4* is controlled by the circadian clock (Yamashino et al., 2003; Kidokoro et al., 2009), it is possible that the downregulation of *PIF4* in the *elo3-6* mutant is a consequence of the downregulation of *CCA1* and Elongator target *LHY*.

Gene expression in the *elo3-6* mutant in light

Expression levels of genes encoding the main regulators of skoto- and photomorphogenesis, the light response, cell wall-related biosynthesis and brassinosteroid biosynthesis were assayed by qPCR in 4-day-old *elo3-6* and Col-0 seedlings grown in continuous red, far-red or blue light. The genes encoding positive regulators of photomorphogenesis (*HY5*, *HYH* and *HFR1*) and skotomorphogenesis (*EID1*) were downregulated under at least one light condition. By contrast, *PIF4*, which is downregulated in darkness, was upregulated in far-red and blue light (Fig. 5A). The *HY5* gene, encoding the main positive photomorphogenesis regulator, was downregulated in all light qualities, but *HYH* and *HFR1*, encoding two HY5 interactors, were downregulated in red light. *HYH*, which plays an important role in blue light photomorphogenesis, also showed lower transcript levels in blue light. Reduced expression of these regulators, which cooperate in the inhibition of hypocotyl elongation and in the promotion of apical hook opening and cotyledon growth, was consistent with the increased hypocotyl length and unexpanded and hyponastic cotyledons of the light-grown *elo3-6* seedlings. *HY5* downregulation in *elo3-6* coincided with extreme upregulation of *WALL-ASSOCIATED KINASE 1* (*WAK1*), moderate upregulation of *INCREASED SIZE EXCLUSION LIMIT 2* (*ISE1*) (Fig. 5A), and no difference in expression of *ARF2*, *UBP15*, *ATHB-2*, *ATASE2*, *APG3* and *MSL3*, which are all HY5 target genes (Zhang et al., 2011). *WAK1* is negatively regulated by HY5 (Zhang et al., 2011), plays a positive role in cell elongation (Lally et al., 2001) and is the receptor of oligogalacturonides, which are cell wall-integrity signaling components that induce defense responses. High *WAK1* expression

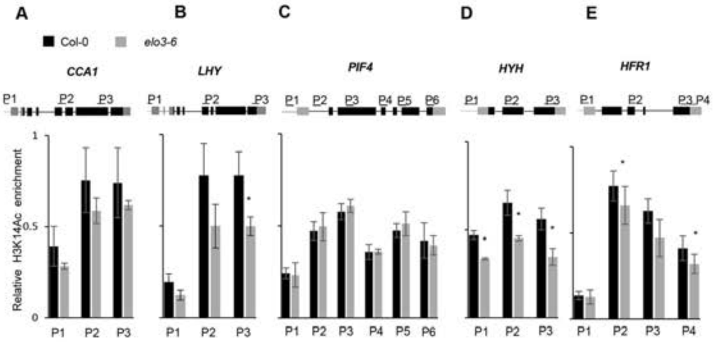

Fig. 4. Histone acetylation of circadian clock and skoto- and photomorphogenesis regulatory genes in the *elo3-6* mutant in darkness. Histone H3K14 acetylation levels in the *CCA1*, *LHY*, *PIF4*, *HYH* and *HFR1* promoter and coding regions. The relative H3K14Ac enrichment was established with antibodies against H3K14Ac for ChIP and primers (P1–P6, Table S5), amplifying fragments of promoter and coding sequences for qPCR. Results were normalized versus input and the actin reference gene. The experiment was repeated four times (*LHY* and *HYH*) or twice (*CCA1*, *PIF4* and *HY5*) with four biological replicates each time. Four-day-old seedlings grown in darkness on half-strength MS medium were analyzed. Bars represent mean±s.d. Differences between mutant and wild type were statistically analyzed with an unpaired two-tailed Student's *t*-test; *$P<0.05$.

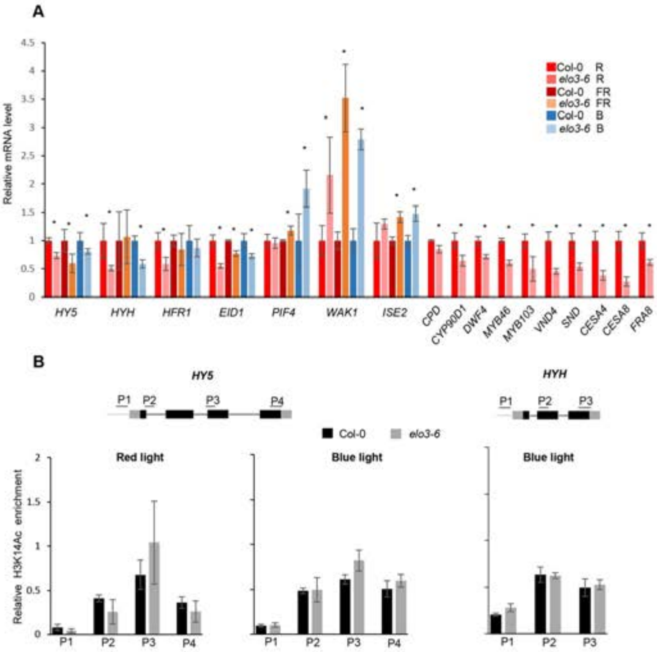

Fig. 5. Expression of genes encoding photomorphogenesis regulators and cell wall biogenesis genes, and histone acetylation of *HY5* and *HYH* in monochromatic light. (A) Relative expression levels of indicated genes determined by qPCR in 4-day-old *elo3-6* and Col-0 seedlings grown under continuous monochromatic light. Expression was normalized using *PP2A* and *SAND* as reference genes. (B) Histone H3K14 acetylation in the *HY5* and *HYH* promoter and coding regions. The relative H3K14Ac enrichment was established with antibodies against H3K14Ac for ChIP and primers (P1–P4, Table S5), amplifying fragments of promoter and coding sequences for qPCR. Results were normalized versus input and the actin reference gene. Average values of six (qPCR) or four (ChIP-qPCR) biological replicates are presented with standard deviation (mean ±s.d.). Differences between mutant and wild type were statistically analyzed with an unpaired two-tailed Student's *t*-test; **P*<0.05.

might contribute to enhanced hypocotyl elongation and/or immune response activation, in line with downregulation of secondary cell wall biogenesis genes under red light (Fig. 5A) (Miedes et al., 2014). Decreased expression of the BR biosynthesis genes *CPD*, *CYP90C11* and *DWFA2* in the *elo3-6* mutant under red light (Fig. 5A) might result from negative feedback regulation by free BZR1 proteins. Free BZR1 might overaccumulate in *elo3-6* because of lower *HY5* levels and, consequently, lower the formation of BZR1/HY5 dimers that suppress hypocotyl elongation (Li and He, 2016). Accordingly, *elo3-6* was hyposensitive to BL and BZR in light (Fig. 3F), confirming that BR signaling was affected in *elo3-6*.

ChIP-qPCR was applied to check whether Elongator promotes photomorphogenesis via histone H3K14 acetylation of the regulatory genes *HY5*, *HYH* and *HFR1* in light. Chromatin isolated from *elo3-6* and Col-0 seedlings grown for 4 days in red, far-red or blue light did not differ in histone acetylation, indicating that Elongator-mediated HAT activity did not target *HY5*, *HYH* (Fig. 5B) or *HFR1* in light. Thus, Elongator is necessary for the expression of *HY5*, *HYH* and *HFR1*, which encode the main photomorphogenesis regulators, and for the downstream pathways controlled by HY5 during photomorphogenesis, but not via Elongator HAT activity.

DISCUSSION

We show that the Elongator complex modulates hypocotyl growth and photomorphogenesis via the regulation of a growth-controlling network consisting of circadian clock regulators, skoto- and photomorphogenesis regulators, hormone pathways and cell wall biogenesis. The regulatory role of Elongator is supported by the hypocotyl phenotypes of *elo3-6* and *elo3-1* and growth-related mutants; identification of the *LHY*, *HYH* and *HFR1* regulators as direct targets of Elongator HAT activity; hormone sensitivity assays; *LUC* reporter gene activity in the *elo3-6* mutant background; and genetic interactions studies with skotomorphogenesis and light response regulators.

Elongator affects early growth in darkness and light through a growth-controlling network

Unlike de-etiolation mutants such as *cop1* and *pif*, which combine short hypocotyls with expanded cotyledons in darkness, *elo3-6* has a short hypocotyl although apical hook and cotyledon folding remain normal. Cotyledons expand in darkness in *cop1* because of high levels of HY5, HYH and/or HFR1; they also expand in multiple *pif* mutants, especially those including mutation in *PIF1*, which is the main cotyledon-folding suppressor in darkness (Leivar et al., 2012). Cotyledons of *elo3-6* do not expand in darkness, because the expression of *HY5*, *HYH* and *HFR1* is lowered and only *PIF4* is downregulated out of all *PIF*s. Hypocotyl phenotypes similar to those of *elo3-6* were observed in *lhy-21*, *lhy-21 cca1-11*, *cca1-11 lhyRNAi* (Fig. 3B), *pif4* (Leivar et al., 2012), and *irx9*, *irx10*, and *irx14-L* (Faik et al., 2014). These plants contain mutations in circadian clock and cell wall biogenesis genes, which are main hubs of the growth-controlling network downregulated in *elo3-6*, indicating that the *elo3-6* hypocotyl

Journal of Cell Science (2018) 131, jcs203927. doi:10.1242/jcs.203927

phenotype is the result of multiple reduced gene activities. This observation is in line with the network topology that consists of upstream regulatory transcription factor pathways converging on cell wall biogenesis and resulting in a cumulative repressing effect on hypocotyl growth. The importance of cell wall biosynthesis for growth and cell elongation has been demonstrated in mutants with impaired cell wall composition (Desnos et al., 1996; McCarthy et al., 2010; Faik et al., 2014). However, growth seems to be reduced in response to cell wall-integrity signaling that activates plant immune responses (Hématy et al., 2007), rather than inhibited directly by a physically weakened cell wall. Mutants defective in the MYB46 regulator of cell wall formation (Ramírez et al., 2011) or in CESA4, CESA7 and CESA8 cellulose synthase subunits required for secondary cell wall synthesis (Hernández-Blanco et al., 2007) activate the plant immune response, leading to growth attenuation (Rojas et al., 2014). Downregulation of over 40 cell wall-related genes (including *MYB46*, *CESA4*, *CESA7* and *CESA8*) and upregulation of defense response genes (including important key regulators) and metabolic genes involved in the plant immune response coincide in *elo3-6*; hence, the hypocotyl growth defects in this mutant might be a result of reduced cell wall biosynthesis and, eventually, activation of the plant immune response (Fig. 6).

Decreased pathogen resistance has been shown for the *elo2* mutant, confirming positive regulation of the plant immune response by Elongator via the targeting of genes encoding important components of the salicylic acid pathway (*NPR1*, *PR2*, *PR5*, *EDS1* and *PAD4*) (Wang et al., 2013) and the jasmonate/ethylene pathway (*WRKY33*, *ORA59* and *PDF1.2*) (Wang et al., 2015) for histone acetylation and/or DNA methylation. Elongator also controls the reactive oxygen species–salicylic acid amplification loop and targets important defense genes for histone acetylation, including the homolog *AtrbohD* that encodes the *Arabidopsis* respiratory burst oxidase, and the salicyclic acid biosynthesis gene *ISOCHORISMATE SYNTHASE1* (An et al., 2017). The incongruences between our data and the results of others (Wang et al., 2013) related to the role of Elongator in the immune response could correspond to different mutants (*elo3* versus *elo2*), diverse developmental stages, or different growth conditions applied in the studies. For example, delayed induction and lower expression of some defense genes (including *PAD4*) in the *elo2* mutant were observed only after pathogen infection, whereas basal

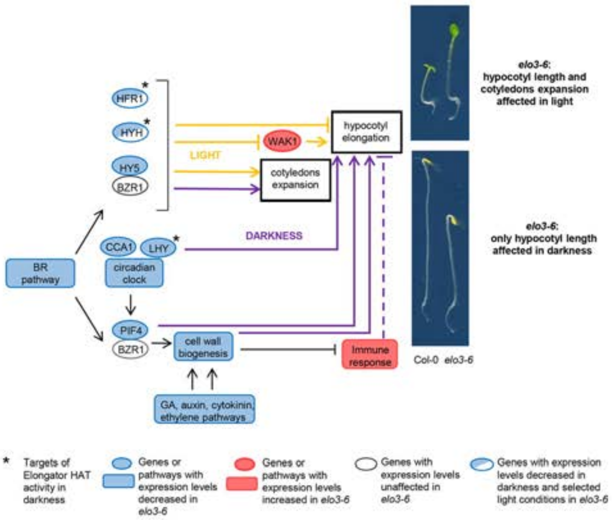
HFR1
HYH
HY5
BZR1
LIGHT
WAK1
hypocotyl elongation
cotyledons expansion
DARKNESS
CCA1
LHY
circadian clock
BR pathway
PIF4
BZR1
cell wall biogenesis
Immune response
GA, auxin, cytokinin, ethylene pathways
elo3-6: hypocotyl length and cotyledons expansion affected in light
elo3-6: only hypocotyl length affected in darkness
Col-0
elo3-6
* Targets of Elongator HAT activity in darkness
Genes or pathways with expression levels decreased in elo3-6
Genes or pathways with expression levels increased in elo3-6
Genes with expression levels unaffected in elo3-6
Genes with expression levels decreased in darkness and selected light conditions in elo3-6

Fig. 6. Model for Elongator transcriptional control of hypocotyl growth in darkness and photomorphogenesis. Elongator controls hypocotyl elongation via several pathways: elongation-suppressing pathways involving positive regulators of photomorphogenesis (HY5, HYH and HFR1) or immune response genes, and elongation-stimulating pathways including circadian clock, PIF4, hormone biosynthesis or signaling, and cell wall biogenesis. In darkness (purple arrows), downregulation of genes in pathways stimulating hypocotyl elongation and upregulation of immune response genes suppressing elongation prevail, resulting in a shorter hypocotyl of the *elo3-6* mutant. In light (yellow arrows), hypocotyl elongation is inhibited very early in the wild type, whereas elongation inhibition fails in the *elo3-6* mutant because of downregulation of positive photomorphogenesis regulators and strong upregulation of WAK1, which stimulates cell elongation and results in a longer hypocotyl. Elongator also regulates cotyledon expansion via positive regulators of photomorphogenesis. The *HY5* gene was downregulated under red, far-red and blue light (blue filling); *HYH* under red and blue light; and *HFR1* under red light only (blue-white filling). Expression of BR pathway and cell wall biogenesis genes was assayed in darkness and red light. Pictures present 4-day-old seedlings grown in darkness (lower panel) or in red light (upper panel). The asterisks indicate targets of Elongator HAT activity in darkness. Blue or red colors indicate, respectively, a lower or higher expression level of the given gene or pathway. Genes half-shaded with blue color have expression levels downregulated in darkness and selected light conditions. The expression level of *BZR1* is unaffected, as indicated by transparent circles. Downregulation of hypocotyl elongation by the immune response is represented by a dashed line because it is not clear whether downregulation of cell wall biogenesis-related genes affects hypocotyl elongation directly or via the immune response, as suggested by higher transcription of genes involved in the immune response in *elo3-6*.

expression was similar in the mutant and the wild type (Wang et al., 2013). Moderately increased expression of selected immunity pathways in *elo3-6* might result in growth inhibition, but does not necessarily trigger constitutive activation of plant defense pathways, which requires high levels of upregulation (usually in response to pathogen infection) to exceed the defense activation threshold (Kwon et al., 2009). Therefore, in addition to well-established direct positive regulation of the plant immune response, under some conditions Elongator might play an opposite and possibly indirect role as a positive regulator of cell wall-related genes. Elongator might contribute independently and inversely to different immune response pathways, and thus modulate the growth–defense balance (Hématy et al., 2007).

Alternatively, a negative role of Elongator in the plant response to wounding is suggested by the increased levels of jasmonic acid (JA), increased JA biogenesis and responsive gene expression levels (Nelissen et al., 2010), and induction of the jasmonate-controlled MYC2 transcriptional cascade (Wang et al., 2015) reported earlier for the *elo* mutants. The plant response to wounding, similar to the immune response, has a negative JA-mediated effect on growth. However, we did not find JA-related genes among those differentially regulated in *elo3-6* in our microarray dataset. Moreover, JA acts during skotomorphogenesis to reduce hypocotyl length, but also promotes cotyledon opening in etiolated seedlings (Zheng et al., 2017), resulting in the constitutively photomorphogenic phenotype. This is not the case for darkness-grown *elo3* seedlings, which are shorter but have normal apical hooks, arguing against the role of JA and wounding in the *elo3* phenotype.

Transcription-based model of the role of Elongator in early plant development

We propose a model for the role of Elongator in early plant development that elucidates why hypocotyl growth of *elo* mutants is slower in darkness but photomorphogenesis is defective in light, resulting in a longer hypocotyl and unexpanded cotyledons (Fig. 6). Elongator regulates hypocotyl elongation and cotyledon expansion by controlling cell wall biogenesis genes and positive photomorphogenesis regulators. Depending on the light conditions, one of the pathways becomes restrictive and Elongator promotes opposite growth behaviors.

In darkness, expression of the circadian clock regulator *LHY* and of the positive photomorphogenesis regulators *HFR1* and *HYH* is activated by Elongator-mediated, transcript elongation-facilitating histone acetylation. As shown by hypocotyl growth analysis of the *lhy-21*, *lhy-21 cca1-11* and *cca1-11 lhyRNAi* mutants, the circadian clock components LHY and CCA1 positively regulate hypocotyl elongation. One of the possible mechanisms of this regulation involves PIF4, which is controlled by the circadian clock (Nozue et al., 2007) at the transcriptional level and stimulates expression of genes involved in hypocotyl elongation. *LHY*, *CCA1* and *PIF4* genes are downregulated in darkness in *elo3-6* mutants, which affects the expression of many transcription factors, such as components of hormonal and cell wall biosynthesis pathways that partially slow down hypocotyl elongation via activation of the plant immune response (Hématy et al., 2007). A lower level of PIF4 reduces formation of complexes with the BZR1 transcription factor of the BR pathway and compromises induction of cell wall biogenesis genes (Lozano-Durán et al., 2013). In conclusion, in darkness, the *elo3-6* hypocotyl phenotype is determined by the combined effect of decreased levels of cell wall biogenesis genes, reduced expression of clock regulators and decreased expression of *HY5*, *HYH* and *HFR1*, consequently inhibiting hypocotyl elongation. The final phenotype of short hypocotyls indicates that the defect in cell wall biogenesis prevails. Low expression of *HY5*, *HYH* and *HFR1* also prevents cotyledon expansion in *elo3-6*.

Elongator is also required for light responses, because the genes of the major positive photomorphogenesis regulators *HY5*, *HYH* and *HFR1* are downregulated in *elo3-6* although, strikingly, their H3K14Ac levels are unaffected in light. The HAT activity of Elongator might be very dynamic and difficult to capture in a ChIP-qPCR assay using acetylated histone antibodies, which could explain the limited number of genes targeted for Elongator-mediated histone acetylation. In plants, the interaction between Elongator subunits and the SPT4/SPT5 transcript elongation complex (Van Lijsebettens et al., 2014) suggests that Elongator might affect RNAPII transcript elongation indirectly, next to its histone acetylation activity (Antosz et al., 2017). An alternative explanation is that, in light, another epigenetic activity of Elongator such as DNA demethylation (DeFraia et al., 2013; Wang et al., 2013) or processing of primary microRNAs (Fang et al., 2015) might be responsible for decreased expression of *HY5*, *HYH* and *HFR1*. In light, hypocotyl elongation is inhibited very early in wild-type seedlings by diverse factors including HY5, HYH and HFR1, possibly involving suppression of the cell elongation activity of WAK1 (Fig. 6B). In the *elo3-6* mutant, decreased expression of *HY5* leads to a higher accumulation of *WAK1* mRNA and induced hypocotyl elongation. On the other hand, upregulation of *WAK1* might trigger immune responses, as suggested by decreased levels of cell wall biogenesis genes, and might suppress hypocotyl elongation. The two pathways contribute to a final hypocotyl length that is longer in *elo3-6* than in the wild type, indicating that the pathway promoting cell elongation prevails. Lower expression of *HY5*, *HYH* and *HFR1* in the mutant also results in less expanded cotyledons, yielding the phenotype typical of photomorphogenesis defect.

In conclusion, Elongator is known as an enzymatic complex with diverse activities that directly or indirectly, positively or negatively, influence expression of genes located in various pathways. Here, we show that Elongator acts as an interface between growth, immune responses and photomorphogenesis and plays a fine-tuning role in mutual regulatory interactions of those processes at the transcriptional level.

MATERIALS AND METHODS

Plant mutants and reporter lines

The *drl1-2* (Nelissen et al., 2003), *elo1-1*, *elo2-1*, *elo3-1* and *elo4* (Nelissen et al., 2005) mutants corresponding to alleles of *ELP4*, *ELP1*, *ELP3* and *DRL1* genes in Ler and the *elo3-6* mutant in Col-0 (GABI-KAT collection code GABI555_H06, Nelissen et al., 2010) are described previously. *pCCA1::LUC* (Salome and McClung, 2005) and *pTOC1::LUC* (Portolés and Más, 2007) are reporter lines in Col-0. The mutants *phyB-9*, *hfr1-101* and *pif3-3 pif4-2* in Col-0 and *phyA-201*, *phyB-1* and *phyA-201 phyB-5* in Ler were purchased at the Nottingham *Arabidopsis* Stock Centre (NASC). The *lhy-21 cca1-11* (N9380) and *lhy-21* (N9379) mutants in Ws background were also obtained from NASC. The *cca1-11 lhyRNAi* mutant in Ws background was a kind gift from Steve Kay (The Scripps Research Institute, La Jolla, CA, USA). The double or triple mutants *elo3-6 hfr1*, *elo3-6 pif3-3 pif4-2*, *elo3-1 phyB-1* and *elo3-1 phyA-201* were generated by crossing. Homozygous individuals were identified by PCR genotyping with the primers listed in Table S3.

Growth conditions and assays

For hypocotyl assays, seeds were sterilized in 5% (v/v) bleach containing 0.05% (v/v) Tween 20 for 10 min, washed in water, sown on half-strength Murashige

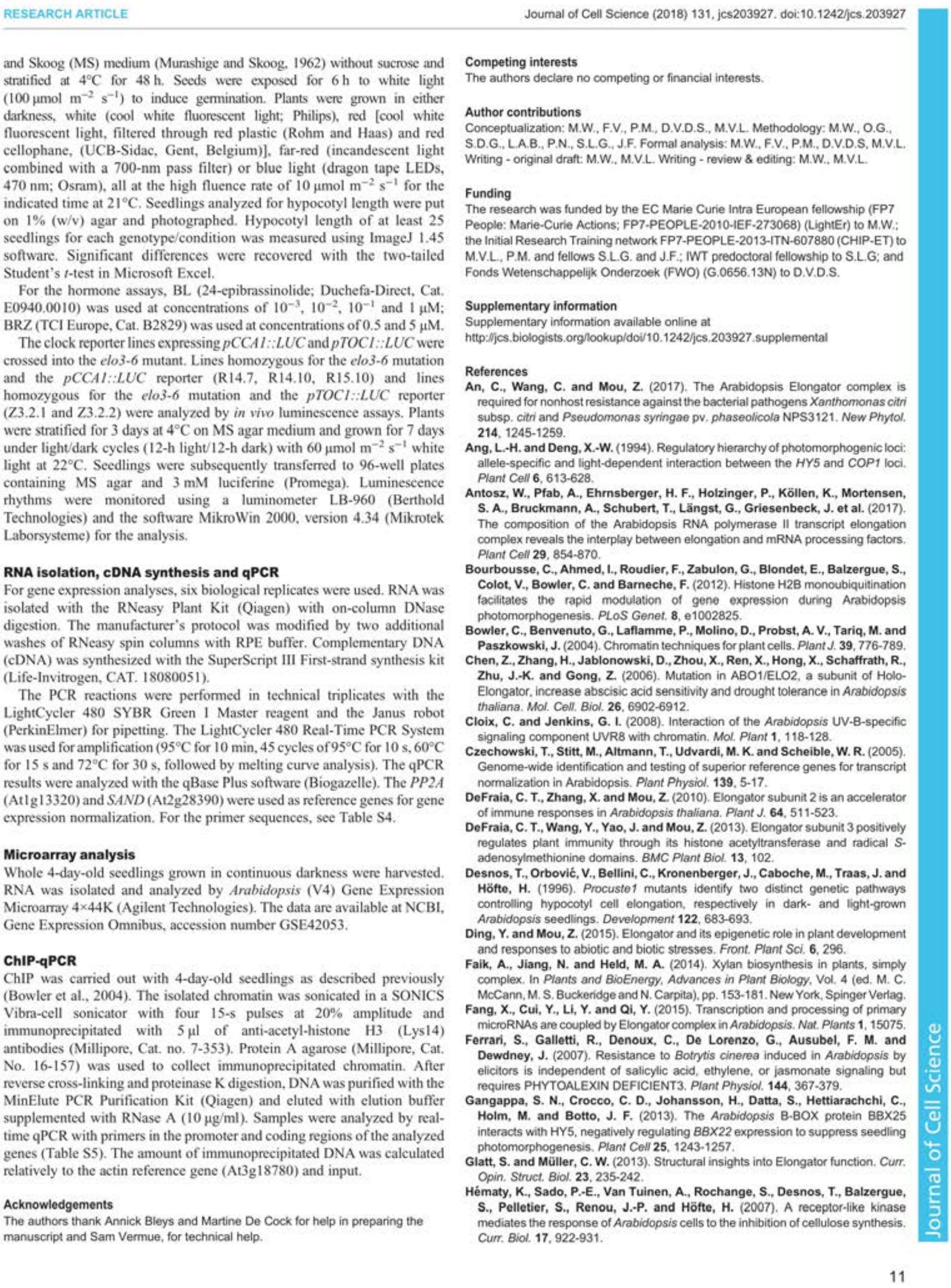

and Skoog (MS) medium (Murashige and Skoog, 1962) without sucrose and stratified at 4°C for 48 h. Seeds were exposed for 6 h to white light (100 µmol m^{-2} s^{-1}) to induce germination. Plants were grown in either darkness, white (cool white fluorescent light; Philips), red [cool white fluorescent light, filtered through red plastic (Rohm and Haas) and red cellophane, (UCB-Sidac, Gent, Belgium)], far-red (incandescent light combined with a 700-nm pass filter) or blue light (dragon tape LEDs, 470 nm; Osram), all at the high fluence rate of 10 µmol m^{-2} s^{-1} for the indicated time at 21°C. Seedlings analyzed for hypocotyl length were put on 1% (w/v) agar and photographed. Hypocotyl length of at least 25 seedlings for each genotype/condition was measured using ImageJ 1.45 software. Significant differences were recovered with the two-tailed Student's *t*-test in Microsoft Excel.

For the hormone assays, BL (24-epibrassinolide; Duchefa-Direct, Cat. E0940.0010) was used at concentrations of 10^{-3}, 10^{-2}, 10^{-1} and 1 µM; BRZ (TCI Europe, Cat. B2829) was used at concentrations of 0.5 and 5 µM.

The clock reporter lines expressing *pCCA1::LUC* and *pTOC1::LUC* were crossed into the *elo3-6* mutant. Lines homozygous for the *elo3-6* mutation and the *pCCA1::LUC* reporter (R14.7, R14.10, R15.10) and lines homozygous for the *elo3-6* mutation and the *pTOC1::LUC* reporter (Z3.2.1 and Z3.2.2) were analyzed by *in vivo* luminescence assays. Plants were stratified for 3 days at 4°C on MS agar medium and grown for 7 days under light/dark cycles (12-h light/12-h dark) with 60 µmol m^{-2} s^{-1} white light at 22°C. Seedlings were subsequently transferred to 96-well plates containing MS agar and 3 mM luciferine (Promega). Luminescence rhythms were monitored using a luminometer LB-960 (Berthold Technologies) and the software MikroWin 2000, version 4.34 (Mikrotek Laborsysteme) for the analysis.

RNA isolation, cDNA synthesis and qPCR

For gene expression analyses, six biological replicates were used. RNA was isolated with the RNeasy Plant Kit (Qiagen) with on-column DNase digestion. The manufacturer's protocol was modified by two additional washes of RNeasy spin columns with RPE buffer. Complementary DNA (cDNA) was synthesized with the SuperScript III First-strand synthesis kit (Life-Invitrogen, CAT. 18080051).

The PCR reactions were performed in technical triplicates with the LightCycler 480 SYBR Green I Master reagent and the Janus robot (PerkinElmer) for pipetting. The LightCycler 480 Real-Time PCR System was used for amplification (95°C for 10 min, 45 cycles of 95°C for 10 s, 60°C for 15 s and 72°C for 30 s, followed by melting curve analysis). The qPCR results were analyzed with the qBase Plus software (Biogazelle). The *PP2A* (At1g13320) and *SAND* (At2g28390) were used as reference genes for gene expression normalization. For the primer sequences, see Table S4.

Microarray analysis

Whole 4-day-old seedlings grown in continuous darkness were harvested. RNA was isolated and analyzed by *Arabidopsis* (V4) Gene Expression Microarray 4×44K (Agilent Technologies). The data are available at NCBI, Gene Expression Omnibus, accession number GSE42053.

ChIP-qPCR

ChIP was carried out with 4-day-old seedlings as described previously (Bowler et al., 2004). The isolated chromatin was sonicated in a SONICS Vibra-cell sonicator with four 15-s pulses at 20% amplitude and immunoprecipitated with 5 µl of anti-acetyl-histone H3 (Lys14) antibodies (Millipore, Cat. no. 7-353). Protein A agarose (Millipore, Cat. No. 16-157) was used to collect immunoprecipitated chromatin. After reverse cross-linking and proteinase K digestion, DNA was purified with the MinElute PCR Purification Kit (Qiagen) and eluted with elution buffer supplemented with RNase A (10 µg/ml). Samples were analyzed by real-time qPCR with primers in the promoter and coding regions of the analyzed genes (Table S5). The amount of immunoprecipitated DNA was calculated relatively to the actin reference gene (At3g18780) and input.

Acknowledgements

The authors thank Annick Bleys and Martine De Cock for help in preparing the manuscript and Sam Vermue, for technical help.

Competing interests

The authors declare no competing or financial interests.

Author contributions

Conceptualization: M.W., F.V., P.M., D.V.D.S., M.V.L. Methodology: M.W., O.G., S.D.G., L.A.B., P.N., S.L.G., J.F. Formal analysis: M.W., F.V., P.M., D.V.D.S, M.V.L. Writing - original draft: M.W., M.V.L. Writing - review & editing: M.W., M.V.L.

Funding

The research was funded by the EC Marie Curie Intra European fellowship (FP7 People: Marie-Curie Actions; FP7-PEOPLE-2010-IEF-273068) (LightEr) to M.W.; the Initial Research Training network FP7-PEOPLE-2013-ITN-607880 (CHIP-ET) to M.V.L., P.M. and fellows S.L.G. and J.F.; IWT predoctoral fellowship to S.L.G; and Fonds Wetenschappelijk Onderzoek (FWO) (G.0656.13N) to D.V.D.S.

Supplementary information

Supplementary information available online at
http://jcs.biologists.org/lookup/doi/10.1242/jcs.203927.supplemental

References

An, C., Wang, C. and Mou, Z. (2017). The Arabidopsis Elongator complex is required for nonhost resistance against the bacterial pathogens *Xanthomonas citri* subsp. *citri* and *Pseudomonas syringae* pv. *phaseolicola* NPS3121. *New Phytol.* **214**, 1245-1259.

Ang, L.-H. and Deng, X.-W. (1994). Regulatory hierarchy of photomorphogenic loci: allele-specific and light-dependent interaction between the *HY5* and *COP1* loci. *Plant Cell* **6**, 613-628.

Antosz, W., Pfab, A., Ehrnsberger, H. F., Holzinger, P., Köllen, K., Mortensen, S. A., Bruckmann, A., Schubert, T., Längst, G., Griesenbeck, J. et al. (2017). The composition of the Arabidopsis RNA polymerase II transcript elongation complex reveals the interplay between elongation and mRNA processing factors. *Plant Cell* **29**, 854-870.

Bourbousse, C., Ahmed, I., Roudier, F., Zabulon, G., Blondet, E., Balzergue, S., Colot, V., Bowler, C. and Barneche, F. (2012). Histone H2B monoubiquitination facilitates the rapid modulation of gene expression during Arabidopsis photomorphogenesis. *PLoS Genet.* **8**, e1002825.

Bowler, C., Benvenuto, G., Laflamme, P., Molino, D., Probst, A. V., Tariq, M. and Paszkowski, J. (2004). Chromatin techniques for plant cells. *Plant J.* **39**, 776-789.

Chen, Z., Zhang, H., Jablonowski, D., Zhou, X., Ren, X., Hong, X., Schaffrath, R., Zhu, J.-K. and Gong, Z. (2006). Mutation in ABO1/ELO2, a subunit of Holo-Elongator, increase abscisic acid sensitivity and drought tolerance in *Arabidopsis thaliana*. *Mol. Cell. Biol.* **26**, 6902-6912.

Cloix, C. and Jenkins, G. I. (2008). Interaction of the *Arabidopsis* UV-B-specific signaling component UVR8 with chromatin. *Mol. Plant* **1**, 118-128.

Czechowski, T., Stitt, M., Altmann, T., Udvardi, M. K. and Scheible, W. R. (2005). Genome-wide identification and testing of superior reference genes for transcript normalization in Arabidopsis. *Plant Physiol.* **139**, 5-17.

DeFraia, C. T., Zhang, X. and Mou, Z. (2010). Elongator subunit 2 is an accelerator of immune responses in *Arabidopsis thaliana*. *Plant J.* **64**, 511-523.

DeFraia, C. T., Wang, Y., Yao, J. and Mou, Z. (2013). Elongator subunit 3 positively regulates plant immunity through its histone acetyltransferase and radical *S*-adenosylmethionine domains. *BMC Plant Biol.* **13**, 102.

Desnos, T., Orbović, V., Bellini, C., Kronenberger, J., Caboche, M., Traas, J. and Höfte, H. (1996). *Procuste1* mutants identify two distinct genetic pathways controlling hypocotyl cell elongation, respectively in dark- and light-grown *Arabidopsis* seedlings. *Development* **122**, 683-693.

Ding, Y. and Mou, Z. (2015). Elongator and its epigenetic role in plant development and responses to abiotic and biotic stresses. *Front. Plant Sci.* **6**, 296.

Faik, A., Jiang, N. and Held, M. A. (2014). Xylan biosynthesis in plants, simply complex. In *Plants and BioEnergy, Advances in Plant Biology*, Vol. 4 (ed. M. C. McCann, M. S. Buckeridge and N. Carpita), pp. 153-181. New York, Spinger Verlag.

Fang, X., Cui, Y., Li, Y. and Qi, Y. (2015). Transcription and processing of primary microRNAs are coupled by Elongator complex in *Arabidopsis*. *Nat. Plants* **1**, 15075.

Ferrari, S., Galletti, R., Denoux, C., De Lorenzo, G., Ausubel, F. M. and Dewdney, J. (2007). Resistance to *Botrytis cinerea* induced in *Arabidopsis* by elicitors is independent of salicylic acid, ethylene, or jasmonate signaling but requires PHYTOALEXIN DEFICIENT3. *Plant Physiol.* **144**, 367-379.

Gangappa, S. N., Crocco, C. D., Johansson, H., Datta, S., Hettiarachchi, C., Holm, M. and Botto, J. F. (2013). The *Arabidopsis* B-BOX protein BBX25 interacts with HY5, negatively regulating *BBX22* expression to suppress seedling photomorphogenesis. *Plant Cell* **25**, 1243-1257.

Glatt, S. and Müller, C. W. (2013). Structural insights into Elongator function. *Curr. Opin. Struct. Biol.* **23**, 235-242.

Hématy, K., Sado, P.-E., Van Tuinen, A., Rochange, S., Desnos, T., Balzergue, S., Pelletier, S., Renou, J.-P. and Höfte, H. (2007). A receptor-like kinase mediates the response of *Arabidopsis* cells to the inhibition of cellulose synthesis. *Curr. Biol.* **17**, 922-931.

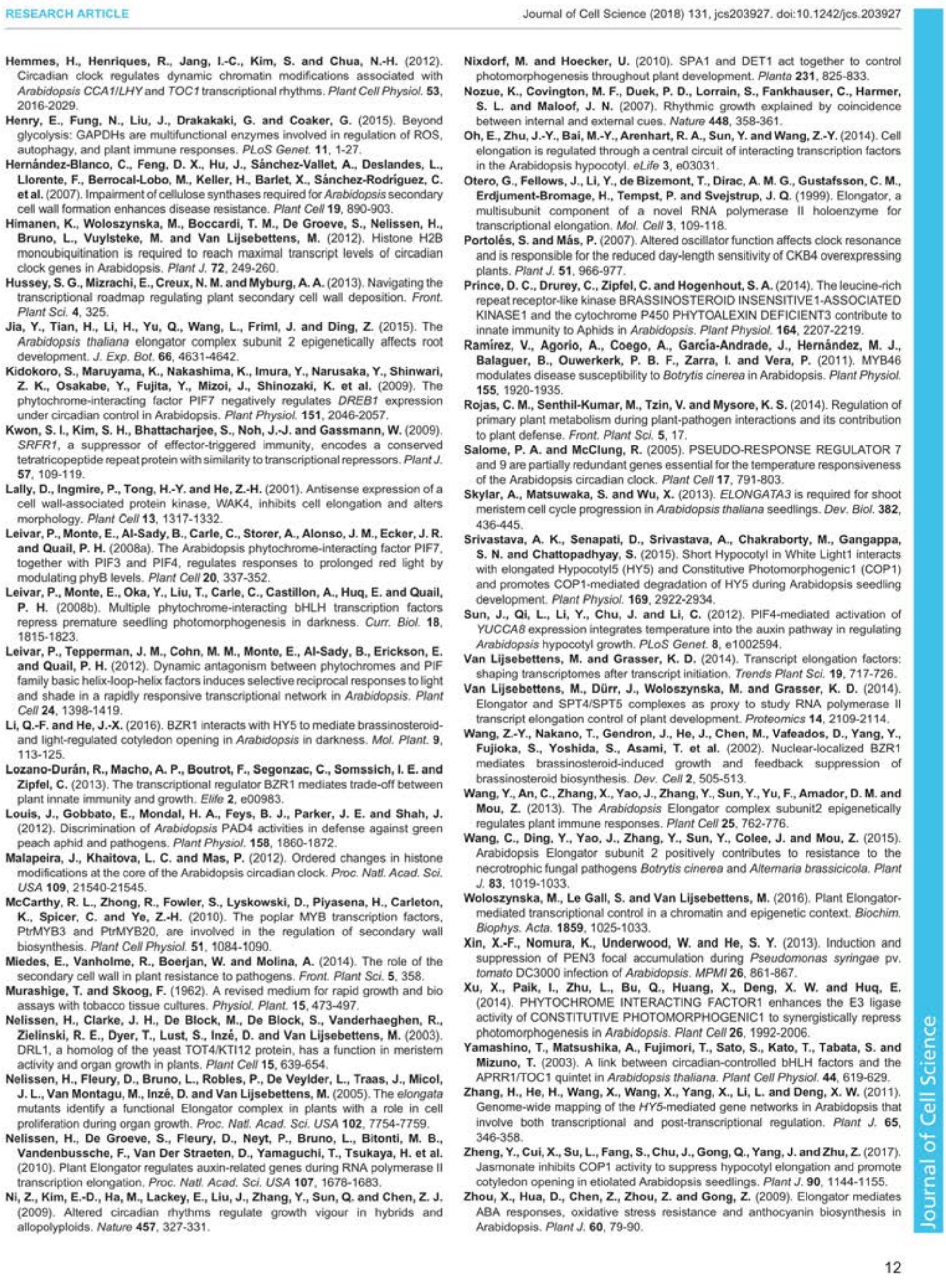

Hemmes, H., Henriques, R., Jang, I.-C., Kim, S. and Chua, N.-H. (2012). Circadian clock regulates dynamic chromatin modifications associated with *Arabidopsis CCA1/LHY* and *TOC1* transcriptional rhythms. *Plant Cell Physiol.* **53**, 2016-2029.

Henry, E., Fung, N., Liu, J., Drakakaki, G. and Coaker, G. (2015). Beyond glycolysis: GAPDHs are multifunctional enzymes involved in regulation of ROS, autophagy, and plant immune responses. *PLoS Genet.* **11**, 1-27.

Hernández-Blanco, C., Feng, D. X., Hu, J., Sánchez-Vallet, A., Deslandes, L., Llorente, F., Berrocal-Lobo, M., Keller, H., Barlet, X., Sánchez-Rodríguez, C. et al. (2007). Impairment of cellulose synthases required for *Arabidopsis* secondary cell wall formation enhances disease resistance. *Plant Cell* **19**, 890-903.

Himanen, K., Woloszynska, M., Boccardi, T. M., De Groeve, S., Nelissen, H., Bruno, L., Vuylsteke, M. and Van Lijsebettens, M. (2012). Histone H2B monoubiquitination is required to reach maximal transcript levels of circadian clock genes in Arabidopsis. *Plant J.* **72**, 249-260.

Hussey, S. G., Mizrachi, E., Creux, N. M. and Myburg, A. A. (2013). Navigating the transcriptional roadmap regulating plant secondary cell wall deposition. *Front. Plant Sci.* **4**, 325.

Jia, Y., Tian, H., Li, H., Yu, Q., Wang, L., Friml, J. and Ding, Z. (2015). The *Arabidopsis thaliana* elongator complex subunit 2 epigenetically affects root development. *J. Exp. Bot.* **66**, 4631-4642.

Kidokoro, S., Maruyama, K., Nakashima, K., Imura, Y., Narusaka, Y., Shinwari, Z. K., Osakabe, Y., Fujita, Y., Mizoi, J., Shinozaki, K. et al. (2009). The phytochrome-interacting factor PIF7 negatively regulates *DREB1* expression under circadian control in Arabidopsis. *Plant Physiol.* **151**, 2046-2057.

Kwon, S. I., Kim, S. H., Bhattacharjee, S., Noh, J.-J. and Gassmann, W. (2009). *SRFR1*, a suppressor of effector-triggered immunity, encodes a conserved tetratricopeptide repeat protein with similarity to transcriptional repressors. *Plant J.* **57**, 109-119.

Lally, D., Ingmire, P., Tong, H.-Y. and He, Z.-H. (2001). Antisense expression of a cell wall-associated protein kinase, WAK4, inhibits cell elongation and alters morphology. *Plant Cell* **13**, 1317-1332.

Leivar, P., Monte, E., Al-Sady, B., Carle, C., Storer, A., Alonso, J. M., Ecker, J. R. and Quail, P. H. (2008a). The Arabidopsis phytochrome-interacting factor PIF7, together with PIF3 and PIF4, regulates responses to prolonged red light by modulating phyB levels. *Plant Cell* **20**, 337-352.

Leivar, P., Monte, E., Oka, Y., Liu, T., Carle, C., Castillon, A., Huq, E. and Quail, P. H. (2008b). Multiple phytochrome-interacting bHLH transcription factors repress premature seedling photomorphogenesis in darkness. *Curr. Biol.* **18**, 1815-1823.

Leivar, P., Tepperman, J. M., Cohn, M. M., Monte, E., Al-Sady, B., Erickson, E. and Quail, P. H. (2012). Dynamic antagonism between phytochromes and PIF family basic helix-loop-helix factors induces selective reciprocal responses to light and shade in a rapidly responsive transcriptional network in *Arabidopsis*. *Plant Cell* **24**, 1398-1419.

Li, Q.-F. and He, J.-X. (2016). BZR1 interacts with HY5 to mediate brassinosteroid- and light-regulated cotyledon opening in *Arabidopsis* in darkness. *Mol. Plant.* **9**, 113-125.

Lozano-Durán, R., Macho, A. P., Boutrot, F., Segonzac, C., Somssich, I. E. and Zipfel, C. (2013). The transcriptional regulator BZR1 mediates trade-off between plant innate immunity and growth. *Elife* **2**, e00983.

Louis, J., Gobbato, E., Mondal, H. A., Feys, B. J., Parker, J. E. and Shah, J. (2012). Discrimination of *Arabidopsis* PAD4 activities in defense against green peach aphid and pathogens. *Plant Physiol.* **158**, 1860-1872.

Malapeira, J., Khaitova, L. C. and Mas, P. (2012). Ordered changes in histone modifications at the core of the Arabidopsis circadian clock. *Proc. Natl. Acad. Sci. USA* **109**, 21540-21545.

McCarthy, R. L., Zhong, R., Fowler, S., Lyskowski, D., Piyasena, H., Carleton, K., Spicer, C. and Ye, Z.-H. (2010). The poplar MYB transcription factors, PtrMYB3 and PtrMYB20, are involved in the regulation of secondary wall biosynthesis. *Plant Cell Physiol.* **51**, 1084-1090.

Miedes, E., Vanholme, R., Boerjan, W. and Molina, A. (2014). The role of the secondary cell wall in plant resistance to pathogens. *Front. Plant Sci.* **5**, 358.

Murashige, T. and Skoog, F. (1962). A revised medium for rapid growth and bio assays with tobacco tissue cultures. *Physiol. Plant.* **15**, 473-497.

Nelissen, H., Clarke, J. H., De Block, M., De Block, S., Vanderhaeghen, R., Zielinski, R. E., Dyer, T., Lust, S., Inzé, D. and Van Lijsebettens, M. (2003). DRL1, a homolog of the yeast TOT4/KTI12 protein, has a function in meristem activity and organ growth in plants. *Plant Cell* **15**, 639-654.

Nelissen, H., Fleury, D., Bruno, L., Robles, P., De Veylder, L., Traas, J., Micol, J. L., Van Montagu, M., Inzé, D. and Van Lijsebettens, M. (2005). The *elongata* mutants identify a functional Elongator complex in plants with a role in cell proliferation during organ growth. *Proc. Natl. Acad. Sci. USA* **102**, 7754-7759.

Nelissen, H., De Groeve, S., Fleury, D., Neyt, P., Bruno, L., Bitonti, M. B., Vandenbussche, F., Van Der Straeten, D., Yamaguchi, T., Tsukaya, H. et al. (2010). Plant Elongator regulates auxin-related genes during RNA polymerase II transcription elongation. *Proc. Natl. Acad. Sci. USA* **107**, 1678-1683.

Ni, Z., Kim, E.-D., Ha, M., Lackey, E., Liu, J., Zhang, Y., Sun, Q. and Chen, Z. J. (2009). Altered circadian rhythms regulate growth vigour in hybrids and allopolyploids. *Nature* **457**, 327-331.

Nixdorf, M. and Hoecker, U. (2010). SPA1 and DET1 act together to control photomorphogenesis throughout plant development. *Planta* **231**, 825-833.

Nozue, K., Covington, M. F., Duek, P. D., Lorrain, S., Fankhauser, C., Harmer, S. L. and Maloof, J. N. (2007). Rhythmic growth explained by coincidence between internal and external cues. *Nature* **448**, 358-361.

Oh, E., Zhu, J.-Y., Bai, M.-Y., Arenhart, R. A., Sun, Y. and Wang, Z.-Y. (2014). Cell elongation is regulated through a central circuit of interacting transcription factors in the Arabidopsis hypocotyl. *eLife* **3**, e03031.

Otero, G., Fellows, J., Li, Y., de Bizemont, T., Dirac, A. M. G., Gustafsson, C. M., Erdjument-Bromage, H., Tempst, P. and Svejstrup, J. Q. (1999). Elongator, a multisubunit component of a novel RNA polymerase II holoenzyme for transcriptional elongation. *Mol. Cell* **3**, 109-118.

Portolés, S. and Más, P. (2007). Altered oscillator function affects clock resonance and is responsible for the reduced day-length sensitivity of CKB4 overexpressing plants. *Plant J.* **51**, 966-977.

Prince, D. C., Drurey, C., Zipfel, C. and Hogenhout, S. A. (2014). The leucine-rich repeat receptor-like kinase BRASSINOSTEROID INSENSITIVE1-ASSOCIATED KINASE1 and the cytochrome P450 PHYTOALEXIN DEFICIENT3 contribute to innate immunity to Aphids in *Arabidopsis*. *Plant Physiol.* **164**, 2207-2219.

Ramírez, V., Agorio, A., Coego, A., García-Andrade, J., Hernández, M. J., Balaguer, B., Ouwerkerk, P. B. F., Zarra, I. and Vera, P. (2011). MYB46 modulates disease susceptibility to *Botrytis cinerea* in Arabidopsis. *Plant Physiol.* **155**, 1920-1935.

Rojas, C. M., Senthil-Kumar, M., Tzin, V. and Mysore, K. S. (2014). Regulation of primary plant metabolism during plant-pathogen interactions and its contribution to plant defense. *Front. Plant Sci.* **5**, 17.

Salome, P. A. and McClung, R. (2005). PSEUDO-RESPONSE REGULATOR 7 and 9 are partially redundant genes essential for the temperature responsiveness of the Arabidopsis circadian clock. *Plant Cell* **17**, 791-803.

Skylar, A., Matsuwaka, S. and Wu, X. (2013). *ELONGATA3* is required for shoot meristem cell cycle progression in *Arabidopsis thaliana* seedlings. *Dev. Biol.* **382**, 436-445.

Srivastava, A. K., Senapati, D., Srivastava, A., Chakraborty, M., Gangappa, S. N. and Chattopadhyay, S. (2015). Short Hypocotyl in White Light1 interacts with elongated Hypocotyl5 (HY5) and Constitutive Photomorphogenic1 (COP1) and promotes COP1-mediated degradation of HY5 during Arabidopsis seedling development. *Plant Physiol.* **169**, 2922-2934.

Sun, J., Qi, L., Li, Y., Chu, J. and Li, C. (2012). PIF4-mediated activation of *YUCCA8* expression integrates temperature into the auxin pathway in regulating *Arabidopsis* hypocotyl growth. *PLoS Genet.* **8**, e1002594.

Van Lijsebettens, M. and Grasser, K. D. (2014). Transcript elongation factors: shaping transcriptomes after transcript initiation. *Trends Plant Sci.* **19**, 717-726.

Van Lijsebettens, M., Dürr, J., Woloszynska, M. and Grasser, K. D. (2014). Elongator and SPT4/SPT5 complexes as proxy to study RNA polymerase II transcript elongation control of plant development. *Proteomics* **14**, 2109-2114.

Wang, Z.-Y., Nakano, T., Gendron, J., He, J., Chen, M., Vafeados, D., Yang, Y., Fujioka, S., Yoshida, S., Asami, T. et al. (2002). Nuclear-localized BZR1 mediates brassinosteroid-induced growth and feedback suppression of brassinosteroid biosynthesis. *Dev. Cell* **2**, 505-513.

Wang, Y., An, C., Zhang, X., Yao, J., Zhang, Y., Sun, Y., Yu, F., Amador, D. M. and Mou, Z. (2013). The *Arabidopsis* Elongator complex subunit2 epigenetically regulates plant immune responses. *Plant Cell* **25**, 762-776.

Wang, C., Ding, Y., Yao, J., Zhang, Y., Sun, Y., Colee, J. and Mou, Z. (2015). Arabidopsis Elongator subunit 2 positively contributes to resistance to the necrotrophic fungal pathogens *Botrytis cinerea* and *Alternaria brassicicola*. *Plant J.* **83**, 1019-1033.

Woloszynska, M., Le Gall, S. and Van Lijsebettens, M. (2016). Plant Elongator-mediated transcriptional control in a chromatin and epigenetic context. *Biochim. Biophys. Acta.* **1859**, 1025-1033.

Xin, X.-F., Nomura, K., Underwood, W. and He, S. Y. (2013). Induction and suppression of PEN3 focal accumulation during *Pseudomonas syringae* pv. *tomato* DC3000 infection of *Arabidopsis*. *MPMI* **26**, 861-867.

Xu, X., Paik, I., Zhu, L., Bu, Q., Huang, X., Deng, X. W. and Huq, E. (2014). PHYTOCHROME INTERACTING FACTOR1 enhances the E3 ligase activity of CONSTITUTIVE PHOTOMORPHOGENIC1 to synergistically repress photomorphogenesis in *Arabidopsis*. *Plant Cell* **26**, 1992-2006.

Yamashino, T., Matsushika, A., Fujimori, T., Sato, S., Kato, T., Tabata, S. and Mizuno, T. (2003). A link between circadian-controlled bHLH factors and the APRR1/TOC1 quintet in *Arabidopsis thaliana*. *Plant Cell Physiol.* **44**, 619-629.

Zhang, H., He, H., Wang, X., Wang, X., Yang, X., Li, L. and Deng, X. W. (2011). Genome-wide mapping of the *HY5*-mediated gene networks in Arabidopsis that involve both transcriptional and post-transcriptional regulation. *Plant J.* **65**, 346-358.

Zheng, Y., Cui, X., Su, L., Fang, S., Chu, J., Gong, Q., Yang, J. and Zhu, Z. (2017). Jasmonate inhibits COP1 activity to suppress hypocotyl elongation and promote cotyledon opening in etiolated Arabidopsis seedlings. *Plant J.* **90**, 1144-1155.

Zhou, X., Hua, D., Chen, Z., Zhou, Z. and Gong, Z. (2009). Elongator mediates ABA responses, oxidative stress resistance and anthocyanin biosynthesis in Arabidopsis. *Plant J.* **60**, 79-90.